# Understanding the ecohydrology of shallow, drained and marginal blanket peatlands

Submitted by David John Luscombe to the University of Exeter

as a thesis for the degree of

Doctor of Philosophy In Geography

In August 2014



I certify that all material in this thesis which is not my own work has been identified and that no material has previously been submitted and approved for the award of a degree by this or any other University.

Signature: ……..

# *Acknowledgements*

Throughout the course of this PhD I have been fortunate enough to have been guided and supported by two fantastic supervisors, whom have both been kind enough to share their knowledge and insight whenever it has been needed. I would like to thank Richard Brazier for always having an open door, a cup of coffee and for reminding me of the bigger picture. I would also like to thank Karen Anderson for managing to supervise my work with such enthusiasm and focus, and often from so far away.

This PhD has provided me with a unique opportunity to work as part of a fantastic research team and wider “mires” project. Without the funding provided from South West Water my research would simply not have taken place. In this respect I am particularly thankful to David Smith at South West Water and the financial, technical and managerial support of my colleagues from the other project partners, including the Environment Agency, Exmoor National Park, Dartmoor National Park and Natural England.

I would also like to expressly thank my fellow postgraduate research students and colleagues with whom I have spent innumerable days in the field, office and pub, and with whom I have had many discussions which have undoubtedly strengthened this thesis. Specifically I would like to thank Emilie Grand-Clement, Naomi Gatis, Alan Puttock, Pia Benaud and Josie Ashe for their insights. I would also like to thank Neville England for his genius in making and fixing so much field equipment.

Finally, I would like to thank my family for their endless support and my wife Polly for her love, support and friendship throughout every day and every bump in the road.

# *Abstract*

Peatlands are unique and important landscape systems, providing valuable ecosystem services such as water and carbon storage, water supply and flood attenuation. They are known to account for more than 10% of the world's terrestrial carbon store and represent 50 – 70% of the global wetland resource. The UK government's decision to support the IUCN, UK Peatland Program Commission of Inquiry on Peatlands, recognises the importance and urgency with which action is needed to understand and restore damaged peatland landscapes, and their associated ecosystem services. To meet this need, it is recognised that peatlands in the South West of the UK are important as bio-climatically and functionally marginal peatlands that are undergoing extensive restoration to reinstate key ecological and hydrological function.

This thesis aims to improve understanding of the temporal and spatial variability of the ecohydrological structure and function of peatland ecosystems in the South West UK, and will provide the first baseline for the spatially distributed extrapolation of change across larger landscape extents. The research seeks to characterise the structure and function of peatland ecohydrology across multiple spatial and temporal scales. This is accomplished by bringing together remote sensing analyses of ecohydrological structure and function coupled with an integrated and high resolution hydrological monitoring system to characterise the spatial and temporal variability of runoff production and water storage across two headwater catchments.

Key outcomes of this research are: 1. The development of novel methods to assess the spatial distribution of near surface hydrology in upland ecosystems using airborne thermal imaging data, 2. Improved understanding of how laser altimetry data can be used to measure the ecohydrology of landscapes more appropriately. 3. An empirical understanding of both the spatial and temporal variability of hydrology across representative sites within the moorlands of the South West UK. The high-resolution monitoring data are the first to describe the hydrological processes operating in these peatlands systems effectively, and provide an insight into how these processes are controlled by the anthropogenic drainage networks that are present throughout this shallow marginal peatland system.

# Contents

# *List of Tables*

# *List of Figures*

# 1 Introduction

Once regarded as empty wastelands or treacherous wilderness (Tebbutt, 2004), peat covered landscapes are now becoming recognised for their wide ranging environmental and anthropogenic importance (Hubacek et al., 2009). Many studies recognise the significance of peatlands in providing valuable ecosystem services such as water and carbon storage, water supply and flood attenuation (Cannell et al., 1993, Joosten and Clarke, 2002, Bellamy et al., 2005, Grand-Clement et al., 2013). Globally, peat soils cover 3% of the land mass, however, despite this relatively small fraction, they account for more than 10% of the world's terrestrial carbon store (Holden, 2005) and represent 50 – 70% of the global wetland resource (Joosten and Clarke, 2002), making them the most widespread of all wetlands. Peatlands are thought to cover 6-21% of the UK land area (Lindsay, 2010, Ramchunder et al., 2009). The inconsistency of such estimates arises from variability in estimation methods, peatland definitions and the uncertainty associated with the peat depths and soil properties in such landscape systems (Morris et al., 2011). "Pristine" and functionally intact peatlands are now nationally and globally sparse, with as little as 1.25% of blanket bog in England in an undamaged and peat-forming state (Reed et al., 2009). The UK government's decision to support the outcomes of the International Union for the Conservation of Nature (IUCN), UK Peatland Program Commission of Inquiry on Peatlands, recognises the importance and urgency with which action is needed to restore damaged peatland landscapes, and their associated ecosystem services (Bain et al., 2011).

Peatlands in the South West of the UK have formed at the southern and western limit of the bio-climatic envelope of peat-forming ecosystems, where conditions are appropriate to sustain carbon sequestering processes (Gallego-Sala et al., 2010). This results in a unique geographic position and marginal potential for future peat accumulation in these peatlands (Clark et al., 2010). For that reason, the functioning of these peatlands is important, not only as a carbon store, water resource and important habitat, but also as a key indicator of climate related changes expected in more northerly peatlands, in the UK and elsewhere. The relative importance of these marginal peatlands is further enhanced by the anthropogenic pressures upon these landscapes. Specifically, the extensive implementation of numerous surface drainage ditches, which

were cut into the relatively shallow peat deposits in the 19th century from approximately 1852 onwards, with the aim of improving the quality of the vegetation for grazing (pers. comm. Exmoor National Park, 2014). These drainage ditch networks have left peatlands in the South West increasingly vulnerable to erosion, and ecological and hydrological degradation (Holden et al., 2007a, Pawson et al., 2012, Ramchunder et al., 2009). It is now widely acknowledged that this type of widespread drainage has caused significant change to the ecohydrology (i.e. the interplay between ecological and hydrological structure and function) of these peatlands, without delivering the promised increases in agricultural productivity (Holden et al., 2006b, Allott et al., 2009, Stewart and Lance, 1991, Wilson et al., 2011c).

Given the societal importance of these peatland landscapes and the widespread anthropogenic modification of their related ecosystem services, there is now an imperative to improve understanding of the ecohydrological processes governing the dynamics of these systems. Given this imperative, this research looks to characterise the ecohydrological structure and function of degraded blanket peatlands in Exmoor, in the South West of the UK. Specifically, the overall focus of this work is to undertake the first spatio-temporal and ecohydrologically focused study of two degraded upland peatland catchments in this area, so that the ongoing management of these landscapes may be better informed. The research seeks to understand the contribution of the ecosystem services that these peatlands deliver (e.g. flood attenuation and carbon storage) in a degraded and drained state. This work will also facilitate an understanding of the future vulnerability of these ecosystem services in light of scheduled hydrological restoration.

Understanding the temporal and spatial variability in the ecohydrological function of these peatlands landscapes will also provide the first baseline for the spatially distributed extrapolation of change across larger landscape extents. Specifically, the research characterises the structure and function of peatland ecohydrology across multiple spatial and temporal scales, to improve scientific understanding of how such landscapes behave with respect to the historic anthropogenic drainage interventions. An enhanced understanding of the spatiotemporal variability in these systems will also provide a baseline for

restoration interventions and support the improved targeting of ongoing restoration interventions across comparable landscapes elsewhere.

## 1.1 Thesis structure

Following this chapter, A literature review (chapter 2) is included to provide a context for the research outlined in this thesis. A detailed site description and study methods section (chapter 3) is included following chapter 2 and prior to the primary research included in this thesis (chapters 4 to 7) in order to provide a methodological and experimental context throughout the rest of this thesis.

The primary research content of this thesis is presented as four self-contained papers that characterise the ecohydrological structure and function across the Aclands and Spooners experimental headwater catchments detailed in chapter 2. The first two papers each form a stand-alone body of work, with the following two papers presented as a two-part paper with a more extensive inter-referential narrative, linking spatial and temporal aspects of hydrological function. To address the characterisation of ecohydrological structure and function over a range of spatial and temporal scales, this research is arranged around two methodological themes:

### *1.1.1 Theme one: remote sensing analysis for spatial characterisation of upland peatland ecohydrology*

Papers one and two (chapters 4 and 5) address this theme, where airborne remote sensing data have been used to characterise the spatially distributed characteristics and ecohydrological status of two experimental catchments prior to restoration. The work undertaken and presented here is novel because this was the first time that (a) airborne LiDAR data were evaluated in relation to ground-based laser scanning data on upland degraded peatlands, with a view towards improving spatial determination of ecohydrological structure and (b) airborne thermographic analysis was used and validated to show spatial patterns in near surface wetness in peatlands. The approach used these data alongside extensive ground validation data to address the following hypotheses:

1. Terrestrial Laser Scanning (TLS) data can be used to validate the information content of a LiDAR DSM in an upland peatland context,

thereby allowing improved spatial characterisation of ecohydrological structures such as above-ground biomass and surface-flow pathways.

2. Airborne LiDAR data allow the discrimination of different ecohydrologically relevant vegetation communities in upland peatlands.
3. Airborne LiDAR data are capable of detecting the presence and position of anthropogenic landscape features such as drains and archaeological remains which may alter hydrological function in peatlands.
4. Patterning evident in unprocessed relative emissivity data from Thermal airborne imaging data (TABI) is spatially associated with the position of anthropogenic drainage networks.
5. Structural data from LiDAR datasets covering the same extent as relative emissivity data distinguishes areas where structure or wetness dominates emissivity measurements.
6. Structurally normalized TABI relative emissivity data are related to the spatial distribution of near surface wetness in an upland peatland.

The development and scientific rational behind these hypotheses are explained more fully in chapters 4 and 5 of this thesis. However, the overarching objective of these hypotheses is to examine the assumption that ecological and topographic structures are key indicators of ecohydrological condition in peatlands (Korpela et al., 2009, Anderson et al., 2010). The research undertaken to address hypotheses 1-3 above (chapter 4) allowed for a detailed assessment of the ability of laser altimetry data of contrasting spatial resolutions to capture complex ecohydrological structure across landscape extents. Building on the results of this work, hypotheses 4-6 above (chapter 5) utilise structural proxies derived from LiDAR data to interpret proxies of land surface hydrology using airborne thermal imaging data.

### *1.1.2 Theme two: in-field high resolution hydrological monitoring of degraded upland headwater catchments*

The second theme, encompassing a two-part paper (chapters 6 and 7), analyses the ability of a novel, high-resolution, *in situ* hydrological monitoring

system (where the sampling design was developed by the author) to characterise the spatial and temporal variability in runoff production and water storage across multiple spatial and temporal scales in both of the studied headwater catchments. This work utilises six separate “experimental pools” (EPs) and two monitored catchment outflows distributed across both catchments, to characterise the hydrological response of these systems to precipitation inputs and periods of drought. This research was unique in the spatial design of the catchment monitoring scheme used. Large numbers of spatially distributed monitoring locations (n >100), measuring depth (below ground surface) to water table (DWT) parameters instantaneously, over short time steps (15 minutes) and continuously over long (multi-annual) periods has provided a state-of-the-art dataset describing the spatial variation in depth to water table across multiple spatial and temporal scales. To date, the *in situ* monitoring scheme has generated approximately 7.74 million data points describing near surface peatland hydrology. Existing literature describing the hydrological process operating in shallow peatlands, such as those in the south west of the UK, is currently very limited (see section 3.1). Resultantly, the research required examination of the empirical hydrological behaviour of the studied catchments using these datasets. In order to address this requirement, the second research theme specifically addresses the following hypotheses.

1. Flow regimes in shallow, drained peatlands are dominated by flashy (i.e. rapid and short lived) storm flows and low base flow conditions.
2. The primary control on runoff (Q) in shallow, drained peatlands is rainfall, with antecedent water tables and rainfall, exerting a secondary control.
3. Event discharge is generated only when water tables are close to the soil surface and rapid, saturation excess near surface flow occurs.
4. Spatial variability of rainfall-runoff response is proportional to the size of the drainage channel and the spatial attributes of its topographic contributing area.
5. Mean (and variance) of depth to water table (DWT) is greatest proximal to functioning drainage features, decreasing with distance from the drain.
6. Variance in depth to water tables can be explained by position of the drainage ditches with respect to local topography.

Building on the spatial characterisation of ecohydrological structure discussed under theme one, these hypothesis enable the temporal (hypotheses 1-3 above, chapter 6) and spatial (hypotheses 4-6 above, chapter 7) analyses of the hydrological function across both experimental headwater catchments. Importantly, the research undertaken to address these hypotheses enables the characterisation of the hydrological processes operating these shallow blanket mire systems in the context of research undertaken in deeper peatland systems. Secondly, these data provide an important baseline with which the effects of landscape rewetting can be more fully understood in the future. Baseline data are recognised in the scientific literature as key to understanding the complex effects that landscape re-wetting has in restoring ecohydrological function, and the associated ecosystem services these landscapes provide (Bragg and Tallis, 2001, Holden et al., 2004, Holden et al., 2011, Parry et al., 2014).

In bringing together the remote sensing analyses with the hydrological analysis, this project has enabled a thorough, spatially-distributed understanding of the two peatland catchments to be gathered, leading to enhanced knowledge about the ecohydrological structure and function of these peatlands. This is discussed further in chapter 3 and in a concise concluding chapter (8) bringing together the findings of this body of research in light of the ongoing landscape management and hydrological monitoring currently underway in these catchments.

## 1.2 Statement of contribution

I am the first author on all four of the papers included in this study and confirm that I am the primary author, data collector and primary data analyst for all of the papers included. Some of the work included here has already been published – chapters 4 and 5 appear in Luscombe et al. (2014a) and Luscombe et al. (2014b) respectively. Further work (chapters 6 and 7) is due to be submitted to the journal “Hydrological Processes” after completion of the thesis. The list of papers below summarises both the published research in the thesis and that which has been co-authored as part of the wider ‘Mires’ project. The papers included in this study have multiple co-authors – this is because the research has been supported by other members of the research group,

particularly in areas such as fieldwork assistance, installation and maintenance of dipwell timeseries and in commenting on papers after the initial draft was produced by me. During the course of my PhD research I have also been included as a co–author on two further papers produced from my wider research group (Grand-Clement et al., 2013, Grand-Clement et al., 2014). These papers do not form part of this thesis but they are related to my contribution to the wider 'Mires' project and they are therefore cited in the text. All of the relevant publications and citations for conference proceeding/papers related to this research are also listed below.

Peer-reviewed publications arising from work undertaken for the thesis.

- Luscombe, D. J., Anderson, K., Gatis, N., Wetherelt, A., Grand-Clement, E. & Brazier, R. E. 2014. What does airborne LiDAR really measure in upland ecosystems? *Ecohydrology*. DOI: 10.1002/eco.1527.

- Luscombe, D. J., Anderson, K., Gatis, N., Grand-Clement, E. & Brazier, R. E. 2014. Using airborne thermal imaging data to measure near-surface hydrology in upland ecosystems. *Hydrological Processes*. DOI: 10.1002/hyp.10285

Papers in preparation for publication and included in thesis.

- Luscombe, D. J., Anderson, K., Grand-Clement, E., Gatis, N., Ashe, J., Benaud, P., Smith, D. & Brazier, R. E. Forthcoming. Understanding the hydrology of shallow, drained and marginal peatlands: 1. Temporal variability. *Hydrological Processes*.

- Luscombe, D. J., Anderson, K., Grand-Clement, E., Gatis, N., Ashe, J., Benaud, P., Smith, D. & Brazier, R. E. Forthcoming. Understanding the hydrology of shallow, drained and marginal peatlands: 2. Spatial variability. *Hydrological Processes*.

Co-authored publications not included in this thesis, but which are cited in the text.

- Grand-Clement, E., Luscombe, D. J., Anderson, K., Gatis, N., Benaud, P. & Brazier, R. E. 2014. Antecedent conditions control carbon loss and downstream water quality from shallow, damaged peatlands. *Science of The Total Environment,* 493**,** 961-973.

- Grand-Clement, E., Anderson, K., Smith, D., Luscombe, D., Gatis, N., Ross, M. & Brazier, R. E. 2013. Evaluating ecosystem goods and

services after restoration of marginal upland peatlands in South-West England. *Journal of Applied Ecology*, 50, 324-334.

References from conference proceedings and papers related to the research in this thesis.

- Luscombe, D., Grand-Clement, E., Anderson, K., Gatis, N., Ashe, J. & Brazier, R. Short-term effects of restoration on the hydrology of shallow blanket peatlands in the South West UK. EGU General Assembly Conference Abstracts, 2014. 7132.

- Luscombe, D., Anderson, K., Wetherelt, A., Grand-Clement, E., Le-Feuvre, N., Smith, D. & Brazier, R. 2012. Understanding the structure of Exmoor's peatland ecosystems using laser-scanning technologies. EGU General Assembly Conference Abstracts.

- Luscombe, D., Anderson, K., Grand-Clement, E., Le-Feuvre, N., Smith, D. & Brazier, R. Assessing the ecohydrological status of a drained peatland: Combining thermal airborne imaging, laser scanning technologies and ground water monitoring. EGU General Assembly Conference Abstracts, 2012. 740.

- Luscombe, D., Anderson, K., Wetherelt, A., Grand-Clement, E., Smith, D. & Brazier, R. Monitoring Exmoor’s upland peatland systems using laser scanning technologies pre- and post-restoration. Earth Observation in a Changing world, 13th-15th September 2011 Bournemouth, UK. Remote Sensing and Photogrammetry Society.

# 2 Literature Review

This review aims to synthesise the current scientific literature as relevant to the study of blanket peatland systems, and to contextualise key terms, principles and theory concerned with understanding the ecohydrology of shallow, drained and marginal blanket peatlands. Given the differing nature of peatlands in the South West of the UK, and particularly those found on Exmoor, this review considers how the current understanding of peatland landscapes elsewhere in temperate zones may be applied to the shallower blanket peatlands studied here. Contextualising the peatlands in the South West of the UK with respect to their deeper more northerly equivalents is important in more fully understanding the ecological and hydrological processes operating in these systems, and how these relate to the important ecosystem services these landscapes provide.

## 2.1 Definitions of Peat

Peat soil is formed in waterlogged anaerobic conditions where the reduced decomposition rate of plant material leads to an *in-situ* build-up of plant detritus (Lindsay, 2010, Lindsay, 1995). The accumulation of the partially decomposed or un-decomposed remains of plant material gives rise to the high percentage of preserved organic matter which is the key component of peat soils (Evans and Warburton, 2010, Ingram, 1978). The classification of soils as peat is, accordingly, based on this relatively high organic matter content. Various conventions define this fraction at a variety of percentages from 30% to virtually 100% (Lindsay, 2010). However, Charman (2002) suggests a dry mass fraction of at least 65% organic matter as a suitable and commonly used fraction to characterise such soils. As the preserved organic material in these soils is a very high fraction of the dry mass, it follows that the soil material can inherit some textural properties from the parent vegetation (Ovenden, 1990). The degree of humification (i.e. decomposition into humus), also affects the textural properties of the peat and can occur as vertically stratified layers in response to a historic shift in the water logging, or changes in climate and therefore precipitation regime. The resulting soil texture can vary in both space, and over time, and can be described as amorphous granular (more humified), fine fibrous and course fibrous (less humified) (Hobbs, 1986). Typically the more fibrous the material, the lower the degree of humification (Evans and Warburton, 2010).

Humification rates can also vary spatially across the landscape, especially as a response to the drying out of the peat mass (Minkkinen and Laine, 1998).

## 2.2 Peatlands

Peatlands are a subset of wetland landscapes which are characterised by a living plant layer and accumulations of preserved organic matter as peat (Charman, 2002). These are commonly defined as landscapes where the dominant superficial deposits are peat soils in excess of 30-40 cm (Charman, 2002; Evans and Warburton, 2010). Peatlands are a global landscape constituent, occurring within many different biomes and with a huge topographic and latitudinal distribution (Joosten and Clarke, 2002).

### *2.2.1 Types of peatlands*

The term peatland can describe peat accumulations that are both actively forming peat, and those landscape elements that contain reserves or stores of peat deposited in the past. Any peatland that is still accumulating peat is termed a ‘mire’ (Joosten and Clarke, 2002). Bogs and fens are the two principal types of mire, with important abiotic and often biotic differentiation. In areas of the landscape where groundwater collects and leads to water logging, the resulting accumulation of peat is relatively minerotrophic, alkaline and supports “fen” or “geogenous” vegetation (i.e. marsh valerian *Valeriana uliginosa*, marsh pennywort *Hydrocotyle vulgaris*) and marsh orchids *Dactylorhiza majalis*) adapted to growing in these conditions (Lindsay, 1995, Joosten and Clarke, 2002). In areas where precipitation is great enough throughout the non-frozen part of the year, peat may accumulate beyond the level of the surrounding mineral groundwater in saturated conditions (Lindsay, 2010), forming a rain-fed and therefore relatively nutrient poor “ombrotrophic” peat system. Such a system is commonly termed a “bog” and supports its own suite of vegetation adapted to growing with low nutrient availability and in a relatively acidic environment. This vegetation is often dominated by bryophytes such as the *Sphagnum* spp. that contribute significantly to the accumulation of organic material, but also includes species such as cotton grasses (*Eriophorum* spp.) and insectivorous sundew (*Drosera* spp.) amongst many others (Rydin and Jeglum, 2013). Such ecosystems are now recognised for their important

biodiversity and are conservation priorities which are designated habitats of principal importance under Section 41 of the Natural Environment and Rural Communities (NERC) Act 2006 and UK Biodiversity Action Plan habitats.

### *2.2.2 Blanket mire complexes*

Peatlands in the UK contain both upland and lowland deposits and include both bog and fen peatland habitats. Data collated by Natural England (2010) suggests that of these peatlands upland mires are the largest in terms of spatial coverage and are dominated by mires occurring as blanket complexes (Figure 2.2). Blanket peatland complexes form over large areas of the ground surface where precipitation is sufficient to keep the soil saturated for much of the non-frozen part of the year (Lindsay, 2010, Moore and Bellamy, 1974). Blanket mire complexes are predominantly found in the upland and mountainous areas of the UK, principally in the West and North (van der Wal et al., 2011, Clark et al., 2010). As such, the peatlands of Exmoor, Dartmoor and Bodmin Moor in the South West of the UK are considered to be at the periphery of the bioclimatic envelope associated with these ecosystems (Gallego-Sala et al., 2010). Such blanket peatland systems often contain almost continuous peatland coverage over large areas and tend to be dominated by ombrotrophic (i.e. rain-fed, nutrient poor) systems, hence the common term “blanket bog” (Bragg and Tallis, 2001). However, blanket mire complexes generally contain a range of peatland ecohydrological units (Figure 2.1), including “bog” and “fen” types. For instance, they are likely to include areas of ombrotrophic mire, minerotrophic mire, non-peat forming organic deposits and associated transitional zones (Charman, 2002).

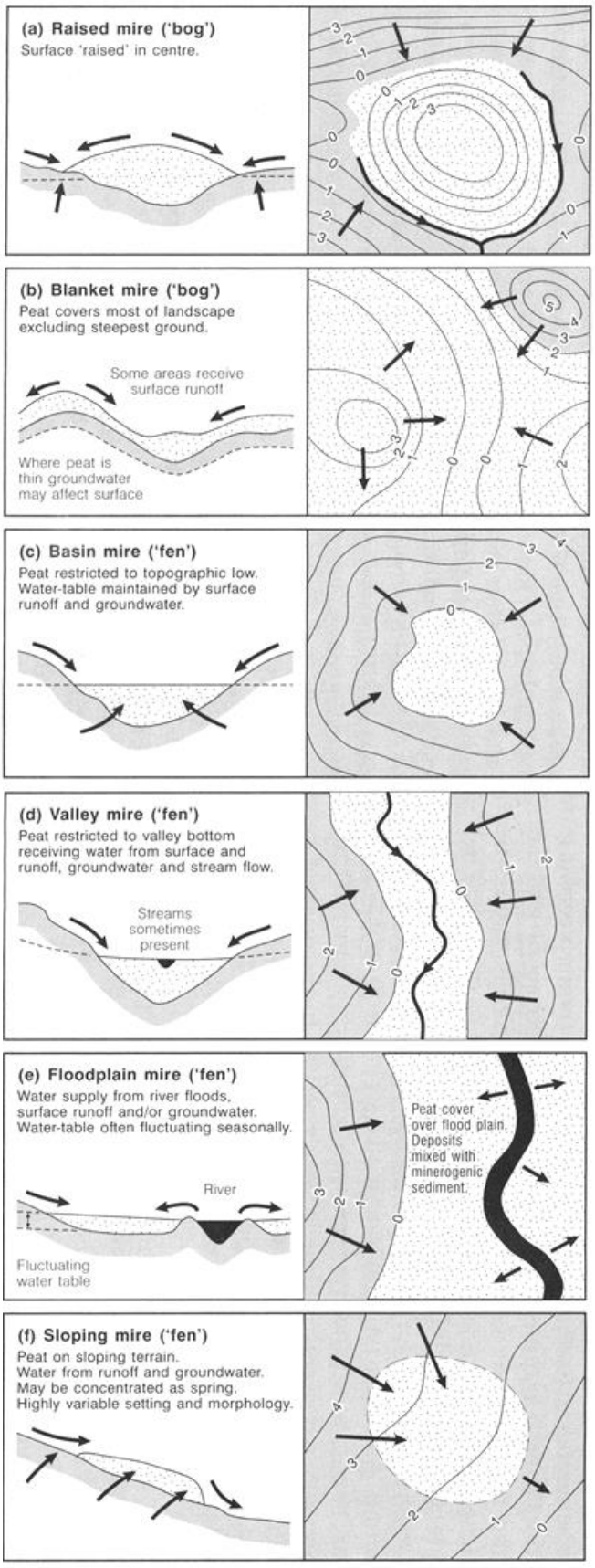


**Figure 2.1: The classification of key hydromorphological blanket mire units, from Charman (2002). These units are found throughout blanket peatlands, and combine together across landscape extents to form the blanket peat matrix.**

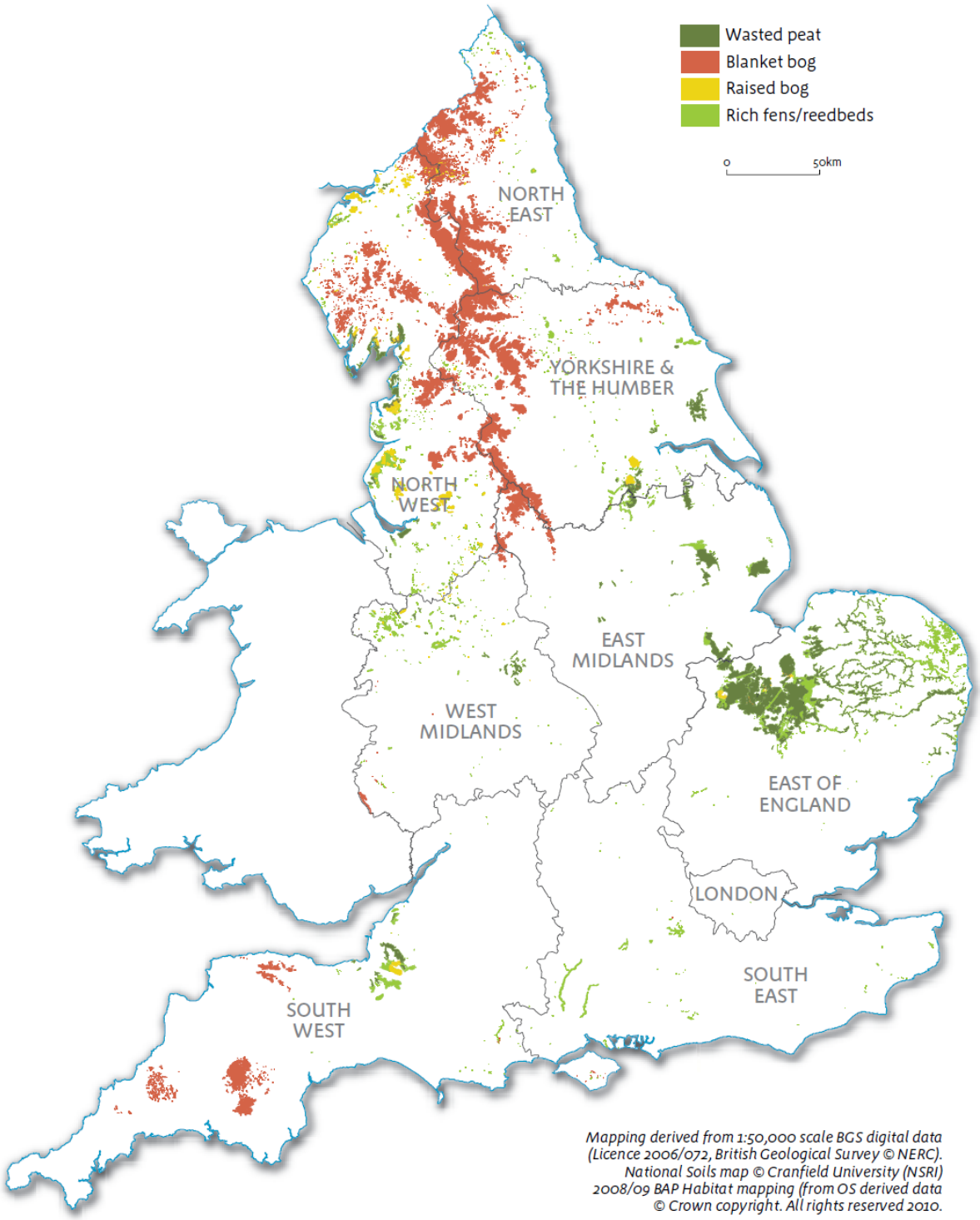


**Figure 2.2: The distribution of mire types in England, from Natural England (2010). The spatial distribution of blanket peatlands in England is seen to be concentrated in the north and west, with the blanket peatlands in the south west persisting at the southern extent of this distribution.**

Given the observable complexity in the organisation of these peatland landscapes, it can be considered that a combined hydro-morphological approach to the classification of blanket mire complex components is probably the only universally applicable and practical system for classifying such peatlands (Charman, 2002, Evans and Warburton, 2010, Lindsay, 1995). As water chemistry, vegetation structure and floristic composition are largely determined by the hydrology and morphology of the system (Daniels, 1978), this hydro-morphological classification describes most of the observable variation in peatland landscapes. A combined hydromorphological approach provides broad categories of mire and describes the shape of the peat deposit and underlying morphology, as well as the source and destination of water which accumulates within the system (Charman, 2002, Lindsay, 1995). Figure 2.1 defines the key hydromorphological mire types which occur within a blanket mire complex.

## 2.3 Ecology and microtopography - peatland structure and function

The structure and function of the ecological components of landscape systems has been shown to be critical in understanding the landscape processes governing their formation and persistence (Turnbull et al., 2008, Forman and Godron, 1981, Turner, 1989). This applies to a range of systems, including, but not limited to, peatlands. For example, changes in the type cover and spatial distribution of vegetation in semi-arid environments has been shown to lead to concomitant changes to erosion rates of soils, and properties such as bulk density and nutrient availability (Turnbull et al., 2008, Turnbull et al., 2010). Similarly in the sub-tropics large scale deforestation has been shown to have significant impacts on the hydrological regime of humid sub-tropical forest ecosystems, decreasing storage and increasing total runoff (Siriwardena et al., 2006). The feedback mechanisms associated with the interactions between biotic and abiotic landscape components may also explain the relationships between the heterogeneity in the distribution of landscape structures at a range of spatial scales (Turnbull et al., 2010).

In the case of mire landscape systems, many studies have identified that as the organic components of mire systems are so related to the availability of water, it is impossible to understand the ecology of these systems without considering their hydrological characteristics (Bragg, 2002, Morris et al., 2011). Specifically it is the close interdependence of water, soil and plants in peatlands that determines the characteristics of the system and its operation (Schumann and Joosten, 2008) (Figure 2.3).

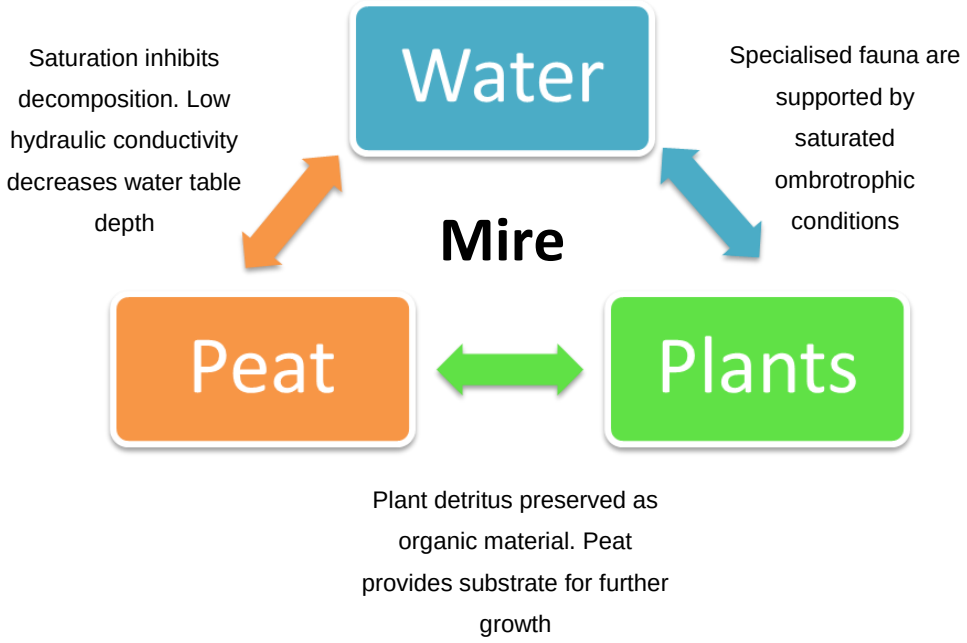


**Figure 2.3: A conceptual illustration of the implicit interrelations of biotic and abiotic mire components in the formation of mire systems.**

In order to understand the structure and function of upland blanket mire complexes at any spatial scale (i.e. plot scale, landscape scale) it is necessary to consider and characterise the ecohydrological structures present at a similarly appropriate spatial scale. In blanket peatland landscapes, characterising these structures hierarchically enables understanding of influence and response to functional systems and processes at a similar range of scales. The following sections consider these components, their scaling and their connectivity with the rest of the system.

### *2.3.1 Peat soil structure and accumulation*

Understanding the processes regulating peat accumulation in intact blanket mires is critical in understanding both the vegetation structure and the

morphological form of peatland systems. In an undisturbed peat bog that has developed naturally, the vegetation and soil structure can be considered as a system with distinct layers that contribute to the “growth” of the peat deposit and the fixing of atmospheric carbon as preserved plant detritus (Holden, 2005, Charman, 2002).

The soil layers present in intact mire systems are considered as distinct from those of mineral soils and are characterised by Ingram (1978) as a diplotelmic (or two layered) soil systems. In this conceptual model of a mature, intact peatland, the topmost layer in an ombrotrophic mire system is thin compared to the overall peat mass, varying from a few centimetres to over 75 cm (Lindsay, 2010). This layer is occupied by the living plant material and is often composed primarily of bryophytes such as the *Sphagnum* species. These organisms differ from higher plants by dying upwards from the base and therefore as they grow, they leave their remains below them, forming a loose and open structure of organic detritus (Lindsay, 2010). Sphagnum species, alongside other vascular plants growing in this region contribute to the *in-situ* accumulation of organic detritus and growth of the peat mass. This topmost layer is known as the **acrotelm** which is normally the zone of water table fluctuation in undamaged systems that are hydrologically intact (Lindsay, 1995, Ingram, 1978). This zone in which the water level may shift in response to seasonal shifts in evapotranspiration, and to precipitation events is also known as the zone of aeration.

Below the acrotelm is the remainder of the peat mass, this layer is termed the **catotelm** (Ingram, 1978). In the catotelm plant detritus is further decomposed/compressed and forms a denser structure with a higher overall bulk density (Charman, 2002). This layer is normally below the water table and therefore oxygen penetration, and is consequently primarily anaerobic (Lindsay, 1995). This layer is therefore less “active” than the acrotelm (Charman, 2002) with decomposition occurring at a slower rate, fuelling peat accumulation (Sjörs, 1948). It is this property of the peat that prevents the ongoing decomposition of the organic matter in an undamaged mire system and therefore facilitates the sequestration of carbon into storage as peat soil. Due to the decomposition of some of the peat mass over time this layer also exports some carbon as methane gas and dissolved organic carbon (DOC) in the soil water (Grand-

Clement et al., 2014, Strack et al., 2004). The storage and sequestration of carbon is described in more detail in section 2.5 and 2.6.1 as this process is an important ecosystem service associated with peatland function.

### *2.3.2 Microtopography*

This description of the acrotelm and catotelm structure of peat accumulation is necessarily simplistic. Vegetation community assemblages are also known to be highly related to the spatial heterogeneity in the hydrological characteristics of a mire surface, i.e. mean depth to water table and surface water availability (Pellerin et al., 2009). Consequently, over the spatial extent of the mire surface this dual layer structure will vary in its floristic composition and morphology. Over long (millennial) temporal scales, this in turn will ultimately lead to patterning of the peat surface and an irregular formation of peat soil, with a heterogeneous distribution of peat depths, vegetation assemblages, and open pools. (Belyea and Lancaster, 2002, Lindsay et al., 1988, Moore and Bellamy, 1974). The initiation and subsequent evolution of spatial patterning seen in peatlands is a consequence of multiple feedback mechanisms operating on existing fine grained heterogeneity in peat accumulation following external disturbance (Evans and Warburton, 2010, Belyea and Clymo, 2001, Belyea and Lancaster, 2002). The characteristic fine scale microtopographic variations present in such peatlands are the hummock/hollow structures found in intact blanket mire systems. This type of structure is a common indicator of intact ombrotrophic peatlands and forms the principle components of the larger scale patterning (Figure 2.4) that occurs across these systems (Couwenberg and Joosten, 2005).

Although over large (landscape) extents, the surface morphology of blanket mire systems can appear fairly homogeneous, over smaller extents the microtopography forms a heterogenic covering of water-filled hollows and drier raised hummock features (Figure 2.4). This microtopography is both a function of, and a control on the vegetation patterning found in these systems (Sjörs, 1948, Moore and Bellamy, 1974). Although *Sphagnum* species remain the backbone of the vegetation over both hummocks and hollows in most functionally intact bog systems (Lindsay, 1995), the species composition varies across the gradient in response to water availability. Indeed the type of

*Sphagnum* species found may even shift along this gradient in response to drier climatic conditions. The species of *Sphagnum* that tolerate driest soil moisture conditions (i.e. *Sphagnum imbricatum* and *Sphagnum rubellum*) are also more effective at binding water into their structure and subsequently such a shift in species composition toward these species can help maintain surface water-logging and prevent peat decomposition (Lindsay 1995). This gradient also supports the presence of heathland community outliers on the hummock tops and more sedge-dominated communities in the hollows (Lindsay, 2010). Other such examples of mire microforms are the presence of permanent pools, peat mounds and erosion features such as gullies and haggs (Evans and Warburton, 2010). However, it is unlikely that hummock/hollow features would persist in areas where such features have become established and water tables have subsequently lowered, and this is discussed further later in this review (section 2.6) (Lindsay, 1995, Woike et al., 1980).

### *2.3.3 Scale specific classification*

When examining mires at larger landscape scales, it is important to understand how the categorisation of the fine-grained variation in hydro-morphology (i.e. hummock-hollow), relates to the overall mire complex. Lindsay (1995) notes that mire complexes in the uplands occur where the mire units are present over a large area and are “fused” together to cloak the landscape. Within this fused landscape, the small-scale vegetation/morphology described above (i.e. hummock/hollow) can be termed a **Microtope.** In the overall mire complex, an area containing a distinct patterning of microtope, and with a single centre of peat formation (i.e. watershed mire) is termed a **mesotope** (Evans and Warburton, 2010, Lindsay, 2010, Lindsay, 1995, Lindsay et al., 1988). In this scaling the **macrotope** is the entire mire complex itself. It can also be noted that any structure identified within a microtope can also be termed a **Nanotope**, i.e. a hummock. Figure 2.4 illustrates the scale of the major topes within the landscape in more detail and how these may occur as a constituent of a blanket complex.

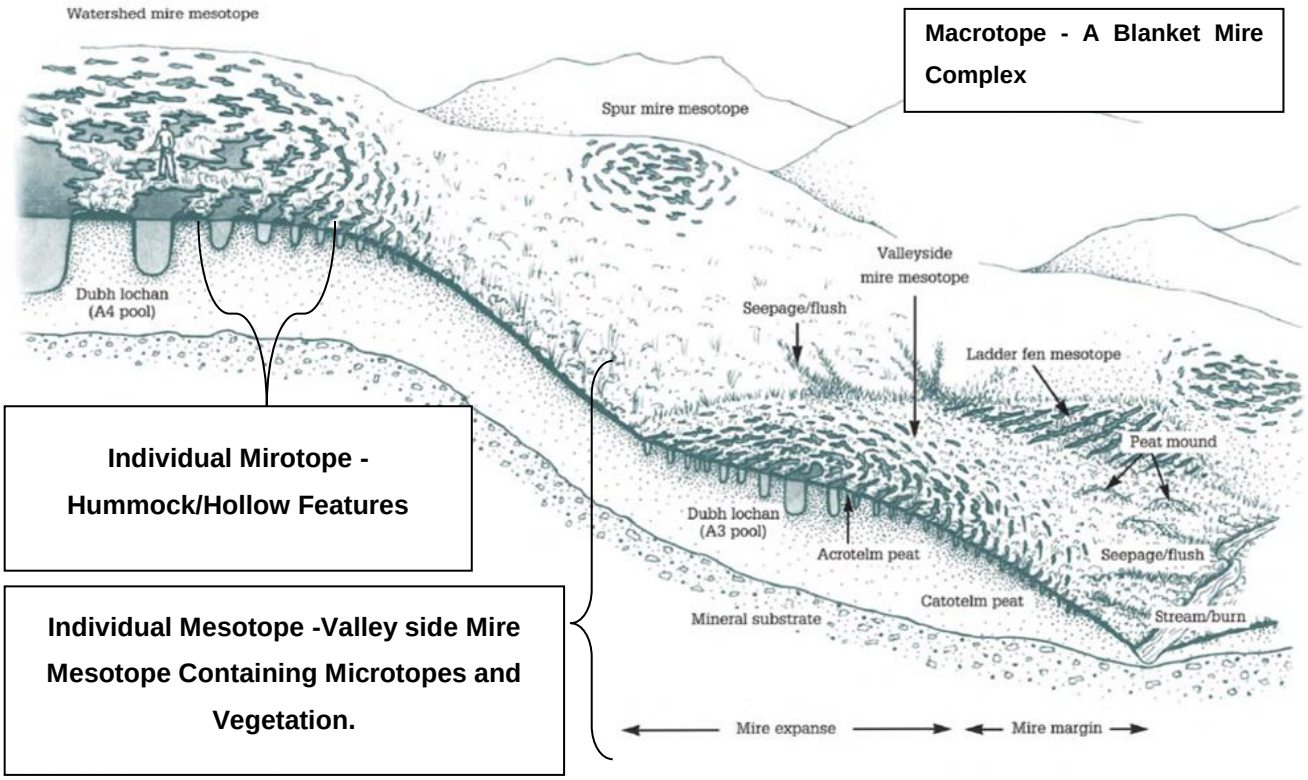


**Figure 2.4: The spatial hierarchy and scale of features in a blanket mire complex, from Lindsay (1995).**

## 2.4 Flow generation and hydrology

Upland blanket mire complexes provide significant hydrological inputs to the municipal water supply system in the UK (Worrall et al., 2007b) and are the headwaters of some of the UK's flashiest rivers (Holden et al., 2006). Ongoing pressures on anthropogenic water resources and the socio-economic implications of increased flood risk highlight the need to ensure the integrated catchment scale management of these systems (Grand-Clement et al., 2013, Vojinovic and Abbott, 2012). The following section summarises the key hydrological processes which regulate flow generation and storage in intact peatland systems. Section 2.6.2 goes on to discuss these processes further with respect to anthropogenically modified (i.e. drained and eroded) peatland systems.

### *2.4.1 Water retention in peatlands*

Peat soils have characteristics that Hobbs (1986) describes as both ordinary and extraordinary. The principal "extraordinary" property of peat is its ability to

hold large quantities of water, varying from about 200% to >2000% of its dry weight (Evans and Warburton, 2010), and as a consequence peat is highly compressible, and can increase in density under load. However, the material can behave similarly to consolidated clay (i.e. “ordinarily”) and possess significant shear strength despite its wet mass being largely composed of water (Hobbs, 1986). Much of this water is held as intra-cellular and intra-particle water and, therefore, increased water logging does not necessarily dictate a reduction in the mechanical strength of the material (Evans and Warburton, 2010). The fibrous nature of the material is key to this strength due to its reinforcing effects under stress (Hobbs 1986). These characteristics mean that intact mires with high water tables are theoretically more robust and resistant to mechanical load bearing than the composition of the soil mass may suggest. As less humified peats retain more cell structures and fibrous material, it follows that shear strength will decrease with the humification of the organic material. Consequently, it may be expected that damaged or drained peatlands, with higher humification rates, could be more susceptible to erosion and gullying, as discussed later in section 2.6. This susceptibility to damage has important implications to the management of degraded peatlands, including the intensity of livestock grazing which such a system may be able to support without significant erosion (Stewart and Lance, 1991, Wilson et al., 2011c). For example, periodically or permanently rewet degraded peatlands may not be able to support stocking densities as high as those in intact systems without the risk of damaging the mire surface further.

### *2.4.2 Hydraulic conductivity*

As well as determining some of its physical characteristics, the amount of water contained within the soil matrix also has considerable effects on the hydrological processes operating within the soil. Hydrologically, the key physical property of intact peat soil is its variable hydraulic conductivity (Evans and Warburton, 2010), and particularly its relationship with humification. Although peat forms in areas where the water table is at or near the surface, as a function of high precipitation and low evapotranspiration, its relatively low hydraulic conductivity at depth also helps the water table to persist at higher levels and encourage peat formation (Ise et al., 2008).

The hydraulic conductivity in the acrotelm is typically high due to the presence of a less consolidated structure of vegetation and detritus. Although this drops off rapidly with depth, high conductivity is why this region of the soil profile experiences high water table (and therefore oxygen) flux compared to the catotelm, and why the initial rapid decomposition of the vegetation can occur prior to the collapse of this matrix (Evans and Warburton, 2010, Ingram, 1978). As the organic material in peat becomes more humified the pore space found within the soil matrix decreases and bulk density increases, consequently both water content and hydraulic conductivity decrease proportionately (Evans and Warburton, 2010). However, as peat is also compressible independently of humification, increased loadings can also decrease the level of hydraulic conductivity (Holden and Burt, 2003a) and therefore compound or mirror the effect of humification. Such loading can even be from the head of water itself, which may apply a significant pressure, in deeper peatlands, further compressing the peat matrix.

### *2.4.3 Ground water flow pathways*

Ground water flow patterns in intact peatlands are largely controlled by the vertical and lateral hydraulic conductivity of the soil. Generally it is perceived that the flow in peat is diffuse and therefore limited by the hydraulic gradient and variation in hydraulic conductivity (Evans and Warburton, 2010). Given this, the spatial heterogeneity previously discussed in peat humification (section 2.1) can have a significant effect on the routing of this flow within the peat mass (Morris et al., 2011).

The patterns of groundwater flow in peatlands are normally considered to be parallel to the surface (Evans and Warburton, 2010) due to increased conductivity in these directions (i.e. within strata, Figure 2.5). The diplotelmic structure of the soil strata also creates variations in the relative speed with which ground water flow occurs within the soil profile. For example, although acrotelm through-flow is more rapid than deep (catotelm) through-flow, water loss via macropore can result in extremely high deep groundwater velocities following rainfall, where such structures occur (Holden and Burt, 2003a, Holden and Burt, 2003b, Holden et al., 2011).

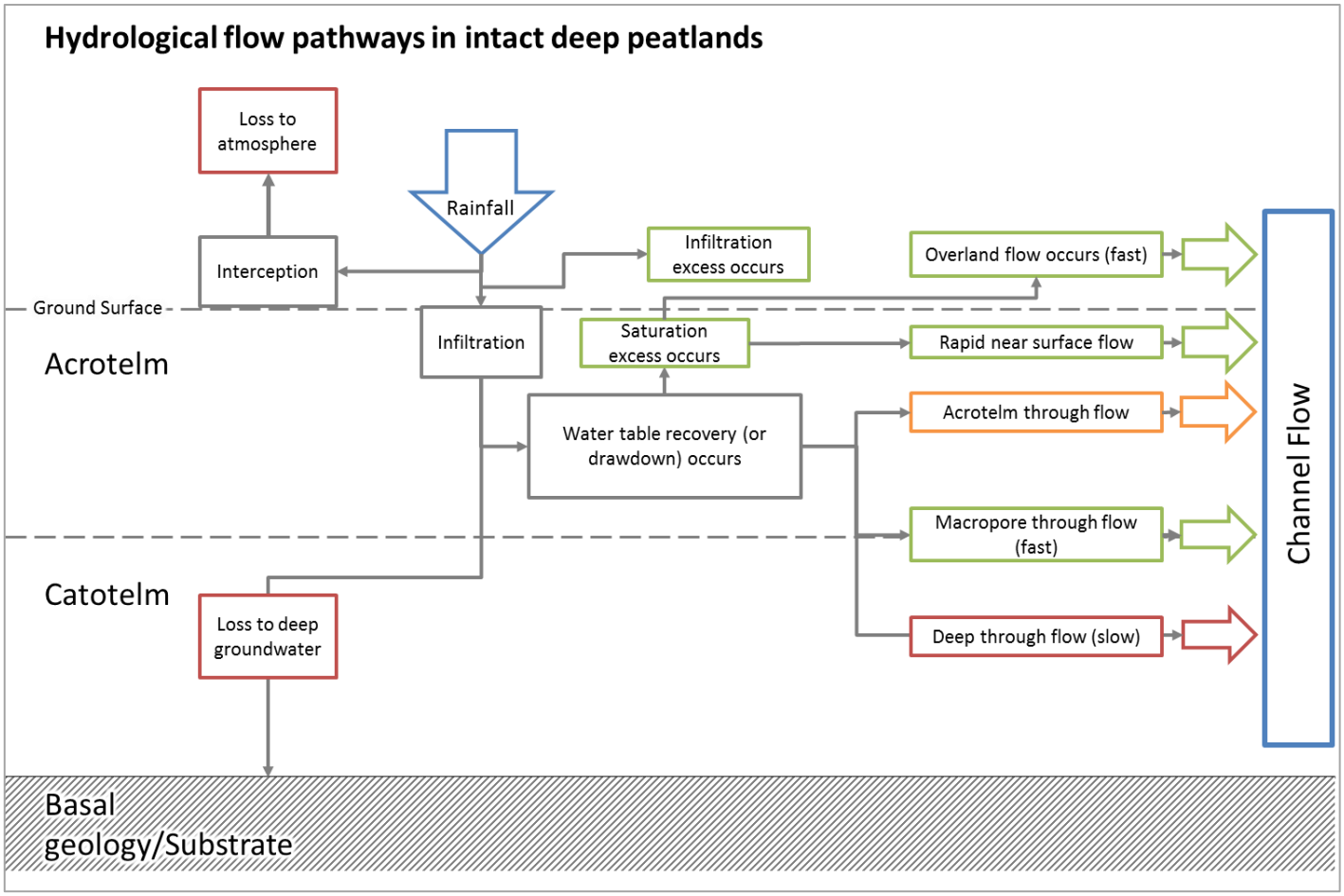


**Figure 2.5: Hydrological flow pathways in intact deep peatland systems. The relative speed of the pathway is highlighted by the colour of the box. Green corresponds to faster pathways and orange and red to slower pathways.**

There is also some evidence that, in drought conditions, vertical movement of ground water in peat can help to recharge the surface layers (Fraser et al., 2001) maintaining water availability and increasing the availability of nutrients to the acrotelm (Fraser et al., 2001). Generally, the relatively low hydraulic conductivity in the catotelm peat means deep ground water flow in intact peatland systems is low and water table levels are well maintained. As a result, intact peatland systems can actually be relatively poor at maintaining significant base flow during periods of no rainfall where acrotelm through-flow is exhausted (Holden, 2005).

### *2.4.4 Rainfall-runoff pathways*

The high water table of peatlands is important in determining the hydrological response of this type of landscape to precipitation events. Intact, upland ombrotrophic mire complexes, are often (mistakenly) perceived as having the ability to significantly attenuate peak flow in storm events by buffering the discharge of water as an “absorbent system” (Holden, 2005). However, intact mire systems have a high water table, as defined above, and low hydraulic conductivity at depth. Such systems therefore, could be considered poor at regulating flow as saturation excess can quickly lead to rapid near surface flow (Figure 2.5). Indeed, during storm events Grayson et al. (2010) demonstrated that the ability of the vegetated peat to absorb rainfall can be poor and give rise to extensive saturation excess overland which is often the predominant discharge from such systems (Charman, 2002).

It is the case however, that intact *Sphagnum* rich peatlands offer some level of buffer compared to a eroded peatland surface (Grayson et al., 2010), due to the relatively high hydraulic conductivity of the thin acrotelm (which is also the area facilitating the most near surface runoff), and the physical storage of water in the surface microtopography (Charman, 2002, Moore and Bellamy, 1974, Ingram, 1978). The extent to which this buffering is effective is often largely dependent on preceding dry conditions and therefore volumetric capacity of such features (Charman, 2002, Holden, 2005, Evans et al., 1999, Daniels et al., 2008). It is partly the loss of these structures via drainage and peat decomposition that can account for the increased flashiness (i.e. rapid rainfall runoff) in damaged peatland systems, as will be discussed later.

The presence of soil pipes or macropores in the soil matrix is a common feature of UK blanket peatlands (Charman, 2002). These are generally considered more common in drained systems (Holden et al., 2006b) and can account for between 10% and 23% of the overall runoff in intense rainfall events compared to around 1% in intact systems (Charman, 2002, Holden et al., 2006b). The effect of peatland drainage is discussed further in section 2.6, however, this type of feature consequently has important compounding effects on the increased discharge peak of drained systems. The persistence of these features following hydrological restoration also has the ability to limit the

effectiveness of efforts to fully rewet the peat mass with the use of surface drain blocks.

The complex processes regulating the generation of flow in these systems can, therefore, be seen to present challenges to those studying these landscapes, as both intact and damaged systems may prove to exhibit extremely flashy runoff regimes. The effects of peatland drainage are more fully discussed in section 2.6.2. In the peatlands studied in this thesis, the shallower and often degraded nature of the peat deposit also poses questions as to the flow response that may be expected in either an intact or damaged state.

## 2.5 Carbon storage and sequestration

Peatlands are known to store around 15-30% of the world's soil carbon (Limpens et al., 2008). Studies suggest that peatlands (including bogs and fens) are the UK's largest terrestrial carbon store (Cannell et al., 1993, Bellamy et al., 2005). Lindsay (2010) suggests a minimum estimate for the total UK terrestrial store at ca. 3121 Mt of carbon. However, the complexities of characterising the depth, extent and bulk density of this soil resource means that the exact quantification of this store has not yet been obtained, and consequently estimates vary considerably (Lindsay, 2010). Some total estimates are as high as 7814 Mt of carbon (Bradley et al., 2005) highlighting the uncertainty in these data. Uncertainty in these estimations of carbon storage have important implications for the value of this landscape resource in managing future climate change. Recent work from Natural England (2010) has brought together findings from a range of locations in the UK to give an estimate of the carbon content of peat soils in England. These data are summarised in Table 2.1 and illustrate that upland blanket mire complexes specifically, may represent the largest terrestrial carbon store not under intensive agricultural production. It should be noted that the error implicit in these data are large and they therefore only form an initial indicator of total storage. However, carbon stored in these uplands is clearly very considerable and of high importance in contributing toward the understanding and management of anthropogenic climate change. As is the case for the Exmoor peatlands considered in this study, the ecosystem services associated with this carbon store have important economic and environmental implications for those charged with the stewardship of these

upland landscapes, including landowners and National Park authorities (Grand-Clement et al., 2013).

**Table 2.1: Estimated total carbon stored in England's deep and shallow peaty soils (tonnes C), from Natural England (2010).**

| Peatland Type. Megatonnes Carbon. | Megatonnes Carbon | % of total peatland carbon |
|---|---|---|
| Blanket bog and Upland Valley Mire | 138 | 24 % |
| Raised bog | 57.5 | 10 % |
| Lowland Fen (deep) | 144 | 25 % |
| Lowland Fen (wasted) | 186.4 | 32 % |
| Shallow Peaty Soils | 58.5 | 10 % |
| All Deep and Shallow Peaty Soils | 584.4 | |

## 2.6 Peatland degradation and drainage

Peatlands in a "pristine" state are now very rare both nationally and globally. Data from the IUCN peatland program suggest that only ca. 1.25% of blanket bog in England is in an undamaged and peat forming state (Reed et al., 2009). Historically, such landscapes have been exploited for both fuel and agricultural reclamation (Holden et al., 2006a, Holden et al., 2006b). Peatlands exploited to provide such additional services have historically been altered with little evidence for the success of the intervention, or without a reasoned or evaluated appreciation of the wider effects of such works (Wilson et al., 2010, Holden et al., 2004). These interventions typically attempt to alter the landscape structures to achieve the desired change in the landscape function or to access a specific resource (i.e. fuel). Critically, the changes to the landscape processes have both direct and indirect influences on wider ecological and hydrological processes operating in these landscape systems, and it is these effects that are highlighted here.

Key examples of such anthropogenic interventions in upland mire complexes involve the use of drainage ditches or "grips" to lower the water table with the hope of improving the grazing for increased livestock densities (Wilson et al.,

2010, Holden et al., 2004). Such “reclamation” may also involve the ploughing of the surface and/or chemical treatments such as “liming” to improve soil fertility or increase pH (Charman, 2002). Given the relatively low hydraulic conductivity of peat soils (Ise et al., 2008), the network of drainage ditches implemented to achieve a significant drop in water tables has to be at regular intervals and of a sufficient density. This means that such features often occur as frequently as every 4 metres (Holden et al., 2004) in highly humified peatlands with low hydraulic conductivity. As well as draining the peat surface, such ditches are often designed to intersect or optimise existing flow lines in order to reduce the residence time of rainfall and enhance run-off rates. The effects of such drainage are discussed further in section 2.6.2. However, it is widely acknowledged that such interventions have caused lasting change to the ecohydrological structure and function of these landscapes, without delivering increases in productivity (Holden et al., 2006b, Allott et al., 2009, Stewart and Lance, 1991, Wilson et al., 2011c). As discussed further in section 2.8, understanding the nature of such drainage is challenging and requires monitoring prior to and following any management interventions to understand any associated change appropriately (Holden et al., 2004).

The long term effect of this drainage on the soil/groundwater characteristics is significant and often persistent. In intact and deep peat systems water tables are predominantly in the top 20 cm, however in a degraded system they are often as low as, or even below, 50 cm (Holden et al., 2004, Wilson et al., 2011b). This periodically drier zone therefore has the opportunity to become more degraded via aerobic (and therefore faster) decomposition, and therefore progressively more humified. As degraded systems often exhibit peat that is more humified and with increased bulk density near to the surface (Holden et al., 2004), the hydraulic conductivity of the soil in this area may also be further reduced. In shallow peatlands, such as those in Exmoor, the thinner peat deposits may therefore be more prone to such humification throughout their entire depth, raising important questions as to the potential of restoration on ‘rewetting’ these soils.

The removal of the peat soil as a resource or fuel is typically not undertaken in order to change the hydrological functioning of the landscape, however the depressions left in the landscape may still alter the drainage and runoff

processes in the longer-term. The exploitation of peatlands for fuel, i.e. the use of dried peat as a combustible fuel, has taken place at a range of scales over many thousands of years (Holden et al., 2004, Wilson et al., 2010). Peat fuel extraction for subsistence, often involving hand cut peat blocks dried in small stacks for personal use in the home still continues in some parts of the UK and Ireland on small scales. Although not a sustainable practice (i.e. the extraction still exceeds accumulation) this method often occurs at a slow enough rate that the soil surface that has been damaged remains predominantly vegetated limiting further mechanical or classical erosion seen in some UK upland peatlands (Pawson et al., 2012). Because such cuttings are not typically connected to wider drainage networks (natural or otherwise) they may not have such a significant effect on the overall water table. Peat extraction also occurs on an industrial scale, and has accounted for some of the most significant peat loss to date (Tomlinson, 2010). Peat extracted commercially has been/is used both as a fuel and as a horticultural product. In such extraction, the peat is often cut mechanically and at a rate that leaves large areas of “cutover” bare peat. This remaining surface is then unstable and can suffer from further loss of peat mass via erosion (Evans and Warburton, 2010).

### *2.6.1 Effects of peatland drainage on carbon storage*

The ability of peatlands to sequester carbon is low compared to the total amount stored. Evidence suggests sequestration rates at ca. 21g $m^{-2}$ $yr^{-1}$ (Anderson, 2002) compared to storage capacity of around 100kg $m^{-2}$ $yr^{-1}$ (based on an average peat depth of ca. 2 m, and ca. 50 kg per $m^3$) (Lindsay, 2010). However, as these systems would very rarely equilibrate in terms of carbon emission/sequestration, it is important that the state of mires as carbon sinks is maintained in order to prevent these landscapes evolving into carbon sources. In addition, over the last decade the concentration of dissolved organic carbon (DOC) in stream flows from upland catchments in the UK has increased by more than 60% (Freeman et al., 2001). This is likely to be both a consequence of climatic warming, and a process that will provide positive feedback to warming via the liberation of further greenhouse gasses from terrestrial storage. The land management of upland peat catchments is also known to have major effects on the amount of carbon released (Yallop and Clutterbuck, 2009). For example, studies show that the annual increase in DOC release due to climatic

shifts will be enhanced in drained catchments from an average of 3% to over 15% (Worrall et al., 2007c). The production of DOC is known to be greater in drained landscapes than intact landscapes (Wallage et al., 2006). This is because highly humified peat deposits, such as those found in drained landscapes are known to release more carbon into solution (Kalbitz and Geyer, 2002). It is also known that the regime of land management by burning can significantly increase carbon export from deep peats (Yallop and Clutterbuck, 2009), due to changes in its mobilisation.

### *2.6.2 Effects on hydrological function*

The connections between the biotic and abiotic components of peatlands are known to provide significant feedbacks between hydrological processes at a range of spatial and temporal scales (Belyea and Lancaster, 2002, Lindsay et al., 1988, Moore and Bellamy, 1974). Land management strategies which modify any such component can therefore have complex effects on hydrological function. For example, activities such as the grazing and burning of blanket peat vegetation is known to effect hydrology, with water tables left nearer the surface after regular burning events and grazing, as a consequence of changing vegetation and soil compaction (Worrall et al., 2007a).

Similarly, the complexities of the effects of drainage in peatland systems give rise to conflicting processes governing the rate of discharge and the amount of system storage (Holden et al., 2004). For example, in a drained system, surface water is known to be less common within ca. 2 m of artificial drainage features and water tables lower up to around 5 m of these features (Wilson et al., 2010, Holden et al., 2004). The effect of such drainage on the rainfall-runoff pathways in drained peatlands is often both profound and complex (Holden et al., 2004, Holden et al., 2006b). For example, lower water tables following drainage may increase the amount of temporary storage available via infiltration and therefore limit saturation excess flow and lower the discharge peak (Figure 2.6) at the catchment outlet. However, the presence of drainage also makes the discharge network more connected and/or shorter, increasing the discharge peak and reducing the lag times between peak rainfall and peak flow (Wilson et al., 2011b, Wilson et al., 2010, Goulsbra et al., 2014). The humification of peat solid following drainage can also significantly increase the occurrence of macropore

structures (Figure 2.5) and concomitantly, rapid macropore through-flow can become a dominant runoff pathway (Holden, 2005).

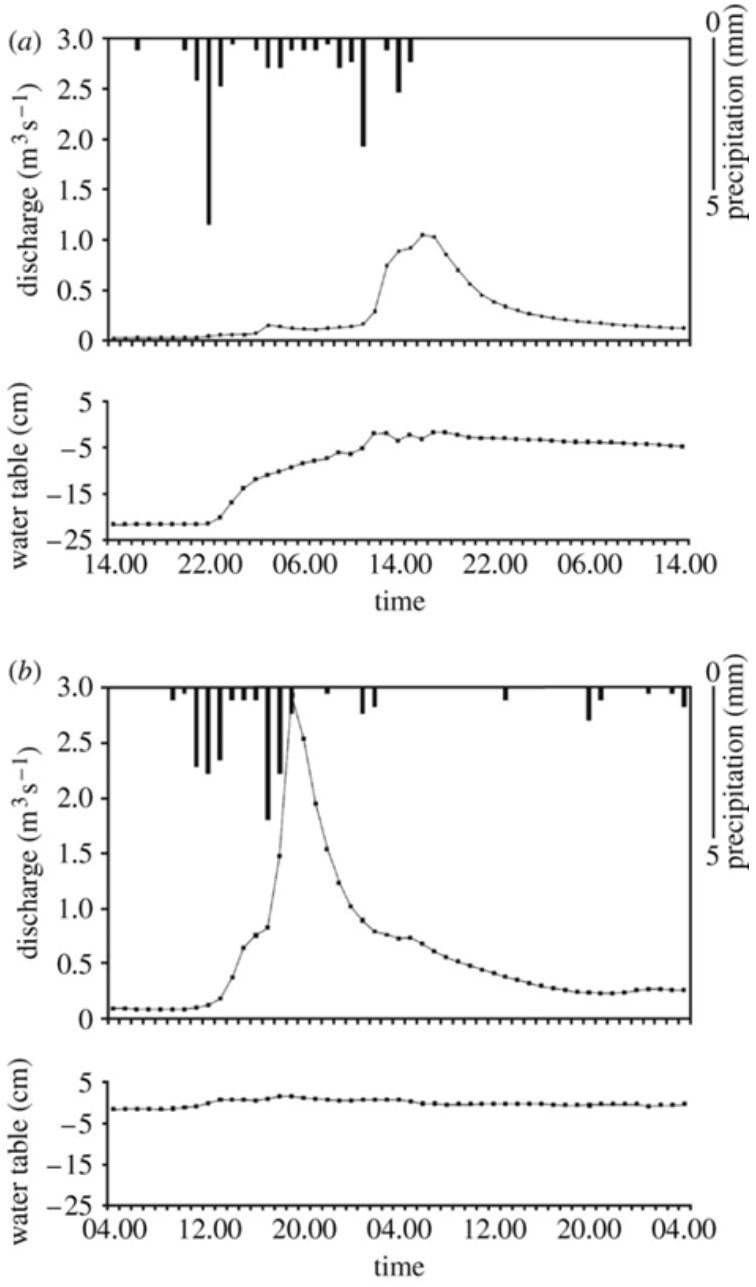


**Figure 2.6: Hydrographs and water-table data from two storms in the Trout Beck catchment; (a) 6 July 1995, (b) 22 May 1996, from Holden (2005).**

In the UK, studies suggest blanket mires are most effective at delaying runoff and preventing the loss of soil and nutrients when they are un-drained (Bragg, 2002, Wilson et al., 2011a, Wilson et al., 2010). The complex relationships in the production of stream flow and the lowering of water tables means that the

exact nature of drainage, and the thickness and vegetation of the peat deposit will markedly change the effects of drainage from site to site. Recent studies have described these types of relationships in deeper peatlands in the north of England (Holden et al., 2006b, Dixon et al., 2013, Allott et al., 2014) and north Wales (Wilson et al., 2010, Wilson et al., 2011a, Wilson et al., 2011b), although similar studies in shallow and bioclimatically marginal peatlands are lacking. Holden et al. (2006b) defines that in a comparative study of analogous drained/undamaged catchments (within the Moor House National Nature Reserve the North Pennines, UK); the drained site had a narrower hydrograph with a steeper rising limb in response to rainfall (Figure 2.7). Similar results are also described by (Wilson et al., 2010), again in deeper peatland systems, where surface drainage has increased the surface connectivity of the system. The effect is also known to persist in the landscape, with examples showing an endurance in excess of 50 years in unrestored peatlands (Holden et al., 2006b). As yet, no such work has been conducted on the shallower peatlands of the South West UK, which has important implications for the funding of schemes which look to modify such runoff characteristics as part of landscape wide rewetting initiatives. Quantifying these hydrological processes in light of the wider literature is therefore an important objective of this research.

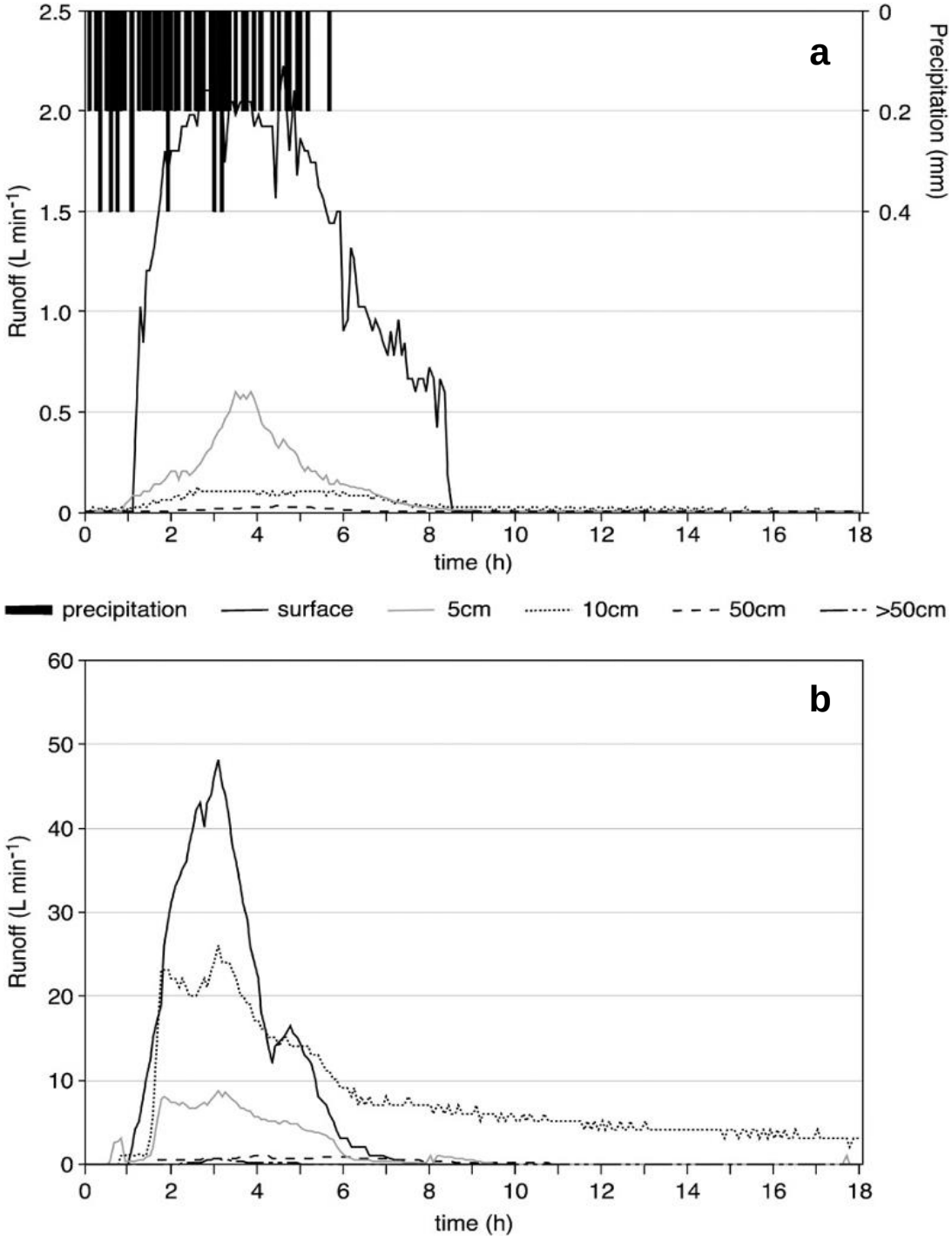


**Figure 2.7: Runoff from automated plots during a storm event 28 Feb. 2003 to 1 Mar. 2004, rainfall and runoff data collected in 5 min intervals: (a) Intact catchment L, (b) Drained catchment S. runoff volumes at the intact catchment plot were greater at the drained plot because the upslope contributing area was larger in the intact catchment since it was not intercepted by drains. Therefore, different y-axes scales are used for (a) and (b), from Holden (2006).**

The timing of flows within these landscapes also has effects on the peak discharge observed. Holden et al. (2004) collated findings from studies dating back to the 1960s in order to examine findings contradictorily describing intact

peatlands producing flashier hydrographs than drained analogues. The scale of the monitoring within these catchments appears to be crucial to these findings. Specifically Holden et al. (2004) suggest that changes in the hill slope scale drainage efficiency, can lead to changes in the synchronisation of flows at the catchment scale, potentially decreasing the overall catchment peak discharge in a drained landscape. Similar results were observed by Goulsbra et al. (2014) where drainage network expansion was observed to be dynamic throughout rainfall events, with concomitant step changes in the relative drainage densities, in a given contributing area. These findings suggest that the spatial and structural characterisation of drained peatlands is critical in predicting and understanding the effect of drainage or restoration in the wider catchment.

The quantification of these effects in the thinner peatlands of South West England is not described in the current literature. Similarly, the number of studies on such effects is limited; particularly with respect to pre-restoration monitoring data, which is lacking from many studies (Bragg and Tallis, 2001, Holden et al., 2004, Holden et al., 2011, Parry et al., 2014). Further research is therefore needed in order to understand the processes regulating these dynamics, across multiple peatland types (including thinner, marginal peatlands) and at multiple locations within each peatland type, at fine spatial scales (Holden, 2005). This would allow the influence of spatial variability of both peatland properties and drainage practices on hydrological processes to be understood and quantified for the first time.

### *2.6.3 Effects on ecological function*

As described previously, vegetation composition and structure shift in response to changes in the hydrological function of peatlands (Lindsay, 1995). The maintenance of the diversity and composition of species in intact blanket mire complexes is known to be a key conservation objective (Natural England, 2010). In blanket mires, vegetation also supports specific species of fauna important to conservation and are a priority habitat under Section 41 of the NERC Act 2006. The British Isles also holds about 10 -15% of the global resource (Wilson et al., 2010) making their preservation an important national conservation objective.

In areas extensively exploited for peat products (e.g. where the peatland surface is cut over) or subject to excessive erosion, the remaining landform may be entirely devoid of vegetation with bare peat exposed at the surface or in gullies (Evans et al., 2005, Rothwell et al., 2005). Evidence confirms that reduced vegetation cover aids runoff, narrows flood hydrographs and increases mean peak storm discharge compared to re-vegetated landscapes (Grayson et al., 2010). The loss or weakening of the vegetation layer can also accelerate the formation of erosion landforms such as gullies (Evans and Warburton, 2010, Pawson et al., 2012) and expedite the loss of DOC/POC from the site as it is transported in runoff (Pawson et al., 2012, Goulsbra et al., 2011, Goulsbra et al., 2012). However, as features such as gullies in drained landscapes can also be responsible for the stripping of vegetation along their flow path (Evans and Warburton, 2010), understanding the dynamics of these systems (e.g. feedbacks between vegetation loss and erosion) is important in interpreting a damaged area. It is also interesting to note that where drainage is implemented on shallower slopes (<4 degrees) anthropogenic drainage ditches have been shown to re-vegetate naturally, mitigating some particulate loss of carbon (Holden et al., 2007a).

Studies also highlight the effects of a drop in water tables on vegetation characteristics. The change in vegetation community composition has been shown to shift along a gradient from ‘wet bog’ species (dominated by species of *Sphagnum)* toward ‘wet heath’ species (e.g. *Erica tetralix*) as a direct response to a loss of surface water and lower water tables (Pellerin et al., 2009). This change in species composition is also evident in the degradation of the surface patterning in damaged peatlands, and an increase in the patch size of the vegetation structure (Anderson et al., 2009, Lindsay, 1995, Lindsay et al., 1988). As a result, observation of vegetation structure and composition form good proxies for gauging the hydrological condition of blanket mires. Furthermore, because these variables may be directly monitored from remote sensing data, this may provide a route for spatial extrapolation of hydrological understanding to the entire peatland extent. However such spatial analysis of peatland ecological structure is lacking from the current literature, despite recent advances in technologies that could support acquisition of relevant data (e.g. LiDAR).

## 2.7 Restoration and land management

Natural England (2010) estimate that only 1% of England's peatlands remain undamaged, and given the prevalence of drained peatlands in the UK there is an increasing focus on their restoration to limit or mitigate these deleterious effects (Wilson et al., 2010, Wallage et al., 2006). However, the term restoration perhaps misleadingly implies the treatment of these landscapes and eventual return to a natural or pseudo-natural structure and functioning. As suggested in previous sections, there is a growing body of scientific evidence that suggests that some properties of damaged systems such as increased bulk density and lower hydraulic conductivity may persist in a restored system (Holden et al., 2004). As such, the goals of restoration may not be to return the landscape to its natural state, rather a state which functions in a manner that maximises ecosystem services (i.e. carbon storage, flood attenuation and biodiversity conservation). For example, restoring the function of the landscape as an overall carbon sink and area of high biodiversity is likely to be a more suitable target that can deliver important societal and environmental benefits via the associated ecosystem services.

### *2.7.1 Ecohydrological restoration*

Most of the targeted ecosystem services desired from restored peatlands are dependent on the reinstatement of a high water table (i.e. biodiversity conversation, carbon storage and water quality improvements) (Wilson et al., 2010). Consequently the removal or blocking of anthropogenic drainage features or drainage features initiated by anthropogenic activity (i.e. erosion following burning) from these landscapes is the primary aim of restoration work. Most restoration techniques in drained upland peatland systems utilise ditch-blocking techniques in order to raise water table levels, prevent stream flow in drains, and decrease the energy in the drainage system (Bain et al., 2011). The blocking of ditches may be achieved through a variety of techniques including peat dams, plastic pile dams, heather bales and wooden dams (Evans et al., 2005). However, some evidence suggests that there are no significant differences in the effect on water table depth and DOC load between these

techniques following restoration (Worrall et al., 2007b). Figure 2.8 demonstrates the type of ditch block employed in larger drainage features in Exmoor peatlands, however smaller blocks may employ any one of these materials (peat blocks, heather bales, wooden dams).

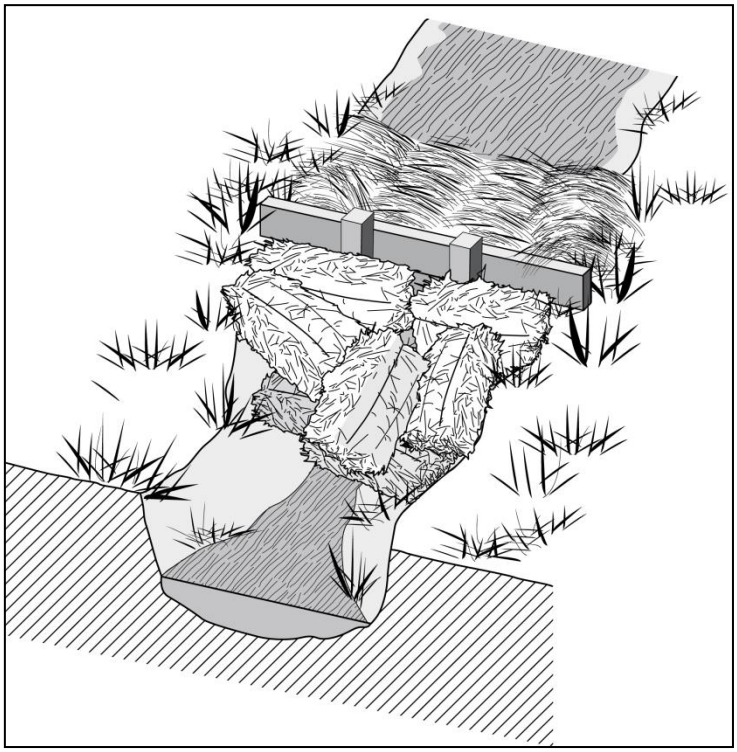

**Figure 2.8: An example of a combination ditch block in a large anthropogenic drainage feature incised into the peat mass.**

Landscapes restored using ditch blocking techniques are known to increase the residence time of water in the system as a consequence of a decrease in the efficiency of the drainage network (Wilson et al., 2010). The system is then less erosive, and the formation of pools behind such features can allow the re-growth of bog vegetation in an analogue of the microtopography found in intact systems. In deeper peatlands, the blocking of ditches and gullies has also been shown to significantly reduce active erosion and fluvial sediment loads (Martin-Ortega et al., 2014). The re-establishment of high water tables is proven to increase the growth of *Sphagnum* species, however, the resulting species are not of the same species assemblages as intact sites and this may limit the speed of the formation of hummock/hollow type topography (Rochefort et al., 2002).

In some studies, the dry zone around drainage features is shown to be reduced or completely removed post restoration and surface waters more common (ca. 40%) (Wilson et al., 2010, Worrall et al., 2007b). Additionally, there is evidence that water table stability is improved during the summer months suggesting an increased ability of the peat to store water within the soil matrix (Wilson et al., 2010). However, the period of recovery of water tables in such landscapes may take longer than a year (Wilson et al., 2010, Holden et al., 2004) and the time and extent of restoration may be dependent on the scale of the damage, and the specific characteristics of the peat mass. For example, around larger drainage features, in areas subject to significant compression or in areas where humification is more advanced throughout the peat mass, the resulting hydraulic conductivity may be so low that the rewetting of the peat mass may take a long (and unknown) period of time. Although a decrease in the depth to water table associated with restoration may conceivably decrease the water storage potential of the catchment, evidence suggests that reducing the peak flows of the system and attenuating the hydrograph shape is still often achieved post restoration (Wilson et al., 2010, Holden and Burt, 2003a, Wilson et al., 2011a). This is likely to be a consequence of the reduced (but not removed) connectivity of the drainage network and a more diffuse flow over the peat surface/through the acrotelm. Although this has important implications for the use of such techniques in catchment scale management of water quantity and quality, without ecosystem specific hydrological monitoring the inference of such results is subject to significant and unquantified uncertainties.

Organic Carbon is often lost from drained and eroding peatland systems as a fluvial particulate load (POC), following the surface and gully erosion of blanket peatlands (Pawson et al., 2012, Goulsbra et al., 2011). Again, evidence suggests that the implementation of ditch and gully blocking to rewet the adjacent peat soil is effective at reducing particulate carbon loss through fluvial suspended sediment (Martin-Ortega et al., 2014). The export of dissolved organic carbon (DOC) from peat is also known to be higher in degraded peatlands as a consequence of a higher level of organic decomposition and humification (Wallage et al., 2006). Evidence suggests that drain blocked peat produces lower DOC concentrations than even intact sites (Wallage et al., 2006). This indicates that the use of restoration techniques such as drain

blocking could go some way in mitigating the annual increase in DOC release due to climatic shifts. Changes in chemical composition of the carbon in solution post restoration are shown to result in more humic acids being flushed from the rewet and humified peat mass, and therefore a higher colour per unit carbon ratio (Wallage et al., 2006) and darker overall water colouration in the shorter term (Worrall et al., 2007b). This may only be a short-term response of the restoration process and long-term evidence of this trend is currently lacking. However, this does have implications in attracting investment in restoration from water companies, to reduce water colouration.

## 2.8 Monitoring approaches

In this section key hydrological and remote sensing monitoring approaches are reviewed with respect to their relevance to the major research questions and objectives outlined in sections 1.1.1 and 1.1.2.

### *2.8.1 In-situ hydrological monitoring*

The use of automated hydrological monitoring for measuring change in hydrological parameters within catchments, and through time is well established (Shaw, 1989, Ward and Robinson, 2000). Broadly, the key hydrological parameters monitored in studies of hydrological processes are rainfall, channel stage and velocity (to derive discharge) and the depth to water table (DWT). Historically the manual measurement of rainfall in a cylindrical receptacle (i.e. a rain gauge) is known to provide rainfall rates at a temporal resolution dictated by the sampling interval of the user. Since the invention of the tipping bucket rain gauge (TBR) in 1722 (Logsdon, 2008) the capability to determine rainfall rates at fine temporal resolution has increased dramatically, and with use of this technology may be logged either mechanically or electronically.

Prior to automation, channel stage and velocity was estimated in the field using relatively rudimentary equipment (i.e. graduated ruler and float). The use of modern depth logging equipment now provides reliable and reproducible datasets describing the changes in stage and velocity over very short, user defined time steps (Shaw, 1989). Common methods of automatically measuring channel stage include float operated chart recorders or, more recently, electronic pressure transducers. Either of these methods may record data

locally from stilling wells mounted in or connected to the stream channel (Shaw, 1989). Using these stage data, channel discharge may be estimated using empirical stage velocity relationships such as Manning's Equation (Manning et al., 1890) where velocity is estimated using appropriate parameterisation of the channel cross section, slope, wetted perimeter and a channel roughness coefficient selected to be representative of the monitored reach (R). Discharge may also be measured either directly at various stages (i.e. check gauges), in order to construct a stage – discharge relationship in a channel of known cross-section and hydrological behaviour, or estimated using real time velocity measurements to derive discharge in "real time" (Shaw, 1989).

The use of pressure transducers to gauge water depth within the soil profile also facilitates the automated collection of depth-to-water-table (DWT) datasets. The measurement of DWT at any specific location is often accomplished with the use of a piezometer or "dip well" set into the soil deposit (Shaw, 1989), which allows direct measurement of the equilibrated water table within the piezometer tube, via perforations along its length. The column of water may then be measured manually from the top, or using a pressure transducer at a known depth below the surface. Data collected can then be logged mechanically, or electronically.

The use of the above methods to monitor key hydrological parameters are common throughout the studies examining the hydrology of peatland landscapes (Evans et al., 1999, Price, 1997, Price, 2003, Daniels et al., 2008, Pawson et al., 2012). However, throughout this literature there is an agreement that the duration, temporal resolution, and spatial resolution of the hydrological monitoring currently used to assess the effect of peatland drainage (and restoration) is lacking (Parry et al., 2014, Ballard et al., 2011, Bragg and Tallis, 2001, Holden, 2005, Holden et al., 2004). Without such data the benefits delivered as a consequence of landscape management are subject to far more uncertainty, which has important repercussions for the economic evaluation of such management. Although this has begun to be addressed in recent years in other peatland landscapes (Wilson et al., 2011b, Wilson et al., 2010) the peatlands in the South West of the UK, including those on Exmoor have still lacked data describing their ecohydrological responses to restoration.

### *2.8.2 Remote sensing techniques for ecohydrological monitoring*

Remote sensing is a familiar and mature scientific tool that has been well explored in a peatland context: e.g. to quantify the extent of peatlands, and their ecological condition and in the study and management of such systems (Schultz and Engman, 2011, Anderson et al., 2009, Anderson et al., 2010, Hopkinson and Allott, 2012, Korpela et al., 2009). Broadly, the technologies available to assess the condition of landscapes of this sort remotely, fall into 2 main categories.

- Active RS Systems, i.e. ranging systems:
    - LiDAR (including full-waveform LiDAR)
    - Radar (altimetry)

- Passive multi- or hyper-spectral reflectance or emission detection technologies such as:
    - Visible cameras, i.e. aerial photography
    - Infrared passive imagers, e.g. thermal airborne broadband imager (TABI)
    - Multispectral sensor systems, e.g. Landsat satellite data.
    - Hyperspectral airborne imagers, e.g. ITRES Compact Airborne Spectrographic Imager (CASI)

Such technologies can be deployed on a range of physical platforms from unmanned aerial vehicles (visible cameras), piloted aircraft (LiDAR, thermal imaging and hyperspectral/multispectral systems) to satellites (multispectral imagers, thermal imagers and RADAR altimetry sensors). The platform used often dictates the resolution of the data (in time and space) and the extent of the areal coverage (Campbell, 1996). The selection of such technologies is therefore dependent on the interest of the observer and the spatial compatibility of the data sets available. For example, the platforms may include geostationary or orbital satellites, airborne platforms at a range of heights, or ground based proximal measurement systems (e.g. laser scanners) and these may be

generating data with a spatial resolution or grain size of between >1 km to <1 cm. Where a user needs data covering a large extent but at a low spatial resolution, data collected from a space-borne platform may present the preferred option. Conversely, where a user needs high spatial resolution data over a small extent, data captured from an Unmanned Aerial Vehicle (UAV) platform (such as a visible photo mosaic) may be preferable. Data collected from UAV platforms are also normally significantly cheaper to acquire than either airborne or space-borne platforms, although sensor payloads are greatly restricted.

This study has a particular focus on data from LiDAR systems and passive thermal imagers (both from piloted aircraft surveys) which were commissioned by Exmoor National Park and made available to the project through collaboration with project partners. As detailed below in sections 2.8.2.1 and 2.8.2.2, these products were chosen because of the multiple research outputs available from the analysis of the resultant structural and thermal datasets. Additionally, the project trialled the use of UAV systems for capturing fine scale air photograph data for describing ecological community distribution across the peatland catchments. Each of these approaches is introduced in-turn in the following subsections.

*2.8.2.1 LiDAR surveys, vegetation mapping and peatland applications*

LiDAR technologies offer the observer the opportunity to quantify the morphological and textural attributes of a landscape at a range of spatial and temporal resolutions by making observations of the elevation or distance of a surface (Cavalli et al., 2008, Chassereau et al., 2011, Eeckhaut et al., 2007, Evans and Lindsay, 2010). While RADAR based systems can offer large extent observations of the ground surface at a coarser scale (often from space borne platforms), laser based “LIght Detection and Ranging” techniques (LiDAR) provide a restricted spatial extent but greatly increased spatial resolution of between 0.2 and 5 m typically. Commercial aerial LiDAR techniques can now survey large areas of the landscape at pixel sizes as fine as 0.2 $m^2$. Ground based terrestrial laser scanning systems can describe a surface elevation with a spatial resolution of <6 mm and an accuracy of <4 mm (Anderson et al., 2009). In the case of peatland ecosystems, such technologies have been shown to

permit the exploration of the relationship between mire topography and specific landscape features. For example, analysis can provide elevation models, which are useful in describing topographical associations of peat erosion and vegetation communities (Evans and Warburton, 2010, Cook et al., 2009). The use of this type of remote sensing data has also provided evidence that intact mire complexes have microtopographic vegetation patterning exhibiting anisotropy with a “patch” size of around 1 m. Contrastingly, damaged areas with differing vegetation communities exhibit larger scales of patchiness, of around 3 m to 4 m (Anderson et al., 2009). These types of data are useful in quantifying the condition of peatlands over larger extents which is critical in understanding anthropogenic damage and the concomitant shifts in ecohydrological organisation across landscape extents.

LiDAR data also provides quantification of the underlying topography of peatlands. Using LiDAR to determine topographic indices of the slope and the modelled flow paths in the landscape can provide insight into the spatial heterogeneity of soil saturation and drainage characteristics and can therefore be useful in guiding restoration efforts to more targeted locations (Holden, 2005, Beven, 2012). This type of interrogation of modelled flow paths in drained landscapes may also enable users to assess the extent to which drainage can affect the fate of runoff in the system and identify the spatial heterogeneity inherent in natural or artificial drainage systems. When such surveys are repeated over time, they are also able to identify how such systems evolve, and how this may relate to system change, such as soil and carbon export into stream flows (James et al., 2007).

*2.8.2.2 Passive remote sensing systems – thermal and optical*

Passive remote sensing technologies for capturing spectral reflectance (i.e. electromagnetic radiation reflected from a material) or emmitance (i.e. electromagnetic radiation emitted by a material) data, offer an additional suite of observations that can provide more information about the content of the landscape and further quantify its condition. Aerial photography can provide accurate data describing the extent of well-defined landscape features, including some vegetation classes. However, the use of the wider spectrum allows observers to gather information on the absorbance/reflectance of various

electromagnetic components. For example, commonly, the relative absorbance of near infrared radiation (low) compared to infrared (high) can be used to identify vegetation assemblages/species, due to the variation in absorption of this part of the electromagnetic spectrum for photosynthesis. These data can therefore be used to characterise the extent of vegetation and estimate variables such as leaf area and green biomass by inference (Mänd et al., 2010). Such methods can also offer information on the spatial distribution of plant condition in similar vegetation types using photosynthesis rates as a proxy of productivity. However recent studies suggest that this technique (normalised difference vegetation index (NDVI)) has limitations in its extensive application (Garbulsky et al., 2010). For example, the radiation use efficiency (RUE) of plants varies from species to species and environmental constraints on both the vegetation and sensing technique can limit the ability to compare measurements temporally (Garbulsky et al., 2010). Nonetheless, emerging techniques such as the photochemical reflectance index (PRI) are shown to produce data describing the vegetation response to stressors and photosynthetic efficiency by examining the difference in reflection at narrow bandwidths 531-570 nm (Mänd et al., 2010, Garbulsky et al., 2010). The difference in reflectance of these bandwidths is dependent on certain photochemical pathways in the leaf, which respond to stress, thereby providing an estimation of photosynthetic condition.

Hyperspectral data and techniques such as NDVI are widely used as proxies for ecological condition or ecosystem mapping. However, this research has a primary focus of understanding the ecohydrological condition of peatland ecosystems across the monitored catchments. In this light, capturing the remotely sensed data able to provide proxies of hydrological condition at a fine spatial scale is desirable. Although the use of active technologies such as SAR are able to provide data describing near surface hydrology (Hoekman, 2007) the coarse nature of these data (ca. 18 $m^2$) limits their use in catchment scale monitoring of peatland hydrology. As a consequence this research examines the potential of alternate passive spectral data to characterise near surface hydrology. Specifically, chapter five examines the use of thermal airborne imaging to identify the thermal signature of water bodies or moisture dominated vegetation such as *Sphagnum Spp.* (Harris and Bryant, 2009).

The use of thermal imagery to spatially describe patterns of near surface hydrology is a relatively unexplored technique, but has been shown to describe spatial parameters of soil wetness in other situations (Price, 1980). Such data may be used to describe patterns of land near surface wetness as the relatively high specific heat capacity of water (4.1855 J/g-$K^{-1}$ at 15°$^{C}$, 101.325 kPa) can cause wetter areas to appear warm relative to their surroundings during cool air temperatures. Advances in the development and deployment of such sensors (e.g. improved spatial resolution and miniaturisation for UAV platforms) provide new opportunities to assess the use of this data resource for understanding hydrological processes over large extents. The complex effect of material emissivity in the interpretation of thermal data has previously limited the use of these data, (Anderson and Wilson, 1984). However, data which describe the structural properties of a surface may prove useful in overcoming this limitation. For example, LiDAR data can provide information that may be used to quantify and normalise the effect of material emissivity on the relative infield temperature measurement (Luscombe et al., 2012). The ongoing development of remote sensing technologies described above, and the emergent field of UAVs as platforms for these sensors also offers new opportunities for spatial data capture (Anderson and Gaston, 2013). One such opportunity is the increased temporal frequency with which measurements may be made, which offers new tools to more fully integrate the spatial and temporal monitoring of remote and inaccessible habitats.

This research employs a variety of complementary remote sensing and in situ monitoring methods that together should be able to quantify landscape attributes and hydrological parameters spatially, and through time. In coupling a detailed in-situ hydrological monitoring study with new remote sensing approaches, this work is intending to address whether scientific understanding of the ecohydrology of upland peatland landscapes can be improved. Chapters four to seven contain specific detailed methodologies relevant to the deployment, acquisition and analysis of the data used in this body of research, which builds on the key techniques reviewed here.

## 2.9 Summary

The literature and understanding outlined here provides a conceptual and experimental understanding of the structure and function associated with both intact and degraded/drained peatland systems. However, almost all the literature currently focusses on deeper blanket peatlands in the north of the UK. These peatlands are both larger in extent than those in the south west and represent the majority of the carbon store associated with this type of landscape in the UK. Nonetheless, these findings provide a key basis for understanding, from which the ecohydrological structure and function of the shallow peatlands in South West England can be assessed.

These peatlands are noticeably different from other more northerly peatlands in that they are shallower than peatlands in northern areas and accordingly, are hypothesised to be affected by drainage and peat cutting in differing ways. Their location on the south western periphery of the geographical extent of UK peatlands may also increase their vulnerability to climate change (Clark et al., 2010) which may serve as an early indicator of change seen in more northerly analogues. Capturing a representative dataset that quantifies the ecohydrological function of these peatlands is therefore critical in supporting and evaluating the landscape management of these areas in the future. It can be seen from the literature reviewed here that a dataset able to satisfy these needs must examine the ecohydrology of these peatlands spatially and temporally in order to appropriately asses this resource, and provide a robust baseline from which future change may be gauged. The following chapters detail the findings from a set of papers that aim to meet this research requirement, and discuss the implications of those findings.

# 3 Site Description and Study Methods

## 3.1 Exmoor's peatlands

Exmoor National Park occupies an area of approximately 686 $km^2$, more than half of which is over 300m above sea level (Davies, 2012). The extent of blanket peat within this area was surveyed by Merryfield (1977) and later by Bowes (2006) who suggest that an area of deep blanket peat (> 50cm) is between 3.5 and 4 $km^2$. It is generally accepted that the extent of thinner blanket peat soils (<50cm) on Exmoor is significantly greater, although this is not currently defined in the literature. These geo-climatically marginal and shallow peatlands in the South West of the UK have recently been subject to significant restoration activities (Gallego-Sala et al., 2010, Clark et al., 2010, Grand-Clement et al., 2013), with over 50 km of drainage ditches already undergoing restoration (pers comm, ENPA, 2014). However, the ecological and hydrological function of these systems remains poorly understood when compared to more northerly and deeper peatlands.

Although recent studies have examined the carbon storage and paleoarchaeological record associated with these peatlands (Fyfe, 2006, Maltby and Crabtree, 1976, Parry and Charman, 2013, Davies, 2012), without a complementary understanding of the contemporary ecohydrological function of these systems, the efficacy of such restoration is uncertain. The shallow Exmoor peatlands are also thought to differ in their ecohydrological structure and function from deeper peats (Grand-Clement et al., 2013, Chambers et al., 1999, Merryfield and Moore, 1974), and as such, may be more sensitive to the effects of climate change (Gallego-Sala et al., 2010, Clark et al., 2010). An improved understanding of the hydrological function of these damaged shallow mires is, consequently, important to determine their sensitivity in a changing climate, and to facilitate effective landscape rewetting following restoration activities (Parry et al., 2014, Bain et al., 2011).

## 3.2 Site selection criteria

In addressing the research imperative defined in chapter 1, this research project needed to ensure that the locations selected for study were suitably characteristic of the thin and bio-climatically marginal upland peatlands found throughout the south west of England, and especially Exmoor, as this was the primary focus of the work (Bowes, 2006, Clark et al., 2010). Consequently, the chosen study locations needed to be representative of several key characteristics:

- The different landscape characteristics found across the Exmoor extent (i.e. slope, aspect, soil type/thickness, land use and management).
- The different types and scales of anthropogenic drainage found in the wider moorland area.
- Vegetation community composition and species diversity.

The site selection and experimental design for the research in this thesis is also linked to the wider “mires on the moors” project, which is part of the “Upstream Thinking” programme funded by South West Water. This project has the aim of improving water quality and managing the quantity of water at source by improved land management (Grand-Clement et al., 2012). As a result, the experimental catchments monitored as part of this study are also used as a platform for complementary research examining the flux of gaseous and dissolved organic carbon in these landscape systems. The locations used for monitoring of drainage discharge and depth to water table as part of this research (see section 6.3) have therefore, also been used to collect water samples using automated pump samplers.

Additionally, the study sites were chosen with careful consideration of the societal and governance issues surrounding the management of this landscape and with the permission and collaboration with the land owners and other environmental stakeholders (e.g. Exmoor National Park, The Environment Agency, Natural England and English Heritage).

## 3.3 Experimental catchment and experimental pool locations

Two principal experimental catchments were selected following extensive consultation with project stake holders in order to facilitate reasonable access and relevant permissions for the monitoring implemented. The two principal study sites are ca. 3 km apart. The westernmost site is “Aclands” [SS 733,384] and “Spooners” [SS 776,374] is the eastern most site (Figure 3.1). Both sites are headwater catchments formed as shallow depressions with height variations of ca. 40 m and are 400 – 450 m above sea level and are headwaters of the river Barle, a tributary to the river Exe. Both catchments are also located within the North Exmoor Site of Special Scientific Interest (SSSI). The position of the watersheds with respect to the local landscape, is shown in Figure 3.1 with watersheds delineated from 50 cm airborne LiDAR data.

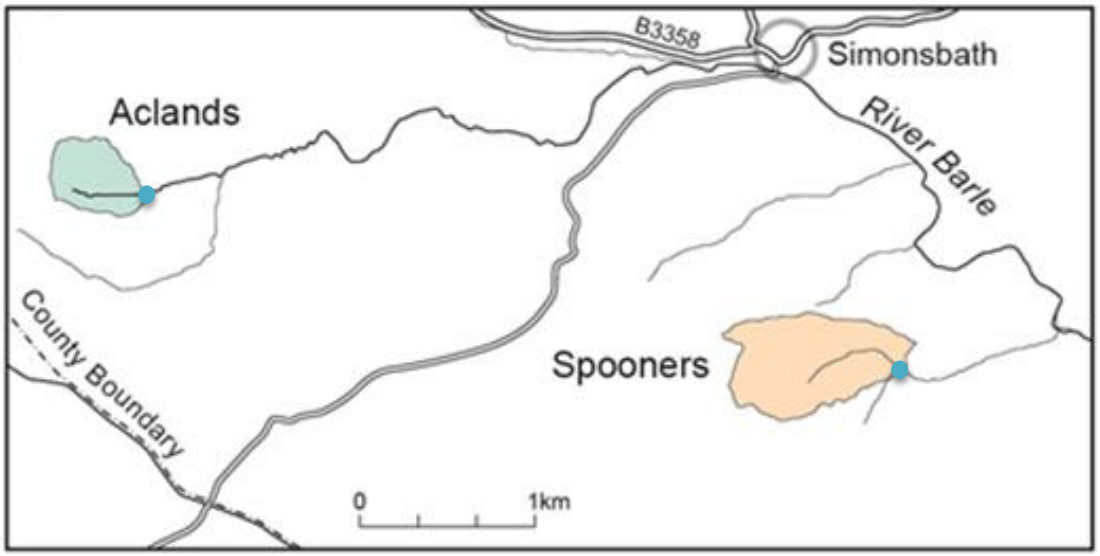


**Figure 3.1: Aclands and Spooners Watershed in Exmoor National Park. The blue marker point (•) shows the location of the catchment outflow location where discharge was monitored.**

Aclands and Spooners contained a representative diversity of the required parameters, including ditches that have appropriate variability in stream order, size and depth (approx. 0.3 m to 0.6 m wide occurring ca. every ~20 m across the catchment extent and on a range of aspects). These catchments cover approximately 16.5% of the blanket peat extent on Exmoor (Davies, 2012) and contain slope morphologies representative of those found throughout the

drained areas of moorland on Exmoor. In addition to these physical characteristics, the catchments both contained moorland vegetation dominated by Purple Moor Grass (*Molinia caerulea*) and also exhibited various assemblages of bog (i.e. *Sphagnum Spp., Eriophorum Spp*. and *Drosera rotundifolia)* and heath (i.e. ericaceous shrub species (e.g. *Calluna vulgaris, Erica tetralix and Erica caerulea*) also characteristic of drained planted blanked mire complexes in Exmoor. The selected sites also represent defined catchments, which exclude land use types not representative of the areas identified as suitable for ecohydrological restoration (i.e. open drained moorland) and have a single drainage outflow of comparable (Strahler) stream orders (see chapter 7 for more details).

Hydrological parameters (Flow discharge [Q] and depth to water table [DWT]) were also collected at three experimental pools [EP] locations within each of the two headwater catchments. Each EP was located within a drainage ditch of a different scale, determined by its geometry measured during site selection trips, giving rise to 8 (nested) scales of hydrological monitoring over the two catchments. These selection criteria ensured that the resultant dataset was as representative as possible of the drainage found across the catchment and Exmoor, although at this stage the relative topographic contributing area of each location was not estimated. At the start of the research project both catchments were also scheduled for full hydrological restoration to be undertaken by project partners, including Exmoor National Park and the Environment Agency, under funding from South West Water under the 'Upstream Thinking' programme (Grand-Clement et al., 2012). The timeline of the research was planned so that there would be a period of at least one year of pre-restoration baseline monitoring at each site prior to restoration being implemented, though this period was flexible and was controlled by the quality/quantity of the data collected via this research.

## 3.4 Study methods and data

The following section summarises the key methods and datasets used in both the remote sensing and hydrology aspects of this thesis where not otherwise referred to in chapters 4 to 7, due to the scientific brevity required for publication. The LiDAR and thermal remote sensing data used in this research

was commissioned, specified and collected by the project funders and partners (ENPA and SWW) prior to commencement of this study. Consequently, the flight path design or other aspects of the data capture were not able to be specified to the benefit of this research prior to acquisition. The LiDAR and TABI data used were also supplied as commercial data products with limited available metadata for users. Personal communications with the EAGG (21/1/2013 and 23/6/14) have expanded the available metadata which is summarised in sections 3.4.1 and 3.4.2. As part of the wider mires project, the research undertaken using this data was designed to maximise the use of these data for the purpose of understanding the ecohydrology of these peatlands. In light of this, this research explores the content of these data products in order to better inform other users of these data, and users of similar commercial LiDAR or thermal imaging products supplied in a "closed" format to users.

### *3.4.1 Airborne LiDAR data acquisition and processing*

Airborne LiDAR data were collected by the Environment Agency Geomatics Group (EAGG) (www.geomatics-group.co.uk) in May 2009 at a 0.5 m spatial resolution (0.3 m diameter footprint). LiDAR data were collected using an ALTM Gemini (08SEN230) LIDAR instrument and were supplied as a pre-derived but minimally filtered DSM dataset, with a 0.5 m × 0.5 m spatial resolution. These data were provided as a 'first return' dataset with only spurious low and high points removed prior to being triangulated and fitted to a regular grid using TerraScan (version 009.004).

The LiDAR dataset was checked for accuracy at 5 separate locations by Geomatics group, using a differential Global Positioning System (DGPS) survey. These ground truth data indicated an average systematic error (or bias) of + 0.0004 m and an average random bias of ± 0.047 m in elevation. The combined RMSE for these data was 0.029 m which was well within the product specification of 0.15 m. The average of all LiDAR surveys from EAGG for the previous two years has been within +/- 8cm (pers. Comm. 2012).

For analysis undertaken in chapter 4 and 7, LiDAR data were also used to derive a numerical model of flow accumulation and routing based on the methods developed by Jenson and Domingue (1988). This model was

implemented for the study catchments in Arc GIS (version 10) using the Arc Hydro toolbox extension. Unless otherwise stated in the text, the methodology used the following stages to derive the modelled watersheds and flow pathways used in this analysis:

1. The removal of topographic sinks from the DSM to ensure flow connectivity.
2. Deriving a flow direction model from the modified DSM.
3. Deriving a flow accumulation model from the modified DSM.
4. Using 2 and 3 as inputs to derive a raster stream model.
5. Vectorisation of stream model.
6. Resulting stream network classified using the Strahler stream order hierarchy (Strahler 1957).
7. Allocation of “pour point” on stream network.
8. Derive watershed using 4 and 7.

### *3.4.2 Airborne thermal imaging data acquisition and initial processing*

The Itres Instruments Thermal Airborne Broadband Imager (TABI) provided thermal imagery at 2 m × 2 m spatial resolution and were collected simultaneously with the LiDAR data discussed in 3.4.1. These data are not calibrated to land surface temperature or material emissivity (the ratio of thermal emission to that of a black body of the same temperature), and are only supplied as relative within-scene temperature pixels for which the sensitivity should be better than 0.1$^{o}$C noise equivalent temperature difference (NEDT). Because the data were collected prior to the beginning of this study it was not possible to ensure that concomitant field validation data were collected describing temperature or emissivity of known points on the ground. As such, the resultant dataset contains measurements describing the temperature of the observed surface combined with the effect of the material emissivity of the target. It is for this reason that this dataset and the data derived from it are only treated as relative measured spatial distributions throughout this thesis.

### *3.4.3 Hydrological monitoring data acquisition and processing*

The fine scale hydrological monitoring used during this research has required the collection of a large volume of timeseries data used for the analysis detailed in chapters 6 and 7 of this thesis. The list below describes the number of points of data that have been collected annually from the water table and flow data collected as part of this study.

- 6 Experimental pools each with 17 sensors.
- Total 104 sensors (including catchment outlets).
- Measurements taken every 15 minutes providing :
    - 35,040 data points per sensor year$^{-1}$
    - Total of 3,644,160 data points year$^{-1}$

The collection of this volume of data over multiannual timescales has resulted in specific challenges related to the management of the resulting dataset, such as:

- The ongoing acquisition and storage of the measurements.
- The management of the data archive.
- The security of the data acquired.

These requirements were fulfilled with the use of a modular telemetry system produced by “adCON” (http://www.adcon.at/). This system was originally developed for agricultural applications and is able to accept various sensor types and feed data back to a server in near real time. Using this system data were collected by a given sensor and transferred, via a wired connection, to a remote telemetry unit. These data were then combined with data from other sensors and transmitted via VHF to a base station within each catchment and transmitted to the server via the GPRS mobile data network. Data was also downloaded to a local computer at the university periodically for pre-processing and backup. The sensors and telemetry system were powered solely via photovoltaic panels with appropriate voltage regulation, charging internal batteries. Data regarding the charge state of these systems and any data delay was also sent back from the telemetry every 15 minutes in order to facilitate the ongoing management and maintenance of this system. The data was also able to be viewed and managed live on the server, which allows for decisions and

actions regarding data collection to be taken remotely, and breakdowns to be resolved quickly.

### *3.4.4 Numerical methods for hydrological analysis*

The large volume of data collected in this study has required significant processing and statistical analysis which is detailed in chapters 6 and 7 of this thesis. Where such analysis has involved more complex statistical examination than descriptive statistics or simple regression, the statistical analysis is summarised in the below table.

**Table 3.1: Key numerical and statistical data analysis undertaken and the specifc outputs associated with this work.**

| Dataset | Test/Analysis | Type | Output | Section |
|---|---|---|---|---|
| Discharge | Q5/Q95 | Probability ratio | Numerical Index of runoff flashiness | 6.4.1 |
| Rainfall and discharge | Spearman's Rank Order | Non-parametric | Direction and significance of relationship | 6.4.2 |
| Rainfall, DWT and discharge | Multiple regression | Parametric regression | Significance and explanatory power of hydrological variables | 6.4.2 |
| Depth to Water Table | Exponential regression with 95% confidence interval | Regression | Inflection point as a proxy of step-change in process | 6.4.3 |
| Rainfall and discharge | One way ANOVA and least difference post hoc analysis | Parametric | Difference in frequency distribution of variables at different locations | 7.4.1 |

## 3.5 Research timeline

At the project outset, it was necessary to establish the *in situ* monitoring scheme for each catchment and to install, set up and maintain the equipment through time. This required extensive fieldwork, details of which are only briefly provided in the subsequent sections, due to the nature of this thesis being written as a set of papers. For this reason, the following section illustrates the time-line for the monitoring setup and remote sensing analysis undertaken for this research (Figure 3.2) and provides a photographic record of key milestones in this process. This includes site selection (Figures 3.3 – 3.7), aerial photography of the selected catchments using a fixed wing UAV to generate broad vegetation classifications for each catchment (Figures 3.8 – 3.10), sampling design, installation, testing and set-up of the hydrological monitoring and telemetry equipment (Figures 3.12 – 3.15) and finally, hydrological restoration of one of the study catchments (Spooners), in Figures 3.16 – 3.20. Locations of Figures 3.3 to 3.20 are illustrated in Figure 3.21.

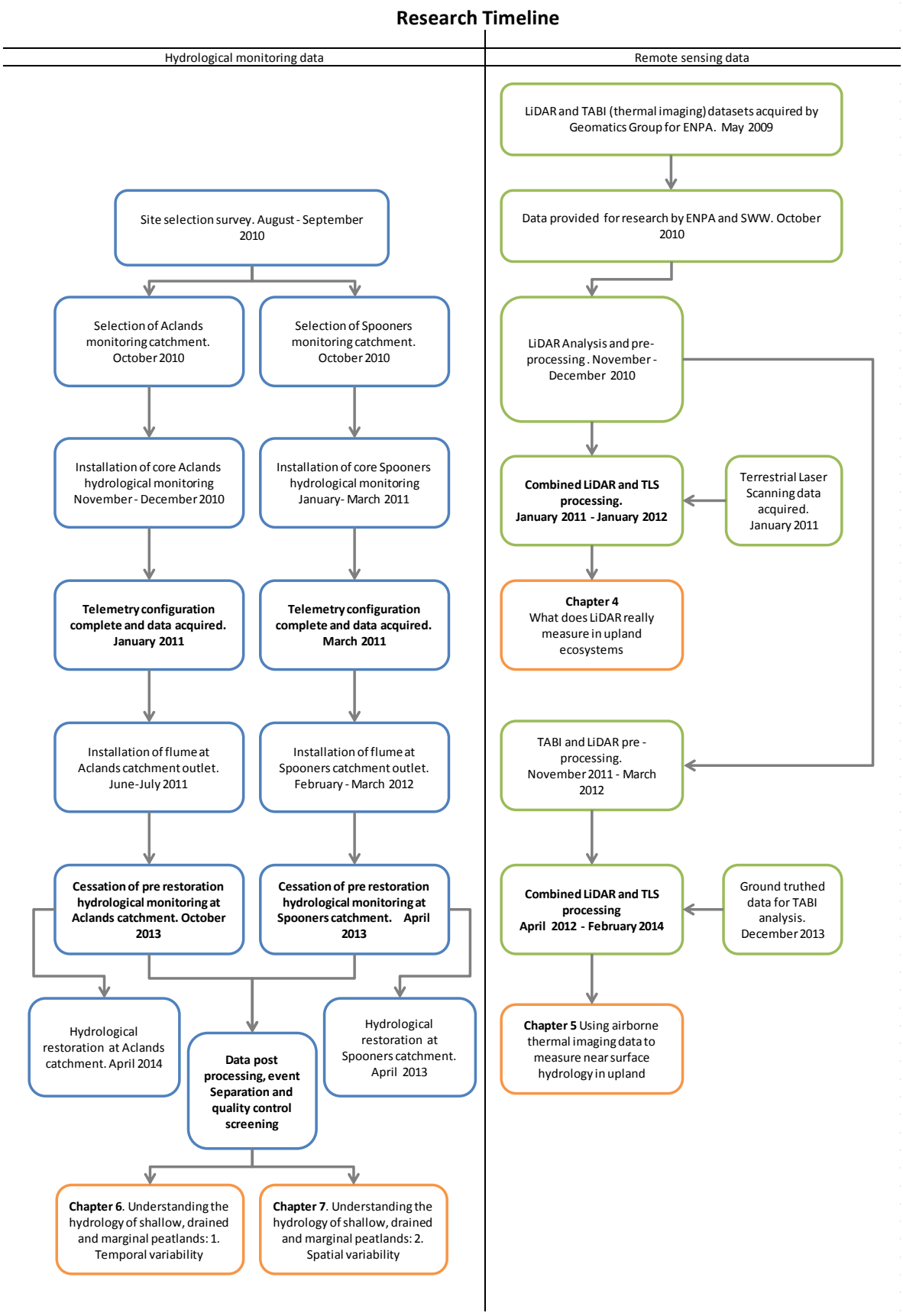


**Figure 3.2: Timeline of key milestones in data acquisition for both remote sensing and hydrological monitoring data throughout PhD research. Blue boxes refer to hydrological datasets and green boxes to remote sensing datasets. Research outputs are highlighted in orange.**

**Figure 3.3: Aclands catchment autumn 2010, pre-restoration. Looking down-slope towards the catchment outlet from the top of the catchment. Of note is the vegetation of the site where *Molinea caerulea* is very dominant.**

**Figure 3.4: Spooners catchment autumn 2010, pre-restoration. Looking down towards the catchment outlet from a mid-catchment position. Again, the vegetation assemblage of the site is dominated by *Molinea caerulea*.**

**Figure 3.5: Aclands catchment autumn 2010, pre-restoration. Looking north along an eroded wall structure.**

**Figure 3.6: Spooners catchment. September 2010. Close up photograph showing summer vegetation growing over an incised anthropogenic drainage feature.**

**Figure 3.7: Spooners catchment. September 2010. Looking west up the main channel overgrown with summer vegetation. Of note is the presence of *Molinea caerulea* tussocks dominating local topography within the drainage feature.**

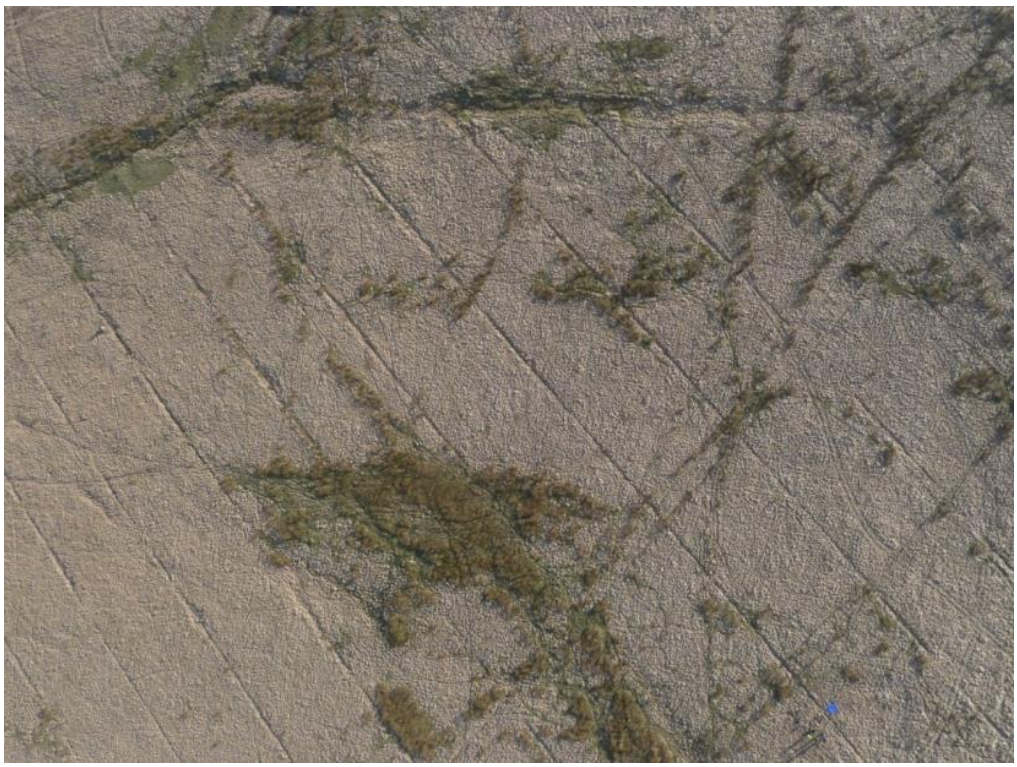

**Figure 3.8: Visible aerial photography collected from a QuestUAV fixed wing aircraft flying at 100 m altitude over the Aclands catchment in March 2012. Linear features running from the top left of the image to the bottom right of the image show the anthropogenic drainage network.**

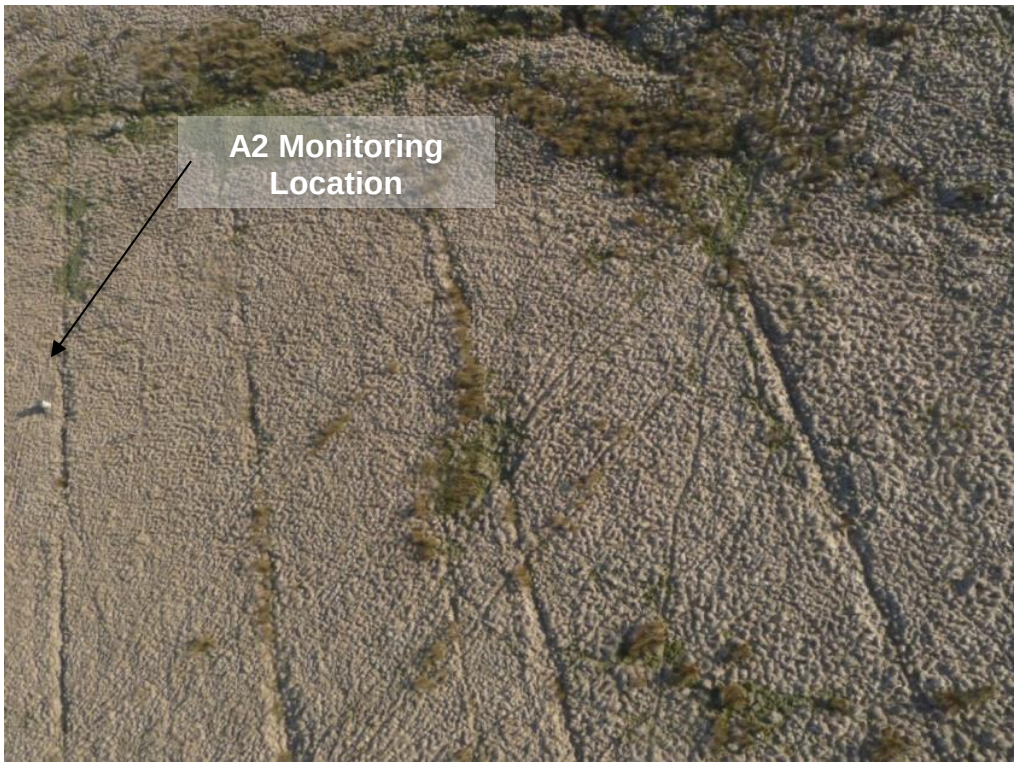


**Figure 3.9: UAV imagery at Aclands catchment surveyed in March 2012 Showing the A2 monitoring location.**

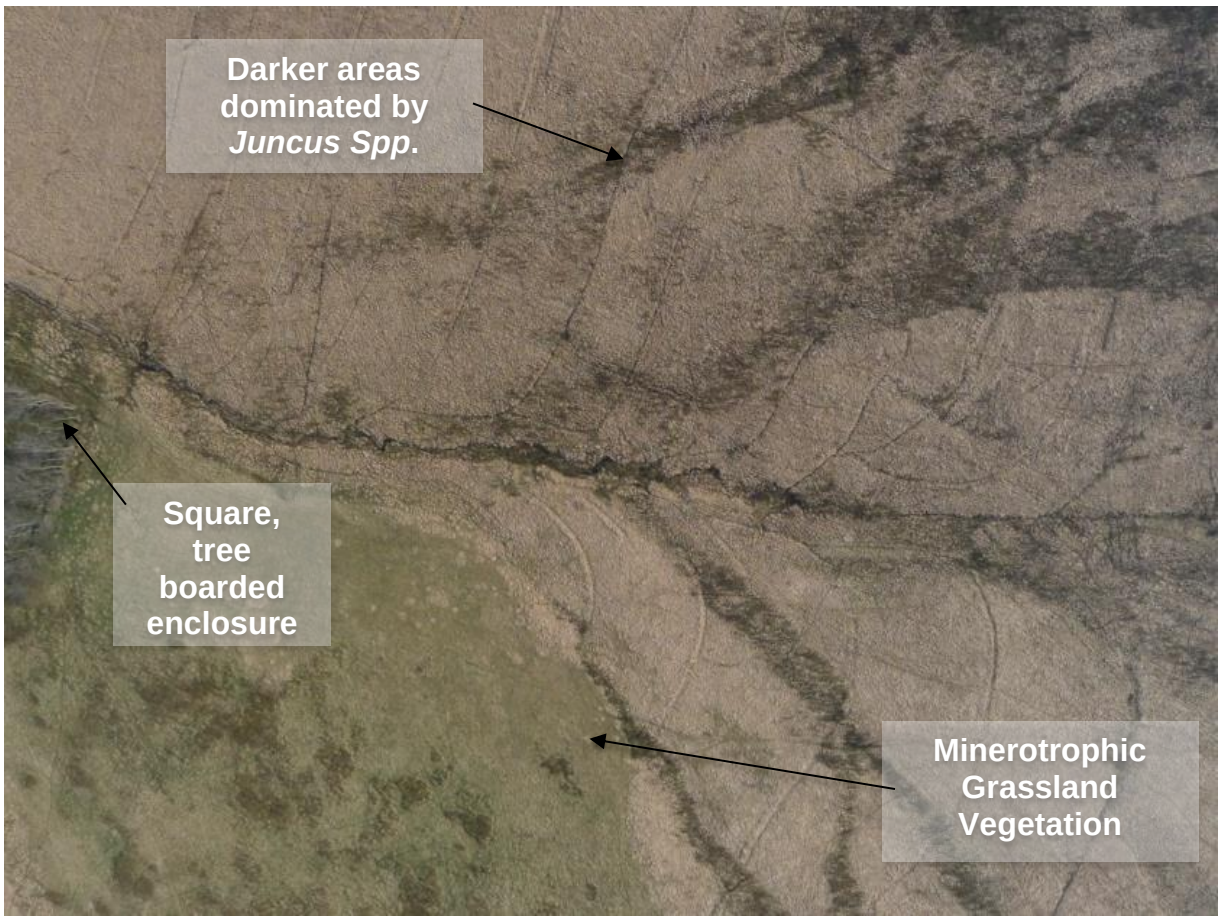


**Figure 3.10: UAV imagery from the Spooners catchment in March 2012. The irregularly spaced anthropogenic drainage network is visible running towards the central drainage channel. Dark areas of vegetation (as highlighted) are hypothesised naturalised flow pathways, and there is an area of minerotrophic vegetation which appears greener than the senescent *Molinea caerulea* community.**

**Figure 3.11: Field photograph of the square, tree bordered enclosure visible in Figure 3.10. This structure is easily identifiable in the airborne thermal imaging data discussed in chapter 5.**

**Figure 3.12: Author installing stage monitoring in the main channel at Aclands prior to flume installation.**

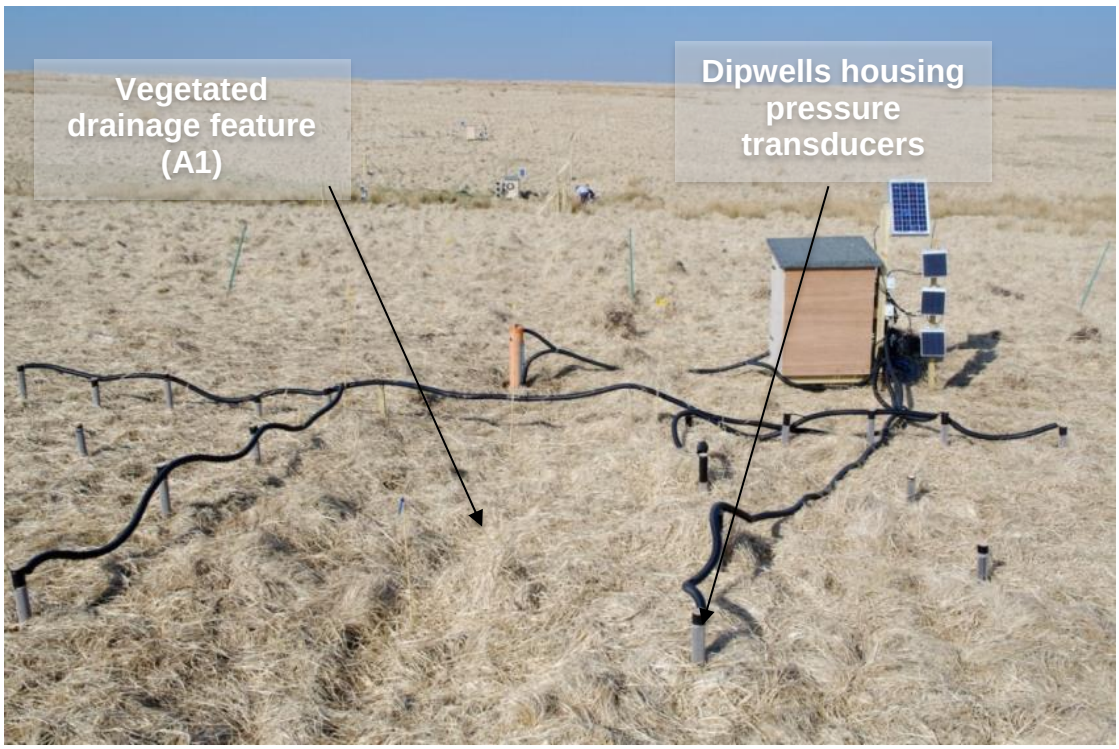


**Figure 3.13: Array of dipwells and in-channel stilling well installed around the small drainage feature (A1) within the Aclands Catchment. January 2011. Wooden cabinet contains telemetry and sampling equipment used to monitor the drainage feature. Dipwells are also clearly visible and contain pressure transducers connected to the telemetry equipment using conducted cables (black piping).**

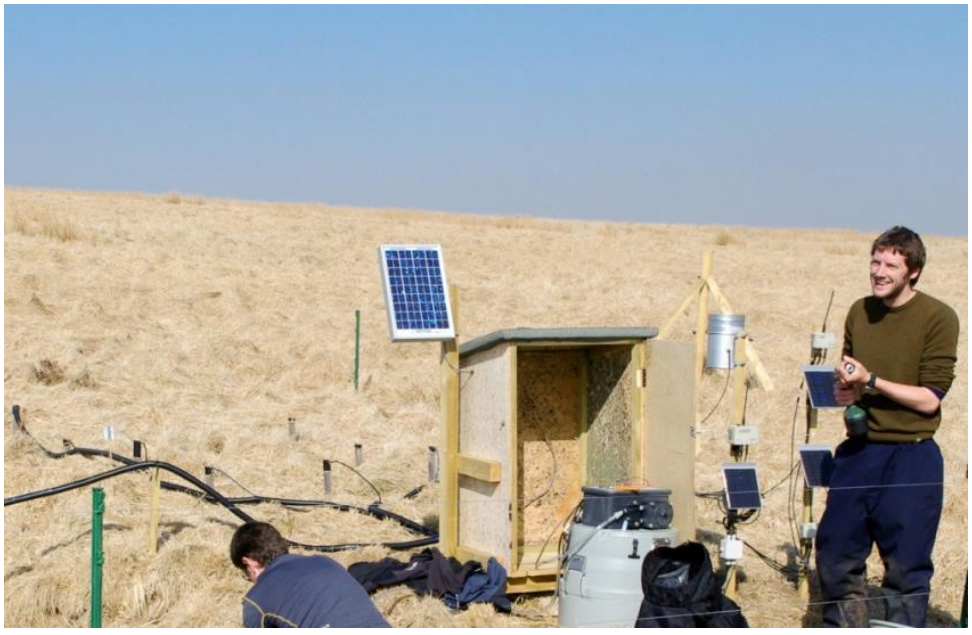

**Figure 3.14: Author installing telemetry equipment at the A2 monitoring location within the Aclands Catchment. January 2011.**

**Figure 3.15: Contractors installing the flume structure at the Aclands catchment outlet, Summer 2011.**

**Figure 3.16: Restoration of the S3 monitoring location in Spooners catchment, March 2013. The photograph shows wooden blocks which were put in place to raise the water table in the surrounding peat soil. Water can clearly be seen collecting upslope of the blocks following installation.**

**Figure 3.17: Restoration of the S1 monitoring location in the Spooners catchment, March 2013.**

**Figure 3.18: This photograph shows the effect of restoration on the S2 monitoring location in the Spooners catchment. Note the water ponding upslope of the installed ditch block. March 2013.**

**Figure 3.19: Close up of ditch block at S1 monitoring location in Spooners catchment, March 2013.**

**Figure 3.20: Main channel immediately following restoration in Spooners catchment, March 2013.**

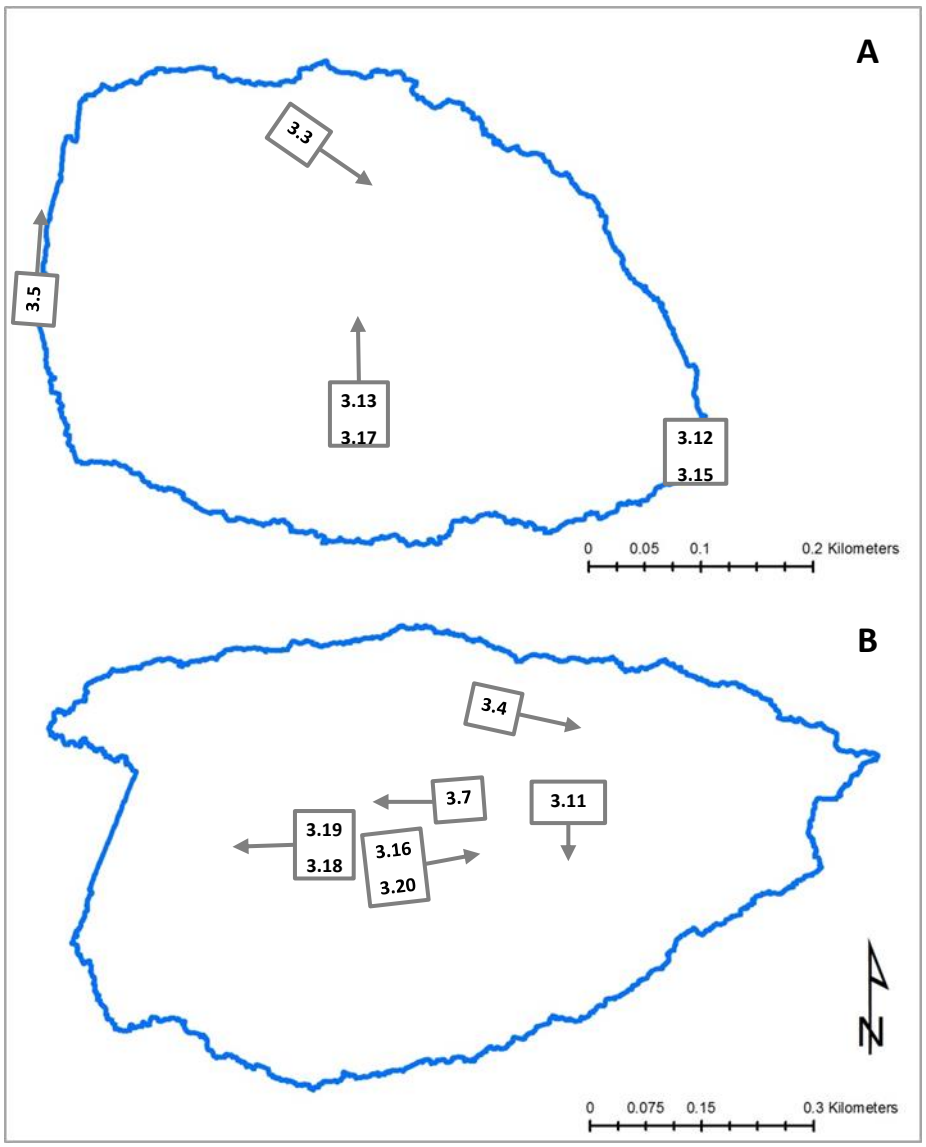


**Figure 3.21: Relative locations of photos in figures 3.3 to 3.20 within the Aclands (A) and Spooners (B) catchment watersheds (blue lines). Grey boxes indicate the location of the photographs and grey arrows the direction**

# 4 What Does Airborne LiDAR Really Measure in Upland Ecosystems?

The following paper is included as the fourth chapter of this thesis and is presented in its published format. This chapter falls under the first theme of this research outlined in chapter 1. All references for this paper are included at the end of this chapter, in publication format. This paper was submitted for publication in the journal Ecohydrology on the 22nd of November 2013 and accepted for publication on the 21st of June 2014.

ECOHYDROLOGY
*Ecohydrol.* (2014)
Published online in Wiley Online Library
(wileyonlinelibrary.com) DOI: 10.1002/eco.1527

# What does airborne LiDAR really measure in upland ecosystems?

David J. Luscombe,[1]* Karen Anderson,[2] Naomi Gatis,[1] Andrew Wetherelt,[3] Emilie Grand-Clement[1] and Richard E. Brazier[1]

[1] *Geography, CLES, University of Exeter, Amory Building, Rennes Drive, Exeter, Devon, EX4 4RG, UK*
[2] *Sustainability Institute, University of Exeter, Cornwall Campus, Treliever Road, Penryn, Cornwall, TR10 9EZ, UK*
[3] *Camborne School of Mines, University of Exeter (Cornwall Campus), Tremough Penryn, Cornwall, TR10 9EZ, UK*

## ABSTRACT

Airborne laser scanning systems (Light Detection And Ranging, LiDAR) are very well suited to the study of landscape and vegetation structure over large extents. Spatially distributed measurements describing the three-dimensional character of landscape surfaces and vegetation architecture can be used to understand eco-geomorphic and ecohydrological processes, and this is particularly pertinent in peatlands given the increasing recognition that these landscapes provide a variety of ecosystem services (water provision, flood mitigation and carbon sequestration). In using LiDAR data for monitoring peatlands, it is important to understand how well peatland surface structures (with fine length scales) can be described. Our approach integrates two laser scanning technologies, namely terrestrial laser scanning (TLS) and airborne LiDAR surveys, to assess how effective airborne LiDAR is at measuring these fine-scale microtopographic ecohydrological structures. By combining airborne and TLS, we demonstrate an improved spatial understanding of the signal measured by the airborne LiDAR. Critically, results demonstrate that LiDAR digital surface models are subject to specific errors related to short-sward ecosystem structure, causing the vegetation canopy height and surface-drainage network depth to be underestimated. TLS is shown to be effective at describing these structures over small extents, allowing the information content and accuracy of airborne LiDAR to be understood and quantified more appropriately. These findings have important implications for the appropriate degree of confidence ecohydrologists can apply to such data when using them as a surrogate for field measurements. They also illustrate the need to couple LiDAR data with ground validation data in order to improve assessment of ecohydrological function in such landscapes. Copyright © 2014 John Wiley & Sons, Ltd.

KEY WORDS LiDAR; terrestrial laser scanning; DSM; uncertainty; peatlands; uplands; ecohydrology; ecosystem services; Exmoor; UK

*Received 22 November 2013; Revised 20 June 2014; Accepted 21 June 2014*

## INTRODUCTION

There is a new monitoring imperative for peatlands as global policy recognizes the importance of these ecosystems in tackling climate change, water management objectives and biodiversity conservation (Bain *et al*., 2011; Grand-Clement *et al*., 2013). Spatially distributed measurements from airborne laser scanning systems, such as Airborne Light Detection And Ranging (LiDAR), are useful for describing the three-dimensional structure of landscape surfaces and vegetation (Rango *et al*., 2000; Zimble *et al*., 2003; Hutton and Brazier, 2012; Mitchell *et al*., 2012; Emanuel *et al*., 2013), and there is considerable evidence that such data provide valuable information on ecohydrological and eco-geomorphic processes in peatlands (Korpela *et al*., 2009; Anderson *et al*., 2010). In addition, landscape and ecosystem structure have long been recognized as important controls on peatland function (Moore and Bellamy, 1974; Barber, 1981). More recently, Belyea and Clymo (2001) have explored the link between microtopography and peat formation and the ecohydrology of mires, leading to the contemporary understanding of links between microtopography and ecohydrological functioning summarized by Holden (2005) and Lindsay (2010).

The use of laser scanning techniques in peatlands could permit the quantification of how peatland structure and function change through time, leading to a dynamic understanding of landscape-scale ecohydrological behaviour (Turnbull *et al*., 2008; Fisher *et al*., 2009; Lane and D'Amico, 2010). However, progress towards this in an operational sense is limited by our understanding of what the LiDAR signal actually represents in real terms – e.g. can LiDAR deliver robust measurements of both the

*Correspondence to: David J. Luscombe, Geography, CLES, University of Exeter, Amory Building, Rennes Drive, Exeter, Devon EX4 4RG, UK.
E-mail: d.j.luscombe@exeter.ac.uk

short-sward canopy and/or the landscape surface? Spatially distributed information on both of these factors is needed because many temperate peatlands are dominated by low-sward vegetation (Drewitt and Manley, 1997) with structurally subtle microtopographic features (Kincey and Challis, 2009; Lindsay, 2010): both of which impart significant effects on the ecohydrological functioning of peatlands (Holden *et al*., 2004). Small shifts in ecological structure or drainage pattern may, for example, elicit major shifts in the hydrological response of the system.

The LiDAR technologies use a precisely timed laser pulse and measure the return signal to capture accurate altimetry measurements of the Earth's surface, over large spatial extents. When analysing LiDAR datasets at landscape scales, there is often an assumption that the data are directly representative of the three-dimensional habitat structure (e.g. forest canopy) or the true ground surface (Jones *et al*., 2008; Kincey and Challis, 2009). For example, LiDAR-derived digital surface models (DSMs) are often used to calculate hillshade products (Kincey and Challis, 2009; Barbier *et al*., 2011), canopy height models for forestry (Zimble *et al*., 2003), or used to support numerical models of wetness, surface roughness or surface flows (Beven and Freer, 2001; Jones *et al*., 2008; Beven, 2012). Previous work (Ivanov, 1981; Taylor, 1983) highlights the need for accurate representation of peatland surface flows in particular, to characterize peatland systems effectively. As a result, this approach can provide a powerful means of separating ecological and topographic structures (Hinsley *et al*., 2002; Clawges *et al*., 2008; Vierling *et al*., 2008; Horning *et al*., 2010; Chassereau *et al*., 2011; Hutton and Brazier, 2012). However, in using these data, it is important to note that the applicability of LiDAR is always constrained by the spatial resolution of the processed LiDAR surface (i.e. the resolution of the DSM) and the spatial support (or footprint) of the laser beam itself (Fisher and Tate, 2006). Datasets derived from airborne LiDAR are, therefore, subject to implicit (but often unquantified) uncertainty (Aguilar *et al*., 2010).

Although we acknowledge that LiDAR datasets offer an as yet unparalleled ability to understand landscape structure and function (Rango *et al*., 2000; Zimble *et al*., 2003; Vierling *et al*., 2008; Korpela *et al*., 2009; Evans and Lindsay, 2010), herein, we stress the need to better quantify the spatial ($x$, $y$) and vertical ($z$) uncertainty in such data. This would permit an improved interpretation of LiDAR products describing the biotic and abiotic structure of peatlands. One way of approaching the problem is to integrate data from other laser scanning technologies operating at finer spatial resolutions (Danson *et al*., 2007), in order to validate the information content of the LiDAR. Here, we combine data from a terrestrial laser scanner (TLS) with airborne LiDAR surveys of an upland peatland system in the UK to test the following hypotheses:

1. TLS data can be used to validate the information content of a LiDAR DSM in an upland peatland context, thereby allowing improved spatial characterization of ecohydrological structures such as aboveground biomass and surface-flow pathways.
2. Airborne LiDAR data allow the discrimination of different ecohydrologically relevant vegetation communities in peatlands.
3. Airborne LiDAR data are capable of detecting the presence and position of anthropogenic landscape features such as drains and archaeological remains, which may alter hydrological function in peatlands.

## METHODS

### *Airborne LiDAR data acquisition and initial processing*

Airborne LiDAR data were collected by the Environment Agency Geomatics Group (EAGG) (www.geomatics-group.co.uk) in May 2009 at a 0·5-m spatial resolution in the horizontal plane. Two headwater catchments within degraded upland peatland areas in Exmoor National Park, UK, were selected to include a wide range of drainage ditch morphology, slope morphology, aspect and vegetation composition. The location of the watershed of these upland catchments [known locally as 'Aclands' (SS 733,384) and 'Spooners' (SS 776,374)] is shown in Figure 1. LiDAR data supplied by EAGG were provided as a 'first return' dataset (0·3-m diameter footprint) and fitted to an even grid of $0{\cdot}5 \times 0{\cdot}5$ m by the data supplier. These data were then processed within a Geographical Information System (GIS; ArcGIS version 9.3.1) to produce a DSM with a cell size equal to 0·5 m. The LiDAR dataset was checked for accuracy at five separate locations by Geomatics group, using a differential Global Positioning System (DGPS) survey. These ground truth data indicated an average systematic error (or bias) of +0·0004 m and an average random bias of ±0·047 m in elevation. The combined root-mean-square error for these data was 0·029 m, which was well within the product specification of 0·15 m (EAGG 2012, pers. comm).

### *TLS data collection and processing*

Ground-based, terrestrial laser scanning (TLS) systems utilize a similar approach to airborne LiDAR, but typically cover smaller extents at finer spatial resolutions. Unlike airborne LiDAR, TLS systems are deployed from one or more fixed locations on the ground surface and have proven useful in providing data describing spatial structural proxies for peatland ecohydrological condition (Anderson *et al*., 2009; Anderson *et al*., 2010). Here, TLS data were collected *in situ* using a Leica Geosystems HDS 3000 scanner at the Spooners headwater catchment, in January 2011. The scanner collected

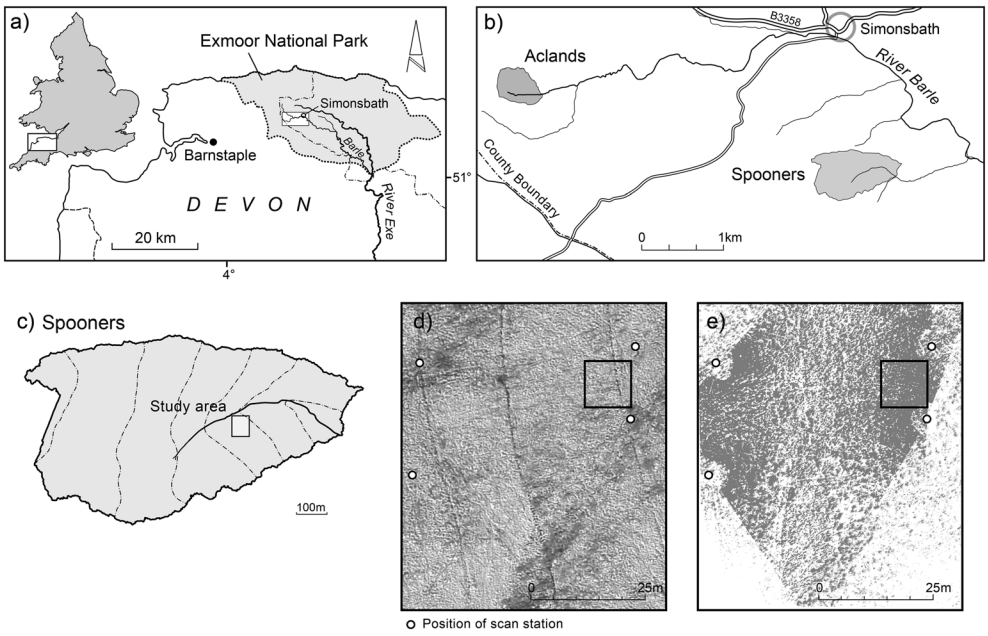


Figure 1. (a) and (b) The location of Aclands and Spooners study catchments and (c) the terrestrial laser scanning (TLS) study area within Spooners watershed defined from airborne Light Detection And Ranging data; (d) and (e) illustrate the study area used for the TLS survey; (d) shows the scan locations and area of interest (AOI) overlaying an aerial photograph of the study area (co-ordinates for upper left 51° 7′23·81″N, 3°45′2·76″W and bottom right 51° 7′ 21·69″N, 3°44′59·70″W); (e) shows the spatial extent of the TLS data collected as a grid, each dot representing one of $>7{\cdot}5\times10^6$ data points.

~1800 points per second spaced at 0·003 m, with a resultant dataset of $>7{\cdot}5\times10^6$ points over a spatial extent of $4{\cdot}2\times10^3\,m^2$ in this example. The instrument uses a green laser (wavelength 532 nm), with a beam size of <6 mm, positional accuracy of <6 mm and range accuracy of <4 mm (at a range of <50 m; Anderson *et al*., 2009). Data were collected from multiple viewpoints above the peatland surface (Figure 2), and were registered into a single point cloud for each site following the method of Anderson *et al.* (2009). Highly visible static stakes were deployed within the survey area to facilitate point cloud registration; their positions were known to an accuracy of 0·005 m following a DGPS survey. To ensure the scanner had sufficient height above the peatland surface and thus an appropriate angle of incidence to the ground, a flat-bedded tracked vehicle was deployed at each of the scan locations providing a stable elevated platform of a consistent height (~2 m) throughout the survey. The site selected for the survey included three artificial drainage ditches measuring approximately 0·3 m × 0·3 m in cross-section and was dominated by vegetation typical of the majority of the hill slope area within the catchment. The vegetation included a mixed soft rush (*Juncus effusus*) and purple moor grass (*Molinia caerulea*) dominated sward in which the *M. caerulea* grew in tussock form.

A DGPS survey was also used to provide validation transects through the TLS scan areas as an independent means of verifying the information content and accuracy of both the TLS and LiDAR datasets during subsequent stages of the analysis. DGPS survey points were taken at 3- to 5-m intervals along a transect, and at each location, the position of the ground surface and the top of the nearest dense grass tussock structures were recorded, creating pairs of measurements along the

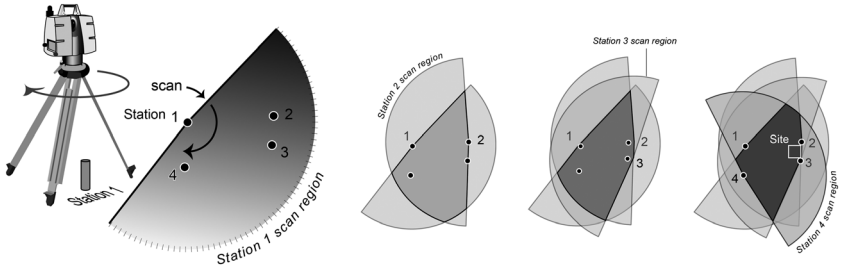


Figure 2. Terrestrial laser scanning data capture locations and respective overlapping scan zones. The darker polygon within the station four-scan region represents the area of greatest point cloud overlap as shown in Figure 1e. The area of interest is indicated, showing that it lies within the zone of maximal point-cloud overlap.

 

transect. The accuracy of the DGPS measurements was ±0·5 cm in *x*, *y* and ±2 cm in *z*. The registered TLS point cloud data were imported into Arc GIS 9.3.1. A 10 m × 10 m area of interest (AOI) was chosen in an area of dense point cloud coverage and to include a known surface-drainage feature.

Subsequent processing aimed to extract the vertical extent of the top of canopy and ground surface, respectively. The highest and lowest *z* values within a moving window filter of 0·05 m × 0·05 m were extracted for the AOI extent and then processed into a 0·01-m discontinuous horizontal grid. A 1-cm grid resolution was chosen to preserve the fine-scale variability of the point cloud in the surface generated. To prevent over-representation of outlying cloud points, the resultant data were then aggregated to a grid with a cell size matching the 0·05 m × 0·05 m filter used. Finally, a continuous 0·01-m grid was interpolated from these data, using the ordinary spherical Kriging method to match the resolution of the discontinuous grid surface. The result was two products – (a) 'TLSmax' – the maximum vertical extent (assumed top of canopy) and (b) 'TLSmin' – the minimum vertical extent (assumed ground surface). For the next stage of processing, the same AOI was extracted from the airborne LiDAR data so that the two datasets could be combined.

### *Combined TLS and LiDAR data analysis*

In order to address hypothesis 1, DSMs generated from both LiDAR and TLS data were compared to understand their information content. A new dataset was derived from the TLSmax, TLSmin and LiDAR data to describe their spatial relationship in three dimensions. Both TLSmax and TLSmin surfaces were classified as either above the height of the LiDAR DSM or below the LiDAR DSM. These classified data were then overlaid on top of a simple hillshade model of both TLSmax and TLSmin to enhance the visual comparison. The percentage of the TLSmax and TLSmin surfaces above and below the LiDAR DSM was then calculated. A transect through both DSMs was plotted alongside the raw TLS point cloud to provide a cross-sectional representation of the relationship between the datasets.

### *LiDAR analysis to discriminate vegetation and anthropogenic structures*

To address hypotheses 2 and 3, a model describing the high frequency spatial variation in LiDAR *z* (height) was needed. Data were filtered using a 'low pass' moving window (11 × 11 pixel neighbourhood) in ERDAS Imagine 2011, resulting in a 'smoothed' surface. These data were subtracted from the original DSM to derive a detrended surface. The low pass window of 11 × 11 pixels was selected to be larger than the maximum patch size of the canopy and microtopographic structure without degrading the signature of the underlying topography. The detrended surface enabled discontinuities in the data to be extracted and classified. For example, step changes could indicate human activity (e.g. drainage ditches or archaeological remains) (Newman, 2010), or areas where the DSM structure changed as a function of shifts in vegetation structure or composition.

Detrended data derived from the LiDAR DSM were used to identify the *x*, *y* position of microtopographic sinks within the peatland (e.g. tussock/hollow topography or drains). Within the detrended data, sinks were identified automatically by selecting pixels with a height (*z*) threshold of −0·11 m. As the *z* values in the detrended data represent the height difference from a smoothed surface, negative values highlighted the microtopographic sinks in the landscape, such as drainage features. A *z* threshold of −11 cm was chosen on the basis of expert field knowledge of this catchment (this was the minimum depth in the model that could highlight known anthropogenic drainage networks). To analyse the resultant layer further, data were processed to calculate the density of the classified pixels in two-dimensional (*x*, *y*) space. Step changes in the density of these pixels were then used to classify the sinks as being either drainage features or vegetation characteristic of wet flushes.

### *Comparison with hydrological models and vegetation maps*

Finally, high-resolution aerial photography (2-cm spatial resolution, collected April 2012) was used for the whole Aclands catchment to define the spatial distribution of six distinct vegetation communities based on the species assemblages outlined by Backshall *et al.* (2001) (wet and dry *M. caerulea*, *Juncus* flush, minerotrophic grassland, wet bog and wet heath). These communities were differentiated using visual changes in canopy structure that were present in the imagery used. The vegetation categories were then manually digitized in order to support interpretation of the RS data analysis under hypothesis 2. Although subjective, this technique identified abrupt changes in vegetation at a finer spatial resolution (0·02 m) than the LiDAR DSM (0·5 m) and was therefore considered sufficiently accurate.

In addition, to support hypothesis 3, the raw LiDAR DSM was interrogated with an overland flow accumulation modelling algorithm based on the methods described in Jenson and Domingue (1988). This methodology includes the removal of topographic sinks to ensure flow connectivity. The resulting stream network was then classified using the Strahler stream order hierarchy (Strahler, 1957). The Jenson and Domingue (1988) model assumes that all precipitation becomes runoff and none is lost to interception or

groundwater. Although this approach is hydrologically simplified, overland flow is often the predominant discharge from upland peatland systems (Charman, 2002; Holden, 2005), and therefore, this simplicity is scientifically justified and appropriate to describe the hypothetical functioning of surface-drainage features in the catchment.

## RESULTS

### *Hypothesis 1: results of combined TLS and LiDAR analysis*

To address hypothesis 1, the difference between topographic patterns from the TLS and LiDAR data was evaluated. The comparison of TLSmin and TLSmax surfaces to the LiDAR DSM (Figure 3) help to quantify the spatial relationship of TLS and LiDAR data in three dimensions. Most strikingly, the patterning evident in Figure 3 illustrates that the linear surface drain feature (highlighted) in the TLSmin surface is almost entirely below the plane of the LiDAR DSM. In the TLSmax surface (Figure 3a), almost all of the areas that are lower than the LiDAR DSM correspond with gaps in the vegetation canopy, and are common to both Figure 3a and b. These locations are visible as shared surface elements and low points in the landscape by both TLSmax and TLSmin. The results in Table I illustrate that 45% of the TLSmin layer is below the plane of the LiDAR DSM. In contrast, for TLSmax, over 87% of the surface is above the plane of the LiDAR DSM. Therefore, if TLS data are considered to be 'correct', LiDAR data overestimate the level of the ground surface in 45% of the AOI and underestimate the vegetation canopy in 87% of the AOI.

Figure 4 provides more detailed illustration of the relationship between these surfaces along an east–west cross-section through the LiDAR- and TLS-derived DSMs within the AOI. The TLS point cloud exhibits significant vertical variation along this transect with an increased density towards the bottom of its range. The TLSmin surface has an overall trend similar to the LiDAR surface (illustrated in Figure 5), although data are more variable than the LiDAR data, falling both above and below the LiDAR DSM in Figure 4. Importantly, there is a region (annotated as Drainage ditch in Figure 4) that falls markedly below the plane of the LiDAR data but also

Table I. Percentage of the TLSmax and TLSmin layers that have $z$ values above and below the plane of the LiDAR-derived DSM.

| Classification | TLSmax surface | TLSmin surface |
|---|---|---|
| % below LiDAR DSM | 13 | 45 |
| % above LiDAR DSM | 87 | 55 |

TLS, terrestrial laser scanning; Light Detection And Ranging, LiDAR; DSM, digital surface model.

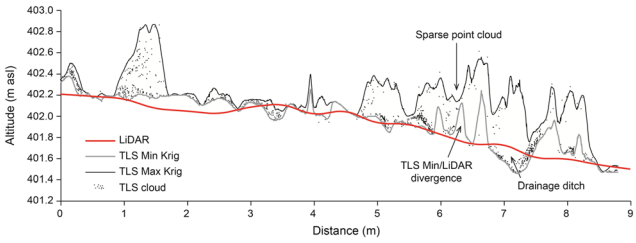


Figure 4. Terrestrial laser scanning (TLS) and Light Detection And Ranging (LiDAR) topographic profiles extracted from the Studied AOI within Spooners Catchment. TLSmax and TLSmin represent the maximum and minimum vertical extent of the TLS data along this transect. Annotations highlight the position of the drainage ditch in the transect and an example of a location where TLSmin and LiDAR surfaces diverge as a result of a sparser point cloud density.

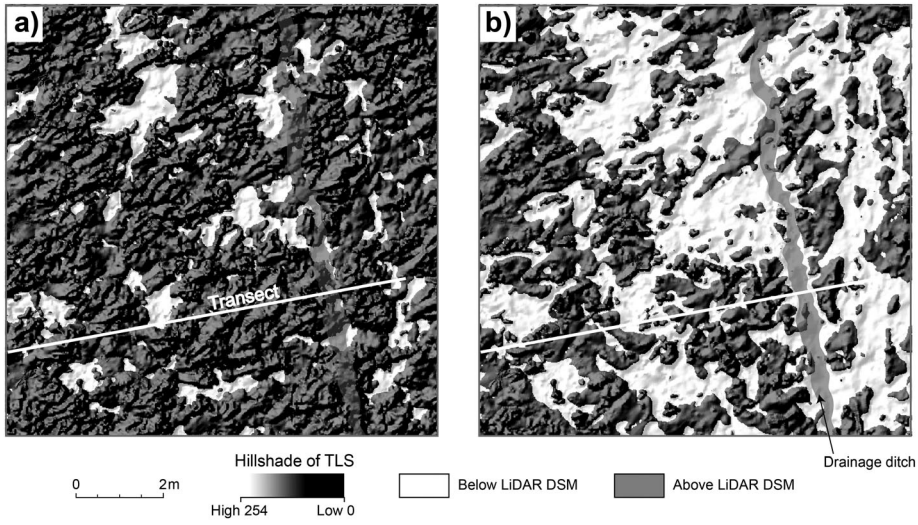


Figure 3. Hillshade models of both (a) terrestrial laser scanning (TLS)max and (b) TLSmin Surfaces for the area of interest. Areas higher than the Light Detection And Ranging (LiDAR) digital surface model (DSM) surface are overlain with black and those below the LiDAR DSM are overlain with white.

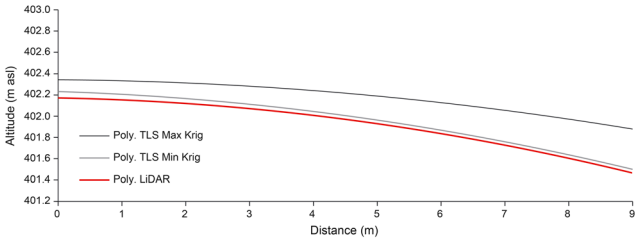


Figure 5. Modelled relationships [second-order polynomial, N = 1040 for terrestrial laser scanning (TLS)max and TLSmin] describing the under-representation of the vegetation canopy (TLSmax) by Light Detection And Ranging (LiDAR) digital surface model data. Data are generated as trends of topographic profiles extracted in Figure 4.

corresponds with the position of a drainage ditch in the landscape. In contrast, the TLSmax surface demonstrates a level consistently above the plane of the LiDAR data both as discrete data (Figure 4) and as an overall trend (Figure 5).

Along this transect, the TLSmax surface also exhibits areas of both high and low variation from the TLSmin surface. In addition, there are six discrete regions in which the TLSmin layer displays increased divergence from the plane of the LiDAR layer (Figure 4). These regions also correspond with positions at which the TLSmax surface peaks and the density of the TLS point cloud noticeably decreases. Plotting DGPS points, measuring the position of the dense tussock structures and the adjacent ground surface across an extended transect, permits a further test of how well the LiDAR data represents the ground surface (Figure 6).

Data in Figure 6 confirm that the LiDAR DSM is largely bounded by the surveyed ground surface and the vertical height of the dense tussock structure in this transect. Furthermore, at any DGPS point pair, the LiDAR surface appears skewed towards *either* the ground surface (DGPS tussock bottom) or the tussock tops, with no consistent bias.

### *Hypotheses 2 and 3: discrimination of vegetation and anthropogenic structures*

The extraction of spatially distinct areas of microtopographic sinks from the detrended LiDAR DSM supports evaluation of both hypotheses 2 and 3. In this analysis, dense areas of microtopographic sinks do not fit the expected position of the discrete linear features known to be anthropogenic drainage features. Figure 7 illustrates the

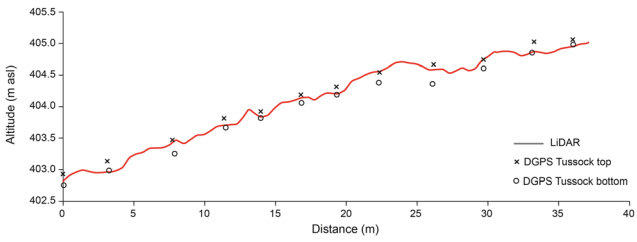


Figure 6. Alternate Light Detection And Ranging (LiDAR) topographic profile extracted from the wider terrestrial laser scanning scan zone (Figure 1) within Spooners catchment. Global Positioning System (DGPS) Survey data describing the maximum and minimum vertical extent of dense vegetation components (tussocks) are included as paired measurements along the transect length.

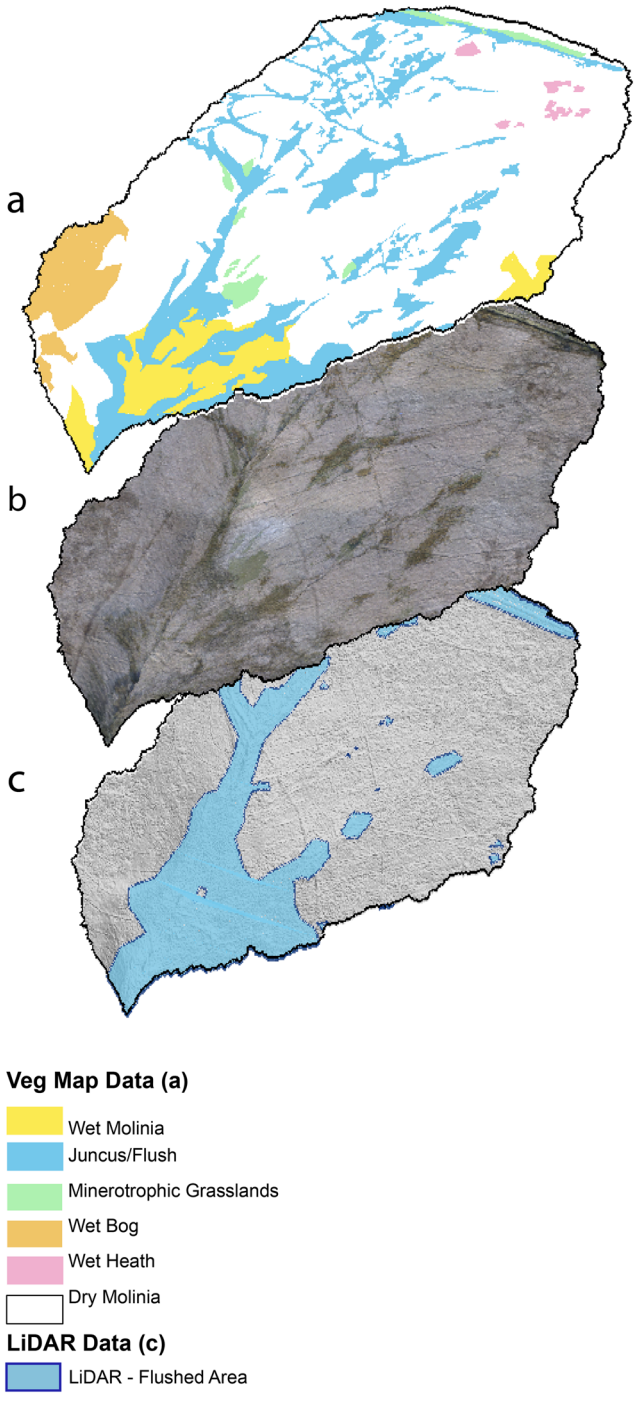


Figure 7. Habitat mapping of Aclands Catchment. (a) Vegetation communities digitized from aerial imagery; (b) high-resolution aerial photograph; (c) flushed vegetation area delineated from classified Light Detection And Ranging (LiDAR) data.

results of manually digitizing dominant vegetation classes across the catchment (Figure 7a) from high-resolution aerial photography (Figure 7b) and comparing these with the dense areas of microtopographic sinks classified from detrended LiDAR data from Figure 7c. Visual comparison of the images suggests that the large extents of wet *M. caerulea* and wet *Juncus* spp. dominated vegetation observed in the catchment are also captured by the LiDAR data as a complex surface characterized by a high density of microtopographic sinks. The contiguous area that is mapped as wet *M. caerulea* and wet *Juncus* spp. from aerial photography represents 15·9% of the catchment, versus 18·6% that the LiDAR classification delineates as dominated by vegetation and microtopography characteristic of flushed areas. The smaller (often linear) areas of *Juncus* spp. in the west of the catchment are, however, not described well by the LiDAR classification.

With respect to hypothesis 3, Figure 8a reveals that anthropogenic landscape features with constrained vertical variation (greater than or equal to −0·11 m) can also be identified and classified using the detrended LiDAR DSM, and the spatial extent of such features delineated and measured. The linear structure of surface drains is visible here as black pixels, alongside the dense areas of microtopographic sinks (blue pixels) used to delineate the flushed (wet *M. caerulea* and wet *Juncus spp dominated*) areas. The linear anthropogenic features extracted using these classifications appear discontinuous across the land surface. Indeed, when the LiDAR DSM is used as an input to simple overland flow routing algorithms (Figure 8b), the anthropogenic drainage features extracted (shown as blue lines) demonstrate only a weak control on these flow pathways (grey scale, darker colours representing higher-order channels). Many higher-order flow accumulation pathways also appear to function entirely independently of the mapped artificial drainage network outlined in blue (Figure 8b), in agreement with the disconnected nature of linear features extracted in Figure 8b. The LiDAR data, although able to detect the two-dimensional location of drainage ditches, do not therefore appear able to quantify whether or not they are continuous drainage features in the landscape.

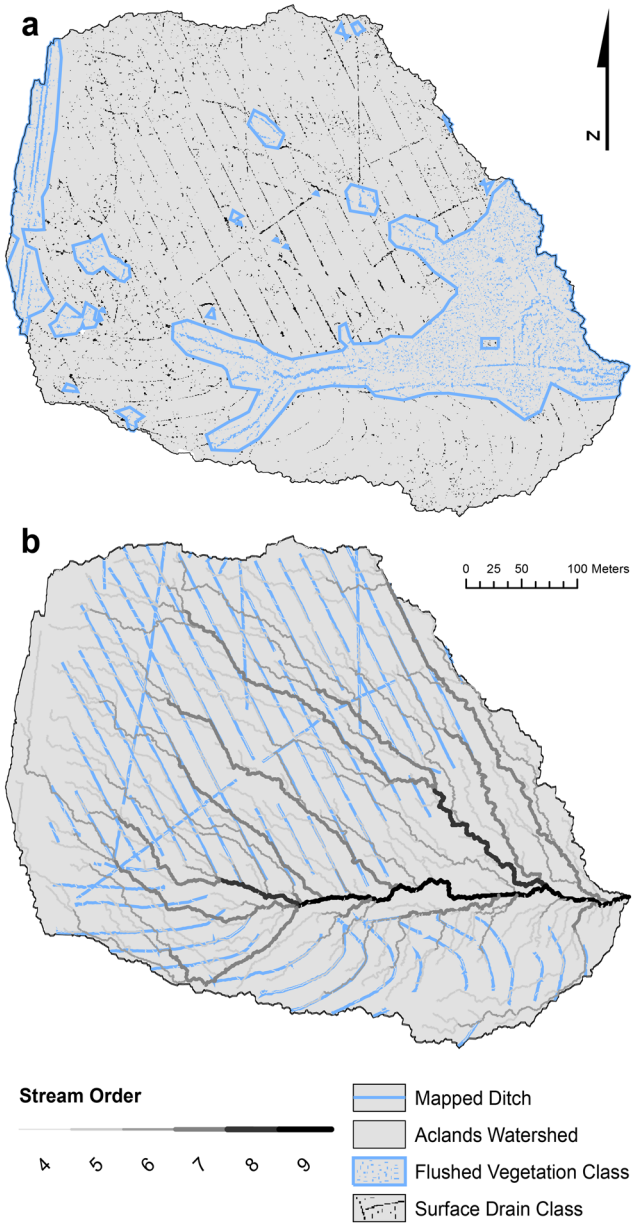


Figure 8. Mapping of surface-drainage. (a) Data extracted from detrended Light Detection And Ranging data (Aclands Catchment) and classified into surface-drainage networks, whether natural or artificial (Black pixels) and rush dominated 'flushed' zones (blue pixels). Pixels were classified using a threshold of pixel density; (b) A simple overland flow accumulation model with streams ordered using the Strahler classification (Strahler, 1957) whereby stream size is classified according to a hierarchy of tributaries. A stream with no tributaries is first order; when two first-order streams meet, they subsequently form a second-order stream and so on. Only fourth- to ninth-order streams are displayed.

## DISCUSSION

Moving beyond qualitative visual analysis of LiDAR data, such as simple hillshade models, is an essential step to quantify landscape-scale ecohydrological functioning and the associated landscape services. Given this, understanding the accuracy with which LiDAR products are able to measure ecohydrologically relevant structures in the uplands is critical if such analysis is to be considered representative of 'real world' structure and subsequent function. This study has shown that although vegetation canopy height and drainage ditch depth are underestimated by airborne LiDAR DSMs, the aerial extent of these features can still be determined in a spatial context. The following sections discuss the various ramifications of these findings.

*Vertical accuracy of LiDAR data – combined LiDAR and TLS analysis*

Hypothesis 1 explored how airborne LiDAR DSMs compare with TLS data, in relation to their abilities to capture structural information about vegetation and topography. Numerous researchers have alluded to the sources of error in a wide range of DSMs (Fisher and Tate, 2006; Li *et al*., 2011; Wise, 2011). However, few authors propose solutions to resolve levels of error with respect to independent measurements (see Aguilar *et al*., 2010; Hodgson and Bresnahan, 2004 for notable exceptions). Herein, we illustrate that the TLSmax and TLSmin surfaces describe the maximum and minimum measured vertical extent of the vegetation canopy at a fine spatial resolution. Therefore, TLS data are extremely useful in describing the information content and error associated with airborne LiDAR data and its ability to describe spatial shifts in vegetation organization. Data presented in Figure 3 illustrate that the LiDAR DSM elevation values correlate with the TLSmin surface far more than they do with the TLSmax surface over the extent of the AOI (87% of TLSmax is above the plane of the LiDAR data). These results demonstrate that the LiDAR data most closely represent the ground surface and not the canopy structure. Furthermore, the highlighted surface drain feature (Figure 3) is entirely below the plane of the LiDAR DSM in the AOI studied. Such underestimation of vegetation canopy heights and the depth of drainage features have important implications where LiDAR-derived structures are used as indicators of ecohydrological condition (Anderson *et al*., 2010), and as inputs to spatially distributed models (Beven, 2012).

More detailed analysis of the magnitude of vertical variation between the LiDAR and TLS layers (Figures 4 and 5) also illustrated that the LiDAR DSM more closely represents a smoothed version of the ground surface (described by the TLSmin data) lacking microtopographic structure. Topographic features, such as the surface-drainage network, are estimated in error in DSM data for the following reasons according to Fisher and Tate (2006):

- variability in the accuracy, density and distribution of source data,
- processing and interpolation and
- characteristics of the terrain surface being modelled.

In this case, the LiDAR DSMs created provide one $x$, $y$, $z$ coordinate for every 0·5-m cell, which is a relatively coarse resolution when compared with the scale of drainage ditch features (often they are only 0·3 m wide in these landscapes). In addition, the dense, low-sward vegetation tussocks disrupt the return of the laser pulse from the ground surface such that microtopographic depressions are not captured consistently, especially when tussock forming grasses occur within, or overhang, surface-drainage pathways (as evident in Figure 3). Therefore, in contrast to forested landscapes, where vegetation is typically less dense and more uniform in height (Vierling *et al*., 2008), it is likely that LiDAR DSMs will always generate an uncertain representation of the ecosystem structure in short-sward ecosystems. In this example, the LiDAR DSM is biased towards the ground surface, as delineated by the TLSmin dataset, which lies consistently close to and above the trend line for the LiDAR DSM (Figure 5).

To understand the specific effect of denser vegetation components on the LiDAR DSM, DGPS survey data were also compared with the LiDAR surface. Figure 6 illustrates that the LiDAR DSM data captured the ground surface *and* dense grass tussock centres reasonably well as a composite surface, with all points falling within the bounds created from the DGPS measurements. This additional data analysis suggests that the LiDAR DSM data represent both the ground surface and the denser components of the vegetation structure *only* and not the sward canopy structure. For an airborne product flown at an altitude of 800–1000 m above ground level, this ability to approximate the range of tussock top-bottom values suggests some promise in using the LiDAR DSM in these low-sward landscapes to assess habitat structure (Vierling *et al*., 2008; Korpela *et al*., 2009; Anderson *et al*., 2010). However, these results highlight the necessity to evaluate the modelled LiDAR surface with finer resolution data prior to inference of ecohydrological structure. Indeed, where LiDAR data are used to provide metrics of habitat condition without three-dimensional validation of observed vegetation structures such as TLS (Streutker and Glenn, 2006; Kincey and Challis, 2009; Korpela *et al*., 2009; Li *et al*., 2011), the certainty with which we can use LiDAR data to understand the condition of these systems spatially is limited.

The TLS data in isolation also provide a useful tool in the quantification of both the ecological and hydrological structure of these upland ecosystems over smaller extents. The technique presented here provides discrete layers, which are useful in measuring vegetation canopy/biomass and the underlying surface structure. Whether used independently or in conjunction with airborne LiDAR, critical evaluation of TLS data is still necessary to ensure robust interpretation. For example, data presented here (Figure 4) illustrate that at locations where the point cloud becomes sparse, the TLSmin layer appears to offer a markedly poorer representation of the underlying ground surface. In agreement with wider studies using TLS (Watt and Donoghue, 2005; Anderson *et al*., 2009), these findings highlight the difficulties of using TLS data to measure complex and fine-scaled vegetation structure *in situ*. In this case, the error is attributable to the method of data generation (Fisher and Tate, 2006), i.e. vegetation canopy completely obscuring the ground from the laser or because the area is subject to shadowing in the point cloud. As such, this deviation of the TLSmin surface from the

LiDAR DSM agrees with the LiDAR data predominantly describing a smoothed ground surface. However, these results illustrate that structural measurements from any platform, even at fine spatial scales, can be subject to the same sources of error in short-sward ecosystem.

*Discrimination of vegetation and anthropogenic structures*

Although the preceding results and discussion demonstrate that LiDAR data underestimate both canopy height and drainage network volume, numerical interrogation of detrended LiDAR data has shown that spatial information on ecohydrologically relevant vegetation communities (hypothesis 2) and anthropogenic drainage features (hypothesis 3) can still be captured. Data in Figure 7 confirm that the detrended LiDAR data can be used to effectively map the extent of flushed (i.e. wetter) vegetation communities. However, the preceding findings suggest that increased surface complexity used to delineate these areas is, in fact, a measurement of the change in the sub-canopy, highlighting microtopographic landforms associated with these waterlogged vegetation communities dominated by *Juncus* spp. and wet *M. caerulea* stands.

Features identified as anthropogenic peatland surface-drainage in this analysis have been validated as being (largely) continuous and connected, following extensive fieldwork and GPS mapping of drainage features at these sites (Figure 8). However, results in Figure 8 suggest that they appear to be highly discontinuous features when detected by LiDAR. Under-representation of microtopographic structure in LiDAR DSMs (Figure 4) explains why such drainage features extracted for the Aclands catchment in Figure 8a appear to be discontinuous. Consequently, these features are shown to have only a limited influence on the flow paths modelled in the flow accumulation model illustrated in Figure 8b, although in reality, they may be highly significant in controlling surface-flow networks. The extent to which such LiDAR data can be relied upon as good representations of microtopography (anthropogenic or otherwise) controlling ecohydrological function is therefore subject to the same implicit error or uncertainty previously discussed (Jones *et al*., 2008). Where such data are used as inputs to numerical hydrological models in peatland landscapes (Rothwell *et al*., 2010), understanding such uncertainty in the representation of drainage structure is critical to ensure the spatial quality of model predictions.

Acknowledging the error and understanding the source of it in such data can also be advantageous to the ecohydrologist. Knowing the nature of the error and its magnitude makes airborne LiDAR data potentially far more powerful as inputs to ecohydrological modelling frameworks. For example, using numerical processing such as 'growing' extracted features (Espindola *et al*., 2006) describing discontinuous drainage features and using these to modify DSM values (Li *et al*., 2011) may allow researchers to represent the connectivity of surface-drainage structures in a modelled catchment more accurately. Subsequently, better predictions of both the spatial distribution of flow routing and resultant downstream hydrographs may result, in turn aiding the quantification of the associated ecohydrological landscape services (Grand-Clement *et al*., 2013). These data also highlight the value of a combined RS approach in confirming assumptions made from any one dataset. For example, cross-validation of modelled surface wetness indices generated from LiDAR and Thermal Airborne Broadband Imager (airborne thermography) data, Luscombe *et al*., 2012 or LiDAR and near infra-red data (Harris and Bryant, 2009) can be performed, enabling the observed ecohydrological patterning to be evaluated prior to integration into numerical modelling of the ecohydrological functioning.

## CONCLUSION

This paper demonstrates that the spatially explicit measurements provided by LiDAR datasets are subject to specific errors, related to both the spatial resolution of the dataset and the interaction of laser ranging systems with short-sward landscapes. Results show that airborne LiDAR data underestimate the vegetation canopy volume/height and volume/depth of surface-drainage networks, both of which are key spatial variables in understanding ecohydrological functioning at a landscape scale. Understanding this uncertainty improves the way in which these data can be used as numerical model inputs, and the confidence that researchers should place on these data when used as a surrogate for field measurements over a variety of disciplines and ecosystems. Furthermore, this work demonstrates that using TLS data, the canopy structure *can* be described at a fine spatial resolution and with greater precision than with LiDAR data, although over far smaller extents. These data illustrate the need to couple LiDAR data with fine spatial resolution altimetry data (i.e. TLS) and field measurements, to improve models of the ecosystem structure and describe the spatial attributes of the ecosystem at a scale that is appropriate to capture the ecohydrological functioning of the landscape.

ACKNOWLEDGEMENTS

We thank the Exmoor Mires Project for helping us with site access and logistics, and the drawing office at the University of Exeter for helping us with maps and figures. We also thank the anonymous referees and the editor for their positive and constructive suggestions during the review process. This research received financial support from South West Water Ltd and the University of Exeter (SK04809).

## REFERENCES


Aguilar FJ, Mills JP, Delgado J, Aguilar MA, Negreiros JG, Perez JL. 2010. Modelling vertical error in LiDAR-derived digital elevation models. *ISPRS Journal of Photogrammetry and Remote Sensing* **65**(1): 103–110.

Anderson K, Bennie J, Wetherelt A. 2009. Laser scanning of fine scale pattern along a hydrological gradient in a peatland ecosystem. *Landscape Ecology* **25**(3): 477–492.

Anderson K, Bennie J, Milton EJ, Hughes PDM, Lindsay R, Meade R. 2010. Combining LiDAR and IKONOS data for eco-hydrological classification of an ombrotrophic peatland. *Journal of Environmental Quality* **39**(1): 260–273.

Backshall J, Manley J, Rebane M. 2001. *The Upland Management Handbook*. English Nature: Peterborough.

Bain CG, Bonn A, Stoneman R, Chapman S, Coupar A, Evans M, Gearey B, Howat M, Joosten H, Keenleyside C, Labadz J, Lindsay R, Littlewood N, Lunt P, Miller CJ, Moxey A, Orr H, Reed M, Smith P, Swales V, Thompson DBA, Thompson PS, Van de Noort R, Wilson JD, Worrall F. 2011. *IUCN UK Commission of Inquiry on Peatlands*. IUCN UK Peatland Programme: Edinburgh.

Barber KE. 1981. *Peat Stratigraphy and Climatic Change*. Balkema: Rotterdam.

Barbier N, Proisy C, Vega C, Sabatier D, Couteron P. 2011. Bidirectional texture function of high resolution optical images of tropical forest: an approach using LiDAR hillshade simulations. *Remote Sensing of Environment* **115**(1): 167–179.

Belyea LR, Clymo RS. 2001. Feedback control of the rate of peat formation. *Proceedings of the Royal Society of London: Biological Sciences* **268**: 1315–1321.

Beven K. 2012. *Rainfall-Runoff Modelling: The Primer*. John Wiley & Sons Ltd.: Chichester.

Beven K, Freer J. 2001. A dynamic TOPMODEL. *Hydrological Processes* **15**(10): 1993–2011.

Charman D. 2002. *Peatlands and Environmental Change*. John Wiley & Sons Ltd.: Chichester.

Chassereau JE, Bell JM, Torres R. 2011. A comparison of GPS and LiDAR salt marsh DEMs. *Earth Surface Processes and Landforms* **36**(13): 1770–1775.

Clawges R, Vierling K, Vierling L, Rowell E. 2008. The use of airborne lidar to assess avian species diversity, density, and occurrence in a pine/aspen forest. *Remote Sensing of Environment* **112**(5): 2064–2073.

Danson FM, Hetherington D, Morsdorf F, Koetz B, Allgower B. 2007. Forest canopy gap fraction from terrestrial laser scanning. *Geoscience and Remote Sensing Letters, IEEE* **4**(1): 157–160.

Drewitt AL, Manley VJ. 1997. The vegetation of the mountains and moorlands of England. English Nature Research Reports. English Nature, pp. 218.

Emanuel RE, Hazen AG, McGlynn BL, Jencso KG. 2013. Vegetation and topographic influences on the connectivity of shallow groundwater between hillslopes and streams. *Ecohydrology* **7**: 887–895. DOI: 10.1002/eco.1409

Espindola GM, Camara G, Reis IA, Bins LS, Monteiro AM. 2006. Parameter selection for region growing image segmentation algorithms using spatial autocorrelation. *International Journal of Remote Sensing* **27**(14): 3035–3040.

Evans M, Lindsay J. 2010. High resolution quantification of gully erosion in upland peatlands at the landscape scale. *Earth Surface Processes and Landforms* **35**(8): 876–886.

Fisher PF, Tate NJ. 2006. Causes and consequences of error in digital elevation models. *Progress in Physical Geography* **30**(4): 467–489.

Fisher B, Turner RK, Morling P. 2009. Defining and classifying ecosystem services for decision making. *Ecological Economics* **68**(3): 643–653.

Grand-Clement E, Anderson K, Smith D, Luscombe DJ, Gatis N, Ross M, Brazier RE. 2013. Evaluating ecosystem goods and services after restoration of marginal upland peatlands in South-West England. *Journal of Applied Ecology* **50**(2): 324–334.

Harris A, Bryant RG. 2009. A multi-scale remote sensing approach for monitoring northern peatland hydrology: present possibilities and future challenges. *Journal of Environmental Management* **90**(7): 2178–2188.

Hinsley SA, Hill RA, Gaveau DLA, Bellamy PE. 2002. Quantifying woodland structure and habitat quality for birds using airborne laser scanning. *Functional Ecology* **16**(6): 851–857.

Hodgson ME, Bresnahan P. 2004. Accuracy of airborne lidar-derived elevation: empirical assessment and error budget. *Photogrametric Engineering and Remote Sensing* **70**(3): 331–340.

Holden, J. 2005. Peatland hydrology and carbon release: why small-scale process matters. *Philosophical Transactions of the Royal Society a-Mathematical Physical and Engineering Sciences* **363**: 2891–2913.

Holden J, Chapman PJ, Labadz JC. 2004. Artificial drainage of peatlands: hydrological and hydrochemical process and wetland restoration. *Progress in Physical Geography* **28**(1): 95–123.

Horning N, Robinson JA, Sterling EJ, Turner W, Spector S (eds). 2010. *Remote Sensing for Ecology and Conservation: A Handbook of Techniques*. Oxford University Press: Oxford and New York.

Hutton C, Brazier RE. 2012. Quantifying riparian zone structure from airborne LiDAR: vegetation filtering, anisotropic interpolation, and uncertainty propagation. *Journal of Hydrology* **442-443**(0): 36–45.

Ivanov KE. 1981. *Water Movement in Mirelands*. Academic Press Inc.: London.

Jenson SK, Domingue JO. 1988. Extracting topographic structure from digital elevation data for geographic information system analysis. *Photogrammetric Engineering and Remote Sensing* **54** (11): 1593–1600.

Jones KL, Poole GC, O'Daniel SJ, Mertes LAK, Stanford JA. 2008. Surface hydrology of low-relief landscapes: assessing surface water flow impedance using LIDAR-derived digital elevation models. *Remote Sensing of Environment* **112**(11): 4148–4158.

Kincey M, Challis K. 2009. Monitoring fragile upland landscapes: the application of airborne lidar. *Journal for Nature Conservation* **18**(2): 126–134.

Korpela I, Koskinen M, Vasander H, Holopainen M, Minkkinen K. 2009. Airborne small-footprint discrete-return LiDAR data in the assessment of boreal mire surface patterns, vegetation, and habitats. *Forest Ecology and Management* **258**(7): 1549–1566.

Lane C, D'Amico E. 2010. Calculating the ecosystem service of water storage in isolated wetlands using LiDAR in north central Florida, USA. *Wetlands* **30**(5): 967–977.

Li S, MacMillan RA, Lobb DA, McConkey BG, Moulin A, Fraser WR. 2011. LiDAR DEM error analyses and topographic depression identification in a hummocky landscape in the prairie region of Canada. *Geomorphology* **129**(3-4): 263–275.

Lindsay R. 2010. *Peatbogs and Carbon*: A Critical Synthesis. University of East London: London.

Luscombe DJ, Anderson K, Grand-Clement E, Le-Feuvre N, Smith D, Brazier RE. 2012. Assessing the ecohydrological status of a drained peatland: combining thermal airborne imaging, laser scanning technologies and ground water monitoring. *EGU General Assembly Conference Abstracts*, Vol. 14, p. 740.

Mitchell PJ, Lane PNJ, Benyon RG. 2012. Capturing within catchment variation in evapotranspiration from montane forests using LiDAR canopy profiles with measured and modelled fluxes of water. *Ecohydrology* **5**(6): 708–720.

Moore PD, Bellamy DJ. 1974. *Peatlands*. Elek Science: London.

Newman P (2010). Domestic and industrial peat cutting on North-Western Dartmoor, Devonshire. An archaeological and historical investigation. In South-West landscape Investigations reports, Dartmoor National Park.

Rango A, Chopping M, Ritchie J, Havstad K, Kustas W, Schmugge T. 2000. Morphological characteristics of shrub coppice dunes in desert grasslands of southern New Mexico derived from scanning LIDAR. *Remote Sensing of Environment* **74**(1): 26–44.

Rothwell JJ, Lindsay JB, Evans MG, Allott THE. 2010. Modelling suspended sediment lead concentrations in contaminated peatland catchments using digital terrain analysis. *Ecological Engineering* **36**(5): 623–630.

Strahler AN. 1957. Quantitative analysis of watershed geomorphology. *American Geophysical Union Transactions* **38**(6): 912–920.

Streutker DR, Glenn NF. 2006. LiDAR measurement of sagebrush steppe vegetation heights. *Remote Sensing of Environment* **102**(1): 135–145.

Taylor J 1983. Peatlands of Great Britain and Ireland. In *Mires: Swamp, Bog, Fen and Moor. 4B Regional Studies (Ecosystems of the World)*, Gore AJP (ed.). Elsevier Scientific: Amsterdam; 1–46.


 

Turnbull L, Wainwright J, Brazier RE. 2008. A conceptual framework for understanding semi-arid land degradation: ecohydrological interactions across multiple-space and time scales. *Ecohydrology* **1** (1): 23–34.

Vierling KT, Vierling LA, Gould WA, Martinuzzi S, Clawges RM. 2008. LiDAR: shedding new light on habitat characterization and modeling. *Frontiers in Ecology and the Environment* **6**(2): 90–98.

Watt PJ, Donoghue DNM. 2005. Measuring forest structure with terrestrial laser scanning. *International Journal of Remote Sensing* **26**(7): 1437–1446.

Wise S. 2011. Cross-validation as a means of investigating DEM interpolation error. *Computers & Geosciences* **37**(8): 978–991.

Zimble DA, Evans DL, Carlson GC, Parker RC, Grado SC, Gerard PD. 2003. Characterizing vertical forest structure using small-footprint airborne LiDAR. *Remote Sensing of Environment* **87**(2-3): 171–182.

# 5 Using Airborne Thermal Imaging Data to Measure Near-Surface Hydrology in Upland Ecosystems

The following paper is included as the fifth chapter of this thesis and is presented in its published format. This chapter falls under the first theme of this research outlined in chapter 1. All references for this paper are included at the end of this chapter, in publication format. This paper was submitted for publication in the journal Hydrological Processes on the 27th of February 2014 and accepted for publication on the 3rd of July 2014.

HYDROLOGICAL PROCESSES
*Hydrol. Process.* (2014)
Published online in Wiley Online Library
(wileyonlinelibrary.com) DOI: 10.1002/hyp.10285

# Using airborne thermal imaging data to measure near-surface hydrology in upland ecosystems

David J. Luscombe,[1]* Karen Anderson,[2] Naomi Gatis,[1] Emilie Grand-Clement[1] and Richard E. Brazier[1]

[1] *Department of Geography, College of Life and Environmental Sciences, University of Exeter, Exeter, Devon, EX4 4RG, UK*
[2] *Environment and Sustainability Institute, University of Exeter, Penryn, Cornwall, TR10 9EZ, UK*

## Abstract:

Upland ecosystems are recognized for their importance in providing valuable ecosystem services including water storage, water supply and flood attenuation alongside carbon storage and biodiversity. The UK contains 10–15% of the global resource of upland blanket peatlands, the hydrology and ecology of which are highly sensitive to external anthropogenic and climatic forcing. In particular, drainage of these landscapes for agricultural intensification and peat extraction has resulted in often unquantified damage to the peatland hydrology, and little is understood about the spatially distributed impacts of these practices on near-surface wetness. This paper develops new techniques to extract spatial data describing the near-surface wetness and hydrological behaviour of drained blanket peatlands using airborne thermal imaging data and airborne Light Detection and Ranging (LiDAR) data. The relative thermal emissivity ($\varepsilon_r$) of the ground surface is mapped and used as a proxy for near-surface wetness. The results show how moorland drainage and land surface structure have an impact on airborne measurements of thermal emissivity. Specifically, we show that information on land surface structure derived from LiDAR can help normalize signals in thermal emissivity data to improve description of hydrological condition across a test catchment in Exmoor, UK. An *in situ* field hydrological survey was used to validate these findings. We discuss how such data could be used to describe the spatially distributed nature of near-surface water resources, to optimize catchment management schemes and to deliver improved understanding of the drivers of hydrological change in analogous ecosystems. Copyright © 2014 John Wiley & Sons, Ltd.

KEY WORDS LiDAR; thermal imagery; peatland; ecohydrology

*Received 27 February 2014; Accepted 3 July 2014*

## INTRODUCTION

Globally, peat-covered landscapes are recognized for their importance in providing valuable ecosystem services such as water and carbon storage, water supply and flood attenuation (Cannell *et al*., 1993; Joosten and Clarke, 2002; Bellamy *et al*., 2005). The UK contains 10–15% of the global resource of upland blanket peatlands (Tallis, 1998; Wilson *et al*., 2010), the formation, functioning and persistence of which are principally controlled by the availability of water and its loss from the system. Downstream, these peatlands also provide significant hydrological inputs to the public water supply system (Worrall *et al*., 2007) and are located at the headwaters of some of the UK's most 'flashy' and therefore flood-prone river systems (Holden *et al*., 2006). However, the hydrology and ecology of peatlands are highly sensitive to anthropogenic disturbance and climatic forcing (Charman, 2002; Reed *et al*., 2009). Surface wetness, water table depth, flow pathways and rainfall run-off dynamics are known to be dramatically modified in damaged and drained peatland landscapes (Holden *et al*., 2004; Holden *et al*., 2006; Wilson *et al*., 2010). Consequently, understanding the spatial heterogeneity of the water resource and topography in these landscapes is crucial in effectively managing the peatland resource and its ecosystem services. Accordingly, there is a growing need for accurate, spatially distributed information describing the hydrological condition of these upland ecosystems (Harris and Bryant, 2009). Such information could be used to optimize and focus catchment management schemes and allow for enhanced understanding of the drivers of hydrological change (Grand-Clement *et al*., 2013).

Currently, baseline and post-restoration monitoring of hydrological parameters in peatlands is limited, and in many cases, data are not fully spatially interrogated or structured (Wilson *et al*., 2010). The widespread availability of fine-scale remote sensing technologies for quantifying landscape structure and function presents an opportunity to improve understanding of the hydrological

*Correspondence to: David J. Luscombe, Department of Geography, College of Life and Environmental Sciences, University of Exeter, Amory Building, Rennes Drive, Exeter, Devon EX4 4RG, UK.
E-mail: d.j.luscombe@exeter.ac.uk

functioning of these systems over landscape extents (Schultz and Engman, 2011). Already, there is evidence that airborne Light Detection and Ranging (LiDAR) data can provide useful data for monitoring habitat vegetation structure and landscape morphology as proxies for hydrological condition (Clawges *et al*., 2008; Vierling *et al*., 2008; Horning *et al*., 2010; Chassereau *et al*., 2011). In peatlands, these data have been used to describe vegetation and surface structure in order to improve interpretation of ecohydrological function (Anderson *et al*., 2009; Anderson *et al*., 2010; Luscombe *et al*., 2014). LiDAR technology is also becoming increasingly widely used by scientists at the landscape scale to describe the complexities of wetland and fluvial ecosystems and to develop numerical models that quantify the hydrological functioning of these systems (James *et al*., 2007; Vierling *et al*., 2008; Korpela *et al*., 2009; Anderson *et al*., 2010; Bertoldi *et al*., 2011; Hutton and Brazier, 2012). For example, studies exist that show the use of LiDAR digital elevation models (DEMs) for deriving flow accumulation, rainfall run-off estimates and indices of spatial near-surface wetness (Lamb *et al*., 1998; Beven and Freer, 2001). All such numerical models are inherently uncertain, (Beven, 2012) and independent spatially distributed information (rather than or in addition to discrete *in situ* observations) describing hydrological parameters or conditions would help towards validating the complex story of water storage and loss in these systems.

There is an opportunity in using multi-sensor approaches to address this challenge, by combining LiDAR with other remote sensing tools that can more directly describe spatial variability in indicators of near-surface wetness. A relatively under-explored option in this domain is the use of airborne thermal imagery (sometimes called 'thermography'), which can characterise spatial patterns in landscape relative thermal emissivity ($\varepsilon_r$). Such data can, in theory, indicate patterns of land near-surface wetness (Price, 1980) because $\varepsilon_r$ is reliant upon the relatively high specific heat capacity (C) of water (4.1855 J g $K^{-1}$ at 15 °C, 101.325 kPa) and its ability to resist heat loss being higher than surrounding landscape components. In cool air temperatures, water masses can consequently appear warm relative to their surroundings, and in a landscape context, this could facilitate detection of the relative moisture content of the soil (Price, 1980; Campbell, 1996). There are some complexities – e.g. $\varepsilon_r$ provides only a relative thermal measurement that will vary according to the thermodynamic properties of the surface (i.e. wet *vs* dry masses) and/or the ability of a material or structure to retain or emit energy (Anderson and Wilson, 1984; Campbell, 1996). Therefore, more highly structured vegetation (e.g. trees) will have higher relative measurements of $\varepsilon_r$. Similarly, changes in topography can affect the mixing of air masses and the measured $\varepsilon_r$ because of the relative position of the sensor (Torgersen *et al*., 2001). Such effects cause equifinality in the interpretation of these data in heterogeneous landscapes and have previously limited the use of thermal airborne imaging (Quattrochi and Luvall, 1999).

Using LiDAR and airborne thermal imagery together, we propose that vegetation composition and structure may be 'disentangled' from other features and used to understand the nature of underlying surface wetness and the associated ecohydrological processes. Furthermore, models of surface flow pathways and wetness indices generated from LiDAR Digital Surface Models (DSMs) may then be integrated alongside the extent of near-surface wetness available from airborne thermal imaging data, to improve the understanding of near-surface water flow pathways in peatlands.

### *Aims and hypotheses*

This paper develops new techniques aimed at understanding the near-surface hydrological information contained within fine-scale thermal remote sensing data of an upland peatland catchment. The study utilized data from the Itres Instruments Thermal Airborne Broadband Imager (TABI) coupled with simultaneously collected data from an airborne LiDAR sensor (ALTM Gemini (08SEN230) LIDAR instrument). The research explores how TABI data can be used to understand, and potentially quantify, near-surface wetness in such wetlands.

This paper tests the following hypotheses:

(1) Patterning evident in unprocessed $\varepsilon_r$ data from airborne TABI thermographs is spatially associated with the position of anthropogenic drainage networks.
(2) Structural data from LiDAR data sets covering the same extent as $\varepsilon_r$ data distinguish areas where structure or wetness dominates emissivity measurements.
(3) Structurally normalized TABI $\varepsilon_r$ data are related to the spatial distribution of near-surface wetness in an upland peatland.

## METHODS

### *Study area and data collection*

Our approach employed airborne LiDAR and TABI data captured and processed by the UK Environment Agency Geomatics Group in May 2009. The Itres Instruments TABI provided thermal imagery at 2 m × 2 m spatial resolution and better than 0.1 °C noise-equivalent temperature difference. LiDAR data were collected using an ALTM Gemini (08SEN230) LIDAR instrument and were supplied as a pre-derived but unfiltered DSM data set, with a 0.5 m × 0.5 m spatial resolution. The LiDAR data set was checked for accuracy at five separate locations by the Geomatics group, using a Differential Global Positioning System survey. These ground truth data indicated an

average systematic error of +0.0004 m and an average random bias of ±0.047 m in elevation. The combined root-mean-square error for these data was 0.029 m, which was within the product specification of 0.15 m (pers. comm. EAGG, 2012).

The $\varepsilon_r$ data from TABI describe the thermal energy emission of an observed mass or structure (Avery and Berlin, 1992). However, as $\varepsilon_r$ data are not fully calibrated to land surface temperature or material emissivity (the ratio of thermal emission to that of a black body of the same temperature), the data obtained only provide relative values. Furthermore, the resultant $\varepsilon_r$ data contain measurements describing the temperature of the observed surface combined with the effect of the material emissivity of the target. The TABI and LiDAR data were collected at a single flying height (800–1000 m above ground level), and because of the different radiometric properties of the two sensors, this gave rise to data sets with different spatial resolutions.

Data were extracted for a highly instrumented experimental headwater catchment in Exmoor National Park named 'Spooners' (51°7′26.77″N, 3°44′55.96″W, elevation range 376–443 m asl). The catchment was selected to include a representative range of drainage ditch morphology, slope morphology, aspect and vegetation composition typical of the area and to exclude land use types not representative of the wider peatland landscape in Exmoor National Park. The location of the watershed of the study catchment is shown in Figure 1 alongside visualizations of the visible and LiDAR data available for that watershed.

*Initial exploration of patterns in the data*

To understand the broad-scale landscape patterning evident in the TABI data set, a preliminary exploration of the data was undertaken. Spatial patterns in $\varepsilon_r$ over the catchment were examined by first overlaying the TABI data set on a LiDAR elevation model and then assigning colours to the measured $\varepsilon_r$ values and stretching the colour ramp to increase visual differentiation of $\varepsilon_r$. The thematic analysis of this data sought to inform later stages of the data processing.

*Association of TABI with surface drainage*

The locations of anthropogenic drainage channels within the Spooners catchment were initially identified using fine-scale aerial photography. Subsequently, in 2011, the channel positions were mapped and verified during detailed site walkovers. A hand-held GPS unit with a spatial accuracy of <1 m (Thales Navigation, MobileMapper CE) was used to record the position of these features. Once identified, each drain was measured by walking the length of the feature, and new line segments were recorded where any step change in the morphology or vegetation on the surface drain was evident. Each line segment therefore had metadata describing the approximate height, width, cross-sectional profile and dominant vegetation recorded. These linear vector features were subsequently exported from the GPS and overlaid onto the TABI $\varepsilon_r$ data set within ArcGIS. This allowed hypothesis 1 to be evaluated as it was then possible to understand the spatial relationship between the locations of drainage features and the patterns evident in the TABI $\varepsilon_r$ data set.

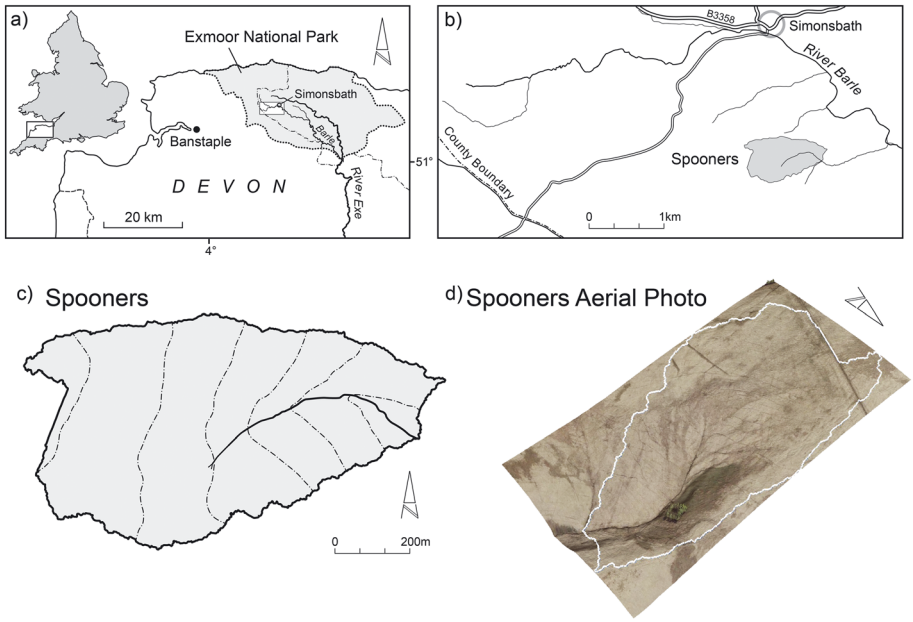


Figure 1. a) Location of the Spooners Catchment within the UK and b) Exmoor national park. c) LiDAR-derived Spooners Watershed and slope contours. d) Aerial photograph of Spooners catchment stretched over LiDAR DEM

*Normalizing TABI data using structure*

*Exploring spatial and vertical structures in vegetation across the catchment*. The first stage in understanding how best to correct the TABI $\varepsilon_r$ data for structural variability was to assess the nature of changes in the surface structure across the catchment. Firstly, data subsets were generated for nine areas of interest (AOIs) measuring approximately 20 m × 20 m. These were three manually selected areas of high (>0.64), intermediate (−1.51 to −2.6) and low (<−2.60) $\varepsilon_r$ pixel values identified in the raw TABI $\varepsilon_r$ data (classified using the Jenks natural breaks method) that were large enough to accommodate the AOI neighbourhood. The location of these is shown in Figure 2.

Using the LiDAR data, each AOI was analysed geostatistically to quantify the scale of surface patterns in the detrended LiDAR DSM. In each case, LiDAR data were first numerically filtered using a 'low pass' moving window across the data using an 11 × 11 pixel neighbourhood, resulting in a 'smoothed' surface. These data were then subtracted from the original data set to derive a 'detrended' data set showing only the high-frequency spatial variation. Secondly, the geostatistical approach employed semivariogram analysis in which dissimilarity ($\gamma$) of pairs of points ($N$) are described as a function of separation distance ($h$) across the surface, as in the empirical variogram in Equation 1. This technique describes the spatial dependence of values in the LiDAR DSM AOI data subsets (Anderson *et al*., 2009).

$$\hat{\gamma}(\boldsymbol{h}) := \frac{1}{|\boldsymbol{N}(\boldsymbol{h})|} \sum_{(i,j)\in \boldsymbol{N}(\boldsymbol{h})} \left|z_i - z_j\right|^2 \qquad (1)$$

An ordinary spherical model was fitted to the resultant data for each AOI as this was found to best fit the empirical semivariograms generated. Alongside the model, three key parameters derived from this analysis are the sill variance, which describes the total variability [of height ($z$) values] in the data, the nugget, which describes error and variability below the sampling interval (pixel size), and the range. Importantly, the range describes the distance at which values cease to show spatial autocorrelation and therefore is indicative of the length scale of the measured surface structure. These parameters were extracted for each of the AOIs for comparison. A descriptive classification of the dominant vegetation community was also created for each AOI from super-high resolution (0.2 × 0.2 m cell size) aerial photography collected in March 2012 and confirmed with field surveying. Vegetation was classified broadly into areas dominated by *Juncus* spp. (soft rush), *Molinia caerulea* (purple moor grass), wet bog communities and minerotrophic grassland communities. *Molinia*-dominated areas were also classified as having 'wet' or 'dry' ground surfaces as this species can physiologically adapt to wetness and persist in both situations. These data were used to inform the optimal method for generating surface roughness estimates from LiDAR.

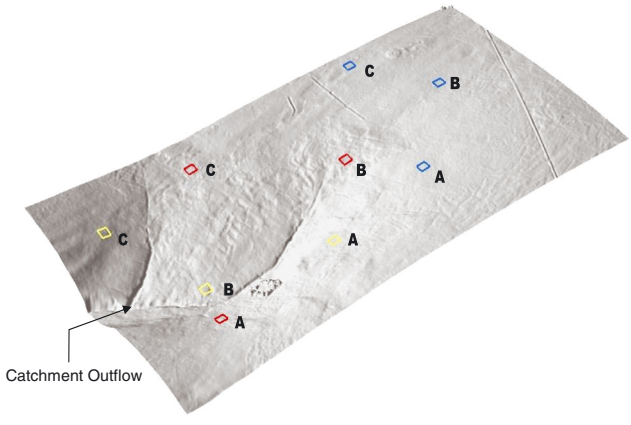


Figure 2. Location of areas of interest (AOIs) measuring approximately 20 m × 20 m. Selected areas of high (red, >0.64), intermediate (yellow, −1.51 to −2.6) and low (blue, <−2.60) pixel values identified from the raw TABI. A, B and C denote each triplicate for each classification

*Generating a structural index of surface roughness from LiDAR*. As $\varepsilon_r$ are known to be in part affected by the structural attributes of an observed surface (Campbell, 1996), it was necessary to take steps towards normalizing the TABI $\varepsilon_r$ data set for surface roughness changes. An index of surface roughness could be easily calculated for each LiDAR pixel. This was achieved using the method described fully in Jenness (2004), whereby the triangular surface area of each pixel is calculated and then divided by the respective planar surface area. The result is a ratio between the planar and the angular surface areas, which is indicative of a surface roughness index (SRI). This method, combined with the fine resolution DSM used, results in a more accurate measure of 3D topographic roughness in the LiDAR than detrending the data and deriving a neighbourhood standard deviation index of roughness (Cavalli *et al*., 2008), because the values in the wider neighbourhood of the pixel do not influence the calculation result (Jenness, 2004). The derived data were deemed most appropriate to test the full structural associations (i.e. $x$, $y$ and $z$ variations) with measured $\varepsilon_r$ values in the TABI data set. These data were also processed in Esri ARCGIS v. 9.3.1, to aggregate pixel values from the 0.5-m LiDAR data to a 2-m resolution, so as to match the spatial resolution of the TABI data set with which it was compared. Prior to full normalization using these data, it was necessary to rescale the SRI data layer and the TABI $\varepsilon_r$ layer to between 0 and 1, to ensure representative control on the output values. The result of this processing was a re-scaled 2-m SRI data set that could be used to normalize the re-scaled TABI $\varepsilon_r$ data.

*Normalizing TABI according to a LiDAR-derived SRI.* The resultant data were used to create a normalized TABI data set of the same extent and spatial resolution by calculating a simple ratio of emissivity to 'roughness', i.e. TABI $\varepsilon_r$ divided by SRI index value. The result was a 2-m normalized TABI $\varepsilon_r$ data set that could be used to assess non-structurally related changes in $\varepsilon_r$ across the catchment in relation to field validation data. Derived data were also non-dimensional (i.e. unitless) however, as TABI data are only examined as relative measurements in this study; this did not affect further analysis.

*Validation of normalized TABI*

In order to validate the hypothesized spatial distribution of surface wetness evident in the TABI data (hypothesis 3), field measurements of surface wetness were required as an independent test data set. Data were collected at 100 randomly located points within the catchment that were predetermined according to a random point generator in ArcGIS version 10. Each of the point locations within the catchment were identified using the same hand-held GPS as previously described and visited in December 2013. The presence or absence of the water table from the surface to a depth of $>10$ cm was recorded at each point, against a nominal four-class scale (Table I). A $0.1\,m \times 0.1\,m \times 0.2\,m$ test pit was used to measure depth of water table where it was not visible at the surface. This classification system was used because instrumentation (delta-t theta probe) trialled at the catchment in 2012 to record soil surface moisture content failed to differentiate water content within any of the peat soils examined, and all readings were returned as showing full saturation. The four-point scale was also straightforward to capture across a large number of points and allowed differentiation between observed surface wetness characteristics throughout the catchment. The locations and values of these 100 points were imported into ArcGIS and overlaid on the normalized TABI data set developed in the previous stage. To aid the visual comparison of these data with $\varepsilon_r$, the points were then interpolated using a simple Natural Neighbour (NN) algorithm in ArcGIS 10. The result was an interpolated map of estimated *in situ* surface wetness that could be used as an independent comparison with the information content of the roughness-normalized TABI $\varepsilon_r$ data. The interpolated data allow for a simple visual comparison of the spatial patterning of these data across the catchment extent. However, as the interpolated data set uses nominal integer values as an input, further quantitative interrogation of these data would include error propagated via the NN interpolation. As such, quantitative analysis was based on the 100-point measured data set.

Table I. Nominal four-point scale for recording near-surface water conditions at the catchment

| Value criteria | Field wetness scale value |
|---|---|
| Depth to water table $>0.1$ m | 1 |
| Depth to water table $<0.1$ m | 2 |
| Depth to water table $=0$ m | 3 |
| Surface water | 4 |

## RESULTS

*Initial exploration of patterns in the data*

Figure 3 shows an overlay of the raw TABI data set over a basic topographic hillshade model from the LiDAR data. Areas of higher emissivity (red) appear to be concentrated in topographic sinks and also form linear and connected features across the wider catchment indicative of the surface flow networks found in upland peatland landscapes. Areas of higher $\varepsilon_r$ also appear coincidental with large structural features such as the square tree-bordered enclosure and the boundary fence lines. These findings supported further examination of the relationship between TABI data and models of land surface structure derived from LiDAR data.

*Association of TABI with surface drainage (hypothesis 1)*

A simple comparison between raw TABI $\varepsilon_r$ and drainage networks (Figure 4) illustrates that in those areas where anthropogenic drainage networks are intact and functional, $\varepsilon_r$ is generally lower. Rapid transitions between higher and lower $\varepsilon_r$ also appear to be coincidental with the direction and location of drainage features (arrow 3, Figure 4). Assuming that those areas where drainage features are present are less likely to hold significant surface water, this finding suggests the areas with higher $\varepsilon_r$ may be wetter. However, areas of high surface structure variability (hitherto referred to as roughness) such as trees (arrow 2, Figure 4) appear to exert a very strong control on the recorded $\varepsilon_r$ value. Some transitions in $\varepsilon_r$ also appear to be independent of any drainage features (arrow 1, Figure 4).

*Normalizing TABI data using structure (hypothesis 2)*

*Exploring spatial and vertical structures in vegetation across the catchment.* The geostatistical interrogation of the detrended LiDAR data in each AOI provides further information on the relationship between roughness and $\varepsilon_r$. The semivariogram models plotted for each AOI in Figure 2 (key statistics extracted in Table II) demonstrate significant variation relating to the vertical scale and variability of the structures present in each area.

Firstly, Figure 5 shows that for the three AOI types shown in Figure 2 [with high (red), intermediate (yellow) and low (blue) thermal emissivity], the semivariogram

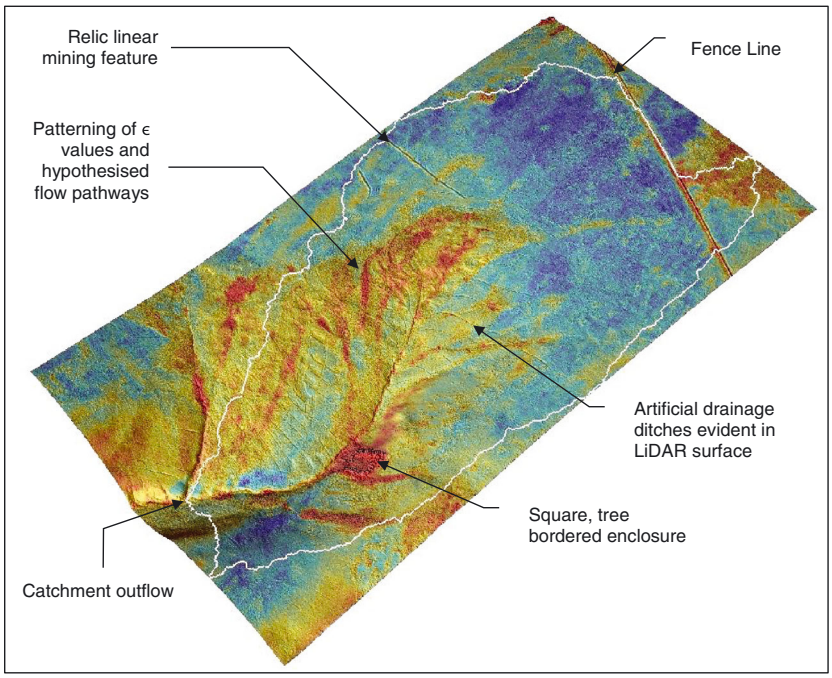


Figure 3. Raw TABI data overlain onto a LiDAR-derived DSM and hillshade model. Red areas denote higher emissivity and blue areas lower emissivity. Features of note are highlighted with arrows and labelled accordingly. White line denotes LiDAR-defined catchment watershed

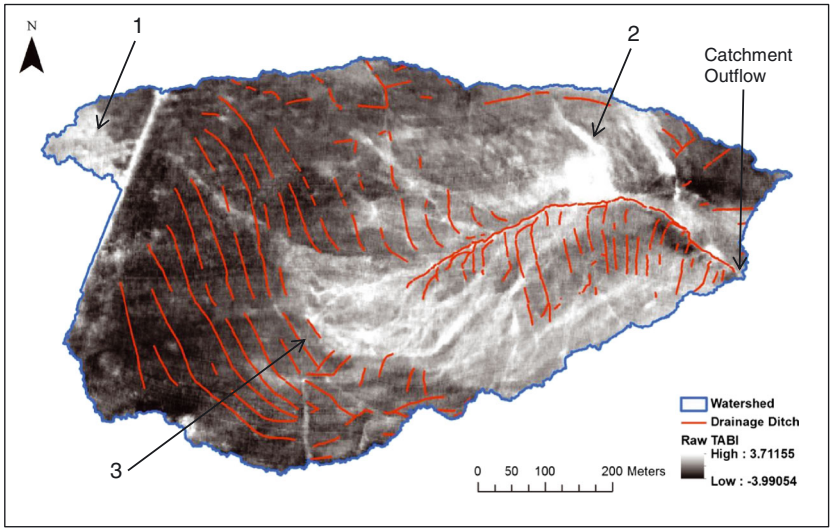


Figure 4. The spatial association of raw TABI data and mapped anthropogenic drainage networks. Arrows labelled as 1, 2 and 3 relate to points made in the accompanying text

range values (Table II) show little variation. Range values are indicative of the length scale (patch size) of surface features within each AOI and only vary between 1.38 and 2.43 m across all of the AOIs studied. This indicates that the patch size of the vegetation exhibits low spatial variation across the catchment and corroborates results from other studies that show similar length scales in peatland vegetation pattern (Anderson *et al.*, 2009). This finding shows that the horizontal scale of the vegetation patterning across these AOIs is quite consistent regardless of $\mathcal{E}_r$.

In contrast, Figure 5 shows that the total variability in DSM height is much more variable from site to site, as indicated by changes in sill variance across these AOIs. AOIs with higher $\mathcal{E}_r$ are shown to have the highest sill variances (and thus the highest total spatial variation in LiDAR DSM height), whereas areas of low $\mathcal{E}_r$ have the lowest sill variances (and thus lower total spatial variation

Table II. Summary statistics, semivariogram model parameters and vegetation classification of each area of interest attributed to each triplet class shown in Figure 2

| Classes of emissivity (see AOIs in Figure 2 and semivariograms in Figure 4) | | Emissivity mean (SD) | Semivariance parameters | | | Dominant land cover |
|---|---|---|---|---|---|---|
| | | | Nugget | Partial sill | Range | |
| Red (high emissivity) | A | −0.39 (0.37) | 0.003 | 0.003 | 2.14 | *Juncus effusus* flush |
| | B | −0.44 (0.26) | 0.001 | 0.003 | 1.90 | Wet bog |
| | C | −0.22 (0.37) | 0.002 | 0.004 | 2.37 | Wet *Molinea caerulea* |
| Yellow (intermediate emissivity) | A | −2.05 (0.15) | 0.000 | 0.001 | 1.93 | Minerotrophic grassland |
| | B | −2.11 (0.15) | 0.003 | 0.003 | 1.78 | *Molinea caerulea* |
| | C | −2.15 (0.32) | 0.002 | 0.003 | 2.43 | Dry, with stands of *Molinea caerulea* |
| Blue (low emissivity) | A | −2.94 (0.16) | 0.001 | 0.001 | 1.53 | Dry, with stands of *Molinea caerulea* |
| | B | −3.12 (0.13) | 0.001 | 0.001 | 1.38 | Dry, with stands of *Molinea caerulea* and *Juncus effusus* |
| | C | −2.97 (0.15) | 0.001 | 0.001 | 1.78 | Dry *Molinea caerulea* |

AOIs, areas of interest; SD, standard deviation.

in LiDAR height). Areas of intermediate $\varepsilon_r$ are seen to have a spread of sill variance values. This relationship may suggest that the areas with higher $\varepsilon_r$, which may be wetter, exhibit taller and more variable vegetation or microtopographic structure, e.g. dense *Juncus effusus* rush stands or separated *Molinia* tussocks where the vegetation and surface structure is more spatially separated allowing water to flow between plants. Indeed, the vegetation classes associated with these AOIs support this assumption with all three of the AOIs with the highest $\varepsilon_r$ values having characteristic 'wet' vegetation communities (Table II). Given this finding, and the assumption that roughness may directly affect $\varepsilon_r$ values, it was necessary to take steps to normalize the effect of this structure on recorded $\varepsilon_r$.

*Generating a structural index of surface roughness from LiDAR*. The index of roughness (SRI) generated from LiDAR data resulted in a raster data set with distinct patternation illustrating a square tree-bordered enclosure, multiple anthropogenic drainage ditches and patternation indicative of shifts in ecological structure across the catchment (Figure 6). Once aggregated to a pixel size equivalent to that of the TABI data set (2 m), these data were used to derive fine-scale normalization of the TABI data using this structural proxy.

*Normalizing TABI according to a LiDAR-derived SRI*. The normalization of the TABI data generated a data set describing $\varepsilon_r$ without the direct influence of vegetation and surface structure. Figure 7 illustrates that the square tree-bordered enclosure and key areas of the channel network (with incised fluvial topography) are 'corrected' so that they now show reduced relative $\varepsilon_r$ values. This result suggested that the method was successful in mitigating the effect of structure on $\varepsilon_r$.

*Validation of normalized TABI (hypothesis 3)*

*Field survey of surface moisture variations*. Data displayed in Figure 7 illustrate a clear spatial relationship between those areas with a higher mapped wetness value and higher normalized $\varepsilon_r$, with both hypothesized areas of surface wetness and known drainage features corresponding well. Assuming that $\varepsilon_r$ is describing wetness to some level, this relationship suggests that patterns of $\varepsilon_r$ in this catchment are describing patterns of wetness related to important hydrological processes. It is important to note that there was a time lag between the remote sensing survey and the ground wetness survey, but hydrological conditions were not known to have changed between these dates, so the comparison should be robust.

*Interpolated model of field-validated surface moisture variation*. Interpolation of these field wetness measurements using an NN algorithm produced a clear visualization of results previously shown in Figure 7. These data (Figure 8) also support the spatial association between surface wetness and $\varepsilon_r$ across the entire catchment. However, as this interpolation technique is numerically simple and unconstrained by surface channels or drainage features, some areas of wetness appear to be overrepresented in the resultant data set.

*Intercomparison of $\varepsilon_r$ and field model*. The spatial association between the normalized TABI values and recorded surface wetness are illustrated in Figure 9 as a boxplot of the normalized $\varepsilon_r$ recorded at each of the field survey points ($n = 100$), split into each of the four wetness classes (table I). These data illustrate that $\varepsilon_r$ increases with increasing surface wetness and that the areas with the highest measured surface wetness demonstrate a consis-

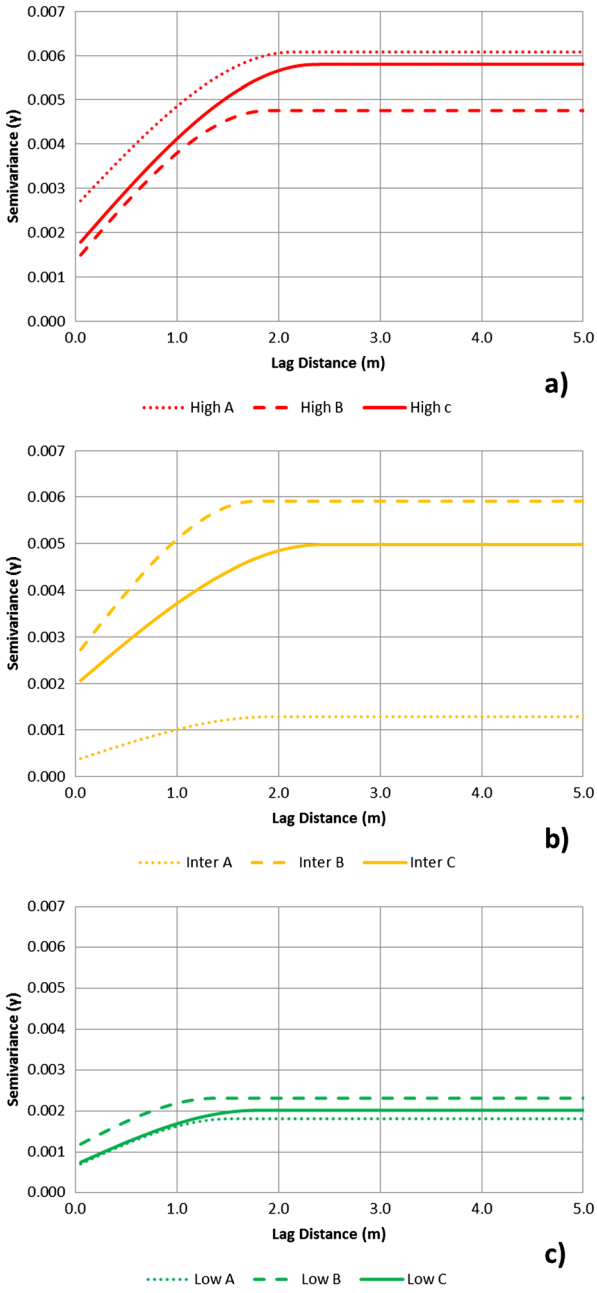


Figure 5. Ordinary spherical semivariogram models for the detrended LiDAR data AOI subsets shown in Figure 2. Each plot groups each AOI triplet that exhibit statistically similar ε values in the TABI data set. a) high, b) intermediate and c) low ε values. For all semivariogram models, the lag size used to create the plot is the same as the spatial resolution of the data (0.5 m)

tently higher $\varepsilon_r$ value. Variation evident in these data is likely to be due to the compound effect of several factors:

(1) unconstrained interpolation of wetness associated with constrained wetness pathways, i.e. drainage channels and ditches;
(2) temporal separation in the sampling of the data sets;
(3) microclimatic variation due to the topographic/structural constraint of air masses; and
(4) the direct effect of using integer scores in assessing $\varepsilon_r$; i.e. as wetness values at each location are discrete, the modelled or actual values of surface wetness are always subject to an implicit uncertainty.

Simple statistical analysis of the variance in $\varepsilon_r$ within each wetness class, (Kruskal–Wallis test) suggests that overall, emissivity values vary significantly ($p < 0.001$) between the wetness classes. Further post hoc analysis of these data (Mann–Whitney *u*-test) suggests that alternate groups (i.e. 1–3 and 2–4) are statistically different from one another ($p < 0.05$) and that the direct difference between groups 3 and 4 is also significant ($p < 0.05$). These data, therefore, are strongly suggestive of wetness directly controlling the measured $\varepsilon_r$.

## DISCUSSION

A spatial understanding of how the water is distributed in peatland landscapes is key to understanding ecosystem services and modelling hydrological functioning of peatland catchments (Harris and Bryant, 2009). For a peatland landscape that may be dominated by saturation excess overland flow (Charman, 2002; Grayson *et al.*, 2010), the spatial distribution of near-surface wetness over large spatial extents provides important information in the understanding of hydrological and ecological conditions (Goward *et al.*, 2002). Although numerous studies model the spatial distribution of surface wetness (Lamb *et al.*, 1998; Beven and Freer, 2001; Gallart *et al.*, 2007), there are few studies that show how near-surface wetness can be measured across large spatial extents to support such work. In response to our three hypotheses, we have found the following:

(1) Patterning evident in unprocessed $\varepsilon_r$ data from airborne TABI thermographs is spatially associated with the position of anthropogenic drainage networks.

Our initial analysis shown in Figure 4 indicated a visual spatial association between areas of high and low emissivity from TABI and the presence of anthropogenic drainage channels in the catchment. Given the position of the patterning in raw $\varepsilon_r$ relative to channels in the peatland (Figure 4), it is reasonable to conclude that these data could be used to describe relative near-surface wetness across the catchment and that this technique presents a new method to evaluate and map the distribution of near-surface water in analogous catchment systems.

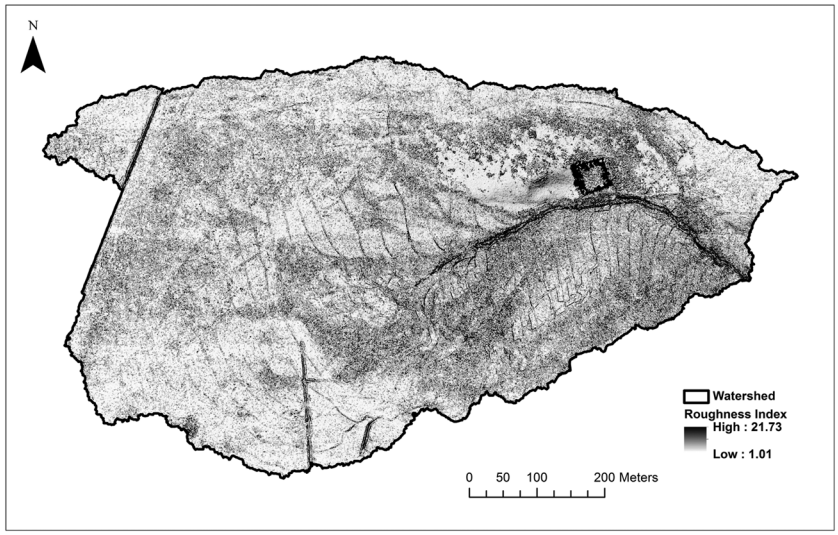


Figure 6. Surface roughness index used to normalize TABI data for land surface and vegetation structure

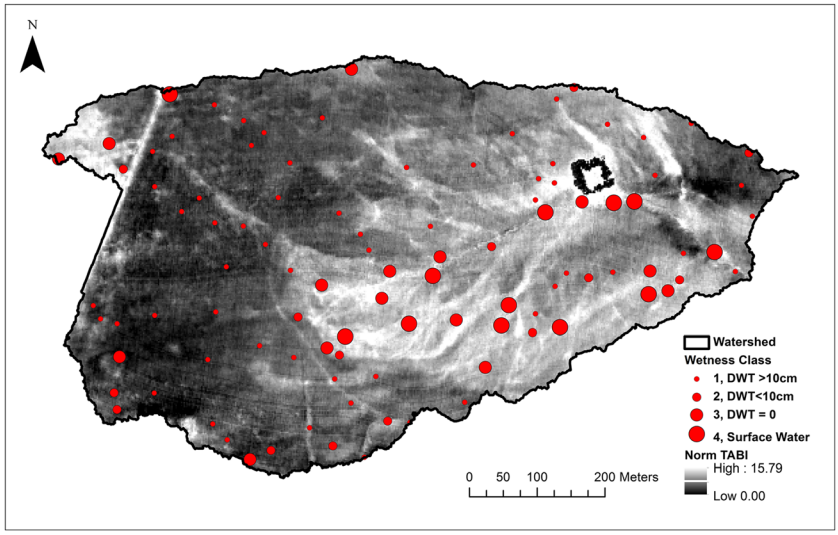


Figure 7. Results from field survey of soil surface wetness (December 2013). Points are randomly distributed within the catchment, with a minimum allowable distance of 20 m. Larger red dots signify the wettest sampled locations

(2) Structural data from LiDAR data sets covering the same extent as $\varepsilon_r$ data distinguish areas where structure or wetness dominates emissivity measurements.

One key aspect that needs to be borne in mind when using thermography for surface wetness mapping is that other landscape variables can also impact on the values of $\varepsilon_r$ measured by a system such as TABI. In this work, surface structure is shown to be a major control on patterns of $\varepsilon_r$ and needs to be corrected or normalized before the data can be used as a relative index of near-surface wetness. Geostatistical analysis (Figure 5, Table II) of the LiDAR data set demonstrated that at a plot scale, textural characteristics of the peatland surface relate to $\varepsilon_r$ (i.e. the inferred relative wetness of that area), because of the effect of the local wetness on ecohydrological organization. However, the nature of the variation in these data (LiDAR) indicates that structural differences may be occurring as a response to wetness (observed in the thermal imaging) and not operating as a strong feedback on the measurement of $\varepsilon_r$. This relationship between wetness, structure and $\varepsilon_r$ supports the need to normalize the effect of ecosystem structure on measurements of $\varepsilon_r$, in order to better interpolate surface wetness. Our approach utilized a fine-scale LiDAR data set that was able to describe changes

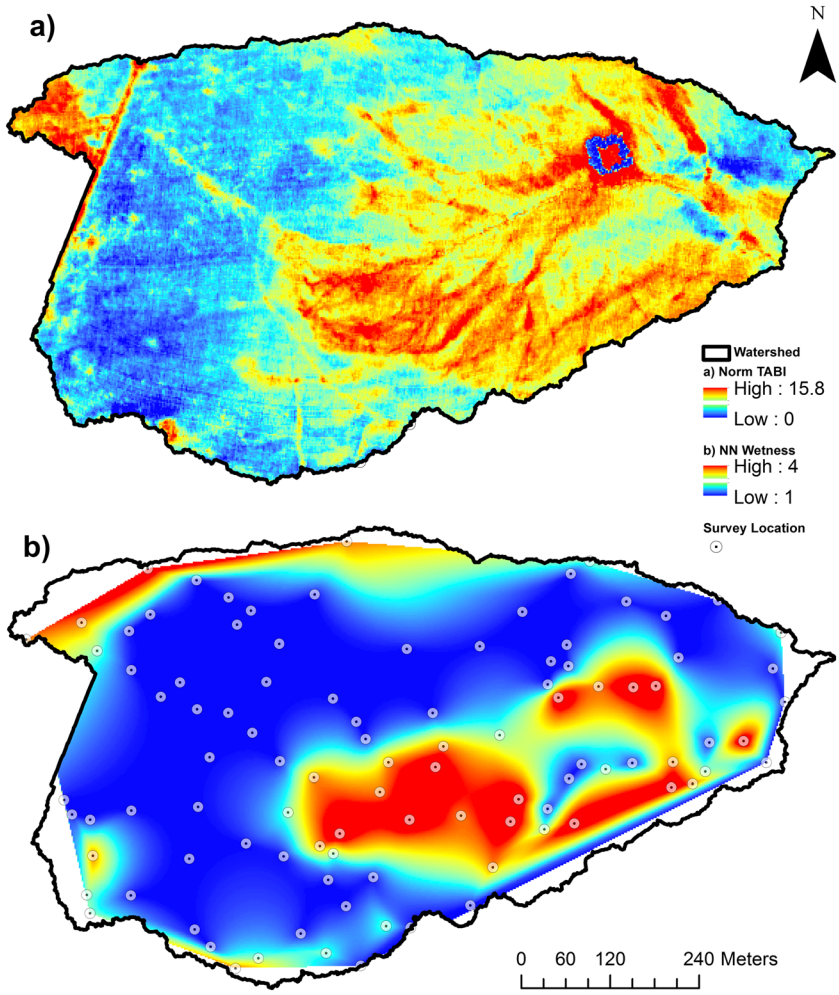


Figure 8. Visual comparison of a) normalized TABI data shown in Figure 7 and b) Natural Neighbour (NN) interpolation of wetness values collected at 100 survey points

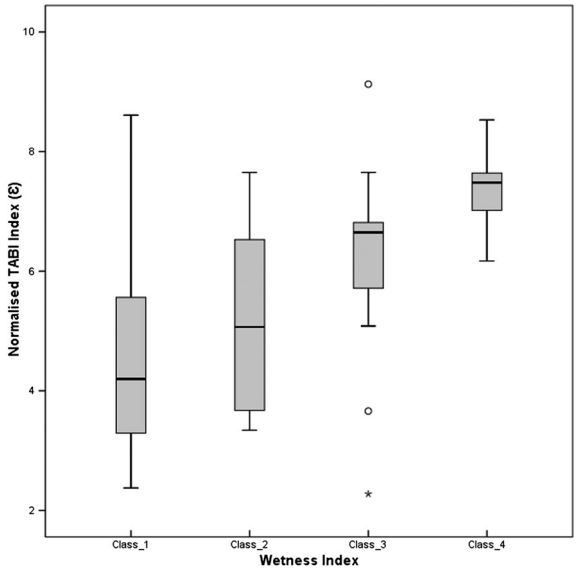


Figure 9. Boxplot of normalized TABI values that occur at survey location in each separate wetness category (Table I), $N = 100$

in surface roughness across the catchment, in this case caused by different ecological communities in different hydrological zones. The resultant data demonstrate that in areas where raw $\text{Ɛ}_r$ measurements were higher due to more complex ecological or morphological structure, this approach was effective at normalizing these data. The data set derived therefore allows us to distinguish between areas of greater near-surface wetness and structural anomalies (i.e. trees, banks and fences) affecting $\text{Ɛ}_r$ (Figure 6). However, there are areas of the resultant data set that still appear to exhibit higher relative $\text{Ɛ}_r$ than may be expected. For example, the area surrounding (and within) the tree enclosure exhibits high $\text{Ɛ}_r$ that may be indicative of regional microclimatic variations influencing the measured temperature and $\text{Ɛ}_r$. Therefore, although this technique is useful for minimizing the effects of surface roughness on $\text{Ɛ}_r$, there are extraneous factors that must also be considered as potential causes of changes in $\text{Ɛ}_r$ and that are not moisture related.

(3) Structurally normalized TABI $\varepsilon_r$ data are related to the spatial distribution of near-surface wetness in an upland peatland.

The results have shown that in using the LiDAR roughness to normalize $\varepsilon_r$ values, it was possible to derive a data set describing surface wetness well, when compared with *in situ* field measurements of near-surface wetness (Figures 8 and 9). The analysis of *in situ* measurements of surface wetness and $\varepsilon_r$ shows a statistically significant relationship between wetness measurements and TABI-derived $\varepsilon_r$ (Figure 9). Furthermore, the spatial information in the structurally normalized TABI data set exceeds that of the *in situ* wetness data set, which are relatively coarse in comparison. Although structurally normalized TABI data are still subject to added uncertainty in $\varepsilon_r$ from microclimatic and topographical drivers, the results suggest that these techniques will be useful in understanding surface wetness across similar landscapes. The coupled data approach presented here also provides useful cross evaluation of findings in both LiDAR and TABI data sets (Hyde *et al*., 2006; Vierling *et al*., 2008).

Unlike the deployment of such technologies from space-borne platforms (Quattrochi and Luvall, 1999), the ability of these airborne technologies in combination to characterize both the hydrological and ecological conditions of these landscapes at a fine spatial scale also makes them highly appropriate to be used as an ongoing management tool on annual or decadal scales. For instance, vegetation communities with characteristic architecture and with known tolerance to soil saturation could be differentiated (i.e. stands of *Juncus* spp. or areas dominated by *Sphagnum* spp.) and their extents mapped. Similarly, regularly repeated surveys of these data sets could be used to quantify the fine-scale shifts in ecohydrological structure in intact or degraded peatlands (Quattrochi and Luvall, 1999), such as the degradation of hummock-hollow microtopography in response to drier soils conditions (Korpela *et al*., 2009). When data capture is repeated on a pre/post-landscape restoration basis, this approach could offer potential as a tool for understanding the extent to which landscape alteration, such as artificial drainage, affects ecohydrological processes and pathways and the effectiveness of landscape restoration schemes in mitigating these affects and restoring ecosystem services. This technique could provide a quantitative measurement of the increase in surface wetness following restoration measures, such as the blocking of drains and ditches. Furthermore, this coupled technique allows us to measure the nature (i.e. diffuse or concentrated) and position of the surface flow pathways reinstated under such works, which is important in understanding the run-off dynamics in these modified systems. Repeating data collection with a high temporal frequency may also enable us to assess shifts in the storage of water in both surface pools and as near-surface wetness across the upland landscapes.

Data manipulated in this way can also be used to aid in the parameterization (or evaluation) of spatially distributed rainfall run-off models. Using distributed internal catchment measurements to parameterize numerical models has been shown to reduce uncertainty in numerical predictions of catchment behaviour (Lamb *et al*., 1998; Gallart *et al*., 2007). DSMs, such as those derived from LiDAR data, are key in developing numerical indices of hydrological behaviour used within rainfall run-off models such as TOPMODEL (Beven, 2012). Such indices form spatially integrated inputs to these models such as relative topographic wetness, relative local storage deficits, flow accumulation and contributing areas. Using TABI data in combination with DSM data to evaluate the spatial accuracy of these model predictions provides an opportunity to assess, modify and improve the spatial representation of the DSM-derived inputs into such models and constrain model uncertainty and spatial equifinality (Brazier *et al*., 2010). Using such data to improve the spatial quality of catchment models would improve the extent that landscape restoration effects can be predicted for many other analogous landscapes where comparable DSMs are available (Vierling *et al*., 2008). Subsequently, those managing these landscapes and/or quantifying the impact of restoration works could be better able to predict effects across larger extents that are appropriate to the scale at which they need to plan restoration works and prove the efficacy of their interventions (Holden *et al*., 2004).

## CONCLUSIONS

This analysis demonstrates that patterning evident in the airborne thermal imagery is consistent with the positioning of anthropogenic drainage networks in this peatland. Airborne thermal imagery (TABI) and LiDAR data used in conjunction are also shown to aid interpretation of $\varepsilon_r$ measurements and describe the extent of near-surface wetness in many areas of the studied landscape. Furthermore, this coupled approach proves to be useful in further interrogating the spatial patterning of vegetation types in response to wetness in upland landscapes. The data sets derived from this coupled approach also demonstrate potential for integration into other multi-scale approaches to understand analogous landscapes, including numerical rainfall run-off modelling, spatially distributed hydrological monitoring approaches and conventional plot-based monitoring of vegetation communities. Critically, these data cover far larger extents and remote locations than field-based monitoring would normally be able to achieve and can be used to cross-validate/supplement traditional monitoring of this type.

Repeats of this analysis over different extents and utilizing thermal data of a higher resolution would further test this methodology and help develop data sets of near-surface wetness useful to those managing peatland landscapes. Importantly, repeated data capture following landscape restoration could enable the change in patterns of near-surface wetness to be ascertained and therefore evaluate the effectiveness of restoration techniques on raising water tables at landscape scales.

ACKNOWLEDGEMENTS

The authors would like to thank the Exmoor Mires Project for their help with site access and the drawing office at the University of Exeter for their help with maps and figures. We also thank the anonymous referees and the editor for their positive and constructive suggestions during the review process. This research received financial support from South West Water Ltd and the University of Exeter (SK04809).

REFERENCES

Anderson JM, Wilson SB. 1984. Review Article. The physical basis of current infrared remote-sensing techniques and the interpretation of data from aerial surveys. *International Journal of Remote Sensing* **5**: 1–18. DOI: 10.1080/01431168408948786.

Anderson K, Bennie J, Wetherelt A. 2009. Laser scanning of fine scale pattern along a hydrological gradient in a peatland ecosystem. *Landscape Ecology* **25**: 477–492. DOI: 10.1007/s10980-009-9408-y.

Anderson K, Bennie JJ, Milton EJ, Hughes PDM, Lindsay R, Meade R. 2010. Combining LiDAR and IKONOS data for eco-hydrological classification of an ombrotrophic peatland. *Journal of Environmental Quality* **39**: 260–273. DOI: 10.2134/jeq2009.0093.

Avery TE, Berlin TE. 1992. *Fundamentals of Remote Sensing and Airphoto Interpretation*. Macmillan: California.

Bellamy PH, Loveland PJ, Bradley RI, Lark RM, Kirk GJD. 2005. Carbon losses from all soils across England and Wales 1978-2003. *Nature* **437**: 245–248.

Bertoldi W, Gurnell AM, Drake NA. 2011. The topographic signature of vegetation development along a braided river: results of a combined analysis of airborne lidar, color air photographs, and ground measurements. *Water Resources Research* **47**: W06525. DOI: 10.1029/2010wr010319.

Beven K. 2012. *Rainfall-runoff Modelling, The Primer* (2nd edn). John Wiley & Sons, Ltd.: Chichester.

Beven K, Freer J. 2001. A dynamic TOPMODEL. *Hydrological Processes* **15**: 1993–2011. DOI: 10.1002/hyp.252.

Brazier RE, Hutton CJ, Parsons AJ, Wainwright J. 2010. In *Handbook of Erosion Modelling*, Morgan RPC, Nearing MA (eds.) Blackwell: London; 98–117.

Campbell JB. 1996. *Introduction to Remote Sensing* (2nd edn). Taylor and Francis: London.

Cannell MGR, Dewar RC, PYATT DG. 1993. Conifer plantations on drained peatlands in Britain: a net gain or loss of carbon? *Forestry* **66**: 353–369. DOI: 10.1093/forestry/66.4.353.

Cavalli M, Tarolli P, Marchi L, Dalla Fontana G. 2008. The effectiveness of airborne LiDAR data in the recognition of channel-bed morphology. *Catena* **73**: 249–260.

Charman D. 2002. *Peatlands and Environmental Change*. John Wiley & Sons Ltd.: Chichester.

Chassereau JE, Bell JM, Torres R. 2011. A comparison of GPS and lidar salt marsh DEMs. *Earth Surface Processes and Landforms* **36**: 1770–1775. DOI: 10.1002/esp.2199.

Clawges R, Vierling K, Vierling L, Rowell E. 2008. The use of airborne lidar to assess avian species diversity, density, and occurrence in a pine/aspen forest. *Remote Sensing of Environment* **112**: 2064–2073.

Gallart F, Latron Jrm, Llorens P, Beven K. 2007. Using internal catchment information to reduce the uncertainty of discharge and baseflow predictions. *Advances in Water Resources* **30**: 808–823. DOI: 10.1016/j.advwatres.2006.06.005.

Goward SN, Xue Y, Czajkowski KP. 2002. Evaluating land surface moisture conditions from the remotely sensed temperature/vegetation index measurements: an exploration with the simplified simple biosphere model. *Remote Sensing of Environment* **79**: 225–242.

Grand-Clement E, Anderson K, Smith D, Luscombe D, Gatis N, Ross M, Brazier RE. 2013. Evaluating ecosystem goods and services after restoration of marginal upland peatlands in South-West England. *Journal of Applied Ecology* **50**: 324–334. DOI: 10.1111/1365-2664.12039.

Grayson R, Holden J, Rose R. 2010. Long-term change in storm hydrographs in response to peatland vegetation change. *Journal of Hydrology* **389**: 336–343.

Harris A, Bryant RG. 2009. A multi-scale remote sensing approach for monitoring northern peatland hydrology: present possibilities and future challenges. *Journal of Environmental Management* **90**: 2178–2188.

Holden J, Chapman PJ, Labadz JC. 2004. Artificial drainage of peatlands: hydrological and hydrochemical process and wetland restoration. *Progress in Physical Geography* **28**: 95–123.

Holden J, Evans MG, Burt TP, Horton M. 2006. Impact of land drainage on peatland hydrology. *Journal of Environmental Quality* **35**: 1764–1778. DOI: 10.2134/jeq2005.0477.

Horning N, Robinson JA, Sterling EJ, Turner W, Spector S. 2010. *Remote Sensing for Ecology and Conservation: A Handbook of Techniques*. Oxford University Press: Oxford.

Hutton C, Brazier RE. 2012. Quantifying riparian zone structure from airborne LiDAR: vegetation filtering, anisotropic interpolation, and uncertainty propagation. *Journal of Hydrology* **442-443**: 36–45.

Hyde P, Dubayah R, Walker W, Blair JB, Hofton M, Hunsaker C. 2006. Mapping forest structure for wildlife habitat analysis using multi-sensor (LiDAR, SAR/InSAR, ETM+, Quickbird) synergy. *Remote Sensing of Environment*, **102**: 63–73.

James LA, Watson DG, Hansen WF. 2007. Using LiDAR data to map gullies and headwater streams under forest canopy: South Carolina, USA. *Catena* **71**: 132–144.

Jenness JS. 2004. Calculating landscape surface area from digital elevation models. *Wildlife Society Bulletin* **32**: 829–839. DOI: 10.2193/0091-7648(2004)032[0829:clsafd]2.0.co;2.

Joosten H, Clarke D. 2002. *Wise Use of Mires and Peatlands*. International Mire Conversation Group and International Peat Society: Totnes.

Korpela I, Koskinen M, Vasander H, Holopainen M, Minkkinen K. 2009. Airborne small-footprint discrete-return LiDAR data in the assessment of boreal mire surface patterns, vegetation, and habitats. *Forest Ecology and Management* **258**: 1549–1566.

Lamb R, Beven K, Myrab S. 1998. Use of spatially distributed water table observations to constrain uncertainty in a rainfall-runoff model. *Advances in Water Resources* **22**: 305–317. DOI: 10.1016/S0309-1708(98)00020-7.

Luscombe DJ, Anderson K, Gatis N, Wetherelt A, Grand-Clement E, Brazier RE. 2014. What does airborne LiDAR really measure in upland ecosystems? *Ecohydrology*. DOI: 10.1002/eco.1527.

Price JC. 1980. The potential of remotely sensed thermal infrared data to infer surface soil moisture and evaporation. *Water Resources Research*, **16**: 787–795. DOI: 10.1029/WR016i004p00787.

Quattrochi DA, Luvall JC. 1999. Thermal infrared remote sensing for analysis of landscape ecological processes: methods and applications. *Landscape Ecology* **14**: 577–598. DOI: 10.1023/a:1008168910634.

Reed MS, Bonn A, Slee W, Beharry-Borg N, Birch J, Brown I, Burt TP, Chapman D, Chapman PJ, Clay GD, Cornell SJ, Fraser EDG, Glass JH,

 

Holden J, Hodgson JA, Hubacek K, Irvine B, Jin N, Kirkby MJ, Kunin WE, Moore O, Moseley D, Prell C, Price MF, Quinn CH, Redpath S, Reid C, Stagl S, Stringer LC, Termansen M, Thorp S, Towers W, Worrall F. 2009. The future of the uplands. *Land Use Policy* **26**(Supplement 1): S204–S216.

Schultz GA, Engman ET. 2011. *Remote Sensing in Hydrology and Water Management*. Springer: Berlin, Heidelberg.

Tallis JH. 1998. The southern Pennine experience: an overview of blanket mire degradation. In *Blanket Mire Degradation*, Tallis JH, Meade R, Hulme PD (eds.) British Ecological Society: Macaulay, Aberdeen; 7–15.

Torgersen CE, Faux RN, McIntosh BA, Poage NJ, Norton DJ. 2001. Airborne thermal remote sensing for water temperature assessment in rivers and streams. *Remote Sensing of Environment* **76**: 386–398.

Vierling KT, Vierling LA, Gould WA, Martinuzzi S, Clawges RM. 2008. Lidar: shedding new light on habitat characterization and modeling. *Frontiers in Ecology and the Environment* **6**: 90–98. DOI: 10.1890/070001.

Wilson L, Wilson J, Holden J, Johnstone I, Armstrong A, Morris M. 2010. Recovery of water tables in Welsh blanket bog after drain blocking: discharge rates, time scales and the influence of local conditions. *Journal of Hydrology* **391**: 377–386.

Worrall F, Armstrong A, Holden J. 2007. Short-term impact of peat drain-blocking on water colour, dissolved organic carbon concentration, and water table depth. *Journal of Hydrology* **337**: 315–325.

 

# 6 Understanding the hydrology of shallow, drained and marginal peatlands: 1. Temporal variability

David J. Luscombe[1], Karen Anderson[2], Emilie Grand-Clement[1], Naomi Gatis[1], Josie Ashe[1], Pia Benaud[1], David Smith[3] and Richard E. Brazier[1]

1. Geography, CLES, University of Exeter, Amory Building, Rennes Drive, Exeter, Devon EX4 4RG

2. Environment and Sustainability Institute, University of Exeter, Cornwall Campus, Treliever Road, Penryn, Cornwall, TR10 9EZ

3. South West Water, Peninsula House, Rydon Lane, Exeter. Devon EX2 7HR

## 6.1 Abstract

There is a growing recognition that upland peatland landscapes provide a host of critical ecosystem services (carbon sequestration, water provision and flood mitigation). Understanding the spatio-temporal dynamics of peatland hydrological function and the response of these peatlands to management is critical in achieving the UK government's target of restoring 1 million ha of damaged UK peatlands by 2020. The complex relationships governing water storage and flow generation in these landscapes are hard to quantify and may result in equifinal downstream discharge over longer measurement intervals. This paper describes the results of a high-resolution monitoring program, which provides insights into the processes driving storm flow, base flow and water storage in two damaged shallow peatlands in Exmoor, UK. Hydrological responses were captured simultaneously at 104 monitoring points within a spatial monitoring scheme at a high temporal frequency (15 minute time-step) within two upland, peatland catchments. Results show that flow regimes in these shallow, drained and marginal peatlands exhibit a flashy runoff response and poorly maintained base flow. Additionally, a combination of thin peat soils and extensive anthropogenic drainage networks, mean that antecedent hydrological conditions (precipitation and depth to water table) exert little control on the total or peak flow produced, explaining as little as 3% observed variance during monitored rainfall-runoff events (n = 56 - 98). These findings provide a robust baseline for the hydrological function in these damaged peatland

systems and suggest that restoration has the potential to significantly reduce flow generated during rainfall events, attenuating hydrograph peaks and increasing base flow duration and magnitude.

## 6.2 Introduction

The recent commitment by UK government to support the outcomes of the International Union for the Conservation of Nature (IUCN) UK Peatland Program recognises the importance and urgency with which action is needed to restore damaged peatland landscapes (Bain et al., 2011). Much restoration work has already been undertaken on the heavily damaged northern peatlands in the UK (Holden et al., 2006b, Holden et al., 2004, Worrall et al., 2007b, Grayson et al., 2010, Dixon et al., 2013). Recently, the geo-climatically marginal and shallow peatlands in the South West of the UK have also been subject to significant restoration activities (Grand-Clement et al., 2013, Mills et al., 2010), where the aim is to restore ecohydrological function following drainage implemented over the last 200 years (Ramchunder et al., 2009, Allott et al., 2009, Allott et al., 2014, Wilson et al., 2010, Wilson et al., 2011b). However, the hydrology and ecology of these shallow blanket peatlands is less well understood than the deeper peat systems studied in the north of the UK, with many contemporary studies focusing on their paleo-ecological significance (Bowes, 2006, Davies, 2012, Fyfe, 2006). Importantly, Exmoor's peatlands are also thought to differ in their structure and function from deeper peats (Grand-Clement et al., 2013, Chambers et al., 1999, Merryfield and Moore, 1974), and as such, may be more sensitive to climate change due to their maritime location (Gallego-Sala et al., 2010, Clark et al., 2010). Improved understanding of the hydrological function of these damaged shallow mires is therefore critical to determine the sensitivity of such peatlands in a changing climate (Parry et al., 2014), and to facilitate effective restoration towards the IUCN target of up to 1 million ha of restored UK peatlands by 2020 (Bain et al., 2011).

Water movement and storage in all peatlands is intrinsic to their formation, persistence and ecohydrological function (Evans and Warburton, 2010, Charman, 2002, Lindsay, 1995). Contemporary understanding of peatland hydrology acknowledges the complex relationships governing water storage and flow generation in these landscapes (Wilson et al., 2010, Wilson et al.,

2011b, Holden et al., 2004). Indeed, the complex nature of processes governing runoff generation and storage in peatland catchments can result in equifinality (i.e. where an end state can be reached by many potential scenarios) of downstream discharge over long temporal scales, masking the finer-scale processes taking place (Beven, 2012, Holden et al., 2006b, Beven, 2006, Lamb et al., 1998). Monitoring hydrological responses at multiple locations within a peatland catchment simultaneously, continuously and at a high temporal frequency, provides unique and important opportunities to describe the fine scale temporal dynamics governing flow generation and storage in upland peatlands (Ballard et al., 2011, Holden, 2005, Holden et al., 2011, Parry et al., 2014). For example, the relationship between saturation of the peat matrix and the production of channel flow (i.e. saturation excess overland flow) is difficult to quantify without multiple water table measurements across the catchment extent; as such temporal dynamics may be spatially heterogeneous (Morris et al., 2011). Such measurements, collected over short time steps, would be able to record the temporal variability of response to rainfall, which has been shown to be significant at regulating flow elsewhere in degraded peatlands (Evans et al., 1999). Also of interest is the length of time over which base flow is maintained by ground water storage in a damaged peatland system, as this information relates to the resilience of the peatland to store water – a key feature of blanket bogs that is compromised when drainage is implemented (Wallage et al., 2006, Wilson et al., 2010, Wilson et al., 2011b). The monitoring strategy that is required to capture this information must be spatially distributed and must run continuously, capturing the variability across the whole hydrological year, including during dry periods, when maintenance of base flows may be artificially low, due to the effects of drainage (Holden, 2005, Parry et al., 2014).

To address these requirements, this paper describes the results of a high-temporal and fine-spatial resolution monitoring program, which provides insights into the processes driving storm flow, base flow and water storage in damaged shallow peatlands. This study utilises a full range of hydrological parameters (rainfall at 2 locations, depth to water table at 96 locations, open channel discharge estimation at 6 locations and gauged catchment outlet discharge at 2 locations) captured simultaneously, on 15 minute time steps and continuously

over long (multi-year) temporal scales. Data provided here have the potential to inform the restoration and long-term management of these landscapes by better enabling managers to understand the fine scale processes driving water storage and flow generation in such marginal peatlands before they are restored. Specifically this work focuses upon temporal variability (part two of this paper, Luscombe et al., forthcoming, describes spatial variability) and seeks to quantify:

- The mechanisms governing the “flashiness” of rainfall-runoff events in shallow damaged peatlands and;
- How these mechanisms relate to the regulation of ground water storage and base flow discharge from the two studied catchments.

The following hypotheses are tested:

### *6.2.1 Hypothesis A*

**Flow regimes in shallow, drained peatlands are dominated by flashy (i.e. rapid and short lived) storm flows and low base flow conditions.**

In an intact peatland system where soil is saturated year-round, fast flow pathways including overland flow would dominate, generating rapid, saturation-excess rainfall-runoff responses (Holden and Burt, 2002). A drained/damaged system may be characterised by increased connectivity as a consequence of linear drainage flow paths, and humified (shallow) peat soils. In such a system, increased near surface through-flow may occur through pathways including rapid erosional acrotelm flow generation (Daniels et al., 2008) and macropore/soil pipe generation (Holden et al., 2007b) acting alongside increased surface flow connectivity (Pawson et al., 2012), accentuating the flashy character of the flow regime and producing even more rapid runoff than intact systems. Assessing the relationship between discharge variables and rainfall parameters will help to test this hypothesis and quantify the rainfall-runoff response times of the study catchments.

### *6.2.2 Hypothesis B*

**The primary control on runoff (Q) in shallow, drained peatlands is rainfall, with antecedent water tables and rainfall, exerting a secondary control.**

Building on hypothesis A which tests assumptions around the flashiness of storm response and the characteristics of base flow, this hypothesis will test whether the observed hydrograph responses are purely a function of the rainfall, or are additionally regulated by more complex processes (such as antecedent rainfall and event spacing/timing through the hydrological year). Previous studies in deep peatlands have demonstrated that drained peatlands can provide additional storage capacity due to lower water tables (Holden, 2005). Where such additional storage exists, antecedent conditions (i.e. rainfall and water table) may limit such storage and exert a control on catchment discharge (Daniels et al., 2008). Addressing this hypothesis will enable inference to be drawn as to which processes govern how these catchments respond to rainfall under a wide range of environmental conditions.

### *6.2.3 Hypothesis C*

**Event discharge is generated only when water tables are close to the soil surface and rapid, saturation excess near surface flow occurs.**

Establishing the extent to which water tables exert a control on flow production in shallow, drained peatlands will improve understanding of which flow pathways are dominant in the study catchments, and therefore what process drive storm flow in these peatlands. In intact peatland systems, saturation excess overland/near surface flow is often dominant due to persistent and high water tables (Holden and Burt, 2002). However, in damaged systems, other flow pathways may produce rapid runoff, including Hortonian (infiltration excess) overland flow or rapid macropore through-flow (Daniels et al., 2008, Holden et al., 2007b), which can occur even when water tables are drawn-down following drought. As such, determining the dominant flow pathways in these shallower peatland will provide an improved mechanistic understanding of the how these landscapes have been hydrologically modified following anthropogenic drainage.

## 6.3 Methods

### *6.3.1 Experimental design*

Within degraded upland peatland areas in Exmoor National Park, two headwater catchments were selected that were representative of typical shallow blanket mire complexes. The sites were extensively surveyed as part of the Exmoor Mires project and included representative drainage ditch morphology, drainage density, peat depth, slope morphology, aspect and vegetation composition. The location of these upland catchments (known locally as 'Aclands' [SS 733,384] and 'Spooners' [SS 776,374]) is shown in Figure 6.1. Peat depths across the studied catchments were known to be low (Bowes, 2006), and deposits were found to vary between 0.29 m and 0.71 m deep during site surveys.

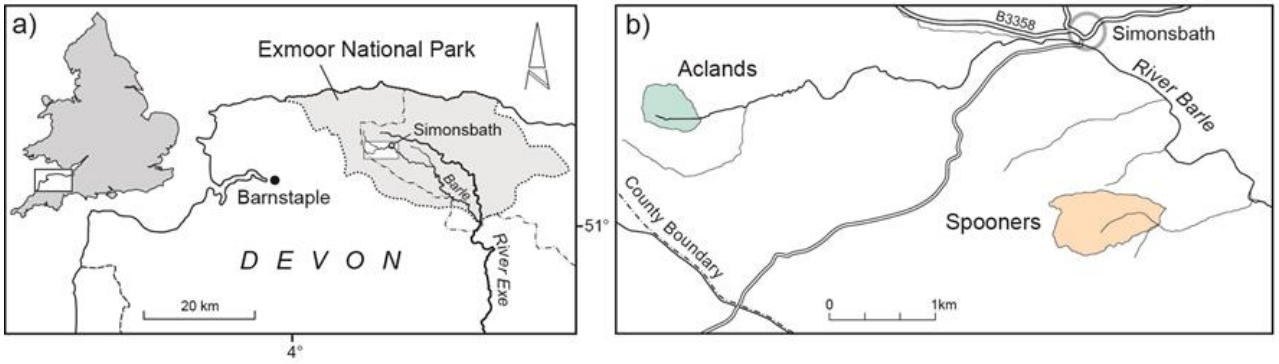


**Figure 6.1: Location of experimental headwater catchments a) within the Exmoor National Park, and b) with respect to the local river systems. NGF 'Aclands' [SS 733,384] and 'Spooners' [SS 776,374].**

Discharge at the outlets of the two catchments was estimated using flume structures mounted into the main channel. Stage data were converted to discharge (Q) using flow ratings calculated for each structure, based on >20,000 in-flume observations of flow velocity and depth measured with a 2150 Area Velocity Module, (Teledyne Isco).

Flow discharge (Q) and depth to water table (DWT) data were also collected at three locations (experimental pools [EP]) within each of the two headwater catchments (Figure 6.2). Each EP was located within a drainage ditch complex of a different scale, determined by its geometry and stream-order (Table 6.1).

Each monitored EP was labelled relative to its estimated drainage scale at installation (from one, small, to three, large) and was also identified to its overall catchment (S = Spooners, A = Aclands). Data for the overall catchment outlet are also included and denoted as f (flume site), giving rise to 8 scales of hydrological monitoring over the two catchments (i.e. A1, A2, A3, Af, S1, S2, S3, Sf).

Within each experimental pool, flow was monitored using pressure transducers which logged depth (stage) within small stilling wells, mounted in the open ditches. Previous hydrological monitoring on Exmoor (Mills et al., 2010) demonstrated that ditch size and the dense, deciduous grass vegetation cover (*Molinia caerulea*) prevented flow monitoring structures from functioning, without significant alteration to either flow or channel properties. Similarly, the shallow and vegetated nature of the EP channels prevented the independent construction of a robust stage – velocity relationship. Q was therefore modelled in these features using Manning's equation (below), with an 'n' value of 0.10 to reflect the rough, vegetated nature of the channels (Chow, 1969). Although high, this value ensures that estimations of discharge are conservative for the monitored drainage features, reducing over-representation of monitored flows. Due to significant, static pooling in the bottom of drainage features, storm derived flow was extracted from these data using a 48 h moving minimum window to remove the artificially elevated "baseflow" component. The derived time series was subsequently quality controlled in detail to remove time steps which indicated short periods of equipment failure or erroneous data capture. Any stage data collected that exhibited artificially induced signal noise (due to equipment failure) was also filtered to interpolate the underlying data signal. This was accomplished using a 4 h moving window filter of mean discharge plus one standard deviation, to isolate the signal of the channel discharge.

$$V = \frac{k}{n} {R_h}^{2/3} S^{1/2}$$

**Equation 1: where V is the cross-sectional average velocity; k is a conversion factor for SI, or U.S. customary units; n is the Gauckler–Manning coefficient (unitless); Rh is the hydraulic radius; S is the slope of the channel bed.**

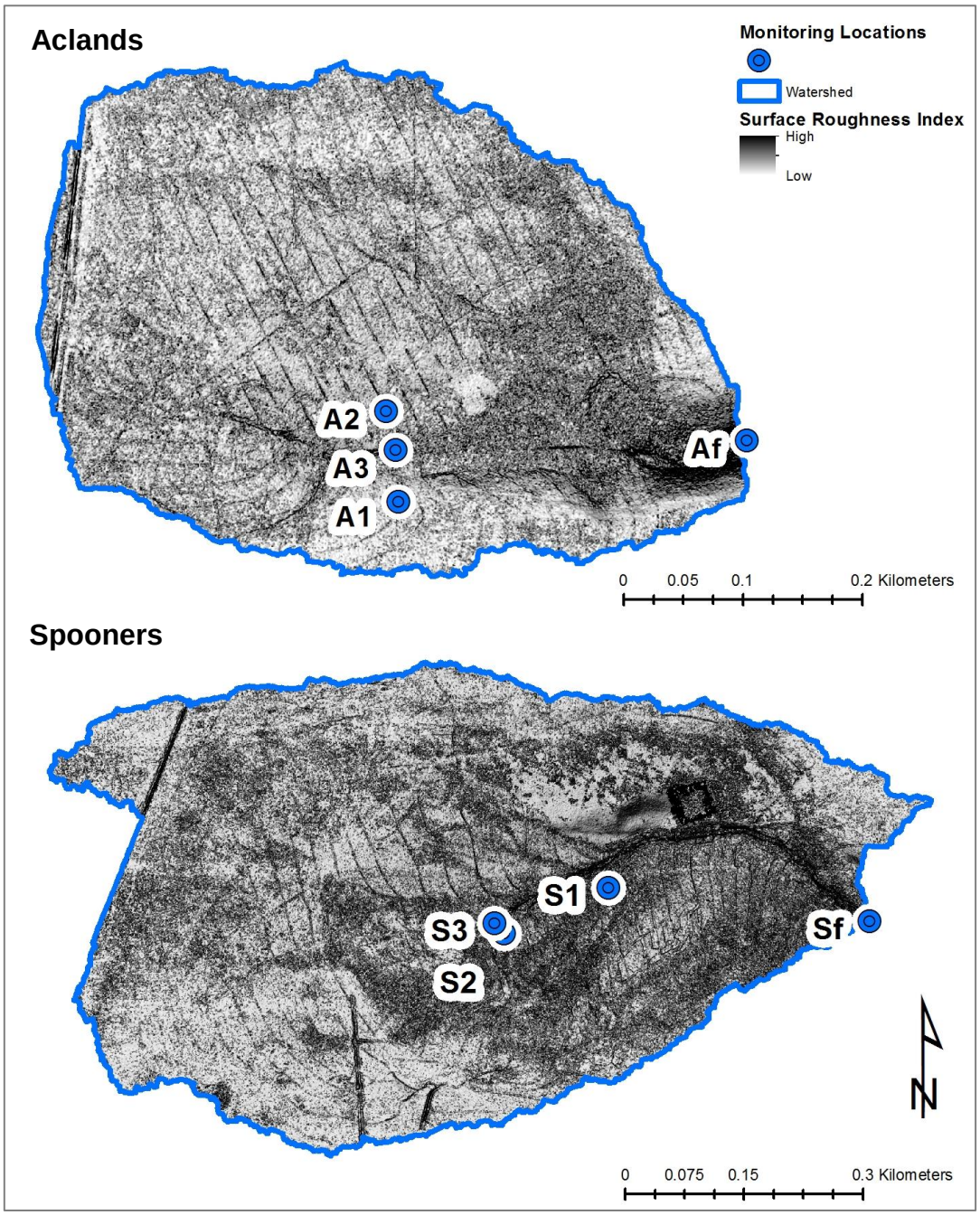


**Figure 6.2: Location of experimental pools within the Aclands and Spooners experimental headwater catchments. The catchment extents illustrate the topographic contributing area for Sf and Af monitoring locations, as delineated using a 50 cm LiDAR DSM. The background surface raster represents an index of surface roughness (SRI) as described in Chapter 5.**

In previously ungauged landscapes, *a priori* knowledge of the resolution of monitoring required to capture the spatio-temporal dynamics of hydrology is lacking. Therefore, an experimental design was implemented which would allow for detailed understanding of hydrology at four scales of interest within each catchment. Within each experimental pool, depth to water table was recorded at

16 locations surrounding the selected drainage feature, using dipwells set into the full depth of the peat mass. Depth to water table was calculated from pressure transducers mounted in dipwells at known depths at the peat base. Dipwells had 0.8mm Ø holes along two axes screened with fine nylon mesh to prevent peat particles building up within the cylinder. Dipwells were distributed in even numbers on both sides of the studied drainage features. As illustrated in Figure 6.3, dipwells were also distributed along two axes to understand variation in DWT both parallel to and perpendicular with, the flow direction in the drainage feature. Rainfall data were collected via a tipping bucket rain gauge mounted centrally within each of the catchments. DGPS locations of dipwell tops were recorded to ensure accurate understanding of their spatial distribution with each EP and within the wider catchment with spatial accuracy of 2 cm in *x*, *y* and 3 cm in *z* (Anderson et al., 2010).

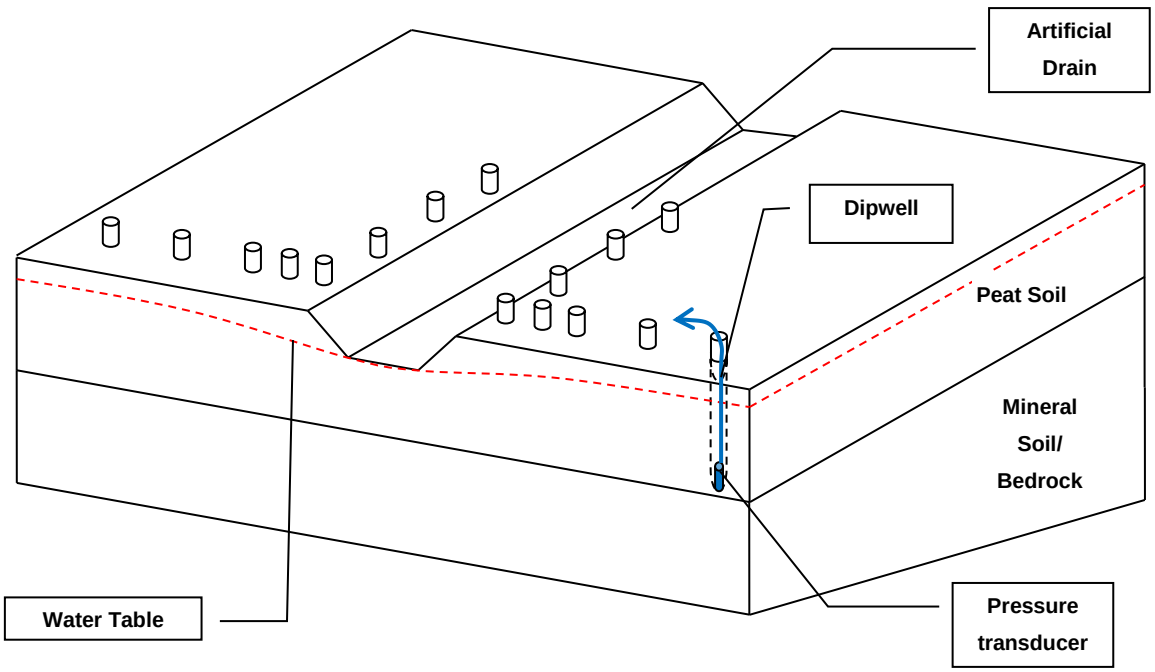


**Figure 6.3: Design of experimental pools dipwell arrays. Conceptual design locating mini piezometers (dipwells) distributed along two axes adjacent to an anthropogenic drainage feature. The blue arrow represents the wired connection of each dipwell to the telemetry system.**

**Table 6.1: Key drainage characteristics for all 8 nested scales of monitoring. Contributing area (cont. area) is defined on the basis of surface topography alone.**

| Parameter | Cont. area | Channel Depth | Channel Width | Strahler Stream order |
|---|---|---|---|---|
| **Unit** | $m^2$ | m | M | ND |
| **SF** | 464825 | Flume | Flume | 8 |
| **S3** | 5335 | 0.86 | 5.6 | 4 |
| **S2** | 499 | 0.49 | 2 | 3 |
| **S1** | 1770 | 0.31 | 1 | 3 |
| **AF** | 195025 | Flume | Flume | 7 |
| **A3** | 53161 | 0.55 | 2.7 | 6 |
| **A2** | 11220 | 0.34 | 1.6 | 4 |
| **A1** | 1428 | 0.15 | 1.4 | 3 |

### *6.3.2 Data acquisition and quality control*

All stage, rainfall and DWT measurements were logged continuously every 15 minutes in the field using an Adcon-based remote telemetry system (Adcon Telemetry GmbH). Data were simultaneously fed back to a local base station via VHF transmission on the 15 minute time step and were then uploaded to a remote server using a high gain GPRS transmitter. This telemetry system also allowed for a short period of data buffering (ca. two days) in the field during periods of degraded connectivity via the GPRS network. Timeseries extracted from the telemetry server were all cross-checked to eliminate any erroneous periods of data acquisition or equipment failure.

### *6.3.3 Analytical design*

To address the proposed hypotheses, time series data describing rainfall and runoff at each scale were automatically split into “rainfall-runoff events” and “base-flow” periods using logic-derived data sorting protocols. These protocols were trained on the real flow data observed at each catchment outlet, building on the work of Deasy et al. (2009) and Glendell et al. (2014). This technique identified periods where the discharge data met criteria outlined in Table 6.2. Rainfall events were classified as periods where precipitation was continuous for more than 15 minutes and where breaks in the rainfall were for less than 60

minutes. Rainfall events that fell within periods of elevated flow and those that occurred within 6 hours of the lowest stage preceding elevated discharge were included as “event rainfall”. All such events were automatically numbered and key summary statistics calculated. A final, visual inspection of the time series was used to quality control these data and ensure that all significant rainfall and flow events were extracted from the dataset. Extracted events were then classified 1 to 4 according to the criteria in Table 6.3, in an effort to group events according to how complex the flow response was. For the analysis undertaken, class 1 and 2 events only were used so as to ensure the most robust comparison between the geometry of the studied hydrographs with the best quality data observed.

**Table 6.2: Event separation criteria used in discharge data pre-processing.**

| | | |
|---|---|---|
| **Aclands** | % change in Q over 4 hours | 12% |
| | Minimum threshold of Q for an event ($m^3 s^{-1}$) | 0.008 |
| | Minimum magnitude of event Q ($m^3 s^{-1}$) | 0.01 |
| **Spooners** | % change in Q over 4 hours | 10% |
| | Minimum threshold of Q for an event ($m^3 s^{-1}$) | 0.03 |
| | Minimum magnitude of event Q ($m^3 s^{-1}$) | 0.03 |

**Table 6.3: Secondary event classification criteria.**

| Event Categories | Definition |
|---|---|
| **1** | Unimodal event |
| **2** | Bimodal or multimodal with continuous elevated flow |
| **3** | Bimodal or multimodal with discontinuous elevated flow |
| **4** | Null: Defining something other than a true rainfall response event |

All rainfall–runoff events identified for the monitored period had standardised summary statistics derived via a simple relational database and logic query procedure, enabling direct comparison of event parameters and hydrograph geometry. Table 6.4 summarises those statistics derived and the hypotheses that they address. Summary statistics were also derived for all inter-event

periods using an identical technique and automatic sequential numbering of these data blocks.

**Table 6.4: Metrics derived from rainfall-runoff event time series.**

| | Rainfall – Runoff metric | Hypothesis tested |
|---|---|---|
| **Rainfall** | Total rainfall (mm) | 2 |
| | Peak rainfall intensity (mm $h^{-1}$) | 2 |
| | 2 Day antecedent rainfall (mm) | 2 |
| **Runoff** | Total Q ($m^3$) | 2 |
| | Peak event Q ($m^3$ $s^{-1}$) | 2 |
| | Event duration (min) | 2 |
| | Lag from peak of rainfall intensity to peak Q (min) | 1 |
| | Flashiness (peak flow: total flow ratio) | 2 |
| | 2 day antecedent depth to water table depth | 2,3 |

### *6.3.4 Data and statistical analysis*

In addition to the simple metrics calculated in Table 6.4, the Q5:Q95 ratio (i.e. ratio of discharge (Q) at $p$ = 0.05 to $p$ = 0.95) was used to provide longer term and multi-event quantification of event flashiness throughout the measured time series (Jordan et al., 2005, Jordan and Cassidy, 2011). This metric was calculated by non-linearly regressing (using a power relationship, γ=χ^n) the probability for each average daily flow occurring in a given month (i.e. where χ=probability and γ= flume discharge) and using the result to derive flow at $p$ = 0.05 and $p$ = 0.95. This value was then expressed as a ratio for each month in the time series and simply illustrates the ratio of the probability that flow is very low, to very high.

Further statistical analysis was conducted on parameters extracted for individual rainfall runoff events (and inter-event periods). This analysis was conducted using two methods. Firstly, a conservative, non-parametric Spearman's Rank-Order correlation was chosen as a simple mechanism to explore the nature and significance of the relationships present, whilst using a dataset subject to large kurtosis and skew. Values were calculated using IBM SPSS statistics 20 and compiled in Microsoft Excel 2010. Secondly, following appropriate transformation (log10), multiple regression analysis was used to analyse the extent to which the antecedent conditions explained any additional

variance in the flow data, after rainfall was considered. This analysis was also conducted in IBM SPSS statistics 20.

Finally, the DWT and discharge time series were regressed using a two term exponential model ( $y = ae^{bx} + ce^{dx}$ ) to address hypothesis c. For each monitoring location the Spearman's rank correlation coefficients, $r^2$ values and the inflexion points of the fitted curves were extracted and recorded for comparison across the experimental pools and catchments monitored.

## 6.4 Results

### *6.4.1 Hypothesis A*

**Flow regimes in shallow, drained peatlands are dominated by flashy storm flows and low base flow conditions**

***Discharge time series***

Figure 6.4 illustrates an excerpt of the rainfall-runoff timeseries collected at the eight monitoring scales across the Spooners and Aclands catchments. Flow responses are shown to be immediate following rainfall, although differences are apparent between the two catchments and the four scales of drainage observed. It also appears that hydrograph geometry was more similar within each catchment than between each catchment, indicative of the spatial separation of these catchments. Flow responses were generally more pronounced in the Spooners catchment, with peak flows regularly exceeding 0.3 $m^3 s^{-1}$, whereas highest peak flows in the Aclands catchment were ca. 0.18 $m^3 s^{-1}$. Base flow was maintained at the catchment outlet of Spooners more often than at Aclands and at higher levels, with average low flow being ca. 0.03 $m^3 s^{-1}$, compared with >0.01 $m^3 s^{-1}$. At Aclands, discharge scaled well with the size of the drainage feature (as indicated by channel depth/width, Table 6.1). Here discharge increases as channel depth and contributing area increase, although similar discharge values observed at EP3 (largest drain) and the catchment outlet are perhaps unusual given the spatial separation of these locations. At the Spooners catchment EP discharge scales with the catchment outlet discharge (black line). However, EP 2 and 3 do not scale as expected and are in fact reversed in terms of cross-sectional and contributing area suggesting other factors are responsible for regulating discharge from these locations.

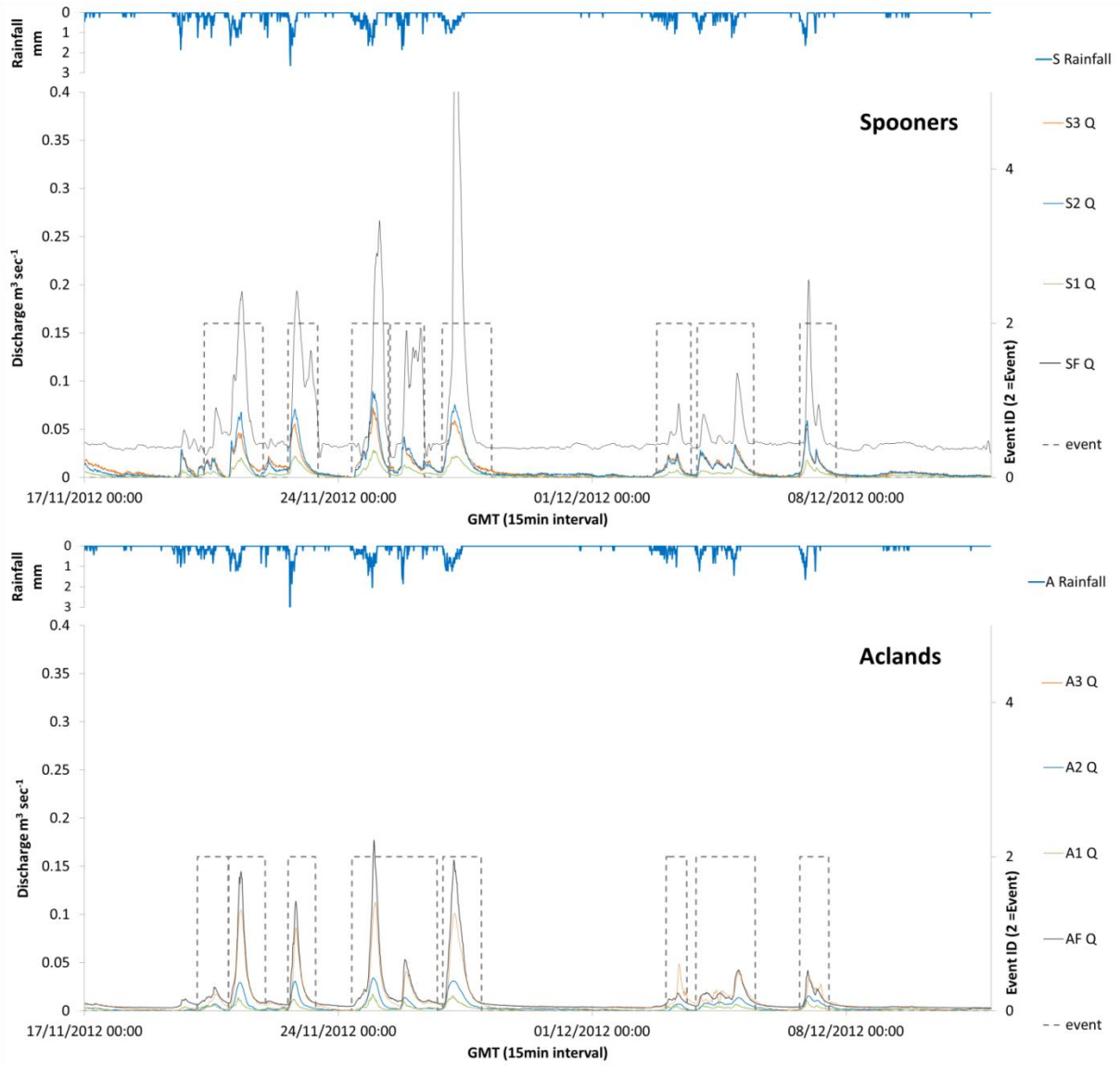


**Figure 6.4: Extract of discharge time series data collected from both catchments from July to August 2012 inclusive. All data are reported as estimated discharge in $m^3$ $s^{-1}$ and sampled on a 15 min time step. The delineation of the automatic event separation analysis is also illustrated as a dotted line in each graph.**

In order to quantify the storm and base flow contributions to hydrographs at drains of different scales in more detail, summary values were calculated to describe the average discharge during three periods: base-flow, storm flow and peak storm flow (Figure 6.5). Both mean base-flow discharge and mean total discharge are very low compared to the peak flow observed at each drainage feature, indicative of a runoff regime dominated by flashy storm flow and poorly maintained base flow discharge. At Aclands (Figure 6.5 c,d), the mean base flow, total flow and peak flows scaled well with respect to the size of the drainage feature, increasing as the contributing area increased, corroborating

results shown in Figure 6.4 for the wider timeseries. Similarly at the Spooners catchment (Figure 6.5 a, b) these discharge metrics varied with drainage scale. However, at Spooners EP2 and EP3 were found to have similar values whilst EP2 had a larger observed maximum and total flow over the period monitored (Table 6.5), again corroborating results shown in Figure 6.4.

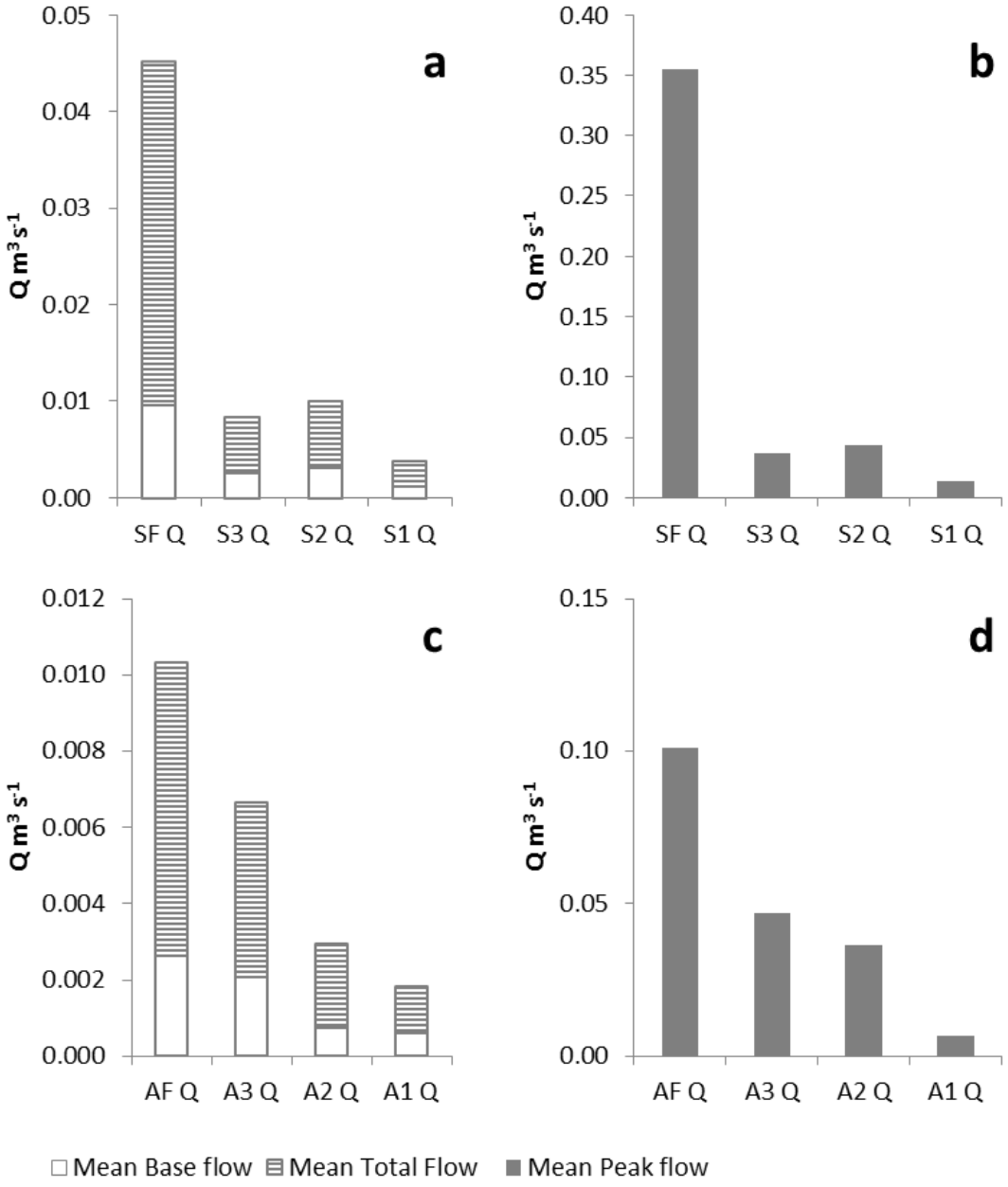


**Figure 6.5: Breakdown of the average (mean) base flow (i.e. non rainfall event flow), average of rainfall event peak flows and average of total flows (i.e. baseflow and stormflow) across each scale of drainage and across both catchments (a,b, Spooners and c,d, Aclands).**

Further summary statistics for the whole discharge time series are collated in Table 6.5. The total days of observations vary due to changes in monitoring duration and the dates at which restoration was undertaken at the Spooners catchment (March 2013).

**Table 6.5: Summary statistics for the discharge measured across all catchments and at all scales of drainage.**

| | AF Q | A3 Q | A2 Q | A1 Q | SF Q | S3 Q | S2 Q | S1 Q |
|---|---|---|---|---|---|---|---|---|
| **Days of Observations** | 831 | 938 | 630 | 506 | 414 | 704 | 795 | 770 |
| **Total Observed Flow $m^3$** | 552,236 | 371,898 | 120,872 | 52,978 | 1,268,360 | 354,525 | 472,299 | 171,746 |
| **Max Observed Flow $m^3$ $s^{-1}$** | 0.842 | 0.192 | 0.097 | 0.029 | 3.117 | 0.157 | 0.164 | 0.062 |
| **Average daily flow $m^3$** | 664 | 396 | 192 | 105 | 3064 | 504 | 594 | 223 |

***Indicators of flashiness***

In order to address hypothesis 'A' further, lag times between peak rainfall and peak flow across all eight monitoring sites were calculated. Figure 6.6 illustrates lags were short, with lag times most commonly (mode) between 30 minutes and 1:45 hours (mean values of between 3:21 hours and 5:13 hours) across all monitoring locations (σ = 3:10 to 8:39). These data also demonstrate a consistent positive skew ($g_1$ ranging from 1.55 at SF to 7.50 at S3) showing a more frequent occurrence of the shorter lag times (below 3 hours). Data also show significant leptokurtosis ($g_2$ ranging from 2 [SF] to 61 at [S3]) with the majority of the observations falling nearer to the mean observation, suggesting that longer lag times are uncommon.

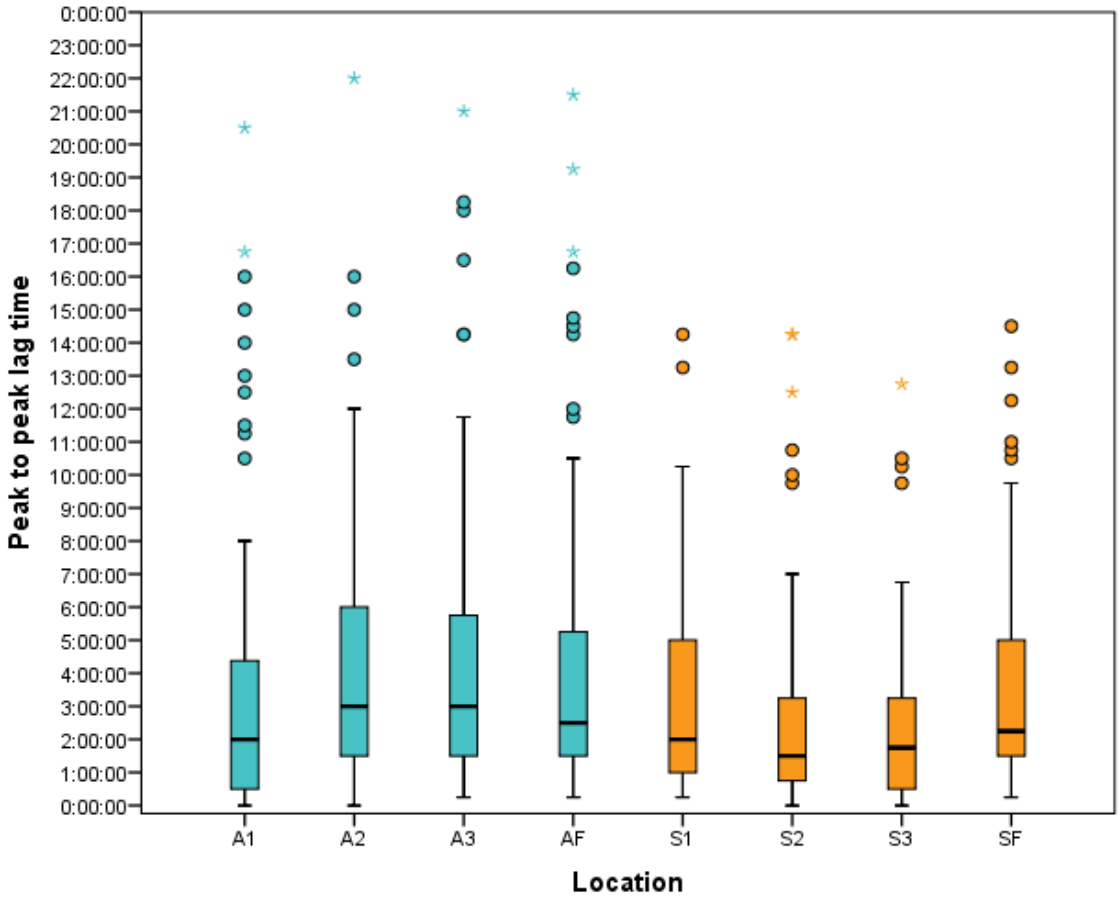


**Figure 6.6: Lag times calculated for all rainfall runoff events observed at each monitoring scale. The number of rainfall-runoff events used to derive these values are: A1 = 87, A2 = 56, A3 =95, AF=98, S1=79, S2=78, S3=78, SF=85. Table 6.5 summarises the number rainfall runoff events used to derive the lag times summarised here.**

Examination of the monthly ratio of Q5:Q95; an index of stream system flashiness (Jordan et al., 2005), demonstrates that at the outlet of Aclands (the smaller catchment of the two), a consistently flashier runoff response is observed (Figure 6.7) with baseflow often returning close to 0 and Q95 regularly exceeding Q5 by a factor of 20. On average, the Q95 at Aclands is 25 times larger than the Q5, whereas at Spooners the Q95 is typically only seven times the Q5. In addition, the monthly variation in this index shows correlation between the two catchments ($R_s$ = 0.74), suggesting that despite the different magnitudes of flow and the different overall flashiness of each catchment, the two landscapes respond in a synchronous manner.

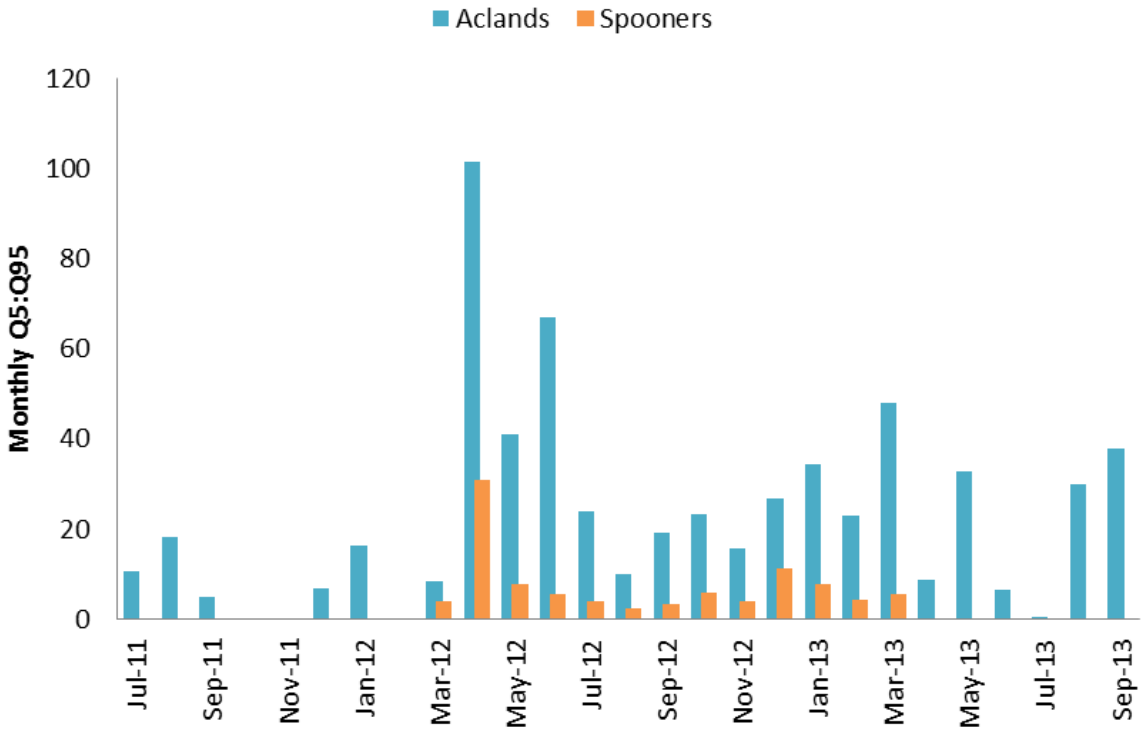


**Figure 6.7: Monthly Q5:Q95 Ratio for both catchment outlets discharge timeseries. The truncation of the Spooners timeseries due to catchment wide restoration activities.**

### *6.4.2 Hypothesis B*

**The primary control on runoff (Q) in shallow, drained peatlands is rainfall, with antecedent water tables and rainfall, exerting a secondary control.**

In order to understand the effect of precipitation on controlling the generation of discharge, key precipitation and channel flow parameters extracted from the automatic event separation dataset (Table 6.3) were analysed alongside the full timeseries. In order to explore relationships between a large range of rainfall and flow parameters, the spearman's rank correlation coefficient and p–value were calculated for all extracted rainfall and runoff parameter combinations described in Table 6.4. These data are compiled in Table 6.6 and significance is highlighted as at either $p$ <0.01 or $p$ <0.05 levels. Coefficients between total rainfall ($r_t$) and peak/total flow ($Q_p/Q_t$) are high ($R_s$ 0.57 to 0.90) and significant at $p$ <0.01. The correlations of $r_t$ and $Q_t$ are marginally higher than for $Q_p$, at the majority of locations. Peak rainfall intensity ($r_p$) is shown to correlate more weakly with $Q_p$ and $Q_t$ ($R_s$ 0.22 to 0.63), however these correlations remain significant at $p$ <0.01.

In order to explore whether other factors exert a significant control on flow in addition to rainfall, spearman's rank correlation coefficients were also calculated for antecedent conditions, (expressed here as rainfall which fell within the last two days and depth of water table) against flow response at all observation scales. At the Spooners catchment antecedent rainfall is shown to have a weak but significant correlation with the peak event discharge ($R_s$ 0.38 to 0.48) (Table 6.6). Antecedent rainfall was shown to have no significant correlation with discharge in the Aclands catchment. Similarly, average antecedent depth to water table for the two days preceding an event is shown to have no significant correlation with event discharge characteristics at any location (at $p$ <0.05, Table 6.6).

**Table 6.6: Spearmans Correlations of discharge and rainfall parameters. Columns refer to input parameters (water table and rainfall) and rows refer to output (flow) parameters.**

| | **, Correlation is significant at the 0.01level (2-tailed). *. Correlation is significant at the 0.05 level (2-tailed). | | **2 day Anticedent DWT cm A3/S3** | **2 day Anticedent DWT cm A2/S2** | **2 day Anticedent DWT cm A1/S1** | **Anticedent Rainfall - 2 days mm** | **Peak Event Rainfall Intensity** | **Total Event Rainfall** |
|---|---|---|---|---|---|---|---|---|
| Aclands N = 76 - 93 | Peak Discharge A3 | R | -0.09 | | | 0.14 | **0.38**** | **0.76**** |
| | Total Event Discharge A3 | R | -0.10 | | | 0.11 | **0.22*** | **0.89**** |
| | Peak Discharge A2 | R | | 0.23 | | 0.00 | **0.30**** | **0.65**** |
| | Total Event Discharge A2 | R | | 0.19 | | -0.04 | 0.19 | **0.79**** |
| | Peak Discharge A1 | R | | | -0.12 | 0.06 | **0.35**** | **0.69**** |
| | Total Event Discharge A1 | R | | | -0.20 | 0.07 | 0.06 | **0.86**** |
| | Peak Discharge Af | R | -0.12 | 0.00 | -0.11 | 0.08 | **0.40**** | **0.86**** |
| | Total Event Discharge Af | R | -0.11 | -0.03 | -0.14 | 0.05 | **0.23*** | **0.90**** |
| Spooners N = 33 - 38 | Peak Discharge S3 | R | 0.28 | | | **0.39*** | **0.51**** | **0.82**** |
| | Total Event Discharge S3 | R | 0.10 | | | 0.18 | -0.02 | **0.57**** |
| | Peak Discharge S2 | R | | 0.02 | | **0.48**** | **0.64**** | **0.79**** |
| | Total Event Discharge S2 | R | | -0.13 | | **.327*** | **.338*** | **.902**** |
| | Peak Discharge S1 | R | | | 0.00 | **.381*** | **.531**** | **.879**** |
| | Total Event Discharge S1 | R | | | -0.14 | 0.29 | 0.30 | **.901**** |
| | Peak Discharge Sf | R | 0.07 | -0.15 | -0.12 | **.426**** | **.464**** | **.759**** |
| | Total Event Discharge Sf | R | 0.04 | -.359* | -0.25 | 0.26 | 0.21 | **.708**** |

To explore the relationships of the variables identified in Table 6.6 further, total and peak rainfall were regressed against total and peak discharge across both sites and all scales (Figure 6.8). Total event rainfall is shown to have a strong relationship with both peak discharge and total event discharge (Figure 6.8), with the latter explaining up to 93% of the observed variation. However, this is not true in all cases, with total rainfall only explaining 35% of the variance in total flow at A2. Peak rainfall explained significantly less variance in both total and peak event discharge with maximum $r^2$ values of 0.4 to 0.3.

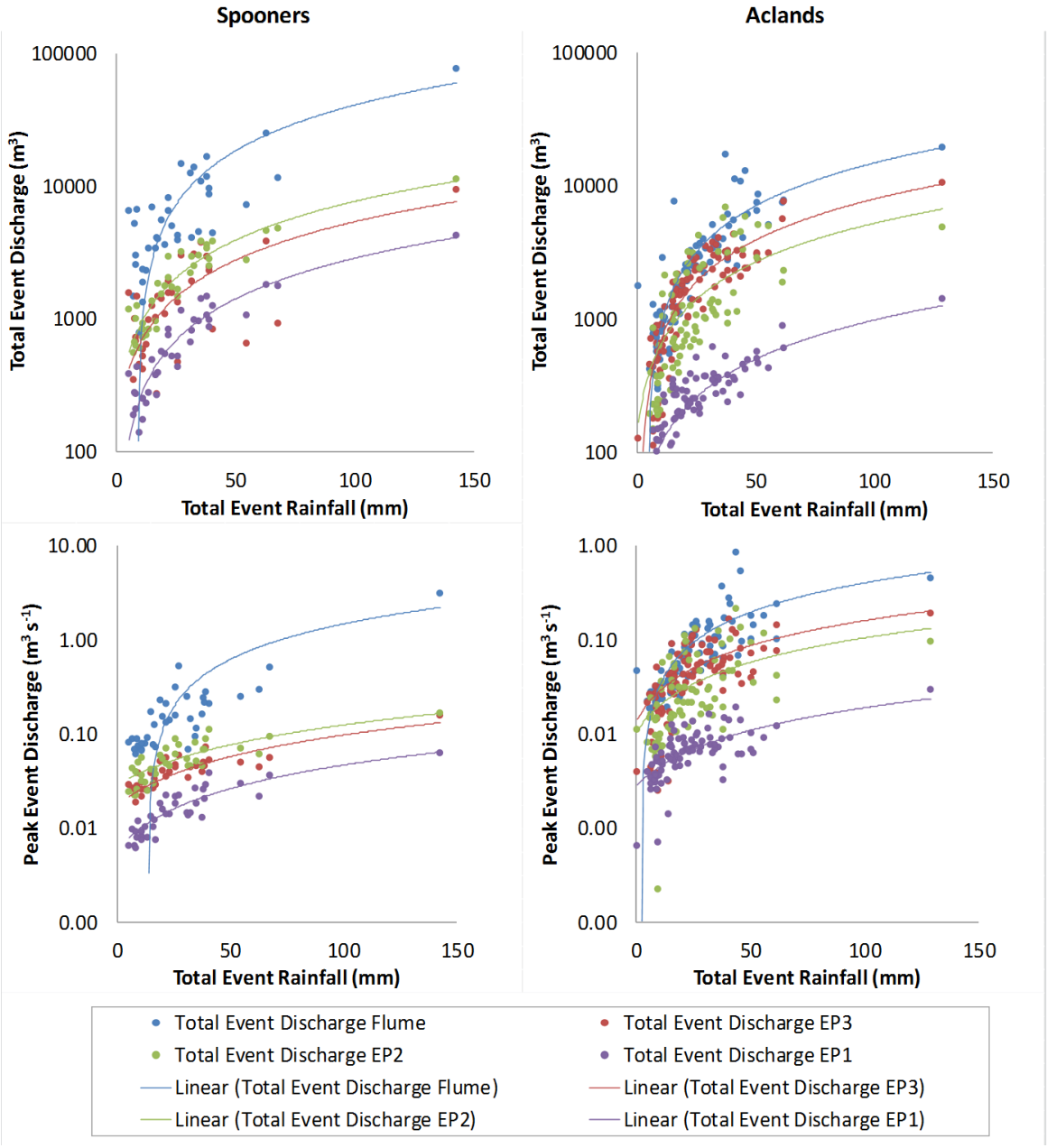


**Figure 6.8: Total event rainfall measurements versus total event flow parameters for all monitored rainfall runoff events and across all scales of monitoring.**

The data in Table 6.6 and Figure 6.8 suggest that the total rainfall is the primary driver of flow production in these catchments. Although antecedent hydrological conditions are shown to exert a weak secondary control on flow production (Table 6.6), understanding whether the additive explanatory power of these variables explains significantly more of the variation in event discharge may be useful. For this reason, multiple regression was conducted in SPSS, following transformation to ensure normalisation of the data (log10). This analysis (Table 6.7) illustrated that in all locations (except A1) the explanatory contribution of the antecedent DWT in predicting $Q_t$ is not significant at $p$ <0.05. Excluding DWT from the regression, the additive explanatory power of including antecedent rainfall and peak rainfall intensity, to predict $Q_t$ ranges from 3% (S2) to 16% (S3). This decreases from 1% to 11% when antecedent rainfall is also removed.

Similarly to $Q_t$, in all locations (except A1) the explanatory contribution of the antecedent water table in predicting $Q_p$ is insignificant at $p$ <0.05. The difference in explanatory power provided by the additional independent variables ($r_p$, $_ar$, $_a$DWT) has an inconsistent effect across the monitored locations. Specifically, at Aclands the additional variables are shown to reduce the predictive power of the model by up to 30%. Conversely, at Spooners the additional variables are shown to improve the prediction by up to 47%.

**Table 6.7: Multiple regression analysis deriving $r^2$ statistics for Event Discharge and Rainfall statistics. Variables are $Q_t$ = Total Discharge, $R_t$ = Total Rainfall, $R_p$ = Peak Rainfall, aR = Antecedent Rainfall, aDWT = antecedent depth to water table.**

| Location | Predictors of $Q_t$ | | | | | | | Predictors of $Q_p$ | | |
|---|---|---|---|---|---|---|---|---|---|---|
| | $R^2$ $Q_t$ and $R_t$, $R_p$, aR, aDWT | $R^2$ $Q_t$ - $R_t$, $R_p$, aR | $R^2$ $Q_t$ - $R_t$, $R_p$ | $R^2$ $Q_t$, - $R_t$ | Explanatory contribution of $R_p$ | Explanatory contribution of $R_p$, aR | Explanatory contribution of $R_p$, aR, aDWT | $R^2$ $Q_p$ - $R_t$, $R_p$, aR, aDWT | $R^2$ $Q_p$ - $R_t$ | explanatory contribution of $R_p$, aR, aDWT |
| Sf | na | 0.64 | 0.59 | 0.56 | 0.03 | 0.08 | na | na | 0.63 | |
| S3 | 0.60 | 0.54 | 0.50 | 0.38 | 0.11 | 0.16 | 0.22 | 0.63 | 0.69 | -0.06 |
| S2 | 0.87 | 0.86 | 0.84 | 0.83 | 0.01 | 0.03 | 0.04 | 0.34 | 0.65 | -0.31 |
| S1 | 0.87 | 0.87 | 0.85 | 0.82 | 0.03 | 0.05 | 0.05 | 0.65 | 0.79 | -0.14 |
| Af | na | 0.68 | 0.64 | 0.62 | 0.02 | 0.06 | na | na | 0.57 | |
| A3 | 0.73 | 0.70 | 0.65 | 0.64 | 0.01 | 0.06 | 0.09 | 0.73 | 0.53 | 0.20 |
| A2 | 0.73 | 0.70 | 0.65 | 0.64 | 0.01 | 0.06 | 0.09 | 0.78 | 0.31 | 0.47 |
| A1 | 0.76 | 0.69 | 0.65 | 0.63 | 0.03 | 0.07 | 0.13 | 0.84 | 0.54 | 0.30 |

### *6.4.3 Hypothesis C*

**Event discharge is generated only when water tables are close to the soil surface and rapid, saturation excess near surface flow occurs.**

To test hypothesis C the mean depth to water table and modelled channel discharge data are plotted for the whole of the recorded time series at each of the six locations where DWT was monitored and for a catchment wide mean DWT alongside the catchment outlets flow data, n = 68,000 to 86,000 (Figure 6.9). These data illustrate that in all EPs significantly elevated flow only occurs once the water table approaches the maximum of the observed range (though not always the soil surface). Both the inflexion point of the fitted line (Table 6.8) and minimum water table depth required to generate flow also appears to vary without respect to drainage scale (A3 and S3 representing the largest). Data in Table 6.8 also confirm that in all cases these relationships are significant at $p < 0.01$, although the coefficients derived illustrate a stronger correlation in the Spooners catchment.

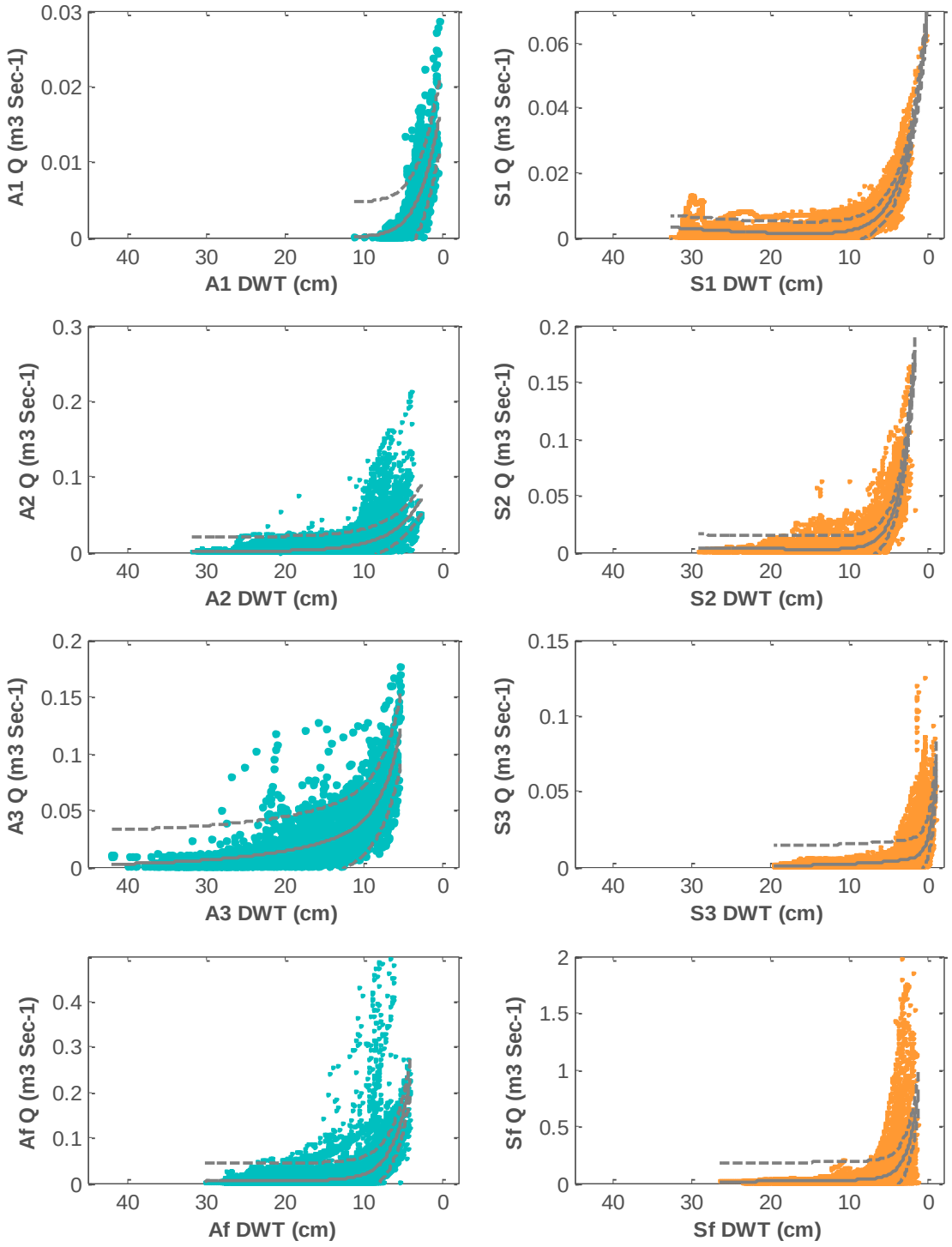


**Figure 6.9: Discharge vs water table depth plotted for the whole of the observed time series and across all experimental pool scales (n = 68,000 to 86,000). A two term exponential model is fitted to each plot and is bounded by a 95% confidence interval (dashed line).**

**Table 6.8: Statistics describing the discharge and water table depth relationship across all monitoring locations. Spearman's rank correlation coefficients describing the relationship between mean depth to water table as the controlling variable on discharge (including significance for all data plotted in Figure 6.9). Exponential regression $r^2$ values for all locations and the inflexion of the regressions used.**

| **. Correlation is significant at the 0.01 level (2-tailed). | S1 | S2 | S3 | A1 | A2 | A3 |
|---|---|---|---|---|---|---|
| **Coefficient** | **-.491**** | **-.567**** | **-.435**** | **-.838**** | **-.645**** | **-.694**** |
| **Sig. (2-tailed)** | 0.000 | 0.000 | 0.000 | 0.000 | 0.000 | 0.000 |
| **N** | 63633 | 68386 | 59107 | 44302 | 60684 | 74375 |
| **Exponential regression $r^2$** | 0.739 | 0.682 | 0.282 | 0.576 | 0.387 | 0.618 |
| **Depth to water table at inflexion** | 6.49 | 4.93 | 0.52 | 5.04 | 6.53 | 8.96 |

To confirm the results in Figure 6.9, analysis of the lag between peak DWT and peak Q was conducted over the full time series monitored (Table 6.9). This indicates that average lag between peak DWT and peak Q was often less than 30 minutes and where it was longer, the mean values were affected by significant skewness in the observed dataset. To illustrate this temporal relationship at an event scale Figure 6.10 demonstrates the average DWT and ditch discharge over 48 hours, during a rainfall runoff event on the 8/12/11 at Aclands EP2. The response of the water table was rapid in both wet-up and draw-down as evidenced by the steep ascending and descending limbs of the graph. The drawdown of the water table also appears to be largely complete within the response of the elevated channel discharge, and returns close to the pre-event level just over 24 hours following the start of the water table response. The grey dashed line highlights the synchronicity between water table wet-up and flow generation in the drainage ditch. Finally, it is seen that once water tables have reached maximum height, peak discharge follows virtually concurrently, illustrating the short lag times measured across the wider dataset and detailed in Table 6.9.

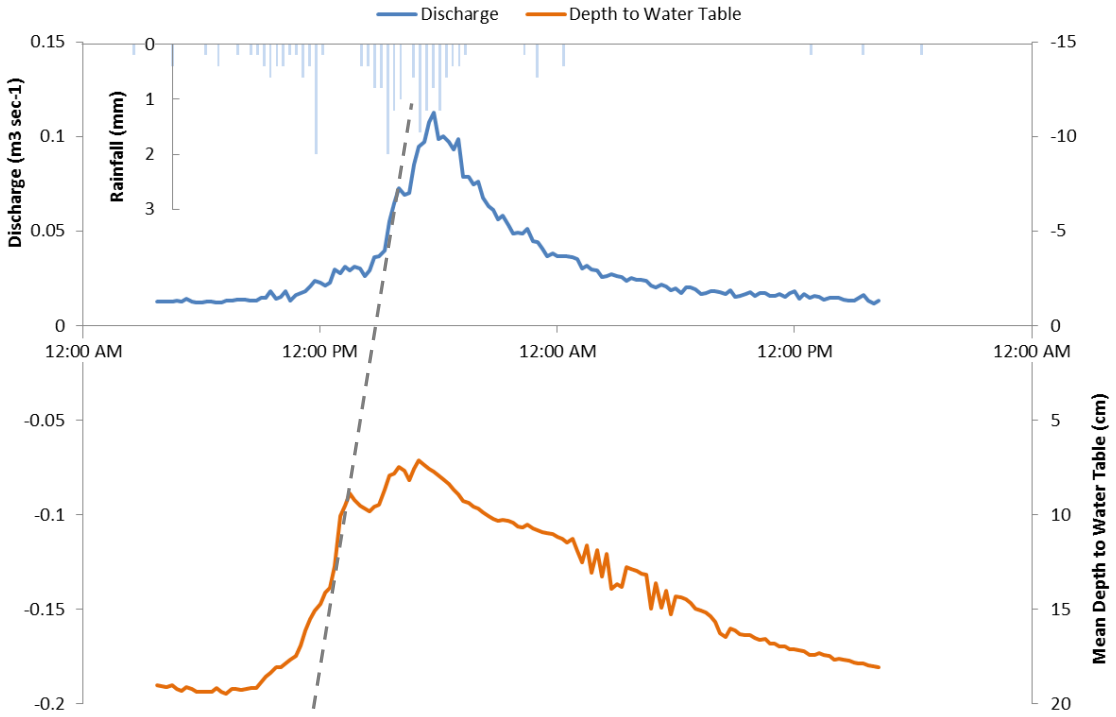


**Figure 6.10: Example average depth to water table and ditch discharge over 48 hours, during a rainfall runoff event on the 8/12/11 at Aclands EP2. Grey dashed line used to highlight the synchronicity between water table wet-up and flow generation in drainage ditch.**

**Table 6.9: Analysis of the lag between peak DWT and peak Q was conducted over the full time series and across all monitored locations recording DWT and Q.**

| | | S3 | S2 | S1 | A3 | A2 | A1 |
|---|---|---|---|---|---|---|---|
| | **Mean** | 0:15:33 | 0:08:36 | -0:33:20 | -3:40:33 | -1:44:26 | 0:16:56 |
| **95% Confidence Interval for Mean** | **Lower Bound** | -0:05:14 | -0:09:58 | -0:55:56 | -5:43:31 | -3:43:57 | 0:02:48 |
| | **Upper Bound** | 0:36:21 | 0:27:12 | -0:10:43 | -1:37:34 | 0:15:04 | 0:31:05 |
| | **Skewness** | -1.561 | .067 | -1.55 | -3.74 | -3.30 | 2.53 |
| | **Kurtosis** | 6.907 | 2.502 | 2.39 | 15.55 | 14.55 | 10.91 |

Figure 6.11 confirms that during periods isolated as “non rainfall-runoff events”, further water table drawdown outside of events is marginal and occurs over longer time periods (approximately 1000, 15 min time steps or around 10.4 days) therefore illustrating that the majority of water table drawdown happens

within the monitored event period and further water table drawdown is limited to extended periods of low rainfall.

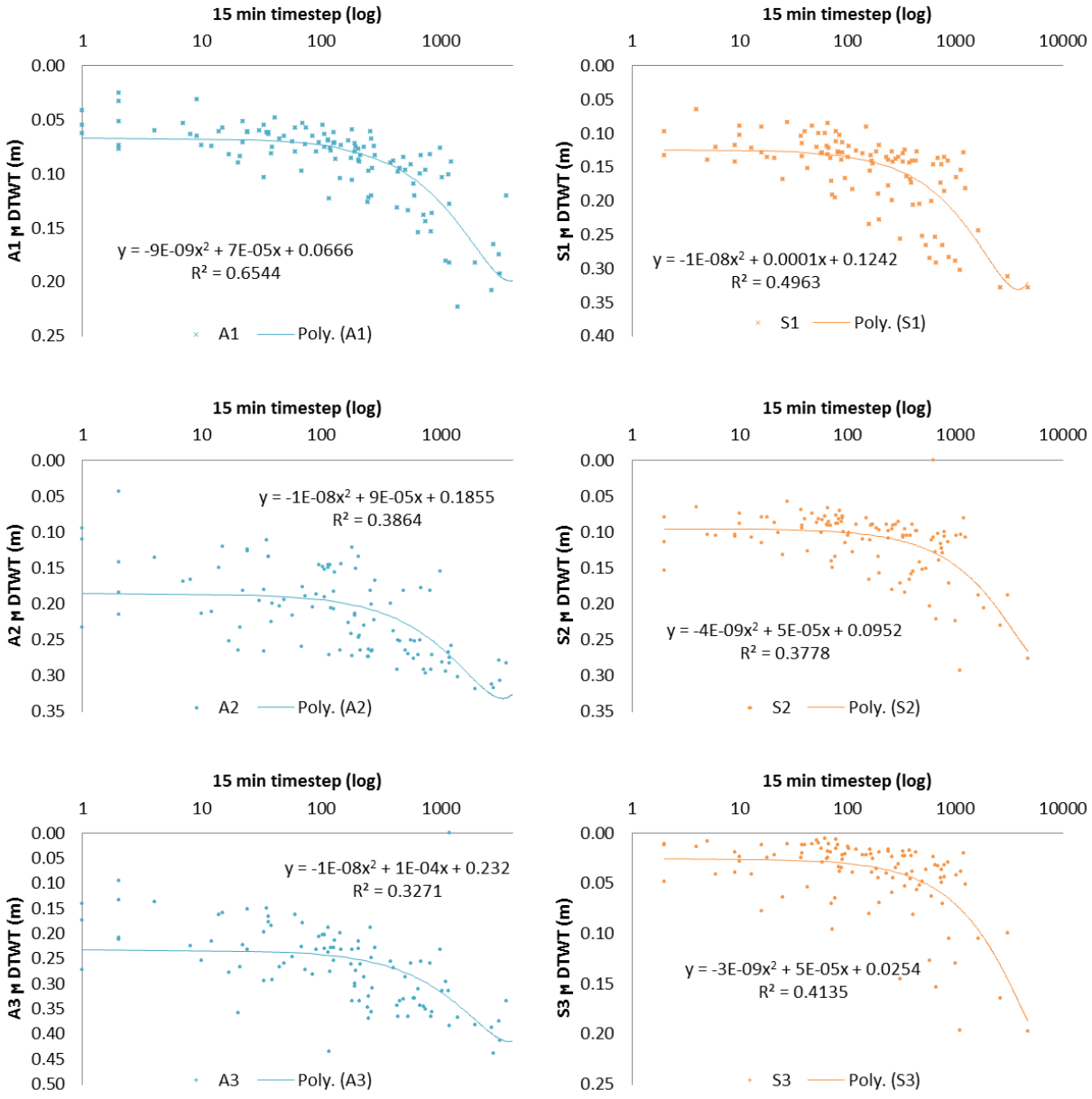


**Figure 6.11: Lowest measured mean water table (DTWT) during all observed "non-event" time series periods.**

## 6.5 Discussion

### *6.5.1 Hypothesis A*

**Flow regimes in shallow, drained peatlands are dominated by flashy storm flows and low base flow conditions**

In a damaged peatland landscape it may be expected that the introduction of anthropogenic drainage ditches will increase the hydrological connectivity of the peatland surface and reduce the capacity of ground water storage (Wilson et al., 2011b, Wilson et al., 2010, Goulsbra et al., 2014). A number of studies on deep peat landscapes have shown that ecosystems modified by drainage and erosion have concurrently higher rates of storm runoff and shorter lag times between peak rainfall and runoff (Holden et al., 2006b, Allott et al., 2014, Grayson et al., 2010). The flow time series collected for the two shallow peat catchments monitored in this study (Figure 6.4), demonstrates that at the outlet of both catchments flow regimes are dominated by very low base flow conditions that (especially at the Aclands catchment) are ephemeral during periods of low rainfall. Similarly, Figure 6.4 and Figure 6.5 both illustrate that during rainfall–runoff events peak discharge is proportionately high and immediate, across all the scales of drainage feature monitored.

Analysis of parameters quantifying the flashiness of the catchment and sub-catchment runoff responses of these shallow, damaged peatlands (Figures 6.5, 6.6 and 6.7), agrees with wider findings, again from deep peatlands, that rainfall/runoff responses are fast and highly connected (Grayson et al., 2010, Holden et al., 2006b). In addition, the lag times for each scale of drainage feature (Figure 6.6) demonstrate that the generation of flow is rapid across the studied catchments, and the lack of scaling in the lag times (intra-catchment), suggests that flow generation is reasonably synchronous across the whole catchment extent. The few instances of longer lag times observed appear to be a direct result of the inclusion of complex multimodal flow responses (with complex rainfall inputs) as part of this analysis. Data in Figure 6.7 describing the ratio between Q5 and Q95 (high flow probability and low flow probability), show that on a monthly basis the smaller of the two catchments (Aclands) exhibits a generally flashier flow response, despite notably lower recorded flows (Figure

6.5, Table 6.5). These data also demonstrate a good temporal correlation between flow responses in the two catchments suggesting that the drainage of these landscapes, whilst exhibiting local differences, has resulted in a broadly similar alteration to the hydrology of both catchments.

Average (mean) catchment lag times of between 3:34 hours and 4:22 hours are comparable to those recorded in headwater catchments found in the deeper re-vegetated peats of the Moor House National Nature Reserve described by Holden and Burt (2003b) in which average recorded lags were between 2:06 and 3:12 hours. However, data collected in this experiment are shown to exhibit significant skew, with lags more commonly between 0:30 and 1:45 hours (mode), indicating the lack of explanatory power implicit in using average data alone to understand temporal dynamics of this type. Indeed, the influence that such short lag times may exert on the fast flood response that is often seen in rivers in the South West of the UK, such as the Exe, may be significant (Kidson, 1953).

### *6.5.2 Hypothesis B*

**The primary control on runoff (Q) in shallow, drained peatlands is rainfall, with antecedent water tables and rainfall, exerting a secondary control.**

Parameters generated from the automatic rainfall-runoff event extraction enabled hypothesis B to be tested for all monitored events across all drainage scales in the time series. As found elsewhere, in these damaged peatland systems, precipitation exerts a strong control on discharge (Evans et al., 1999). In the shallow peatlands observed here, the correlation between total rainfall and event runoff (Figure 6.8 & Table 6.6) is consistently strong and positive, with total rainfall describing up to 90% of the variance in runoff response. Peak rainfall intensity is also shown to be a far weaker driver of either total or peak discharge. The lack of correlation between peak rainfall and flow may indicate that, at these locations, the infiltration capacity of the soil may not be exceeded by the rainfall intensity and thus infiltration excess overland flow may not be significant in generating channel flow responses. As found in other studies, saturation excess flow may therefore, be a stronger driver of runoff in these

landscapes (Holden and Burt, 2003b, Holden and Burt, 2002, Evans et al., 1999).

In a system dominated by saturation excess overland flow (explored further in section 6.5.3), it may also be expected that antecedent water table levels (and by inference rainfall) would exert some control on the generation of flow, particularly during times of greater water table drawdown (Evans et al., 1999, Daniels et al., 2008). However, the data presented in Table 6.7 suggest that, at most locations, the additional explanatory power when antecedent water table or rainfall is included in the multiple regression for total event or peak event discharge is both insignificant and minimal. Importantly, this finding suggests that timing of the rainfall event with respect to previous rainfall does not appear to control flow generation in the way observed in deeper peatland systems (Evans et al., 1999, Daniels et al., 2008)

### *6.5.3 Hypothesis C*

**Event discharge is generated only when water tables are close to the soil surface and rapid, saturation excess near surface flow occurs.**

Given that the antecedent depth to water table does not appear to function strongly in controlling event runoff (hypothesis b), the relationships between discharge and the water table over shorter time steps were examined further to identify the nature of runoff production in relation to DWT measurements. These data (Figure 6.11) illustrate that over the whole of the time series and across all of the scales monitored, the generation of channel flow is empirically linked to the height of the water table, as would be the case in a system dominated by saturation excess flow. Such findings agree with the work of Daniels et al. (2008) and Evans et al. (1999) who also demonstrated a link between raised water tables and flow in damaged peatland systems. Additionally, as these data are plotted from a 15 min time-step series, the dynamics of the change in water table and flow generation can be seen to operate over very short temporal scales. Such findings were also illustrated by Holden (2005) and Goulsbra et al. (2014), but may be especially relevant here, where the peat depths are shallow and any water table changes are intimately linked to surface flow production. Generalising across the monitored locations in Figure 6.9, these

data suggest that once the water table is within 5-10cm of the surface, flow begins to be generated in the adjacent channel feature and that higher flows only occur once the water table is close to its maximum vertical limit (i.e. within 5 cm of the surface). The lack of obvious separation in this trend also suggests that the relationship is relatively consistent for both the rising and falling limbs of the hydrograph.

Lag times between peak water tables and peak flows (Table 6.9) are often also very short (i.e. often less than 30 minutes), suggesting a direct temporal control on flow production when water tables near the surface and lateral near surface flow occur within the acrotelm (Evans et al., 1999). Data in Figure 6.10 illustrate a representative excerpt from the rainfall/flow time series at the Aclands catchment outlet and confirm that the generation of channel flow is directly related to the wet-up of the peat mass, and that this wet-up occurs almost immediately following any significant rainfall. Indeed both the wet-up and drawdown of the water table is shown to occur quickly and within the duration of the hydrograph. The short timescales (i.e. <24 h) over which wet-up/drawdown of the peat mass occurs at these locations explains much of the lack of correlation with antecedent conditions seen in other studies (Daniels et al., 2008, Evans et al., 1999). Indeed, when analysing the lowest recorded depth to water table recorded during all inter-rainfall event periods (Figure 6.11) it is apparent that further drawdown of the water table is only evident after much longer periods of no/low rainfall. Here, further drawdown of the water table is only shown to occur after approximately 10 days (1000 time steps) of inter-event duration, although it is unclear if events following these extended inter-event gaps demonstrate differing runoff production characteristics following rainfall.

### *6.5.4 Summary*

Data presented here indicate that shallow, damaged peatland systems are subject to flashy storm runoff and that this is primarily controlled by the total rainfall amount and not the intensity of this rainfall or antecedent conditions. Although this is broadly as expected in a system with increased drainage (and connectivity)(Evans et al., 1999, Holden et al., 2006b), the shallow nature of these peatlands appear to remove much of the longer term antecedent effect of

water tables on flow generation seen in other studies (Evans et al., 1999, Daniels et al., 2008). Instead, flow is generated quickly; following rapid and short lived wet-up of relatively thin peat soils, giving rise to short-lived saturation excess flow. This illustrates that, in the studied catchments, the effect of drainage in the thinner peat soils increases the drainage efficiency and runoff connectivity without significantly increasing the available storage in the peat mass. Specifically, the extremely rapid wet-up and drawdown seen in the water table as a response to rainfall (Daniels et al., 2008) suggests that the potential for increased buffering and storage in the peat mass (Lane and Milledge, 2013) is mitigated by rapid movement of water laterally through the near surface/eroded (or more appropriately, drain) acrotelm.

Indeed in other studies (Wilson et al., 2010, Wilson et al., 2011b), the decrease in drainage connectivity following restoration (blocking) is seen to lower peak flows, despite increased water tables being recorded concurrently. A decrease in landscape connectivity and an increase in both soil and channel storage following landscape rewetting which is underway in these catchments may therefore result in two important changes to the hydrological functioning of these systems. Firstly, it may be expected that flood hydrographs will be significantly attenuated, both in terms of lower peak flows and also in terms of longer durations (Wilson et al., 2010, Wilson et al., 2011a). This is because a system with decreased connectivity should decrease both the synchronicity and speed of runoff generated. Secondly, storage is likely to be increased both via enhanced water tables, but also due to the surface water storage that occurs upslope of ditch blocks (Worrall et al., 2007b). Consequently we may expect the increase in surface buffering and drainage lengths to produce consistently less flashy flows and response times, throughout a range of hydrological conditions, once these catchments are restored.

## 6.6 Conclusions

This study represents the first time that such a detailed spatio-temporal monitoring scheme has been implemented in shallow and drained peatlands. Results presented demonstrate that overall, flow regimes in shallow, drained and marginal peatlands have a flashy runoff response and poorly maintained base flow. Furthermore, a combination of thin peat soils and extensive

anthropogenic drainage networks, mean that antecedent hydrological conditions exert little control on the total or peak flow produced during rainfall-runoff events.

The findings of this study provide a robust baseline for the hydrological function of damaged peatland systems in analogous landscapes. The number and range of drainage scales studied, and the duration of monitoring, ensure these data are representative of the wider landscape on Exmoor; a great deal of which is currently undergoing rewetting or has recently been restored. These data suggest that restoration has the potential to significantly reduce flow generated during rainfall events, attenuating hydrograph peaks and increasing base flow duration and magnitude. These findings represent a significantly enhanced mechanistic understanding of the hydrological processes operating in these peatlands. Such information is important for those managing these landscapes, and who manage the downstream effects of runoff from these uplands, such as flooding. Ongoing work will quantify the effects of contemporary landscape restoration and in combination with these findings, will provide an important evidence base for the continued investment in the management of similar thin and marginal peatland landscapes. Such findings will also help quantify the potential for future enhancement of key ecosystem services arising from these landscapes, including flood attenuation and carbon storage/sequestration.

Finally, the spatial variability of rainfall-runoff and water table responses in these landscapes are presented in a companion piece to this study; Understanding the hydrology of shallow drained and marginal peatlands: Spatial variability (Luscombe et al., forthcoming, Chapter 7).

# 7 Understanding the hydrology of shallow, drained and marginal peatlands 2. Spatial Variability

David J. Luscombe[1], Karen Anderson[2], Emilie Grand-Clement[1], Naomi Gatis[1], Josie Ashe[1], Pia Benaud[1], David Smith[3] and Richard E. Brazier[1]

1 Geography, CLES, University of Exeter, Amory Building, Rennes Drive, Exeter, Devon EX4 4RG

2 Environment and Sustainability Institute, University of Exeter, Cornwall Campus, Treliever Road, Penryn, Cornwall, TR10 9EZ

3 South West Water, Peninsula House, Rydon Lane, Exeter. Devon EX2 7HR

## 7.1 Abstract

Peatlands in the South West of the UK differ in both their structure and function from deeper, upland peatlands found in more northerly locations. In a companion paper we establish that these drained peatlands demonstrate rapid storm runoff that is primarily controlled by the total rainfall amount and not significantly linked to the rainfall intensity or any antecedent hydrological conditions. The latter are shown to have minimal, secondary controls on runoff responses. However, peatlands are also known to exhibit significant variation in ecohydrological organisation and structure across different spatial scales. Furthermore, predictions of hydrological response using spatially distributed numerical models of rainfall-runoff may be flawed unless they are evaluated with datasets describing the spatial variability of hydrological responses. This paper seeks to quantify whether longer term flow generation and water storage characteristics are also controlled by the spatial attributes of the contributing catchment area or the local drain morphology and geometry. Results from an experiment conducted over multiple nested spatial scales and over long (multiannual) timescales within degraded upland peatland catchments, highlights that the spatial variation in the discharge characteristics from multiple drainage features is significant. Indeed, the detailed monitoring of hydrology at multiple scales highlights the importance of using spatially distributed monitoring to ensure that estimations of discharge across such landscapes are representative. The local scale of the drainage feature (i.e. depth and width), or

the topographic contributing area associated with such drainage is also shown not to be a definitive predictor of discharge metrics at a given location. Furthermore, subtle variations in the local slope and topography are shown to account for key variation in the long-term patterns of water table depth across the catchment.

## 7.2 Introduction

Peatlands in the South West of the UK differ in both their structure and function from deeper, upland peatlands found in more northerly locations (Grand-Clement et al., 2013, Dixon et al., 2013). Due to their maritime position, these shallow and degraded peatlands may be more sensitive to climate change than their more northerly counterparts elsewhere in Europe (Gallego-Sala et al., 2010, Clark et al., 2010). In a companion paper (Luscombe et al., Forthcoming, Chapter 6) we establish that these ecosystems demonstrate rapid storm runoff that is primarily controlled by the total rainfall amount and is not significantly linked to the rainfall intensity or any antecedent hydrological conditions, which demonstrate minimal, secondary controls on runoff responses. Unlike deeper peatlands, where the longer term antecedent conditions have a greater potential to affect water tables and storm flow generation (Daniels et al., 2008, Holden, 2005), in these shallow peatlands (Luscombe et al., Forthcoming, Bowes, 2006), flow is generated quickly following rapid and short lived wet-up of the thinner, heavily drained peat soils.

These insights into the temporal dynamics governing hydrological processes in marginal, damaged peatlands are important as a baseline from which restoration interventions may be evaluated (Schumann and Joosten, 2008). However, these peatlands are also known to exhibit significant variation in ecohydrological organisation and structure in space at multiple scales (Luscombe et al., 2014a, Luscombe et al., 2014b). Given the uncertainty in the spatial distribution and ecohydrological assessment of peatlands more widely (Morris et al., 2011, Lindsay, 2010, Lindsay, 1995, Holden, 2005), it is important to recognise the contribution that fully spatially integrated monitoring of hydrological processes can provide to understand these complex landscapes (Bragg and Tallis, 2001). Several studies acknowledge a lack of monitoring programs able to capture the full spatial heterogeneity of hydrological behaviour

in peatlands (Holden et al., 2011, Holden et al., 2004, Parry et al., 2014), limiting the potential for extrapolation of processed-based understanding of rainfall and runoff response over larger landscape extents (Ballard et al., 2011). Thus, it is proposed that a detailed, spatially explicit and fine spatial resolution monitoring program may overcome these problems.

Furthermore, predictions of hydrological response using spatially distributed numerical models of rainfall-runoff may be flawed unless they are evaluated with datasets describing the spatial variability of hydrological response (Lamb et al., 1998). Indeed, the problem of spatial equifinality, where multiple expressions of a catchment response to rainfall might result in the same catchment outlet hydrograph, is a problem that is rife throughout the hydro-geomorphological literature (Lamb, 1996, Beven and Brazier, 2011, Beven, 2006). Thus, spatially explicit datasets that may help to constrain model predictive uncertainty, by eliminating inappropriate representations of surface flow or wetness, are needed. To meet these needs, this paper argues that the number, spatial distribution and range of drainage scales monitored in part one of this study (Luscombe et al., Forthcoming) represents a dataset appropriately representative of the wider landscape extent. Additionally, the extended duration of monitoring undertaken (multi-annual) ensures that the temporal variation of hydrological processes is sufficiently represented throughout all monitoring locations, thereby allowing for representative inter-site comparisons to be made. In this paper the dataset used in the companion paper (Luscombe et al., Forthcoming) is re-analysed spatially to derive new metrics describing the spatial distribution and spatial variability of the processes governing flow generation and water storage in the anthropogenically altered peatlands of Exmoor National Park.

Specifically, this paper utilises the multiple water table and discharge timeseries collected from the six monitored drainage features across both experimental catchments detailed in part one of this study (Luscombe et al., Forthcoming) to improve understanding of the fine spatial scale hydrological processes which govern water storage and runoff production in these landscapes. These data are used in combination with catchment outlet discharge, rainfall and LiDAR data, to establish both the variability of such measurements in space and establish whether longer term flow generation and water storage characteristics

are also controlled by the spatial attributes of the contributing catchment area or the local drain morphology and geometry. The following hypotheses are tested in order to fulfil the above aims:

### *7.2.1 Hypothesis A*

**Spatial variability of rainfall-runoff response is proportional to the size of the drainage channel and the spatial attributes of its topographic contributing area**.

In part one of this study, these shallow degraded peatlands are shown to produce rapid and short lived storm runoff responses, through a principally synchronous catchment response (Luscombe et al., Forthcoming, Chapter 6). It may therefore, be expected that analogous drainage features on similar hillslope positions will exhibit similar runoff responses that vary proportional to their contributing area or drainage network size (Pilgrim et al., 1982). Accordingly, drainage structures of larger cross-sectional area or higher stream order may be expected to exhibit a stronger response to rainfall inputs. However, the hydrological connectivity of these peatlands is poorly understood due to the complex microtopographic and diplotelmic characteristics of peatland systems (Goulsbra et al., 2014). Similarly, It is well known that topographically derived contributing areas are often misrepresentative of true contributing areas due to transmissive subsurface flow in peatlands (Daniels et al., 2008). Therefore, examining drainage scale/size as a factor related to the regulation of discharge may better inform the conceptual understanding of flow generation and storage across these drained landscapes.

### *7.2.2 Hypothesis B*

**Mean (and variance) of depth to water table (DWT) is greatest proximal to functioning drainage features, decreasing with distance from the drain.**

Given that the monitored drainage features were implemented in order to lower the water table in the adjacent peat mass, establishing the lateral extent of this water table variability will allow an assessment of the distance at which the effect of the drainage channel becomes limited. Additionally this mechanism will permit examination of the variability implicit in the DWT at any given distance

from the drainage feature, both across and between the monitored catchments. Data collected to address this hypothesis will therefore allow an estimation of the potential of rewetting and the variability associated with extrapolating these estimates across the landscape.

### *7.2.3 Hypothesis C*

**Variance in depth to water tables can be explained by position of the drainage ditches with respect to local topography.**

Variance in the observed DWT across all monitored locations will be affected by local heterogeneity in soil properties, soil depth and the hydraulic gradient of the groundwater with respect to localised topography (Allott et al., 2009, Evans et al., 2014, Holden, 2005, Morris et al., 2011, Wilson et al., 2010). Disaggregating DWT measurements across the locations monitored will provide insight into the specific effect of local soil depth and topography in controlling variation in DWT in the studied peatlands. These data will therefore, further enhance the spatial understanding of how drainage affects DWT across larger spatial extents.

## 7.3 Methods

As detailed in the companion paper (Luscombe et al., Forthcoming) and spatially characterised in Luscombe et al. (2014a) and Luscombe et al. (2014b) (Chapter 4, 5 and 6), two headwater catchments were selected within drained upland peatland areas in Exmoor National Park, that were representative of the regional shallow blanket mire complexes. These sites were established to monitor a range of drainage ditch morphologies, drainage densities, peat depth, slope morphology, aspect and vegetation composition. The location of the studied catchments (known locally as ‘Aclands’ [SS 733,384] and ‘Spooners’ [SS 776,374]) is shown in Figure 7.1.

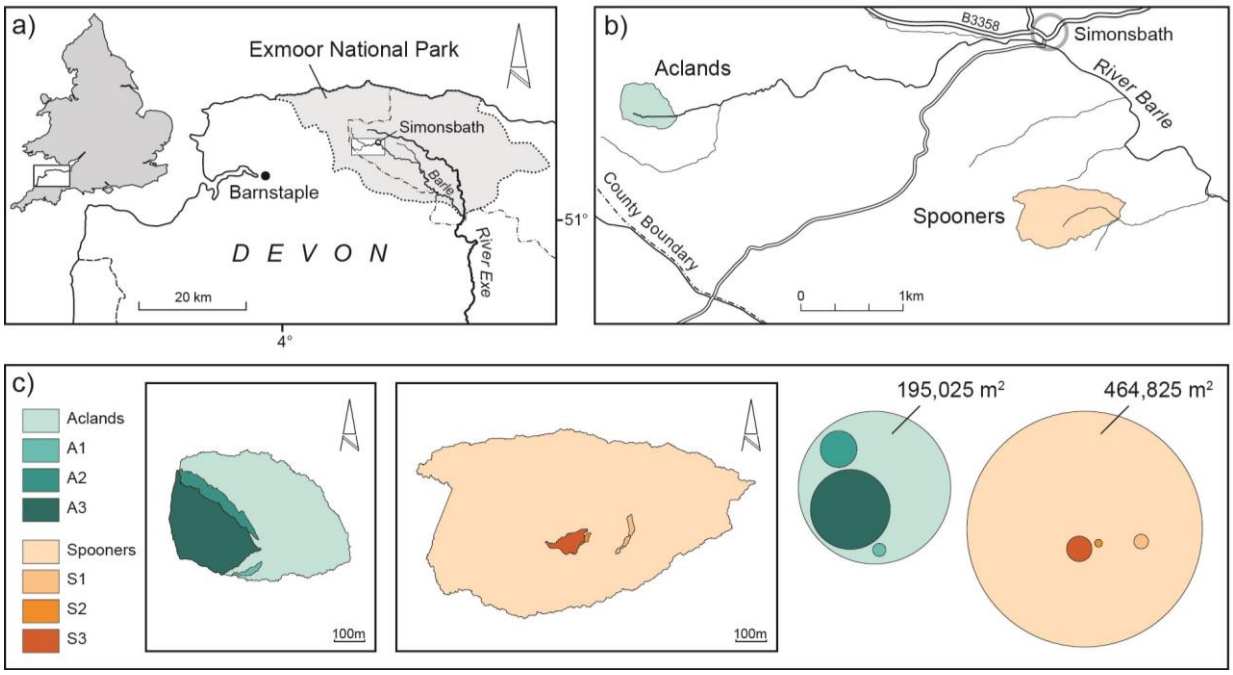


**Figure 7.1: a) and b) location of study catchment in the south west of England. c) relative size of LiDAR delineated sub catchments as both geographically correct and proportional contributing areas.**

A detailed description of the site selection, monitoring design, analytical design and data acquisition methods are also detailed in the companion paper (Luscombe et al., Forthcoming). To briefly summarise, the experimental design and implementation comprises monitoring of DWT at 96 locations and discharge in 8 open channels, across two headwater sub-catchments and at multiple drainage scales. The stage, rainfall and DWT measurements were logged continuously every 15 minutes in the field using a telemetry system, which also returned data continuously via VHF and GPRS connectivity (Adcon remote telemetry system). Flow was modelled at three drainage features, called 'experimental pools' (EP), of differing sizes within each of the two catchments and also estimated at each of the two catchment outlets using rated flume structures and stage/velocity monitoring equipment. Each monitored drainage feature was labelled relative to its perceived drainage scale at installation (from one, small, to three, large) and was also identified to its overall catchment (S = Spooners, A = Aclands). Data for the overall catchment outlet is also included and denoted as f (flume site), giving rise to 8 scales of hydrological monitoring over 2 catchments (i.e. A1, A2, A3, Af, S1, S2, S3, Sf). The geographic position of the monitored drainage features within the studied catchments is described in

detail in the companion paper. DWT measurements were taken at 16 locations around each monitored drainage feature, as detailed in Figure 7.2.

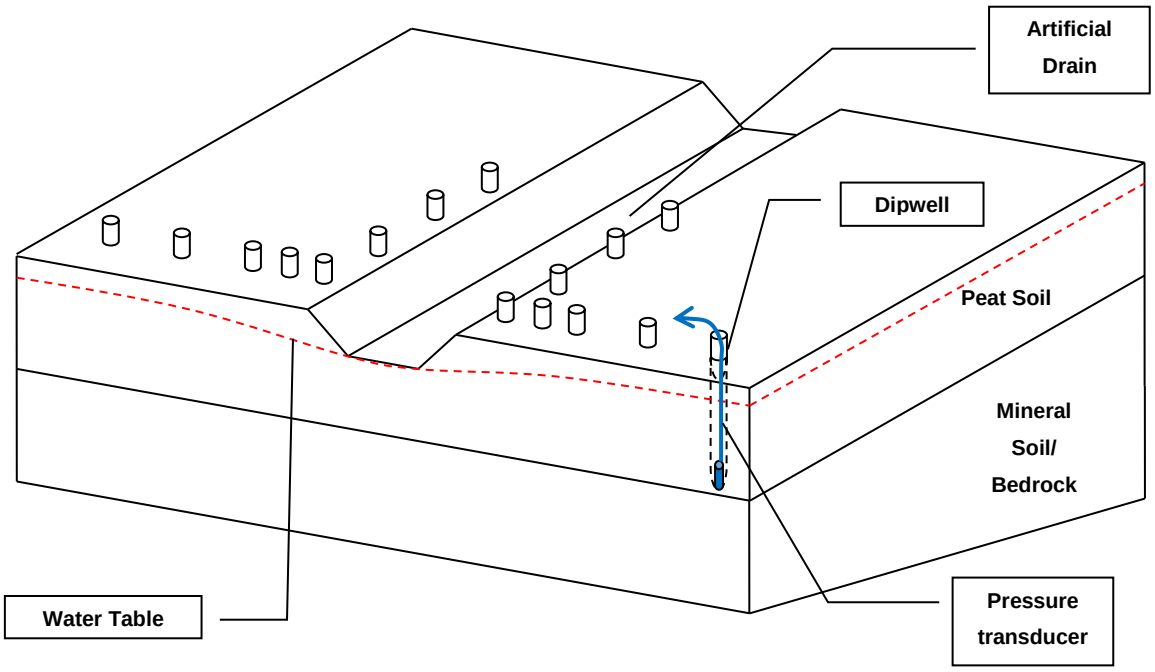


**Figure 7.2 Design of experimental pools dipwell arrays. Conceptual design locating mini piezometers (dipwells) distributed along two axes adjacent to an anthropogenic drainage feature.**

### *7.3.1 Delineation of contributing areas*

Topographic contributing areas for each EP and the wider catchment, were calculated using a LiDAR derived digital surface model (DSM) and a basic flow accumulation modelling algorithm based on the methods described in Jenson and Domingue (1988). This technique models flow accumulation by calculating the accumulated weight of all cells "flowing" into each downslope cell in a given DSM and was implemented using the spatial analyst extension in ArcGIS 10.0. Airborne LiDAR data were collected by the Environment Agency Geomatics Group (www.geomatics-group.co.uk) in May 2009 and provided as a 0.5 m spatial resolution DSM product. LiDAR data were checked for accuracy at five separate locations by the Geomatics group, using a differential Global Positioning System (DGPS) survey. These ground truth data indicated an average systematic error of + 0.0004 m and an average random bias of ± 0.047 m in elevation. The combined root-mean-square error (RMSE) for these data

was 0.029 m i.e. within the product specification of 0.15 m (Luscombe et al., 2014a) (EAGG pers. comm. 2012).

The Jenson and Domingue (1988) model used here, provides only a simple estimation of the topographic contributing area for any given point as all precipitation is assumed to become runoff and not lost to interception or groundwater. Although this approach is hydrologically simplified, previous work on these catchments have suggested that the majority of runoff is generated quickly following rapid and short lived wet-up of the thinner, drained peat soils, producing complex surface flow pathways influenced by artificial drainage features (Luscombe et al., 2014a, Luscombe et al., 2014b, Luscombe et al., Forthcoming). As such, it was hypothesised that the Jenson and Domingue (1988) technique may be useful to delineate the likely contributing area for any given sub-catchment across the area monitored.

In order to maximise the topographic representation of the flow routing model for these catchments, the LiDAR DSM was modified in two ways. Firstly, as the anthropogenic surface drainage network is known to be under represented in the LiDAR DSM due to the concomitant effect of short-sward vegetation structure, (Luscombe et al., 2014a), a manually GPS surveyed position of these networks was used to quantify the depth of the drainage features, and therefore the extent to which they are able to influence the modelled flow pathways. A hand held GPS unit with a spatial accuracy of <1 m (Thales Navigation, MobileMapper CE) was used to record the position of these features which were then rasterised in Arc GIS (version 10.0) with a constant depth value of 0.5 m (to be greater than the local vertical variation) and used to facilitate DSM modification representative of drainage across the studied catchments. Secondly, the DSM surface was optimised to remove spurious topographic sinks that actually reflect complex ecohydrological structure rather than isolated surface depressions (Luscombe et al., 2014a). As vegetation sinks in the DSM are known to relate to areas of higher connectivity in the studied catchments, the method employed a combined “cut and fill” algorithm to remove sink pixels without degrading the underlying surface complexity and connectivity. Using the methods from Soille (2004), sinks were removed by calculating the optimum minimum cost of vertical transformation to achieve connectivity with neighbouring non sink areas. The resulting dataset comprised of a modified

DSM in which surface connectivity was maintained without significant degradation of the surface complexity. The resultant DSM also provided an enhanced representation of the surface drainage, without introducing any further topographic sinks. The derived contributing areas then had their planar area calculated and used to derive summary statistics and frequency distributions for indexes of surface roughness (Jenness, 2004), Strahler stream order delineation (Strahler, 1957) and drainage density. The spatial extent and lateral geometry of these contributing areas is illustrated in Figure 7.1, C.

### *7.3.2 Data and statistical analysis*

As described in sections 6.3.1 – 6.3.4, alongside longer term discharge metrics (i.e. average daily flow, average overall flow etc.) discharge data were extracted automatically for every rainfall runoff event that occurred during the monitoring period (January 2011 to October 2013). Rainfall run-off based statistics used in this analysis are defined as $Q_t$ (total discharge) and $Q_p$ (peak discharge). Long term averages of these data are also used for each location to quantify differences excluding inter event discharge variability (i.e. drought periods). To address hypothesis A, following appropriate transformation (log10) of $Q_t$ and $Q_p$, the frequency distribution for each monitoring scale was extracted and tested using a parametric analysis of variance (one way ANOVA and “least significant difference” post hoc testing). This enabled the significance of the difference between any given pair of data ($Q_t$ or $Q_p$ distributions) to be established. To address hypothesis B, forth order polynomial regression was used to establish the shape and strength of the relationship between DWT and distance from drainage features.

## 7.4 Results

### *7.4.1 Hypothesis A*

**Spatial variability of rainfall-runoff response varies with scale of the drainage system.**

Analysis of the trends in flow characteristics (average base, peak and total flow) observed throughout the examined time series and across all scales of

monitoring (Figure 7.3) shows that the proportion of peak flow, total or base flow is relatively consistent, compared to the spatial variation in the overall magnitude of flow from these locations. For example, average base flow is between 3% and 10% of average peak flow and 27% to 51% of average total flow in Figure 7.3. In contrast, Af has average peak flows 14.7 times larger than A1, and S2 has peak flows 3.2 times larger than S1. This suggests that the spatial variation in the magnitude of discharge is larger than the spatial variation in the discharge characteristics of the flow generated. It can also be noted that, given the selection of the drainage features monitored is based on the scale of the drainage features measured in the field (depth and width, Table 7.1) here, S2 is anomalous in its high values for base, total and peak flow characteristics relative to the other drainage features within the same catchment.

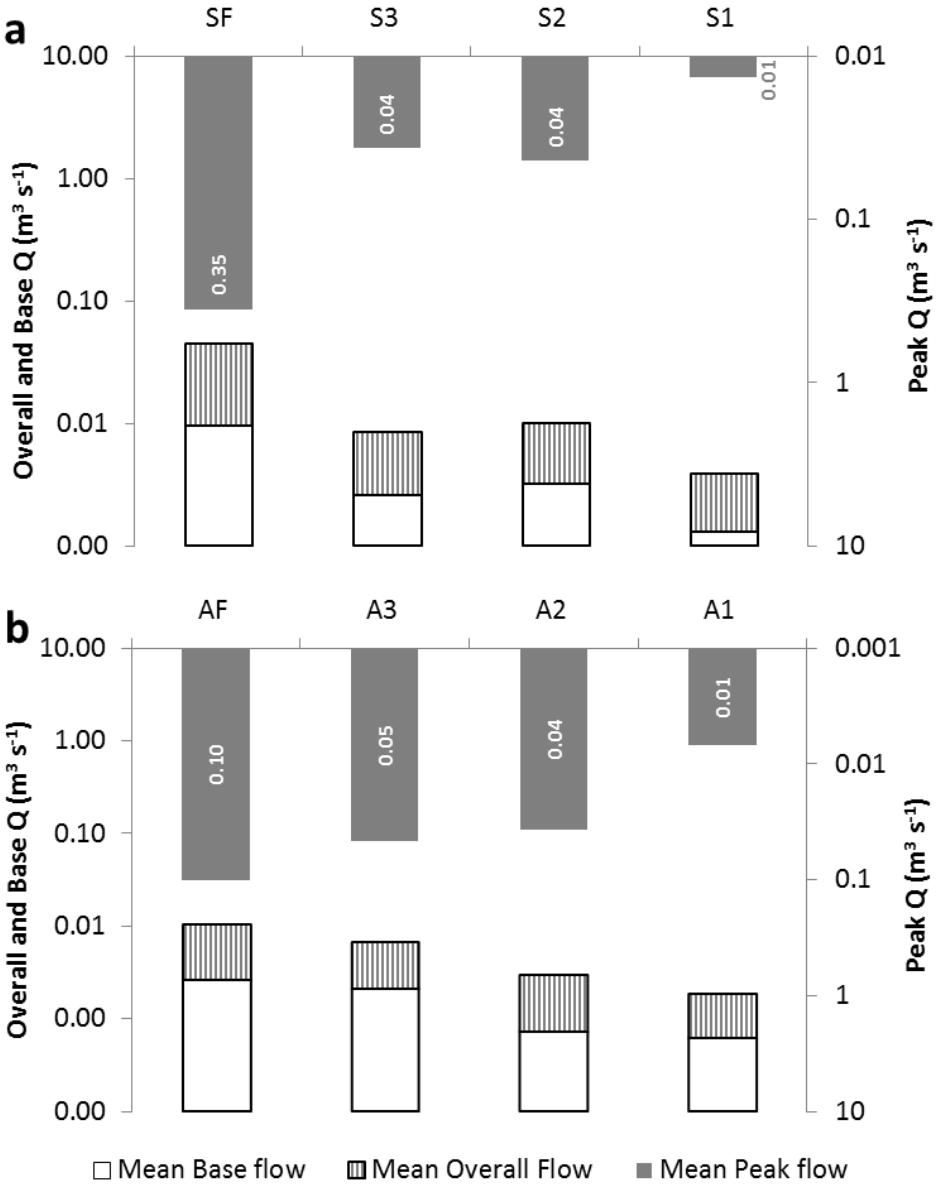


**Figure 7.3: Breakdown of the mean base flow (i.e. non rainfall event flow), mean rainfall event peak flows and mean total flows across each scale of drainage and across both catchments. a. discharge metrics reported for Spooners without any contributing area assumption. b. discharge metrics reported for Aclands without any contributing area assumption.**

The regression of event based rainfall runoff metrics ($Q_{t,}$ and $P_t$ , Figure 7.4) illustrates that the strong control that total event rainfall exerts on estimated total event discharge also largely scales with respect to the size of the drainage feature monitored (depth, width Table 7.1). In both cases the discharge measured at the flume scale is highest, and the smallest monitored drainage feature (A1 and S1) are the lowest. However, again, S2 indicates a disproportionately high response of $Q_t$ mm per unit rainfall.

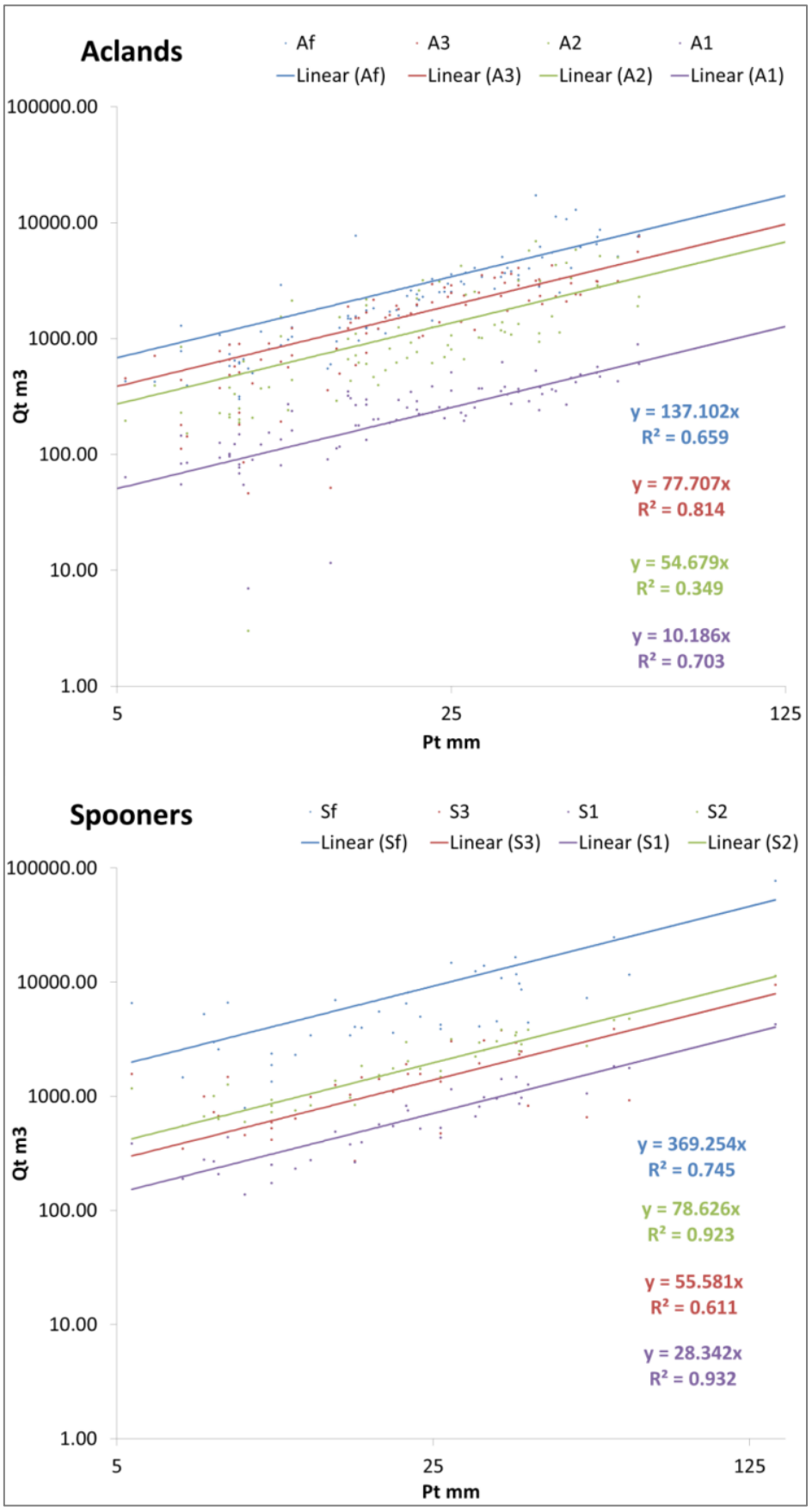


**Figure 7.4: Total event rainfall measurements versus total event flow parameters for all monitored rainfall runoff events, and across all scales of monitoring.**

To explore additional factors that were hypothesised to control the spatial variability of hydrology, (including contributing area and ecohydrological structure) these independent variables have been calculated for each monitoring scale alongside the absolute flow parameters calculated (Table 7.1).

**Table 7.1: Flow characteristics and scale related measurements for each of the monitoring locations analysed, and the associated topographically delineated contributing areas.**

| Parameter | Average Flow | Max Flow | Standard Deviation of Flow | Mean Base flow | Mean Peak flow | Average daily flow | Topographic Cont. area | Channel Depth | Channel Width | Strahler Stream order | Roughness index mean | Drainage density | Mode Peat Depth |
|---|---|---|---|---|---|---|---|---|---|---|---|---|---|
| | Q $m^3 s^{-1}$ | Q $m^3 s^{-1}$ | ND | Q $m^3 s^{-1}$ | Q $m^3 s^{-1}$ | $m^3$ | $m^2$ | m | m | ND | ND | m $m^2$ | cm |
| **SF** | 0.035 | 3.117 | 0.062 | 0.010 | 0.355 | 3064 | 464825 | Flume | Flume | 8 | 187 | 0.02 | No data |
| **S3** | 0.006 | 0.157 | 0.008 | 0.003 | 0.037 | 504 | 5335 | 0.86 | 5.6 | 4 | 192 | 0.01 | No data |
| **S2** | 0.007 | 0.164 | 0.010 | 0.003 | 0.044 | 594 | 499 | 0.49 | 2 | 3 | 234 | 0.05 | No data |
| **S1** | 0.003 | 0.062 | 0.004 | 0.001 | 0.013 | 223 | 1770 | 0.31 | 1 | 3 | 238 | 0.03 | No data |
| **AF** | 0.008 | 0.842 | 0.020 | 0.003 | 0.101 | 664 | 195025 | Flume | Flume | 7 | 168 | 0.04 | 33 |
| **A3** | 0.005 | 0.192 | 0.011 | 0.002 | 0.047 | 396 | 53161 | 0.55 | 2.7 | 6 | 164 | 0.06 | 33 |
| **A2** | 0.002 | 0.097 | 0.005 | 0.001 | 0.037 | 192 | 11220 | 0.34 | 1.6 | 4 | 149 | 0.02 | 38 |
| **A1** | 0.001 | 0.029 | 0.002 | 0.001 | 0.007 | 105 | 1428 | 0.145 | 1.4 | 3 | 106 | 0.07 | 40 |

As both long-term and event-based hydrological metrics appear to exhibit scale-related differences between monitoring locations (Figures 7.3 and 7.4), the frequency distribution of peak and total discharge ($Q_p$ and $Q_t$) measured in individual rainfall – runoff events was analysed (Figure 7.5). Each monitoring scale across both catchments was also ranked according to the LiDAR delineated catchment/sub-catchment area (Table 7.1) as detailed in the methods (right smallest, left largest in Figure 7.5). Analysis of variance (one way ANOVA) between these groups reveals that at least one of the distributions was significantly different for both $Q_p$ and $Q_t$. However, post-hoc analysis reveals that the variation in $Q_t$ and $Q_p$ is not significantly different across all of the scales of monitoring analysed. For example the difference in $Q_t$ between S3, A3 and A2 is not significant at $p$ <0.05, despite the drainage depth varying between 0.34 and 0.86 meters (width 1.6 and 5.6 metres respectively) and

topographically delineated contributing areas varying between 53,161 $m^2$ and 5, 335 $m^2$. Similarly S2 demonstrates no significant difference in $Q_t$ or $Q_p$ to S3 and Af, despite a very small theoretical contributing area of 499 $m^2$. These data illustrate that, although significant differences are evident in the distribution of $Q_t$ and $Q_p$ measured across space, these are not directly related to the scale of the drainage feature or the scale of the topographic contributing area.

As distributions of $Q_t$ across several of the sub-catchment monitoring scales are not significantly different (Table 7.2), despite highly varying surface contributing areas (Table 7.1), normalising total discharge by the contributing area at each scale was not considered appropriate (as discussed in section 7.5.1 later in the paper). However, as the Aclands and Spooners catchments (Af and Sf) do exhibit significantly different distributions of $Q_t$ and $Q_p$ at the largest scale (Figure 7.5, Table 7.2) and contributing areas delineated at higher stream orders are influenced by broader scale topographic change, these scales do allow for some degree of spatial normalisation. Using the topographic catchments areas for Spooners and Aclands, to normalise event $Q_t$ derives distributions of event $Q_t$ and $Q_p$ that are not significantly different at $p < 0.05$. The production of runoff (mm) per unit rainfall (mm) at each catchment following normalisation is also comparable at 69.8% at Aclands and 79.4% at Spooners.

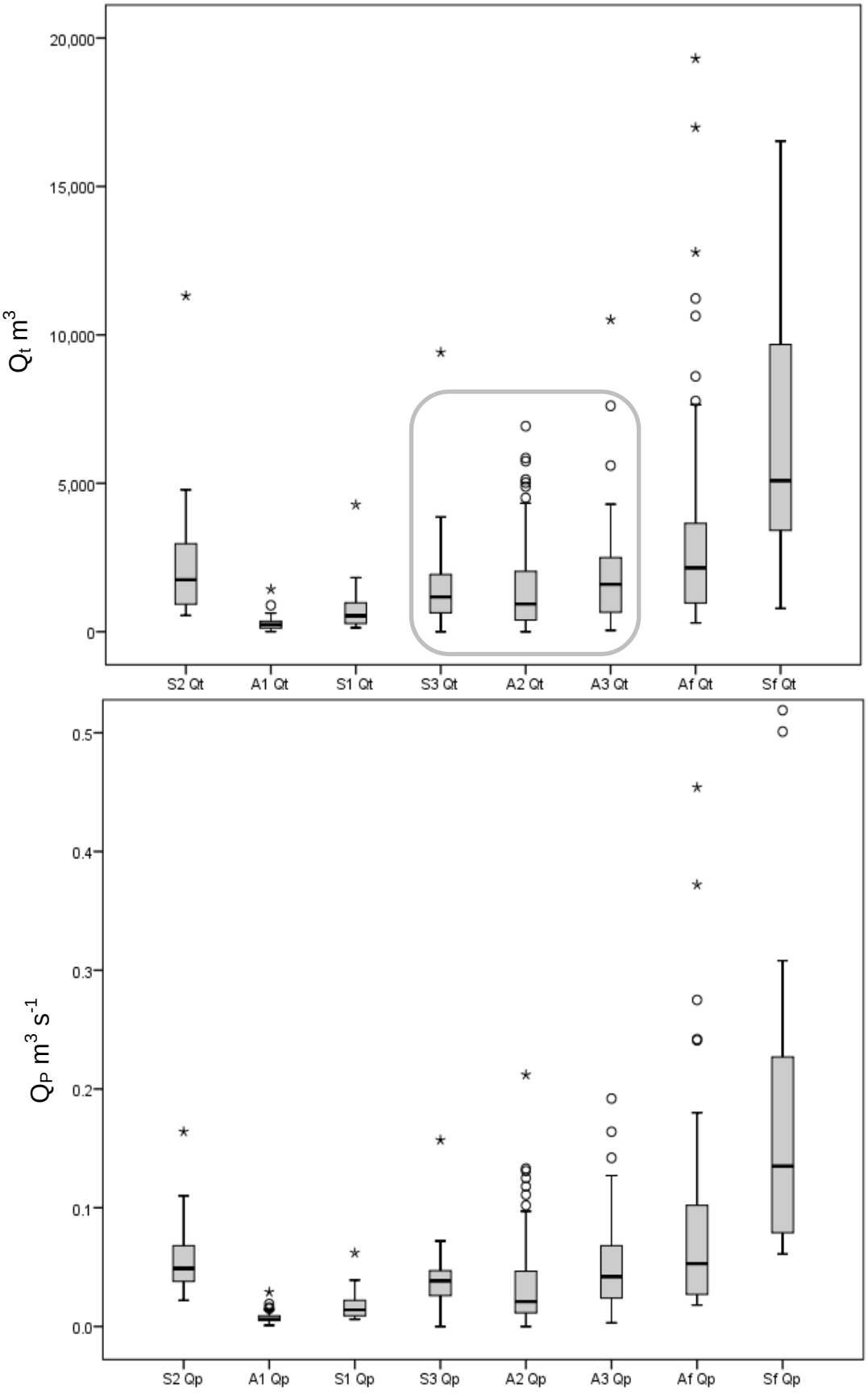


**Figure 7.5: distributions of Qp and Qt for all scales of monitoring, ranked by the relative topographically delineated contributing area (Table 7.1), derived from LiDAR data. This ranges from 499 $m^2$ at S2 (left) to 464,825 $m^2$ at Sf (right).**

**Table 7.2: Summary statistics (mean difference and significance) for one way ANOVA and "least significant difference" post hoc testing of event $Q_t$ and $Q_p$ for each combination of the monitored drainage scales. Combinations with least significant difference ($p > 0.05$) are highlighted in grey.**

| Combination | | Mean Difference $Q_t$ | $Q_t$ Sig. | Mean Difference $Q_p$ | $Q_p$ Sig. |
|---|---|---|---|---|---|
| A3 | S3 | -0.01 | 0.92 | -0.04 | 0.59 |
| Af | S2 | 0.06 | 0.46 | 0.07 | 0.28 |
| S2 | S3 | 0.15 | 0.13 | 0.11 | 0.15 |
| A2 | S3 | -0.14 | 0.09 | -0.21 | 0.00 |
| A3 | S2 | -0.16 | 0.05 | -0.15 | 0.02 |
| A2 | A3 | -0.13 | 0.04 | -0.17 | 0.00 |
| A2 | S1 | 0.20 | 0.02 | 0.21 | 0.00 |
| Af | S3 | 0.21 | 0.01 | 0.19 | 0.01 |
| S1 | S3 | -0.34 | 0.00 | -0.42 | 0.00 |
| A3 | Af | -0.22 | 0.00 | -0.22 | 0.00 |
| A2 | S2 | -0.29 | 0.00 | -0.32 | 0.00 |
| A3 | S1 | 0.33 | 0.00 | 0.38 | 0.00 |
| S1 | S2 | -0.49 | 0.00 | -0.53 | 0.00 |
| S2 | Sf | -0.50 | 0.00 | -0.47 | 0.00 |
| A1 | S1 | -0.44 | 0.00 | -0.38 | 0.00 |
| Af | Sf | -0.44 | 0.00 | -0.40 | 0.00 |
| A2 | Af | -0.35 | 0.00 | -0.39 | 0.00 |
| S3 | Sf | -0.65 | 0.00 | -0.58 | 0.00 |
| Af | S1 | 0.55 | 0.00 | 0.60 | 0.00 |
| A3 | Sf | -0.66 | 0.00 | -0.62 | 0.00 |
| A1 | S3 | -0.78 | 0.00 | -0.80 | 0.00 |
| A2 | Sf | -0.79 | 0.00 | -0.79 | 0.00 |
| A1 | A2 | -0.64 | 0.00 | -0.59 | 0.00 |
| S1 | Sf | -0.99 | 0.00 | -1.00 | 0.00 |
| A1 | S2 | -0.93 | 0.00 | -0.91 | 0.00 |
| A1 | A3 | -0.77 | 0.00 | -0.76 | 0.00 |
| A1 | Af | -0.99 | 0.00 | -0.98 | 0.00 |
| A1 | Sf | -1.43 | 0.00 | -1.38 | 0.00 |

To further explore the spatial relationship between the hydrological responses at the scales of drainage monitored, the time series of discharge across all of the experimental pool locations was plotted together, in three dimensions, for

each monitored drainage ditch in both experimental catchments. These data describe the dynamics of the hydrological response at three locations (i.e. S1, S2 and S3) for any given discharge step. Here, (Figure 7.6) it is evident that the response at Spooners is synchronous across the scales of monitoring implemented and that the variation in the relative discharge between the locations is greatest at lower flows. Aclands displays a similar primary trend in the data, however it can be seen that flow appears to switch to a state in which A2 generates relatively high flow during periods that A1 and A3 produce relatively low flow rates (this feature is annotated with "A").

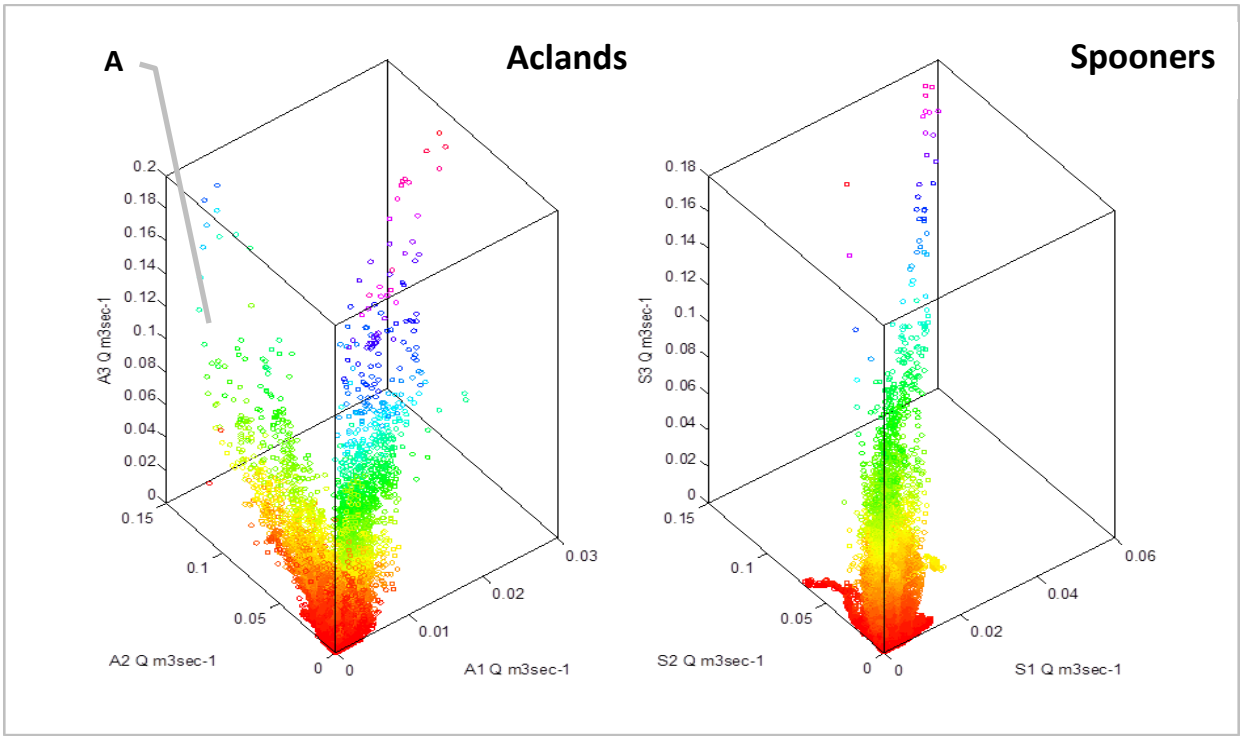


**Figure 7.6: A three-axis scatterplot illustrating the relationship between discharge measured simultaneously in each of the three monitored subcatchments, in both Aclands and Spooners. n = 105,267 in each catchment. The red to violet colour ramp is used to emphasise variation in z with red indicating low and violet indicating high flows on this axis.**

### *7.4.2 Hypothesis B*

**Mean (and variance) of depth to water table (DWT) is greatest proximal to functioning drainage features, decreasing with distance from the drain.**

Regression of the average (+/- standard deviation) DWT for each of the 96 locations across all monitoring location (Figure 7.7) has shown a large degree

of spatial variation in the potential DWT at any given distance from a drainage feature when all monitoring locations are aggregated together. Although the distribution of DWT at locations closer to drainage features indicates an increased potential for lower water tables, the vertical variation observed between data points illustrates heterogeneity of DWT characteristics present in the monitored landscape system. Third order polynomial regression of these data reveals that distance from the edge of a drainage feature explains only 13.6% of the observed variance. Further adjusting these data by the maximum measured DWT within the EP array only improves the explanatory power of drain edge distance by 8.4% to 22%.

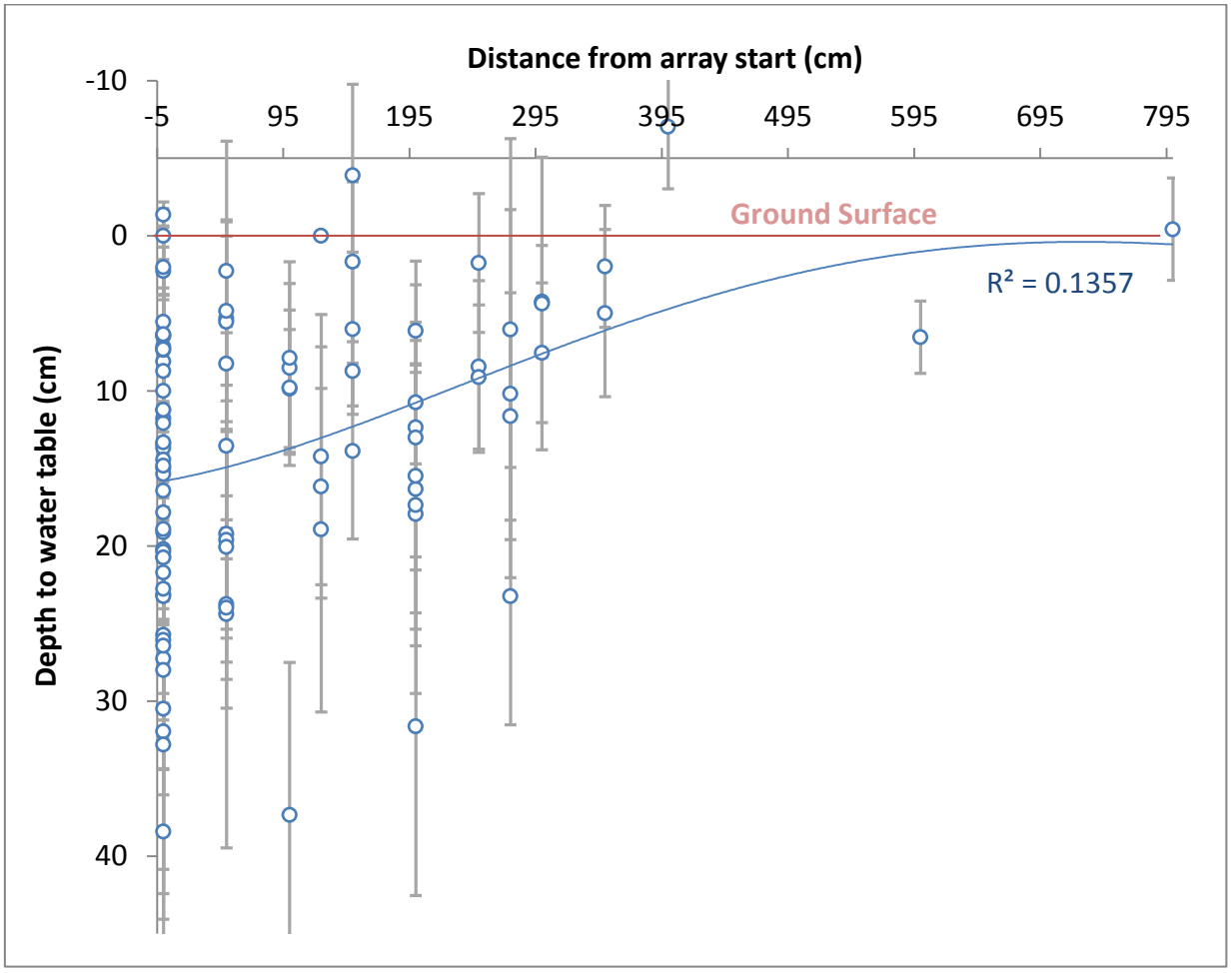


**Figure 7.7: Mean (+/- standard deviation) DWT for each of the 96 locations across all monitoring locations across both monitored catchments.**

### *7.4.3 Hypothesis C*

**Variance in depth to water tables may be explained by position of the drainage ditches with respect to local topography.**

In order to test this hypothesis, data were disaggregated for each drainage feature monitored (n = 6) (Figure 7.8). Here, data are shown for each DWT dataset (n = 69,500 for each location at Spooners and 54,500 at Aclands) collected at each of the monitoring locations perpendicular to a drainage feature, alongside the relative cross slope angle and a conceptual model for the measured slope and water table at each location. It is evident that the DWT measured downslope of drainage features, or where little cross slope gradient is present, is often strongly related to the distance away from these drainage features (e.g. S1 and S2 in Figure 7.8). Although the numbers of points in each location are too few to facilitate quantitative regression, the mean DWT values appear to exhibit constrained variability compared to the simple linear fits included. Conversely, upslope of these areas, far less of the observed variation in DWT appears to be explained by the distance from the drainage features. Conceptual drawing of the relative position of the mean water table is also included and highlights that the monitoring locations with greater cross slope gradient appear to exhibit a stronger downslope control on DWT, despite all measured slopes being relatively subtle (i.e. a maximum of 6% slope).

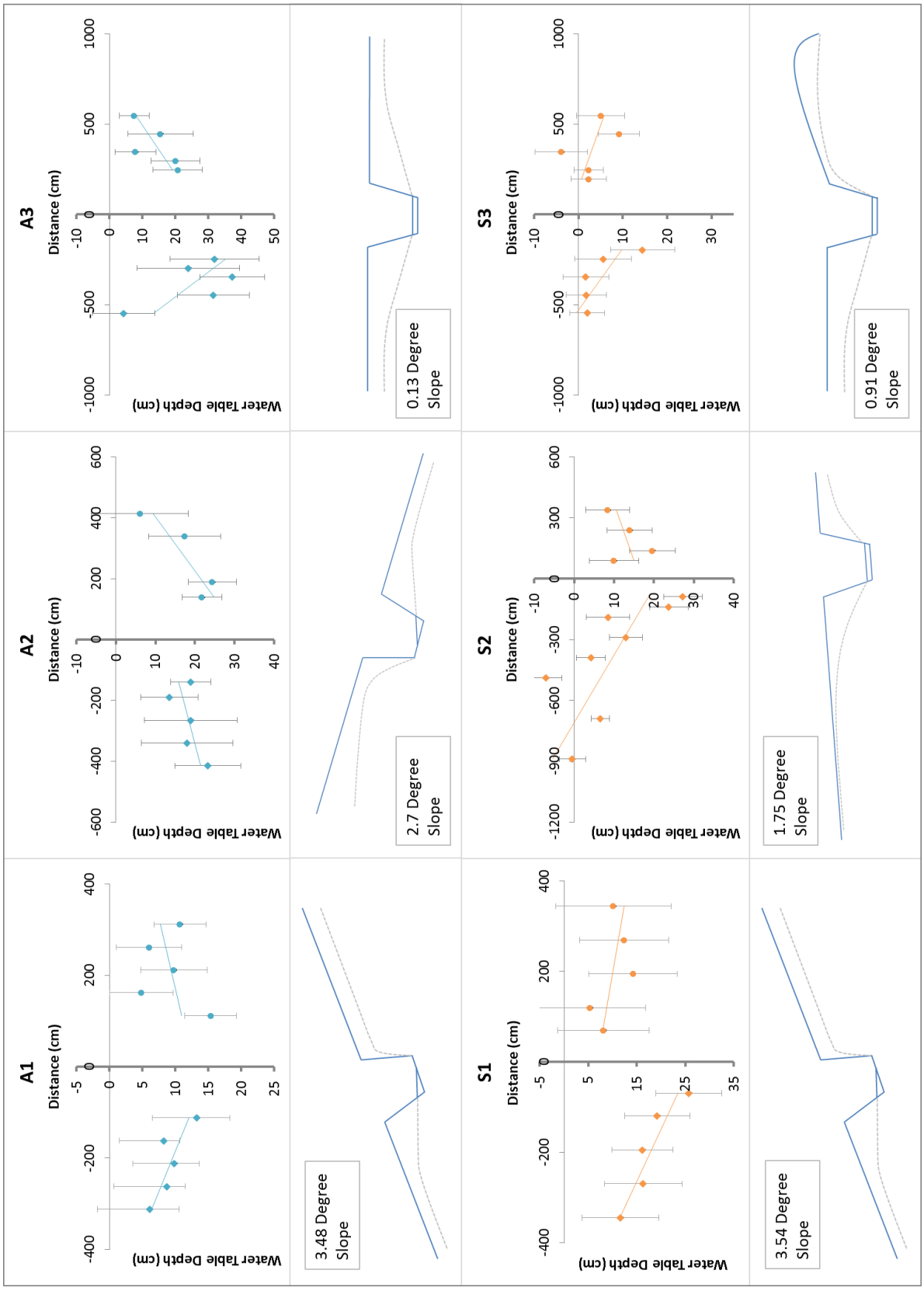


**Figure 7.8: Mean DWT data disaggregated for each drainage feature monitored (n = 6). Here, data are shown for each DWT dataset (n = 69,500 for each location at Spooners and 54,500 at Aclands) collected at each of the monitoring locations perpendicular to a drainage feature, alongside the relative cross slope angle and a conceptual model for the measured slope (blue line) and water table (grey dashed line) at each location.**

## 7.5 Discussion

### *7.5.1 Hypothesis A*

**Spatial variability of rainfall-runoff response varies with scale of the drainage system.**

The data presented provide important insights into the degree that drainage scale or topographic contributing area indicates the potential runoff associated with anthropogenic drainage features in shallow blanket peatlands. The presence of anthropogenic drainage is known to modify runoff generation across landscape extents (Ramchunder et al., 2009). However, the nature of the change in the hydrological regime remains relatively poorly understood (Ballard et al., 2011). In this study, the variation in the longer-term (multi-annual) hydrological characteristics is seen to be significant across the nested spatial scales monitored (Figure 7.3). Data demonstrate that comparable drainage features within close proximity can exhibit significant order of magnitude differences in runoff despite relatively uniform storm flow/base flow ratios, characteristic of anthropogenic drainage networks (Allott et al., 2014, Holden et al., 2006b, Luscombe et al., Forthcoming).

Event based analysis has also shown that the spatial variation in total and peak runoff production (Figure 7.4 and Figure 7.5) is often significantly different between the monitored locations. Additionally, these data indicate that the relationship between drainage scale and discharge is often inconsistent, with drainage features of significantly different geometry and theoretical contributing areas (Table 7.1) producing statistically similar responses to rainfall (Table 7.2) e.g. Af and S2. Specifically, $Q_t$ and $Q_p$ are sometimes shown to scale in relation to the modelled topographic contributing area or drainage size (Figure 7.5 and Table 7.1), particularly in the Aclands catchment. However, a lack of significant variation between key locations (e.g. Af and S2) and significantly larger discharge than may be expected from S2 (Table 7.2, Figure 7.5) suggests that the processes governing the production of flow in these peatlands, are related to factors other than the surface contributing area or drainage scale (Holden and Burt, 2003b, Holden and Burt, 2002, Evans et al., 1999, Luscombe et al., Forthcoming).

For example, the flow discharge metrics recorded for S2, are very high (estimated average daily flow 594 $m^3$) given the topographic contributing area (499 $m^2$) and discharge estimated in comparable drainage features in the landscape. In agreement with other studies in deeper peatlands (Holden and Burt, 2003b, Daniels et al., 2008), this may indicate that additional near surface (<10 cm) or subsurface inputs account for a significant proportion of the flow generated during the rapid wet-up of the peat matrix. Accordingly, the topographic watershed delineation for a location (e.g. S2) may account for only a small fraction of the hydrological source area during a rainfall event, or that topographic contributing areas are subject to step-changes in surface connectivity during rainfall events, as found by Goulsbra et al. (2014). Using this type of surface topography to delineate contributing areas in these shallow peatlands appears to, therefore, be excessively simplistic to quantify the potential source areas for a given drainage feature, anthropogenic or otherwise (Holden, 2005, Goulsbra et al., 2014). In the case of S2, field visits confirm that the immediate upslope contributing area is within an area of historic peat cuttings. Similar to erosion features studied in deeper peat systems, this may demonstrate that such features accumulate flow as a consequence of preferential lateral subsurface/near surface flow from the surrounding, deeper peat mass (Daniels et al., 2008). In many of the drainage features measured within these catchments, the bottom of the drains fall directly onto a basal geology of Morte and Kensisbury series slates and clays (Balchin, 1952) which are less permeable. This therefore, increases the potential fraction of groundwater intercepted by these features, which may include preferential flow lines which form on the interface between the peat mass and the basal substrate.

Three dimensional plots of the spatial relationship between the hydrological responses (Q) at the scales of drainage monitored (Figure 7.6) illustrate that the dynamics of the hydrological response within catchments is predominantly synchronous across the scales of monitoring implemented. Furthermore, variation in the relative discharge between the locations is seen to be greatest at lower flows. However, at Aclands flow does appear to switch to a state of non-synchronous flow generation during base flow periods (Figure 7.6) at A2,

suggesting some (temporally limited) spatial difference in base flow regulation of this area.

Despite the aforementioned limitations of using topographic contributing area as an indicator of flow, there is a no significant difference between area normalised runoff production at the catchment scale (69.8% at Aclands and 79.4% at Spooners). This demonstrates that stream orders (Strahler) of approximately seven and above may incorporate sufficient spatial complexity to sufficiently describe the overall contributing area of headwater catchment outlets. These catchment efficiencies are also useful as a baseline and to compare to those found in other landscapes. For example, Holden and Burt (2003b) record comparable efficiencies of 72% to 82% in a blanket peatland with deposits up to 3 m, in the North Pennines UK.

### *7.5.2 Hypothesis B*

**Mean (and variance) of depth to water table (DWT) is greatest proximal to functioning drainage features, decreasing with distance from the drain.**

Data presented in Figure 7.7 broadly agree with the findings of other studies in deeper peatlands, where the presence of anthropogenic drainage is shown to increase the depth and variability of the DWT in the adjacent peat mass (Daniels et al., 2008, Wilson et al., 2010, Wilson et al., 2011a, Worrall et al., 2007b). However, this analysis has also highlighted that once DWT observations are compiled across all monitoring locations and both studied headwater catchments the overall trend for lower observed DWT distributions at locations closer to the edge of drainage features can only explain 13.6% observed variance. This implies that fine scale processes regulating DWT require analysis that considers more localised controls on DWT. Similarly, it is evident that at some locations adjacent to these relatively subtle drainage features, the water table is able to persist at higher levels than may be expected.

These data are useful in demonstrating the need for a spatially distributed understanding of the DWT characteristics across the catchment extent. Horizontal heterogeneity in the ecohydrological structure and function of such systems is well evidenced (Morris et al., 2011). As discussed in the following

section (7.5.3), the unique way in which the dipwells were spatially distributed across the catchment allowed, for the first time, monitoring of DWT with regard to multiple and specific localised topographic controls. The use of distributed spatio-temporal monitoring networks is therefore, advisable, to improve understanding of the hydrological processes regulating DWT in these peatland landscapes (Holden, 2005, Holden et al., 2011).

### *7.5.3 Hypothesis C*

**Variance in depth to water tables may be explained by position of the drainage ditches with respect to local topography.**

Variation of DWT quantified in Figure 7.7 is compiled across multiple drainage features and normalisation of DWT by maximum water table depth only marginally improves the observed relationship between distance and DWT by 8.4%. It may therefore be expected that further local variation is an important control in the observed DWT at any given location (Holden et al., 2006b). Data in Figure 7.8 illustrates that such subtle variations in the local topography are able to account for some of the observed variation. Specifically it is observed that those locations immediately down slope of a drainage feature appear to exhibit enhanced water table drawdown. This finding agrees with other studies (Holden et al., 2006b) where the local topography is a key control on drainage function. Additionally, water tables upslope of these features do not significantly vary with proximity to the drainage feature. However, this does not infer that drainage is only effective on the down slope side of any drain (Allott et al., 2009). On the upslope side of these features it can be observed that only the highest vertical extent of the water table is close to the surface (i.e. during rainfall events) and the mean DWT measured is often significantly below the surface (i.e. up to 20 cm).

It may also be considered that although the gradient of the slopes measured in these locations is relatively subtle (< 6.2% slope), the shallow nature of the peatlands on Exmoor (Merryfield and Moore, 1974, Chambers et al., 1999) is likely to exaggerate the relative effect of a cross slope gradient on the relative drawdown of water table adjacent to such drainage features. Understanding

these fine scale drivers of DWT is the first step towards more fully estimating the extent that DWT is affected by drainage across larger spatial extents.

## 7.6 Overview and conclusions

This study highlights that the spatial variation in the discharge characteristics from multiple drainage features within comparable upland headwater catchments is significant. This study is the first that has employed such a comprehensive spatio-temporal monitoring approach to examine these processes and it is through this novel approach that it has been possible to understand the fine scale controls on hydrological function in these peatlands. Herein, the detailed monitoring of multiple, nested drainage scales highlights the importance of using spatially distributed monitoring to ensure that estimations of discharge across such landscape systems are representative (Holden, 2005, Holden et al., 2007b). Without such monitoring, the estimation and extrapolation of discharge across landscape extents is subject to greater uncertainty, which is key to those managing these landscapes and their associated ecosystem services.

In the data presented, it is evident that the apparent local scale of the drainage feature (i.e. depth and width), or the theoretical contributing area associated with such drainage is not a definitive predictor of discharge metrics, with features of varying size and topographic area exhibiting statistically similar discharge metrics. It is also interesting to note that the use of surface flow delineation and topographic contributing area is common to many spatially distributed models of rainfall-runoff processes, including the prediction of topographic wetness (Beven, 2012)., We demonstrate that for the shallow, marginal peatlands of Exmoor (Merryfield and Moore, 1974, Chambers et al., 1999), the use of surface topography to predict or spatially normalise discharge metrics is subject to significant uncertainty. Such uncertainty is indicative of the complex processes governing flow generation in peatland landscapes (Holden et al., 2004) and the difficulty of estimating source areas of flow in landscapes that are subject to lateral near-surface flow that may constitute significant sources of both storm-flow and base-flow (Evans et al., 1999, Holden et al., 2006b, Holden, 2005, Daniels et al., 2008). Despite these uncertainties, this analysis does demonstrate that the delineation of catchment watersheds

appears to be more effective at larger spatial extents. Specifically, it is demonstrated that at higher stream orders the delineation of catchment boundaries does appear to incorporate sufficient complexity to effectively delineate these boundaries and subsequently normalise flow characteristics between headwater catchments. This finding has important implications for the spatial quantification of runoff production over larger extents, and is of particular importance to those looking to quantify associated ecosystem services that these uplands may offer, such as flood attenuation.

Data presented here also provide evidence of the effect of the anthropogenic drainage networks on the spatial distribution of water tables within the monitored catchments. Here, the presence of anthropogenic drainage is shown to affect the depth and variability of the water table in the surrounding peat soil, and subtle variations in the local slope and topography are shown to account for some variance observed in the data. The data generated in this study are important as a baseline to gauge the effectiveness of future drain blocking and peat rewetting across these landscapes. The spatially distributed understanding of water table variability that this research provides also has the ability to improve the parameterisation of spatially distributed models of water table depth used by those managing and studying such landscape systems.

All of the locations monitored in this study are scheduled to undergo rewetting as part of a major restoration initiative in the South West of the UK. It may be hypothesised that the changes in surface and subsurface connectivity, and the increased storage capacity of the hillslopes following restoration will significantly alter the runoff characteristics in the monitored features. Future work will quantify the effectiveness of this restoration on altering the hydrological properties of the drainage features and catchments monitored in this study.

# 8 Conclusion

This chapter synthesises the conclusions drawn from chapters four to seven of this thesis and discusses how these findings advance the existing scientific understanding of these landscape systems, to aid the ongoing work carried out by the Exmoor Mires Project. At the outset, this research sought to characterise the ecohydrological structure and function of degraded blanket peatlands in Exmoor, in the South West of the UK. In bringing together remote sensing analyses coupled with hydrological monitoring and analysis, this project has enabled a thorough, spatially-distributed understanding of the two peatland catchments to be assembled. The individual themes used to address this research objective also provide a useful framework with which to evaluate the findings of this work. The four key aims overarching the two thematic lines of research explored in this thesis are as follows:

1. To assess the ability of laser altimetry data of contrasting spatial resolutions to capture complex ecohydrological structure across landscape scale extents.
2. To understand how structural proxies derived from LiDAR data can better interpret proxies of land surface hydrology using airborne thermal imaging data.
3. To characterise the key hydrological processes operating in these shallow blanket mire systems in the context of scientific understanding of other deeper peatland systems.
4. To provide an important baseline with which the effects of landscape rewetting can be more fully understood in the future.

The following sections detail how these aims are addressed under each of those research themes, and the key findings associated with these aims.

## 8.1 Theme one: remote sensing analysis for spatial characterisation of upland peatland ecohydrology

Prior to this research, remote sensing data such as LiDAR and TABI had not been widely used for the detailed spatial assessment of mire ecohydrological

condition. In addressing aim one above, this work has provided a robust evaluation of the data content associated with these technologies. This work has also provided a robust baseline for the structural and hydrological change associated with the ongoing management of these peatland ecosystems. Chapter four specifically, demonstrates a new method in which airborne LiDAR data are shown to be able to describe both the lateral extent of the surface drainage network in these peatlands, and spatial distribution of vegetation assemblages' characteristic of the wetter areas of the catchment. Isolating structural proxies of ecohydrological condition in this way and over larger extents (i.e. all 281 $km^2$ of Exmoor National Park), will provide data that may facilitate more highly targeted restoration interventions. For example, areas that will benefit from rewetting most may be delineated where drainage is identified and vegetation structure/community indicates a dryer soil surface.

This work also quantifies the extent to which LiDAR data underestimate ecosystem structure and the measured depth of surface-drainage networks, in these shallow, marginal peatlands. Understanding this uncertainty significantly improves the way in which these data can be used as a surrogate for field measurements of ecosystem structure or function. For example, methods presented here enable users of LiDAR data to construct more accurate numerical models of mire surface structure (including anthropogenic drainage) across this landscape. Such underrepresentation of anthropogenic drainage can, therefore, be mitigated during modelling as discussed in section 7.3.1 of this thesis. As a result, further work using these techniques will aid scientists and researchers using these data to construct models of peatland drainage and restoration effects with less uncertainty than is currently the case. Estimating the effects of the drainage networks in this way, and modelling the effect of landscape drainage/rewetting more accurately over larger extents will allow users new mechanisms of assessing the effectiveness of landscape rewetting.

Similarly, the data sets derived from the coupled LiDAR – TABI approach (addressing aim two) demonstrate strong potential for integration into other multi-scale approaches to understand the function of these peatlands, such as numerical rainfall run-off modelling. For example, a key component of many spatially distributed models of rainfall – runoff is an index of topographic wetness (TWI) derived from a DEM model and defined as the topographic

contributing area for a given point divided by the Tan of the slope of that grid location (Beven, 2012). The coupled LiDAR TABI approach discussed here may therefore enable enhanced evaluation and validation of TWI products and similar indexes of surface moisture. A lack of spatially distributed parameterisation and validation of such models is a major issue facing researchers in this field and the techniques described here may, therefore, provide key data able to fulfil this scientific requirement. This coupled approach also proves to be useful in understanding the spatial patterning of drainage or vegetation types associated with increased near surface or lack thereof, which provides an important baseline with which change following landscape rewetting may be quantified.

## 8.2 Theme two: in-field high resolution hydrological monitoring of degraded upland headwater catchments

The enhanced understanding of the spatial variability in the ecohydrological organisation of these peatlands provided through this research (theme one) is important for both ongoing management of these landscape systems, and ongoing research into the changes associated with such management. However, without robust *in-situ* hydrological monitoring of these catchments, these findings only provide a theoretical basis for understanding the hydrological processes operating in these peatlands. The second theme of this research has analysed the ability of a novel, integrated and high resolution hydrological monitoring system to characterise the spatial and temporal variability in runoff production and water storage across the studied headwater catchments. This study is the first that has employed such a comprehensive spatio-temporal monitoring approach to examine these processes and it is through this novel approach that it has been possible to uncover the fine scale controls on hydrological function in these peatland systems. (E.g. subtle and short lived controls on runoff production and DWT across the extent of the monitored catchments).

This aspect of the research aimed to understand the hydrological processes operating in shallow blanket mire systems and importantly, also enable these peatland systems to be understood in the context of research undertaken in

deeper peatland systems throughout the UK (aim three). Data presented in chapters six and seven have provided a direct baseline with which the effects of landscape rewetting can be directly compared (aim four). Such benchmarks will form key components of future work establishing the efficacy of such interventions and are therefore, a key outcome of this work. Results presented here provide important scientific insights and demonstrate that, in some respects, the flow regimes in these drained peatlands do behave in a comparable manner to deeper peatland systems found elsewhere. For example, they are characterised by flashy runoff responses and poorly maintained base flow conditions. However, a combination of thinner peat soils and extensive anthropogenic drainage networks, mean that antecedent hydrological conditions exert little of the control on the total or peak flow produced, which is often observed in deeper peatland systems. These findings represent the first time that this level of hydrological understanding has been obtained in these marginal peatlands. Importantly, the empirical understanding that this research provides suggests that landscape rewetting may have substantial effects on attenuating storm flow generation, without significantly reducing the short term soil storage capacity. Utilising this dataset, alongside ongoing monitoring, to evaluate such assumptions represents a key outcome of this research which has direct impact on the ongoing management of and investment in these landscapes.

Analyses of these data has also highlighted that the spatial variation in the discharge characteristics of multiple drainage features within the studied catchments was statistically significant and that neither the scale of the drainage feature, or the associated topographic contributing area, was a definitive predictor of discharge. In light of the results from theme one, these findings suggest that the complex intra-catchment patterns of surface wetness explored in chapter five (i.e. near surface flow pathways) may operate in combination with the topographic contributing areas to regulate source areas of flow production in this drained peatland system. Despite these complexities, this analysis also demonstrates that the delineation of watersheds is effective at catchment scales, where boundaries incorporate sufficient ecohydrological complexity to effectively describe contributing areas and enable the spatial normalisation of flow characteristics.

The complex relationships that govern flow generation in these catchments are also seen to operate on the dynamics of water table depth. Through the deployment of a spatially integrated network of sensors, anthropogenic drainage channels are shown to affect the depth and variability of the water table in the surrounding peat soil, and the topography is shown to account for key variation observed in these data. The fine spatial scale of these data also provides an enhanced ability to predict the effect of restoration on rewetting these peatlands, and raising water tables. For example, the data collected here will enable direct comparison of pre and post restoration water table levels at multiple locations and has sufficient replication to establish if absolute and average DWT are seen to change following rewetting, at multiple monitoring scales. Similarly, these data will be able to establish whether the spatial and temporal variation in DWT measurements varies concurrently with such change. When these results are used in combination with LiDAR and TABI derived datasets, discussed under theme one, these findings may also enable the production of spatially integrated predictions of such rewetting. For example, by enabling the integration of spatially distributed models of near surface hydrology discussed in 8.1, with lateral and vertical estimations of water storage, generated from this new dataset. Such integration, therefore, presents further opportunities to increase the explanatory power of such numerical models of ecosystem function.

## 8.3 Scientific contribution and further work

The findings arising from this research represent a significant contribution toward scientific understanding of the ecohydrological processes operating across these peatland systems, and form a key benchmark from which future change may be gauged. The research included in this thesis also represents unique contributions to wider scientific knowledge. These include the development of novel methods of spatially assessing near surface hydrology in upland ecosystems, and new information on how laser altimetry data can be used to measure and model the ecohydrology of these landscape systems more appropriately. Data presented under chapters six and seven also represent the first time that such an extensive spatially distributed hydrological monitoring program has been successfully deployed in the challenging

environment of the moorlands of the South West UK. The resultant data are therefore, also the first dataset to effectively describe the hydrological processes operating in these peatlands systems, and how these relate to anthropogenic drainage networks.

However, these findings do not represent an end point in this research. Restoration interventions have already taken place in both of the studied catchments following the data collected and presented here. The monitoring implemented has also remained *in-situ* during and following this restoration, providing a unique dataset describing the effect of restoration across the monitoring catchments. These ongoing data measurements represent a unique opportunity to build on the results arising from this thesis and assess how the complex understanding of the ecohydrological structure and function of the drained peatlands presented in this thesis, will change following restoration. Importantly, as a collective body of work this research represents a unique baseline from which myself and other scientists will be able to understand change in these peatland systems following restoration, over decadal timescales in the future.

# 9 References


Allott, T., Evans, M., Agnew, C., Milledge, D., Pilkington, M. & Maskill, R. Impacts of peat restoration on peak flow characteristics of upland headwater catchments. EGU General Assembly Conference Abstracts, 2014. 14505.

Allott, T., Evans, M., Lindsay, J., Agnew, C., Freer, J., Jones, A. & Parnell, M. 2009. Water tables in Peak District blanket peatlands. *Moors for the Future Partnership, Report,* 17.

Anderson, D. E. 2002. Carbon accumulation and C/N ratios of peat bogs in North-West Scotland. *Scottish Geographical Journal,* 118**,** 323 - 341.

Anderson, J. M. & Wilson, S. B. 1984. Review Article.The physical basis of current infrared remote-sensing techniques and the interpretation of data from aerial surveys. *International Journal of Remote Sensing,* 5**,** 1-18.

Anderson, K., Bennie, J. & Wetherelt, A. 2009. Laser scanning of fine scale pattern along a hydrological gradient in a peatland ecosystem. *Landscape Ecology,* 25**,** 477-492.

Anderson, K., Bennie, J. J., Milton, E. J., Hughes, P. D. M., Lindsay, R. & Meade, R. 2010. Combining LiDAR And Ikonos Data For Eco-hydrological Classification Of An Ombrotrophic Peatland. *J. Environ. Qual.,* 39**,** 260-273.

Anderson, K. & Gaston, K. J. 2013. Lightweight unmanned aerial vehicles will revolutionize spatial ecology. *Frontiers in Ecology and the Environment,* 11**,** 138-146.

Bain, C., Bonn, A., Stoneman, R. & Chapman, S. 2011. IUCN UK Commission of Inquiry on Peatlands. Edinburgh: IUCN UK Peatland Programme.

Balchin, W. 1952. The erosion surfaces of Exmoor and adjacent areas. *Geographical Journal***,** 453-472.

Ballard, C. E., Mcintyre, N., Wheater, H. S., Holden, J. & Wallage, Z. E. 2011. Hydrological modelling of drained blanket peatland. *Journal of Hydrology,* In Press, Corrected Proof.

Bellamy, P. H., Loveland, P. J., Bradley, R. I., Lark, R. M. & Kirk, G. J. D. 2005. Carbon losses from all soils across England and Wales 1978-2003. *Nature,* 437**,** 245-248.

Belyea, L. R. & Clymo, R. 2001. Feedback control of the rate of peat formation. *Proceedings of the Royal Society of London. Series B: Biological Sciences,* 268**,** 1315-1321.

Belyea, L. R. & Lancaster, J. 2002. Inferring Landscape Dynamics of Bog Pools from Scaling Relationships and Spatial Patterns. *Journal of Ecology,* 90**,** 223-234.

Beven, K. 2006. A manifesto for the equifinality thesis. *Journal of Hydrology,* 320**,** 18-36.

Beven, K. 2012. *Rainfall-Runoff Modelling, The Primer,* Chichester, John Wiley & Sons, Ltd.

Beven, K. & Brazier, R. E. 2011. Dealing with uncertainty in erosion model predictions. *Handbook of Erosion Modelling***,** 52-79.

Bowes, A. C. 2006. *Exmoor Blanket bog Inventory and restoration plan for English Nature.* MSc Thesis, University of Calgary.

Bradley, R. I., Milne, R., Bell, J., Lilly, A., Jordan, C. & Higgins, A. 2005. A soil carbon and land use database for the United Kingdom. *Soil Use and Management,* 21**,** 363-369.

Bragg, O. M. 2002. Hydrology of peat-forming wetlands in Scotland. *The Science of The Total Environment,* 294**,** 111-129.

Bragg, O. M. & Tallis, J. H. 2001. The sensitivity of peat-covered upland landscapes. *CATENA,* 42**,** 345-360.

Campbell, J. B. 1996. *Introduction to Remote Sensing,* London, Taylor and Francis.

Cannell, M. G. R., Dewar, R. C. & Pyatt, D. G. 1993. Conifer Plantations on Drained Peatlands in Britain: a Net Gain or Loss of Carbon? *Forestry,* 66**,** 353-369.

Cavalli, M., Tarolli, P., Marchi, L. & Dalla Fontana, G. 2008. The effectiveness of airborne LiDAR data in the recognition of channel-bed morphology. *CATENA,* 73**,** 249-260.

Chambers, F. M., Mauquoy, D. & Todd, P. A. 1999. Recent rise to dominance of *Molinia caerulea* in environmentally sensitive areas: new perspectives from palaeoecological data. *Journal of Applied Ecology,* 36**,** 719-733.

Charman, D. 2002. *Peatlands and Environmental Change,* Chichester, John Wiley & Sons Ltd.

Chassereau, J. E., Bell, J. M. & Torres, R. 2011. A comparison of GPS and LiDAR salt marsh DEMs. *Earth Surface Processes and Landforms,* 36**,** 1770-1775.

Chow, V. T. 1969. Spatially varied flow. *Open-Channel Hydraulics.* New York: McGraw-Hill.

Clark, J. M., Gallego-Sala, A. V., Allott, T. E. H., Chapman, S. J., Farewell, T., Freeman, C., House, J. I., Orr, H. G., Prentice, I. C. & Smith, P. 2010. Assessing the vulnerability of blanket peat to climate change using an ensemble of statistical bioclimatic envelope models. *Climate Research,* 45**,** 131-150.

Cook, B. D., Bolstad, P. V., Næsset, E., Anderson, R. S., Garrigues, S., Morisette, J. T., Nickeson, J. & Davis, K. J. 2009. Using LiDAR and quickbird data to model plant production and quantify uncertainties associated with wetland detection and land cover generalizations. *Remote Sensing of Environment,* 113**,** 2366-2379.

Couwenberg, J. & Joosten, H. 2005. Self organization in raised bog patterning: The origin of microtope zonation and mesotope diversity. *Journal of Ecology,* 93**,** 1238-1248.

Daniels, R. E. 1978. Floristic Analyses of British Mires and Mire Communities. *Journal of Ecology,* 66**,** 773-802.

Daniels, S. M., Agnew, C. T., Allott, T. E. H. & Evans, M. G. 2008. Water table variability and runoff generation in an eroded peatland, South Pennines, UK. *Journal of Hydrology,* 361**,** 214-226.

Davies, H. J. 2012. Sustainable management of the historic environment resource in upland peat: a study from Exmoor.

Deasy, C., Brazier, R. E., Heathwaite, A. L. & Hodgkinson, R. 2009. Pathways of runoff and sediment transfer in small agricultural catchments. *Hydrological Processes,* 23**,** 1349-1358.

Dixon, S., Qassim, S., Rowson, J., Worrall, F., Evans, M., Boothroyd, I. & Bonn, A. 2013. Restoration effects on water table depths and CO2 fluxes from climatically marginal blanket bog. *Biogeochemistry***,** 1-18.

Eeckhaut, M. V. D., Poesen, J., Verstraeten, G., Vanacker, V., Nyssen, J., Moeyersons, J., Beek, L. P. H. V. & Vandekerckhove, L. 2007. Use of LiDAR-derived images for mapping old landslides under forest. *Earth Surface Processes and Landforms,* 32**,** 754-769.

Evans, M., Allott, T., Holden, J., Flitcroft, C. & Bonn, A. 2005. Understanding gully blocking in deep peat. *Derbyshire: Moors for the Future Report,* 4.

Evans, M., Allott, T., Worrall, F., Rowson, J. & Maskill, R. Validating a topographically driven model of peatland water table: Implications for understanding land cover controls on water table. EGU General Assembly Conference Abstracts, 2014. 5598.

Evans, M., Burt, T., Holden, J. & Adamson, J. 1999. Runoff generation and water table fluctuations in blanket peat: evidence from UK data spanning the dry summer of 1995. *Journal of Hydrology,* 221**,** 141-160.

Evans, M. & Lindsay, J. 2010. High resolution quantification of gully erosion in upland peatlands at the landscape scale. *Earth Surface Processes and Landforms,* 35**,** 876-886.

Evans, M. & Warburton, J. 2010. *Geomorphology of Upland Peat,* Chichester, John Wiley & Sons Ltd.

Forman, R. T. T. & Godron, M. 1981. Patches and Structural Components for a Landscape Ecology. *BioScience,* 31**,** 733-740.

Fraser, C. J. D., Roulet, N. T. & Lafleur, M. 2001. Groundwater flow patterns in a large peatland. *Journal of Hydrology,* 246**,** 142-154.

Freeman, C., Evans, C. D., Monteith, D. T., Reynolds, B. & Fenner, N. 2001. Export of organic carbon from peat soils. *Nature,* 412**,** 785-785.

Fyfe, R. 2006. Sustainable conservation and management of the historic environment record in upland peat: a view from Exmoor. *International Journal of Biodiversity Science & Management,* 2**,** 146-149.

Gallego-Sala, A., Clark, J., House, J. & Orr, H. 2010. Bioclimatic envelope model of climate change impacts on blanket peatland distribution in Great Britain. *Clim Res,* 45**,** 151-162.

Garbulsky, M. F., Peñuelas, J., Gamon, J., Inoue, Y. & Filella, I. 2010. The photochemical reflectance index (PRI) and the remote sensing of leaf, canopy and ecosystem radiation use efficiencies: A review and meta-analysis. *Remote Sensing of Environment,* 115**,** 281-297.

Glendell, M., Extence, C., Chadd, R. & Brazier, R. E. 2014. Testing the pressure-specific invertebrate index (PSI) as a tool for determining ecologically relevant targets for reducing sedimentation in streams. *Freshwater Biology,* 59**,** 353-367.

Goulsbra, C., Evans, M. & Allott, T. 2011. Oxidation of POC in Floodplain Environments, Evidence from Eroding Blanket Peatlands.

Goulsbra, C., Evans, M. & Allott, T. Oxidation rates of overbank POC deposition in an eroding peatland. EGU General Assembly Conference Abstracts, 2012. 10920.

Goulsbra, C., Evans, M. & Lindsay, J. 2014. Temporary streams in a peatland catchment: pattern, timing, and controls on stream network expansion and contraction. *Earth Surface Processes and Landforms,* 39**,** 790-803.

Grand-Clement, E., Anderson, K., Smith, D., Luscombe, D., Gatis, N., Ross, M. & Brazier, R. E. 2013. Evaluating ecosystem goods and services after restoration of marginal upland peatlands in South-West England. *Journal of Applied Ecology,* 50**,** 324-334.

Grand-Clement, E., Luscombe, D. J., Anderson, K., Gatis, N., Benaud, P. & Brazier, R. E. 2014. Antecedent conditions control carbon loss and downstream water quality from shallow, damaged peatlands. *Science of The Total Environment,* 493**,** 961-973.

Grand-Clement, E., Ross, M., Smith, D., Anderson, K., Luscombe, D., Le Feuvre, N. & Brazier, R. 2012. " Upstream Thinking": the catchment management approach of a water provider. *EGU General Assembly 2012, held 22-27 April, 2012 in Vienna, Austria.***,** p. 4238.

Grayson, R., Holden, J. & Rose, R. 2010. Long-term change in storm hydrographs in response to peatland vegetation change. *Journal of Hydrology,* 389**,** 336-343.

Harris, A. & Bryant, R. G. 2009. A multi-scale remote sensing approach for monitoring northern peatland hydrology: Present possibilities and future challenges. *Journal of Environmental Management,* 90**,** 2178-2188.

Hobbs, N. B. 1986. Mire morphology and the properties and behaviour of some British and foreign peats. *Quarterly Journal of Engineering Geology and Hydrogeology,* 19**,** 7-80.

Hoekman, D. H. 2007. Satellite radar observation of tropical peat swamp forest as a tool for hydrological modelling and environmental protection. *Aquatic Conservation: Marine and Freshwater Ecosystems,* 17**,** 265-275.

Holden, J. 2005. Peatland hydrology and carbon release: why small-scale process matters. *Philosophical Transactions of the Royal Society A: Mathematical Physical and Engineering Sciences,* 363**,** 2891-2913.

Holden, J. & Burt, T. P. 2002. Infiltration, runoff and sediment production in blanket peat catchments: implications of field rainfall simulation experiments. *Hydrological Processes,* 16**,** 2537-2557.

Holden, J. & Burt, T. P. 2003a. Hydraulic conductivity in upland blanket peat: measurement and variability. *Hydrological Processes,* 17**,** 1227-1237.

Holden, J. & Burt, T. P. 2003b. Runoff production in blanket peat covered catchments. *Water Resources Research,* 39**,** 1191.

Holden, J., Chapman, P. J. & Labadz, J. C. 2004. Artificial drainage of peatlands: hydrological and hydrochemical process and wetland restoration. *Progress in Physical Geography,* 28**,** 95–123.

Holden, J., Chapman, P. J., Lane, S. N., Brookes, C., I.P. Martini, A. M. C. & Chesworth, W. 2006a. Chapter 22 Impacts of artificial drainage of peatlands on runoff production and water quality. *Developments in Earth Surface Processes.* Elsevier.

Holden, J., Evans, M. G., Burt, T. P. & Horton, M. 2006b. Impact of Land Drainage on Peatland Hydrology. *J. Environ. Qual.,* 35**,** 1764-1778.

Holden, J., Gascoign, M. & Bosanko, N. R. 2007a. Erosion and natural revegetation associated with surface land drains in upland peatlands. *Earth Surface Processes and Landforms,* 32**,** 1547-1557.

Holden, J., Shotbolt, L., Bonn, A., Burt, T. P., Chapman, P. J., Dougill, A. J., Fraser, E. D. G., Hubacek, K., Irvine, B., Kirkby, M. J., Reed, M. S., Prell, C., Stagl, S., Stringer, L. C., Turner, A. & Worrall, F. 2007b. Environmental change in moorland landscapes. *Earth-Science Reviews,* 82**,** 75-100.

Holden, J., Wallage, Z. E., Lane, S. N. & Mcdonald, A. T. 2011. Water table dynamics in undisturbed, drained and restored blanket peat. *Journal of Hydrology,* 402**,** 103-114.

Hopkinson, E. & Allott, T. 2012. *Employing GIS-based Techniques to Quantify Sub-catchment Erosional Gully Densities in the Upper North Grain in Order to Explore the Relationship Between Gully Erosion and Dissolved Organic Carbon Concentrations*, University of Manchester.

Hubacek, K., Beharry, N., Bonn, A., Burt, T., Holden, J., Ravera, F., Reed, M., Stringer, L. & Tarrasón, D. 2009. Ecosystem services in dynamic and contested landscapes: the case of UK uplands. *What is land for***,** 167-188.

Ingram, H. A. 1978. Soil Layers In Mires: Function And Terminology. *Journal of Soil Science,* 29**,** 224-227.

Ise, T., Dunn, A. L., Wofsy, S. C. & Moorcroft, P. R. 2008. High sensitivity of peat decomposition to climate change through water-table feedback. *Nature Geosci,* 1**,** 763-766.

James, L. A., Watson, D. G. & Hansen, W. F. 2007. Using LiDAR data to map gullies and headwater streams under forest canopy: South Carolina, USA. *CATENA,* 71**,** 132-144.

Jenness, J. S. 2004. Calculating landscape surface area from digital elevation models. *Wildlife Society Bulletin,* 32**,** 829-839.

Jenson, S. K. & Domingue, J. O. 1988. Extracting Topographic Structure from Digital Elevation Data for Geographic Information System Analysis. *Photogrammetric Engineering and Remote Sensing,* 54**,** 1593-1600.

Joosten, H. & Clarke, D. 2002. *Wise Use of Mires and Peatlands,* Totnes, International Mire Conversation Group and International Peat Society.

Jordan, P. & Cassidy, R. 2011. Technical Note: Assessing a 24/7 solution for monitoring water quality loads in small river catchments. *Hydrology & Earth System Sciences,* 15.

Jordan, P., Menary, W., Daly, K., Kiely, G., Morgan, G., Byrne, P. & Moles, R. 2005. Patterns and processes of phosphorus transfer from Irish grassland soils to rivers—integration of laboratory and catchment studies. *Journal of Hydrology,* 304**,** 20-34.

Kalbitz, K. & Geyer, S. 2002. Different effects of peat degradation on dissolved organic carbon and nitrogen. *Organic Geochemistry,* 33**,** 319-326.

Kidson, C. 1953. The Exmoor storm and the Lynmouth floods. *Geography***,** 1-9.

Korpela, I., Koskinen, M., Vasander, H., Holopainen, M. & Minkkinen, K. 2009. Airborne small-footprint discrete-return LiDAR data in the assessment of boreal mire surface patterns, vegetation, and habitats. *Forest Ecology and Management,* 258**,** 1549-1566.

Lamb, R. 1996. *Distributed hydrological predictions using a generalized TOPMODEL formulation.* University of Lancaster, UK.

Lamb, R., Beven, K. & Myrab, S. 1998. Use of spatially distributed water table observations to constrain uncertainty in a rainfall-runoff model. *Advances in Water Resources,* 22**,** 305-317.

Lane, S. N. & Milledge, D. G. 2013. Impacts of upland open drains upon runoff generation: a numerical assessment of catchment-scale impacts. *Hydrological Processes,* 27**,** 1701-1726.

Limpens, J., Berendse, F., Blodau, C., Canadell, J. G., Freeman, C., Holden, J., Roulet, N., Rydin, H. & Schaepman-Strub, G. 2008. Peatlands and the carbon cycle: from local processes to global implications – a synthesis. *Biogeosciences,* 5**,** 1475-1491.

Lindsay, R. 1995. Ecology, classifcation and conservation of obrotrophic mires. Edinburgh: Scotish Natural Heritage

Lindsay, R. 2010. Peatbogs and Carbon: A Critical Synthesis. London: University of East London.

Lindsay, R., Charman, D., Everingham, F., O'reilly, R., Palmer, M., Rowell, T. & Stroud, D. 1988. The flow country: the peatlands of Caithness and Sutherland.

Logsdon, S. D. 2008. *Soil Science: Step-by-step Field Analysis*, ASA-CSSA-SSSA.

Luscombe, D., Anderson, K., Grand-Clement, E., Le-Feuvre, N., Smith, D. & Brazier, R. Assessing the ecohydrological status of a drained peatland: Combining thermal airborne imaging, laser scanning technologies and ground water monitoring. EGU General Assembly Conference Abstracts, 2012. 740.

Luscombe, D. J., Anderson, K., Gatis, N., Grand-Clement, E. & Brazier, R. E. 2014b. Using thermal airborne imagery to measure near surface hydrology in upland ecosystems. *Hydrological Processes***,** n/a-n/a.

Luscombe, D. J., Anderson, K., Gatis, N., Wetherelt, A., Grand-Clement, E. & Brazier, R. E. 2014a. What does airborne LiDAR really measure in upland ecosystems? *Ecohydrology***,** n/a-n/a.

Luscombe, D. J., Anderson, K., Grand-Clement, E., Gatis, N., Ashe, J., Benaud, P., Smith, D. & Brazier, R. E. Forthcoming. Understanding the Hydrology of Shallow, Drained and Marginal Peatlands: 1. Temporal Variability. *Hydrological Processes*.

Maltby, E. & Crabtree, K. 1976. Soil Organic Matter and Peat Accumulation on Exmoor: A Contemporary and Palaeoenvironmental Evaluation. *Transactions of the Institute of British Geographers,* 1**,** 259-278.

Mänd, P., Hallik, L., Peñuelas, J., Nilson, T., Duce, P., Emmett, B. A., Beier, C., Estiarte, M., Garadnai, J., Kalapos, T., Schmidt, I. K., Kovács-Láng, E., Prieto, P., Tietema, A., Westerveld, J. W. & Kull, O. 2010. Responses of the reflectance indices PRI and NDVI to experimental warming and drought in European shrublands along a north-south climatic gradient. *Remote Sensing of Environment,* 114**,** 626-636.

Manning, R., Griffith, J. P., Pigot, T. & Vernon-Harcourt, L. F. 1890. *On the flow of water in open channels and pipes*.

Martin-Ortega, J., Allott, T. E. H., Glenk, K. & Schaafsma, M. 2014. Valuing water quality improvements from peatland restoration: Evidence and challenges. *Ecosystem Services*.

Merryfield, D. L. 1977. *Palynological and Stratigraphical Studies on Exmoor.* King's College London (University of London).

Merryfield, D. L. & Moore, P. D. 1974. Prehistoric human activity and blanket peat initiation on Exmoor. *Nature,* 250**,** 439-441.

Mills, J., Short, C., Ingram, J., Griffiths, B., Dwyer, J., Mcewen, L., Chambers, F., Kirkham, G. & Council, C. 2010. Review of the Exmoor Mires Restoration Project.

Minkkinen, K. & Laine, J. 1998. Effect of forest drainage on the peat bulk density of pine mires in Finland. *Canadian Journal of Forest Research,* 28**,** 178-186.

Moore, P. D. & Bellamy, D. J. 1974. *Peatlands*, Elek Science London.

Morris, P. J., Waddington, J. M., Benscoter, B. W. & Turetsky, M. R. 2011. Conceptual frameworks in peatland ecohydrology: looking beyond the two-layered (acrotelm–catotelm) model. *Ecohydrology,* 4**,** 1-11.

Natural England 2010. Englands Peatlands, Carbon storage and greenhouse gasses. London: Natural England.

Ovenden, L. 1990. Peat accumulation in northern wetlands. *Quaternary Research,* 33**,** 377-386.

Parry, L. E. & Charman, D. J. 2013. Modelling soil organic carbon distribution in blanket peatlands at a landscape scale. *Geoderma,* 211–212**,** 75-84.

Parry, L. E., Holden, J. & Chapman, P. J. 2014. Restoration of blanket peatlands. *Journal of Environmental Management,* 133**,** 193-205.

Pawson, R., Evans, M. & Allott, T. 2012. Fluvial carbon flux from headwater peatland streams: significance of particulate carbon flux. *Earth Surface Processes and Landforms,* 37**,** 1203-1212.

Pellerin, S., Lagneau, L.-A., Lavoie, M. & Larocque, M. 2009. Environmental factors explaining the vegetation patterns in a temperate peatland. *Comptes Rendus Biologies,* 332**,** 720-731.

Pilgrim, D. H., Cordery, I. & Baron, B. C. 1982. Effects of catchment size on runoff relationships. *Journal of Hydrology,* 58**,** 205-221.

Price, J. 1997. Soil moisture, water tension, and water table relationships in a managed cutover bog. *Journal of Hydrology,* 202**,** 21-32.

Price, J. C. 1980. The potential of remotely sensed thermal infrared data to infer surface soil moisture and evaporation. *Water Resour. Res.,* 16**,** 787-795.

Price, J. S. 2003. Role and character of seasonal peat soil deformation on the hydrology of undisturbed and cutover peatlands. *Water Resources Research,* 39.

Ramchunder, S. J., Brown, L. E. & Holden, J. 2009. Environmental effects of drainage, drain-blocking and prescribed vegetation burning in UK upland peatlands. *Progress in Physical Geography,* 33**,** 49-79.

Reed, M. S., Bonn, A., Slee, W., Beharry-Borg, N., Birch, J., Brown, I., Burt, T. P., Chapman, D., Chapman, P. J., Clay, G. D., Cornell, S. J., Fraser, E. D. G., Glass, J. H., Holden, J., Hodgson, J. A., Hubacek, K., Irvine, B., Jin, N., Kirkby, M. J., Kunin, W. E., Moore, O., Moseley, D., Prell, C., Price, M. F., Quinn, C. H., Redpath, S., Reid, C., Stagl, S., Stringer, L. C., Termansen, M., Thorp, S., Towers, W. & Worrall, F. 2009. The future of the uplands. *Land Use Policy,* 26, Supplement 1**,** S204-S216.

Rochefort, L., Campeau, S. & Bugnon, J.-L. 2002. Does prolonged flooding prevent or enhance regeneration and growth of *Sphagnum*? *Aquatic Botany,* 74**,** 327-341.

Rothwell, J. J., Robinson, S. G., Evans, M. G., Yang, J. & Allott, T. E. H. 2005. Heavy metal release by peat erosion in the Peak District, southern Pennines, UK. *Hydrological Processes,* 19**,** 2973-2989.

Rydin, H. & Jeglum, J. K. 2013. *The Biology of Peatlands, 2e*, Oxford University Press.

Schultz, G. A. & Engman, E. T. 2011. *Remote Sensing in Hydrology and Water Management*, Springer Berlin Heidelberg.

Schumann, M. & Joosten, H. 2008. Global Peatland Restoration Manual. Greifswald University,Germany.

Shaw, E. M. 1989. *Hydrology in Practice,* London, Chapman and Hall.

Siriwardena, L., Finlayson, B. L. & Mcmahon, T. A. 2006. The impact of land use change on catchment hydrology in large catchments: The Comet River, Central Queensland, Australia. *Journal of Hydrology,* 326**,** 199-214.

Sjörs, H. 1948. Myrvegetation i Bergslagen. [Mire vegetation in Bergslagen, Sweden]. *Acta Phytogeographica Suecica***,** 1-299.

Soille, P. 2004. Optimal removal of spurious pits in grid digital elevation models. *Water Resources Research,* 40**,** W12509.

Stewart, A. J. & Lance, A. N. 1991. Effects of moor-draining on the hydrology and vegetation of northern Pennine blanket bog. *Journal of Applied Ecology***,** 1105-1117.

Strack, M., Waddington, J. & Tuittila, E. S. 2004. Effect of water table drawdown on northern peatland methane dynamics: Implications for climate change. *Global Biogeochemical Cycles,* 18.

Strahler, A. N. 1957. Quantitative analysis of watershed geomorphology. *American Geophysical Union Transactions,* 38(6)**,** 912-920.

Tebbutt, M. 2004. Landscapes of Loss: Moorlands, Manliness and the First World War. *Landscapes,* 5**,** 114-128.

Tomlinson, R. W. 2010. Changes in the extent of peat extraction in Northern Ireland 1990-2008 and associated changes in carbon loss. *Applied Geography,* 30**,** 294-301.

Turnbull, L., Wainwright, J., Brazier, R. & Bol, R. 2010. Biotic and Abiotic Changes in Ecosystem Structure over a Shrub-Encroachment Gradient in the Southwestern USA. *Ecosystems,* 13**,** 1239-1255.

Turnbull, L., Wainwright, J. & Brazier, R. E. 2008. A conceptual framework for understanding semi-arid land degradation: ecohydrological interactions across multiple-space and time scales. *Ecohydrology,* 1**,** 23-34.

Turner, M. G. 1989. Landscape Ecology: The Effect of Pattern on Process. *Annual Review of Ecology and Systematics,* 20**,** 171-197.

Van Der Wal, R., Bonn, A., Monteith, D. & Reed, M. 2011. Mountains, moorlands and heaths [chapter 5].

Vojinovic, Z. & Abbott, M. B. 2012. Flood Risk and Social Justice. IWA Publishing, London.

Wallage, Z. E., Holden, J. & Mcdonald, A. T. 2006. Drain blocking: An effective treatment for reducing dissolved organic carbon loss and water discolouration in a drained peatland. *Science of The Total Environment,* 367**,** 811-821.

Ward, R. C. & Robinson, M. 2000. *Principles of Hydrology,* Maidenhead, McGraw-Hill.

Wilson, L., Wilson, J., Holden, J., Johnstone, I., Armstrong, A. & Morris, M. 2010. Recovery of water tables in Welsh blanket bog after drain blocking: Discharge rates, time scales and the influence of local conditions. *Journal of Hydrology,* 391**,** 377-386.

Wilson, L., Wilson, J., Holden, J., Johnstone, I., Armstrong, A. & Morris, M. 2011a. Ditch blocking, water chemistry and organic carbon flux: Evidence that blanket bog restoration reduces erosion and fluvial carbon loss. *Science of The Total Environment,* 409**,** 2010-2018.

Wilson, L., Wilson, J., Holden, J., Johnstone, I., Armstrong, A. & Morris, M. 2011b. The impact of drain blocking on an upland blanket bog during storm and drought events, and the importance of sampling-scale. *Journal of Hydrology,* 404**,** 198-208.

Wilson, L., Wilson, J. M. & Johnstone, I. 2011c. The effect of blanket bog drainage on habitat condition and on sheep grazing, evidence from a Welsh upland bog. *Biological Conservation,* 144**,** 193-201.

Woike, M., Schmatzler, E. & Kaule, G. 1980. [Marshes. Importance-protection-regeneration [Germany, FR]]. *Gefaehrdete Lebensstaetten unserer Heimat (Germany, FR)*.

Worrall, F., Armstrong, A. & Adamson, J. K. 2007a. The effects of burning and sheep-grazing on water table depth and soil water quality in a upland peat. *Journal of Hydrology,* 339**,** 1-14.

Worrall, F., Armstrong, A. & Holden, J. 2007b. Short-term impact of peat drain-blocking on water colour, dissolved organic carbon concentration, and water table depth. *Journal of Hydrology,* 337**,** 315-325.

Worrall, F., Gibson, H. S. & Burt, T. P. 2007c. Modelling the impact of drainage and drain-blocking on dissolved organic carbon release from peatlands. *Journal of Hydrology,* 338**,** 15-27.

Yallop, A. R. & Clutterbuck, B. 2009. Land management as a factor controlling dissolved organic carbon release from upland peat soils 1: Spatial variation in DOC productivity. *Science of The Total Environment,* 407**,** 3803-3813.